HU-EP-09/07, HRI-P-09-02-001, RECAPP-HRI-2009-003

The Muon g-2

Fred Jegerlehner [a,b,*], Andreas Nyffeler [c]

[a] *Humboldt-Universität zu Berlin, Institut für Physik, Newtonstrasse 15, D-12489 Berlin, Germany*
[b] *Institute of Physics, University of Silesia, ul. Uniwersytecka 4, PL-40007 Katowice, Poland*
[c] *Regional Centre for Accelerator-based Particle Physics, Harish-Chandra Research Institute, Chhatnag Road, Jhusi, Allahabad - 211 019, India*

Abstract

The muon anomalous magnetic moment is one of the most precisely measured quantities in particle physics. In a recent experiment at Brookhaven it has been measured with a remarkable 14-fold improvement of the previous CERN experiment reaching a precision of 0.54ppm. Since the first results were published, a persisting "discrepancy" between theory and experiment of about 3 standard deviations is observed. It is the largest "established" deviation from the Standard Model seen in a "clean" electroweak observable and thus could be a hint for New Physics to be around the corner. This deviation triggered numerous speculations about the possible origin of the "missing piece" and the increased experimental precision animated a multitude of new theoretical efforts which lead to a substantial improvement of the prediction of the muon anomaly $a_\mu = (g_\mu - 2)/2$. The dominating uncertainty of the prediction, caused by strong interaction effects, could be reduced substantially, due to new hadronic cross section measurements in electron-positron annihilation at low energies. Also the recent electron $g-2$ measurement at Harvard contributes substantially to the progress in this field, as it allows for a much more precise determination of the fine structure constant α as well as a cross check of the status of our theoretical understanding.

In this report we review the theory of the anomalous magnetic moments of the electron and the muon. After an introduction and a brief description of the principle of the muon $g-2$ experiment, we present a review of the status of the theoretical prediction and in particular discuss the role of the hadronic vacuum polarization effects and the hadronic light–by–light scattering correction, including a new evaluation of the dominant pion-exchange contribution. In the end, we find a 3.2 standard deviation discrepancy between experiment and Standard Model prediction. We also present a number of examples of how extensions of the electroweak Standard Model would change the theoretical prediction of the muon anomaly a_μ. Perspectives for future developments in experiment and theory are briefly discussed and critically assessed. The muon $g-2$ will remain one of the hot topics for further investigations.

Key words: muon, anomalous magnetic moment, precision tests
PACS: 14.60.Ef, 13.40.Em

* Corresponding author.
Email addresses: fjeger@physik.hu-berlin.de (Fred Jegerlehner), nyffeler@hri.res.in (Andreas Nyffeler).
URLs: www-com.physik.hu-berlin.de/~fjeger/ (Fred Jegerlehner), www.hri.res.in/~nyffeler (Andreas Nyffeler).

Contents

1. Introduction

The electron's spin and magnetic moment were evidenced from the deflection of atoms in an inhomogeneous magnetic field and the observation of fine structure by optical spectroscopy [1,2]. Ever since, magnetic moments and g–values of particles in general and the $g-2$ experiments with the electron and the muon in particular, together with high precision atomic spectroscopy, have played a central role in establishing the modern theoretical framework for particle physics. That is relativistic quantum field theory in general and quantum electrodynamics in particular, the prototype theory which developed further into the so called "Standard Model" (SM) of electromagnetic, weak and strong interactions based on a local gauge principle and spontaneous symmetry breaking. The muon $g-2$ is one of the most precisely measured and theoretically best investigated quantities in particle physics. Our interest in very high precision measurements is motivated by our eagerness to exploit the limits of our present understanding of nature and to find effects which cannot be explained by the established theory. More than 30 years after its invention this is still the SM of elementary particle interactions, a $SU(3)_c \otimes SU(2)_L \otimes U(1)_Y$ gauge theory broken to $SU(3)_c \otimes U(1)_{\rm em}$ by the Higgs mechanism, which requires a not yet discovered Higgs particle to exist.

Designed to be a local, causal and renormalizable quantum field theory, quarks and leptons are allowed to come only in families in order to be anomaly free and not to conflict with renormalizability. So we have as the first family the quark doublet (u, d) of the up and down quarks accompanied by the lepton doublet (ν_e, e^-) with the electron neutrino and the electron, with the left-handed fields in the doublets and all their right-handed partners in singlets. All normal matter is made up from these 1st family fermions.

Most surprisingly a second and even a third quark–lepton family exist in nature, all with identical quantum numbers, as if nature would repeat itself. The corresponding members in the different families only differ by their mass where the mass scales span an incredible range, from $m_{\nu_e} \lesssim 10^{-3}$ eV for the electron neutrino

to $m_t \simeq 173$ GeV for the top quark. The existence of three families allows for an extremely rich pattern of all kinds of phenomena which derive from the natural possibility of mixing of the horizontal vectors in family space formed by the members with identical quantum numbers. The most prominent new effects only possible with three or more families is CP violation.

The first member of the second family that was discovered was the muon (μ). It was discovered in cosmic rays by Anderson & Neddermeyer in 1936 [3], only a few years after Anderson [4] had discovered (also in cosmic rays) in 1932 antimatter in form of the positron, a "positively charged electron" as predicted by Dirac in 1930 [5]. The μ was another version of an electron, just a heavier copy, and was extremely puzzling for physicists at that time. Its true nature only became clear much later after the first precise $g-2$ experiments had been performed. In fact the muon turns out to be a very special object in many respects as we will see and these particular properties make it to play a crucial role in the development of elementary particle theory.

The charged leptons primarily interact electromagnetically with the photon and weakly via the heavy gauge bosons W and Z, as well as very much weaker also with the Higgs. Puzzling enough, the three leptons e, μ and τ have identical properties, except for the masses which are given by $m_e = 0.511$ MeV, $m_\mu = 105.658$ MeV and $m_\tau = 1776.99$ MeV, respectively. As masses differ by orders of magnitude, the leptons show very different behavior, the most striking being the very different lifetimes. Within the SM the electron is stable on time scales of the age of the universe, while the μ has a short lifetime of $\tau_\mu = 2.197 \times 10^{-6}$ seconds and the τ is even more unstable with a lifetime $\tau_\tau = 2.906 \times 10^{-13}$ seconds only. Also, the decay patterns are very different: the μ decays very close to 100% into electrons plus two neutrinos ($e\bar{\nu}_e\nu_\mu$), however, the τ decays to about 65% into hadronic states $\pi^-\nu_\tau$, $\pi^-\pi^0\nu_\tau$, $, \cdots$ while the main leptonic decay modes only account for 17.36% ($\mu^-\bar{\nu}_\mu\nu_\tau$) and 17.85% ($e^-\bar{\nu}_e\nu_\tau$), respectively. This has a dramatic impact on the possibility to study these particles experimentally and to measure various properties precisely. The most precisely studied lepton is the electron, but the muon can also be explored with extreme precision. Since the muon turns out to be much more sensitive to hypothetical physics beyond the SM than the electron itself, the muon is much more suitable as a "crystal ball" which could give us hints about not yet uncovered physics. The reason is that some effects scale with powers of m_ℓ^2, as we will see below. Unfortunately, the τ, where new physics effects would be even better visible, is so short lived, that corresponding experiments are not possible with present technology.

As important as charge, spin, mass and lifetime, are the magnetic and electric *dipole moments* which are typical for spinning particles like the leptons. Both electrical and magnetic properties have their origin in the electrical *charges and their currents*. Magnetic monopoles are not necessary to obtain magnetic moments. On the classical level, an orbiting particle with electric charge e and mass m exhibits a magnetic dipole moment given by

$$\vec{\mu}_L = \frac{e}{2m}\,\vec{L} \tag{1}$$

where $\vec{L} = m\,\vec{r}\times\vec{v}$ is the orbital angular momentum ($\vec{r}$ position, $\vec{v}$ velocity). An electrical dipole moment can exist due to relative displacements of the centers of positive and negative electrical charge distributions. Magnetic and electric moments contribute to the electromagnetic interaction Hamiltonian with magnetic and electric fields

$$\mathcal{H} = -\vec{\mu}_m\cdot\vec{B} - \vec{d}_e\cdot\vec{E}\,, \tag{2}$$

where $\vec{B}$ and $\vec{E}$ are the magnetic and electric field strengths and $\vec{\mu}_m$ and $\vec{d}_e$ the magnetic and electric dipole moment operators. Usually, we measure magnetic moments in units of the *Bohr magneton* μ_B which is defined as follows

$$\mu_B = \frac{e}{2m_e} = 5.788381804(39)\times 10^{-11}\ \ \mathrm{MeVT}^{-1}\,. \tag{3}$$

Here T as a unit stands for 1 Tesla $= 10^4$ Gauss. [1]

[1] We will use the SI system of units, where $\mathrm{T} = \mathrm{Vsm}^{-2}$ and the electric charge e is measured in Coulomb. The Bohr magneton is then defined by $\mu_B = e\hbar/2m_e$, but we will set $\hbar = c = \epsilon_0 = 1$ throughout this article.

For a particle with spin the magnetic moment is **intrinsic** and obtained by replacing the the angular momentum operator $\vec{L}$ by the *spin operator*

$$\vec{S} = \frac{\vec{\sigma}}{2} \,, \tag{4}$$

where σ_i $(i = 1, 2, 3)$ are the Pauli spin matrices. Thus, generalizing the classical form (1) of the orbital magnetic moment, one writes

$$\vec{\mu}_m = g\, Q\, \mu_0\, \frac{\vec{\sigma}}{2} \quad , \quad \vec{d}_e = \eta\, Q\, \mu_0\, \frac{\vec{\sigma}}{2} \,, \tag{5}$$

where $\mu_0 = e/2m$, Q is the electrical charge in units of e, $Q = -1$ for the leptons $(\ell = e, \mu, \tau)$, $Q = +1$ for the antileptons and m is the mass. The equations define the gyromagnetic ratio g (g-factor) and its electric pendant η, respectively, quantities exhibiting important dynamical information about the leptons as we will see later. The deviation from the Dirac value $g_\ell/2 = 1$, obtained at the classical level, is

$$a_\ell \equiv \frac{g_\ell - 2}{2} \tag{6}$$

the famous *anomalous magnetic moment* and a_μ is the quantity in the focus of this review.

The magnetic interaction term gives rise to the well known *Zeeman effect*: level splitting seen in atomic spectra. If spin is involved one calls it *anomalous Zeeman effect*. The latter obviously is suitable to study the magnetic moment of the electron by investigating atomic spectra in magnetic fields.

The most important condition for the anomalous magnetic moment to be a useful monitor for testing a theory is its unambiguous predictability within that theory. The predictability crucially depends on the following properties of the theory:
– it must be a local relativistic quantum field theory and
– it must be renormalizable.
This implies that $g - 2$ vanishes at tree level and cannot be an independently adjustable parameter in any renormalizable QFT. This in turn implies that for a given theory [model] $g-2$ is an unambiguously calculable quantity and the predicted value can be confronted with experiments. Its model dependence makes a_μ a good monitor for the detection of new physics contributions. The key point is that $g-2$ can be both precisely predicted as well as experimentally measured with very high accuracy. By confronting precise theoretical predictions with precisely measured experimental data it is possible to subject the theory to very stringent tests and to find its possible limitations.

The anomalous magnetic moment of a lepton is a dimensionless quantity, a number, which in QED may be computed order by order as an expansion in the fine structure constant α. Beyond QED, in the SM or extensions of it, weak and strong coupling contributions are calculable. As a matter of fact, the interaction of the lepton with photons or other particles induces an effective interaction term

$$\delta\mathcal{L}_{\rm eff}^{\rm AMM} = -\frac{\delta g}{2}\,\frac{e}{4m}\left\{\bar{\psi}_L(x)\,\sigma^{\mu\nu}F_{\mu\nu}(x)\,\psi_R(x) + \bar{\psi}_R(x)\,\sigma^{\mu\nu}F_{\mu\nu}(x)\,\psi_L(x)\right\} \tag{7}$$

where ψ_L and ψ_R are Dirac fields of negative (left–handed L) and positive (right–handed R) chirality and $F_{\mu\nu} = \partial_\mu A_\nu - \partial_\nu A_\mu$ is the electromagnetic field strength tensor. It corresponds to a dimension 5 operator and since a renormalizable theory is constrained to exhibit terms of dimension 4 or less only, such a term must be absent for any fermion in any renormalizable theory at tree level.

The dipole moments are very interesting quantities for the study of the discrete symmetries. A basic consequence of any relativistic local QFT is *charge conjugation* C, the particle–antiparticle duality [5] or crossing property, which implies in the first place that particles and antiparticles have identical masses and spins. In fact, charge conjugation turned out not to be a universal symmetry in nature. Since an antiparticle may be considered as a particle propagating backwards in time, charge conjugation has to be considered together with *time-reversal* T (time-reflection), which in a relativistic theory has to go together with *parity* P (space-reflection). The CPT theorem says: the product of the three discrete transformations, C, P and T, taken in any order, is a symmetry of any relativistic local QFT. Actually, in contrast to the individual

transformations C, P and T, which are symmetries of the electromagnetic– and strong–interactions only, CPT is a universal symmetry and it is this symmetry which guarantees that particles and antiparticles have identical masses and lifetimes in theories like the SM, where C, P and T are not conserved.

The properties of the dipole moments under C, P and T transformations may be obtained easily by inspecting the interaction Hamiltonian in Eq. (2). Naively, one would expect that electromagnetic (QED) and strong interactions (QCD) are giving the dominant contributions to the dipole moments. However, both preserve P and T and thus the corresponding contributions to (2) must conserve these symmetries as well. On the one hand, both the magnetic and the electric dipole moment $\vec{\mu}_m$ and $\vec{d}_e$ are axial vectors as they are proportional to the spin vector $\vec{\sigma}$. On the other hand, the electromagnetic fields $\vec{E}$ and $\vec{B}$ transform as vector and axial vector, respectively. An axial vector changes sign under T, but not under P, while a vector changes sign under P, but not under T. Hence, in P and/or T conserving theories only the magnetic term $-\vec{\mu}_m \cdot \vec{B}$ is allowed while an electric dipole term $-\vec{d}_e \cdot \vec{E}$ is forbidden. Consequently, η in (5) would have to vanish exactly. However, as the weak interactions violate parity maximally, weak contributions to η cannot be excluded by the parity argument. The actual constraint here comes from T, which by the CPT–theorem is equivalent to CP. CP is also violated by the weak interactions, but only via fermion family mixing in the Yukawa sector of the SM. Therefore, electron and muon electric dipole moments are suppressed by approximate T invariance in the light fermion sector at the level of second order weak interactions (for a theoretical review see [6,7]). In fact experimental bounds tell us that they are very tiny [8]

$$|d_e| < 1.6 \times 10^{-27}\, e \cdot \text{cm at } 90\,\% \text{ C.L.} \tag{8}$$

This limit also plays an important role in the extraction of a_μ from experimental data, as we will see later. A new dedicated experiment for measuring the muon electric dipole moment (EDM) in a storage ring is under discussion [9].

Berestetskii's argument of a dramatically enhanced sensitivity [10] for short distances and for heavy new physics states attracted new attention for the muon anomalous magnetic moment. One of the main features of the anomalous magnetic moment of leptons is that it mediates helicity flip transitions. For massless particles helicity would be conserved by all gauge boson mediated interactions and helicity flips would be forbidden. For massive particles helicity flips are allowed and their transition amplitude is proportional to the mass of the particle. Since the transition probability goes with the modulus square of the amplitude, for the lepton's anomalous magnetic moment this implies that quantum fluctuations due to heavier particles or contributions from higher energy scales are proportional to

$$\delta a_\ell \propto \frac{m_\ell^2}{M^2} \qquad (M \gg m_\ell)\,, \tag{9}$$

where M may be
– the mass of a heavier SM particle, or
– the mass of a hypothetical heavy state beyond the SM, or
– an energy scale or an ultraviolet cut–off where the SM ceases to be valid.
Since the sensitivity to "new physics" grows quadratically with the mass of the lepton, the interesting effects are magnified in a_μ relative to a_e by a factor $(m_\mu/m_e)^2 \sim 4 \times 10^4$ at a given resolution (precision). Yet, the heavier the state, the smaller the effect (it decouples quadratically as $M \to \infty$). Thus we have the best sensitivity for nearby new physics, which has not yet been discovered by other experiments. This is why a_μ is a predestinated "monitor for new physics". By far the best sensitivity we would have for a_τ, if we could measure it with comparable precision. This, however, is beyond present experimental possibilities, because of the very short lifetime of the τ. [2]

Until about 1975 searching for "new physics" via a_μ in fact essentially meant looking for physics beyond QED. As we will see later, also SM hadronic and weak interaction effect carry the enhancement factor $(m_\mu/m_e)^2$, and this is good news and bad news at the same time. Good news because of the enhanced sensitivity to many details of SM physics like the weak gauge boson contributions, bad news because of the

[2] No real measurement exists yet for a_τ. Theory predicts $a_\tau = 117721(5) \times 10^{-8}$; the experimental limit from the LEP experiments OPAL and L3 is $-0.052 < a_\tau < 0.013$ at 95% CL [11].

enhanced sensitivity to the hadronic contributions which are very difficult to control and in fact limit our ability to make predictions at the desired precision. This is why the discussion of the hadronic contributions will cover a large fraction of this review.

The pattern of lepton anomalous magnetic moment physics which emerges is the following: a_e is a quantity which is dominated by QED effects up to very high precision, presently at the .24 parts per billion (ppb) level! The sensitivity to hadronic and weak effects as well as the sensitivity to physics beyond the SM is very small. This allows for a very solid and model independent (essentially pure QED) high precision prediction of a_e. The very precise experimental value and the very good control of the theory part in fact allows us to determine the fine structure constant α with the highest accuracy in comparison with other methods. A very precise value for α of course is needed as an input to be able to make precise predictions for other observables like a_μ, for example. While a_e, theory-wise, does not attract too much attention, although it requires to push QED calculation to high orders, a_μ is a much more interesting and theoretically challenging object, sensitive to all kinds of effects and thus probing the SM to much deeper level. Note that in spite of the fact that a_e has been measured about 2250 times more precisely than a_μ, the sensitivity of the latter to "new physics" is still about 19 times larger. The experimental accuracy achieved in the past few years at BNL is at the level of 0.54 parts per million (ppm) and better than the accuracy of the theoretical predictions which are still obscured by hadronic uncertainties. A small discrepancy at the 2 to 3 σ level persisted [12]–[16] since the first new measurement in 2000 up to the one in 2004 (four independent measurements during this time), the last for the time being. The "disagreement" between theory and experiment, suggested by the first BLN measurement, rejuvenated the interest in the subject and entailed a reconsideration of the theory predictions. Soon afterwards, in Ref. [17] a sign error was discovered in previous calculations of the problematic hadronic light–by–light scattering contribution. The change improved the agreement between theory and experiment by about 1 σ. Problems with the hadronic e^+e^-–annihilation data used to evaluate the hadronic vacuum polarization contribution led to a similar shift in opposite direction, such that a small though noticeable discrepancy persists. Once thought as a QED test, today the precision measurement of the anomalous magnetic moment of the muon is a test of most aspects of the SM, including the electromagnetic, the strong and the weak interaction effects. And more, if we could establish that supersymmetry is responsible for the observed deviation, for example, it would mean that we are testing a supersymmetric extension of the SM and constraining its parameter space, already now. There are many excellent and inspiring introductions and overviews on the subject [18]–[45] which were very useful in preparing this article. The reader can find many more details in the book [46].

1.1. *History*

In principle, the anomalous magnetic moment is an *observable* which can be relatively easily studied experimentally from the precise analysis of the motion of the lepton in an external magnetic field. For rather unstable particles like the muon, not to talk about the τ, obviously the problems are more involved. In case of the electron the observation of magnetic moments started with the Stern-Gerlach experiment [1] in 1924 and with Goudsmit and Uhlenbeck's [2] postulate that an electron has an intrinsic angular momentum $\frac{1}{2}$, and that associated with this spin angular momentum there is a magnetic dipole moment equal to $e/2m_e$. The quantum mechanical theory of the electron spin, where g remains a free parameter, was formulated by Pauli in 1927 [47]. Soon later, in 1928 Dirac presented his relativistic theory of the electron [48].

Unexpectedly but correctly, the Dirac theory predicted $g = 2$ for a free electron [48], twice the value $g = 1$ known to be associated with orbital angular momentum. Already in 1934 Kinster and Houston succeeded in confirming Dirac's prediction $g_e = 2$ [49]. Their measurement strongly supported the Dirac theory, although experimental errors were relatively large. To establish that the electron's magnetic moment actually exceeds 2 by about 0.12%, required more than 20 years of experimental efforts [50]. Essentially as long as it took the theoreticians to establish the first prediction of an "anomalous" contribution Eq. (6) to the magnetic moment. Only after the breakthrough in understanding and handling renormalization of QED (Tomonaga, Schwinger, Feynman, and others around 1948 [51]) unambiguous predictions of higher order effects became possible. In fact the calculation of the leading (one–loop diagram) contribution to the anomalous magnetic

moment by Schwinger in 1948 [52] was one of the very first higher order QED predictions. The result

$$a_\ell^{\mathrm{QED}(2)} = \frac{\alpha}{2\pi} \ , \quad (\ell = e, \mu, \tau) \tag{10}$$

established in theory the effect from quantum fluctuations via virtual electron photon interactions. In QED this value is universal for all leptons. Before theory solved that problem, in 1947 Nafe, Nelson and Rabi [53] reported an anomalous value of about 0.26 % in the hyperfine splitting of hydrogen and deuterium. The result was very quickly confirmed by Nagle et al. [54], and Breit [55] suggested that an anomaly $g \neq 2$ of the magnetic moment of the electron could explain the effect. Kusch and Foley [56] presented the first precision determination of the magnetic moment of the electron $g_e = 2.00238(10)$ in 1948, just before the theoretical result had been settled. They had studied the hyperfine–structure of atomic spectra in a constant magnetic field. Together with Schwinger's result $a_e^{(2)} = \alpha/(2\pi) \simeq 0.00116$ (which accounts for 99 % of the anomaly) this provided one of the first tests of the virtual quantum corrections, predicted by a relativistic quantum field theory. At about the same time, the discovery of the fine structure of the hydrogen spectrum (Lamb–shift) by Lamb and Retherford [57] in 1947 and the corresponding calculations by Bethe, Kroll & Lamb and Weisskopf & French [58] in 1949 provided the second triumph in testing QED by precision experiments beyond the tree level. These events had a dramatic impact in establishing quantum field theory as a general framework for the theory of elementary particles and for our understanding of the fundamental interactions. It stimulated the development of QED in particular and the concepts of quantum field theory in general. The extension to non-Abelian gauge theories finally lead us to the SM, at present our established basis for understanding the world of elementary particles. All this structure today is crucial for obtaining sufficiently precise predictions for the anomalous magnetic moment of the muon as we will see.

In 1956 Berestetskii et al. [10] pointed out that the sensitivity of a_ℓ to short distance physics scales like Eq. (9) where $M = \Lambda$ is an UV cut–off characterizing the scale of new physics. At that time a_e was already well measured by Crane et al. [59], but it was clear that the anomalous magnetic moment of the muon would be a much better probe for possible deviations from QED. But how to measure a_μ?

The breakthrough came in 1957 when Lee and Yang suggested parity violation by weak interaction processes [60]. It immediately became clear that muons produced in weak decays of the pion ($\pi^+ \to \mu^+ +$ neutrino) should be longitudinally polarized. In addition, the decay positron of the muon ($\mu^+ \to e^+ + 2$ neutrinos) could indicate the muon spin direction. Garwin, Lederman and Weinrich [61] and Friedman and Telegdi [62] [3] were able to confirm this pattern in a convincing way. The first of the two papers for the first time determined $g_\mu = 2.00$ within 10% by applying the muon spin precession principle. Now the road was free to seriously think about the experimental investigation of a_μ.

The first measurement of the anomalous magnetic moment of the muon was performed at Columbia University in 1960 [63]. The result $a_\mu = 0.00122(8)$ at a precision of about 5% showed no difference with the electron. Shortly after in 1961, the first precision determination was possible at the CERN cyclotron (1958-1962) [64,65]. Surprisingly, nothing special was observed within the 0.4% level of accuracy of the experiment. This provided the first real evidence that the muon was just a heavy electron. It meant that the muon was a point–like double of the electron and no extra short distance effects could be seen. This latter point of course is a matter of accuracy and the challenge to investigate the muon structure further was evident.

The idea of a *muon storage ring* was put forward next. A first one was successfully realized at CERN (1962-1968) [66,67,68]. It allowed to measure a_μ for both μ^+ and μ^- at the same machine. Results agreed well within errors and provided a precise verification of the CPT theorem for muons. An accuracy of 270 ppm was reached and an insignificant 1.7 σ deviation from theory was found. Nevertheless the latter triggered a reconsideration of theory. It turned out that in the estimate of the three–loop $O(\alpha^3)$ QED contribution the leptonic light–by–light scattering part (dominated by the electron loop) was missing. Aldins et al. [69] then calculated this and after including it, perfect agreement between theory and experiment was obtained.

The first successes of QED predictions and the growing precision of the a_e experiments challenged many particle theorists to tackle the much more difficult higher order calculations for a_e as well as for a_μ. Many of

[3] The latter reference for the first time points out that P and C are violated simultaneously, in fact P is maximally violated while CP is to a very good approximation conserved in this decay.

these calculations were strong motivations for inventing and developing computer algebra codes as advanced tools to solve difficult problems by means of computers. Also the dramatic increase of computer performance and the use of more efficient computing algorithms have been crucial for the progress achieved.

Already in 1959 a new formula for measuring a_μ was found by Bargmann, Michel and Telegdi [70]. At a particular energy, the magic energy, which turned out to be at about 3.1 GeV, a number of systematic difficulties of the existing experiment could be eliminated (see the discussion in Sect. 2.1). This elegant method was realized with the second muon storage ring at CERN (1969-1976) [71]. The precision of 7 ppm reached was an extraordinary achievement at that time. For the first time the m_μ^2/m_e^2–enhanced hadronic contribution came into play. Again no deviations were found. With the achieved precision the muon $g-2$ remained a benchmark for beyond the SM theory builders ever since. Only 20 years later the BNL experiment E821, again a muon storage ring experiment run at the magic energy, was able to set new standards in precision. This will be outlined in Sect. 2.1.

Now, at the present level of accuracy, the complete SM is needed in order to be able to make predictions at the appropriate level of precision. As already mentioned, at present further progress is hampered to some extent by difficulties to include properly the non–perturbative strong interaction part. At a certain level of precision *hadronic effects* become important and we are confronted with the question of how to evaluate them reliably. At low energies QCD gets strongly interacting and a perturbative calculation is not possible. Fortunately, analyticity and unitarity allow us to express the leading hadronic vacuum polarization contributions via a dispersion relation (analyticity) in terms of experimental data [72]. The key relation here is the optical theorem (unitarity) which determines the imaginary part of the vacuum polarization amplitude through the total cross section for electron–positron annihilation into hadrons. First estimations were performed in [73,74,75] after the discovery of the ρ– and the ω–resonances, and in [76], after first e^+e^- cross–section measurements were performed at the e^+e^- colliding beam machines in Novosibirsk [77] and Orsay [78], respectively. One drawback of this method is that now the precision of the theoretical prediction of a_μ is limited by the accuracy of experimental data. Much more accurate e^+e^-–data from experiments at the electron positron storage ring VEPP-2M at Novosibirsk allowed a big step forward in the evaluation of the leading hadronic vacuum polarization effects [79,80,81] (see also [82]). A more detailed analysis based on a complete up–to–date collection of data followed about 10 years later [83]. Further improvements were possible thanks to new hadronic cross section measurements by BES II [84] (BEPC ring) at Beijing and by CMD-2 [85] at Novosibirsk. More recently, cross section measurements via the radiative return mechanism by KLOE [86] (DAΦNE ring) at Frascati and by BaBar at SLAC became available. This will be elaborated in much more detail in Sect. 4.

Another important development was the discovery of reliable methods to control strong interaction dynamics at low energies where perturbative QCD fails to work. At very low energy, the well developed chiral perturbation theory (CHPT) [87] works. At higher energies, CHPT has been extended to a resonance Lagrangian approach [88], which unifies to some extent low energy effective hadronic models. These models play a role in the evaluation of the hadronic light-by-light scattering contribution, which we will discuss in Sect. 5.

Of course it was the hunting for deviations from theory and the theorists speculations about "new physics around the corner" which challenged new experiments again and again. The reader may find more details about historical aspects and the experimental developments in the interesting review: "The 47 years of muon g-2" by Farley and Semertzidis [33].

1.2. *Muon Properties*

Why the muon anomalous magnetic moment is so interesting and plays a key role in elementary particle physics at its fundamental level is due to the fact that it can be predicted by theory with very high accuracy and at the same time can be measured as precisely in an unambiguous experimental setup. That the experimental conditions can be controlled very precisely, with small systematic uncertainties, has to do with the very interesting intrinsic properties of the muon, which we briefly describe in the following.

1.2.1. *Spin Transfer in Production and Decay of Muons*

The muon $g-2$ experiments observe the motion of the spin of the muons on circular orbits in a homogeneous magnetic field. This requires the muons to be polarized. After the discovery of the parity violation in weak interaction it immediately became evident that weak decays of charged pions are producing polarized muons. Thereby the maximal parity violation of charged current processes provides the ideal conditions. The point is that right–handed neutrinos ν_R are not produced in the weak transitions mediated by the charged $W^{\pm}$ gauge bosons. As a consequence the production rate of ν_R's in ordinary weak reactions is practically zero which amounts to lepton number conservation for all practical purposes in laboratory experiments [4] .

Pions may be produced by shooting protons (accumulated in a proton storage ring) on a target material where pions are the most abundant secondary particles. The most effective pion production mechanism proceeds via excitation and subsequent decay of baryon resonances. For pions the dominating channel is the $\Delta_{33} \to N\pi$ isobar.

All muon $g-2$ experiments are based on the decay chain

$$\begin{aligned} \pi &\to \mu + \nu_\mu \\ &\quad \hookrightarrow\ e + \nu_e + \nu_\mu \ , \end{aligned}$$

producing the polarized muons which decay into electrons which carry along with their direction of propagation the muon's polarization (see e.g. [89]).

1) Pion decay:

The π^- is a pseudoscalar bound state $\pi^- = (\bar{u}\gamma_5 d)$ of a d quark and a u antiquark $\bar{u}$. The main decay proceeds via

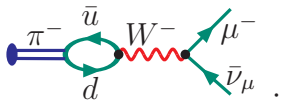

π–decay .

Being a two–body decay, the lepton energy is fixed (monochromatic) and given by $E_\ell = \sqrt{m_\ell^2 + p_\ell^2} = \frac{m_\pi^2+m_\ell^2}{2m_\pi}$, $p_\ell = \frac{m_\pi^2-m_\ell^2}{2m_\pi}$. The part of the Fermi type effective Lagrangian which describes this decay reads

$$\mathcal{L}_{\rm eff,int} = -\frac{G_\mu}{\sqrt{2}} V_{ud} \, (\bar{\mu}\gamma^\alpha \, (1-\gamma_5) \, \nu_\mu) \, (\bar{u}\gamma_\alpha \, (1-\gamma_5) \, d) + \text{h.c.}$$

where G_μ denotes the Fermi constant and V_{ud} the first entry in the CKM matrix. For our purpose $V_{ud} \sim 1$. The basic hadronic matrix element for pion decay is $\langle 0| \, \bar{d} \, \gamma_\mu\gamma_5 \, u \, |\pi(p)\rangle \doteq \mathrm{i} F_\pi p_\mu$ which defines the pion decay constant F_π. The transition matrix–element for the process of our interest then reads

$$T = {}_{\rm out}\!<\mu^-, \bar{\nu}_\mu|\pi^->_{\rm in} = -\mathrm{i}\frac{G_\mu}{\sqrt{2}} V_{ud} \, F_\pi \left(\bar{u}_\mu \gamma^\alpha \, (1-\gamma_5) \, v_{\nu_\mu}\right) \, p_\alpha \ .$$

Since the π^+ has spin 0 and the emitted neutrino is left–handed ($(1-\gamma_5)/2$ projector), by angular momentum conservation, the μ^+ must be left–handed as well. Only the axial part of the weak charged $V-A$ current couples to the pion, as it is a pseudoscalar state. In order to obtain the π^- decay not only particles have to be replaced by antiparticles (C) but also the helicities have to be reversed (P), since a left–handed antineutrino (essentially) does not exist. Note that the decay is possible only due to the non–zero muon mass, which allows for the necessary helicity flip of the muon. How the handedness is correlated with the charge is illustrated in Fig. 1.

[4] Only in recent years phenomenon of neutrino oscillations could be established unambiguously which proves that lepton number in fact is not a perfectly conserved quantum number. Neutrino oscillations are possible only if neutrinos have masses which requires that right–handed neutrinos (ν_R's) exist. In fact, the smallness of the neutrino masses explains the strong suppression of lepton number violating effects.

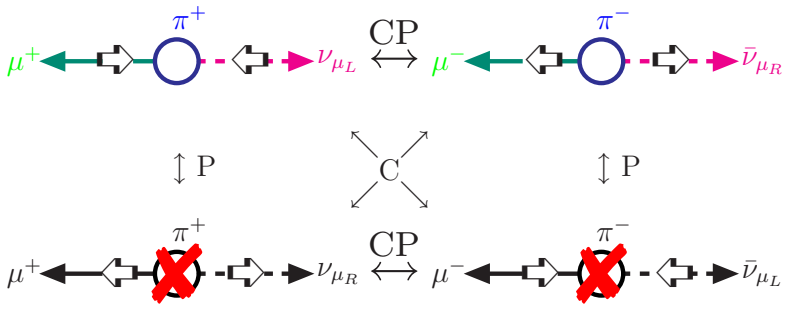

Fig. 1. In the P violating weak pion decays leptons of definite handedness are produced depending on the given charge. μ^- [μ^+] is produced with positive [negative] helicity $h = \vec{S}\cdot\vec{p}/|\vec{p}|$. The physical μ^- and μ^+ decays are related by a CP transformation. The decays obtained by C or P alone are inexistent.

The pion decay rate is given by

$$\Gamma_{\pi^-\to\mu^-\bar{\nu}_\mu} = \frac{G_\mu^2}{8\pi}\,|V_{ud}|^2 F_\pi^2\, m_\pi\, m_\mu^2\,\left(1-\frac{m_\mu^2}{m_\pi^2}\right)^2 \times (1+\delta_{\rm QED})\ , \tag{11}$$

with $\delta_{\rm QED}$ the electromagnetic correction.

2) Muon decay:
The muon is unstable and decays via the weak three body decay $\mu^- \to e^-\bar{\nu}_e\nu_\mu$

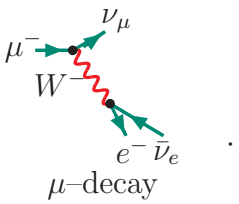

μ–decay

The μ–decay matrix element follows from the relevant part of the effective Lagrangian which reads

$$\mathcal{L}_{\rm eff,int} = -\frac{G_\mu}{\sqrt{2}}\,(\bar{e}\gamma^\alpha\,(1-\gamma_5)\,\nu_e)\,(\bar{\nu}_\mu\gamma_\alpha\,(1-\gamma_5)\,\mu) + \text{h.c.}$$

and is given by

$$T = {}_{\rm out}\!<e^-,\bar{\nu}_e\nu_\mu|\mu^->_{\rm in} = \frac{G_\mu}{\sqrt{2}}\,(\bar{u}_e\gamma^\alpha\,(1-\gamma_5)\,v_{\nu_e})\,(\bar{u}_{\nu_\mu}\gamma_\alpha\,(1-\gamma_5)\,u_\mu)\ .$$

This proves that the μ^- and the e^- have both the same left–handed helicity [the corresponding anti–particles are right–handed] in the massless approximation. This implies the decay scheme of Fig. 2 for the muon. Again

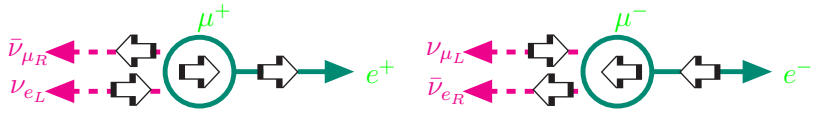

Fig. 2. In μ^- [μ^+] decay the produced e^- [e^+] has negative [positive] helicity, respectively.

it is the P violation which prefers electrons emitted in the direction of the muon spin. Therefore, measuring the direction of the electron momentum provides the direction of the muon spin. After integrating out the two unobservable neutrinos, the differential decay probability to find an $e^\pm$ with reduced energy between x_e and $x_e + dx_e$, emitted at an angle between θ and $\theta + d\theta$, reads

$$\frac{d^2\Gamma^\pm}{dx_e\,d\cos\theta} = \frac{G_\mu^2 m_\mu^5}{192\pi^3}\,x_e^2\,\left(3-2x_e \pm P_\mu\,\cos\theta\,(2x_e-1)\right) \tag{12}$$

and typically is strongly peaked at small angles. The charge sign dependent asymmetry in the production angle θ represents the parity violation. The reduced $e^{\pm}$ energy is $x_e = E_e/W_{\mu e}$ with $W_{\mu e} = \max E_e = (m_\mu^2+m_e^2)/2m_\mu$, the emission angle θ is the angle between the momentum $\vec{p}_e$ of $e^{\pm}$ and the muon polarization vector $\vec{P}_\mu$. The result above holds in the approximation $x_0 = m_e/W_{e\mu} \sim 9.67 \times 10^{-3} \simeq 0$.

1.3. *Lepton Magnetic Moments*

Our particular interest is the motion of a lepton in an external field under consideration of the full relativistic quantum behavior. It is controlled by the QED equations of motion with an external field added

$$\begin{aligned} \left(\mathrm{i}\gamma^\mu\partial_\mu + Q_\ell e\gamma^\mu(A_\mu(x) + A_\mu^{\mathrm{ext}}(x)) - m_\ell\right)\ \psi_\ell(x) \ &= \ 0\ , \\ \left(\Box g^{\mu\nu} - \left(1-\xi^{-1}\right)\partial^\mu\partial^\nu\right) A_\nu(x) \ &= \ -Q_\ell\, e\bar{\psi}_\ell(x)\gamma^\mu\psi_\ell(x)\ . \end{aligned} \tag{13}$$

What we are looking for is the solution of the Dirac equation with an external field, specifically a constant magnetic field, as a relativistic one–particle problem, neglecting the radiation field in a first step. For slowly varying fields $A^{\mu\,\mathrm{ext}} = (\Phi, \vec{A})$ the motion is essentially determined by the generalized Pauli equation (W. Pauli 1927)

$$\mathrm{i}\frac{\partial\varphi}{\partial t} = \boldsymbol{H}\,\varphi = \left(\frac{1}{2m}(\vec{p} - e\vec{A})^2 + e\,\Phi - \frac{e}{2m}\,\vec{\sigma}\cdot\vec{B}\right)\,\varphi\ , \tag{14}$$

which up to the spin term is nothing but the non–relativistic Schrödinger equation and which also serves as a basis for understanding the role of the magnetic moment of a lepton on the classical level. φ is a non–relativistic two-component Pauli–spinor. As we will see, in the absence of electrical fields $\vec{E}$, the quantum correction miraculously may be subsumed in a single number, the anomalous magnetic moment, which is the result of relativistic quantum fluctuations.

To study radiative corrections we have to extend the discussion of the preceding paragraph and consider the full QED interaction Lagrangian

$$\mathcal{L}_{\mathrm{int}}^{\mathrm{QED}}(x) = -e\bar{\psi}(x)\gamma^\mu\psi(x)\ A_\mu(x) \tag{15}$$

for the case where the photon field is part of the dynamics but has an external classical component $A_\mu^{\mathrm{ext}}(x)$: $A_\mu(x) \to A_\mu(x) + A_\mu^{\mathrm{ext}}(x)$. We are thus dealing with QED exhibiting an additional external field insertion "vertex":

$$= -\mathrm{i}e\,\gamma^\mu\ \tilde{A}_\mu^{\mathrm{ext}}\ .$$

Gauge invariance requires that a gauge transformation of the external field $A_\mu^{\mathrm{ext}}(x) \to A_\mu^{\mathrm{ext}}(x) - \partial_\mu\alpha(x)$, for an arbitrary scalar classical field $\alpha(x)$, leaves physics invariant.

The motion of the lepton in the external field is described by a simultaneous expansion in the fine structure constant $\alpha = e^2/4\pi$ and in the external field $A_\mu^{\mathrm{ext}}(x)$ assuming the latter to be weak

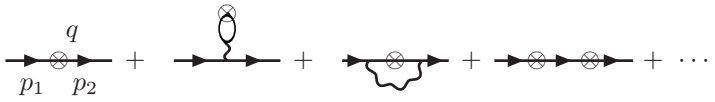

In the following we will use the more customary graphic representation

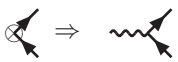

of the external vertex, just as an amputated photon line at zero momentum.

The gyromagnetic ratio of the muon is defined by the ratio of the magnetic moment which couples to the magnetic field in the Hamiltonian and the spin operator in units of $\mu_0 = e/2m_\mu$

$$\vec{\mu} = g_\mu \, \frac{e}{2m_\mu} \, \vec{s} \;\; ; \quad g_\mu = 2\,(1 + a_\mu) \tag{16}$$

and as indicated has a tree level part, the Dirac moment $g_\mu^{(0)} = 2$ [48], and a higher order part a_μ the muon anomaly or anomalous magnetic moment.

In QED a_μ may be calculated in perturbation theory by considering the matrix element

$$\mathcal{M}(x;p) = \langle \mu^-(p_2,r_2)|j^\mu_{\rm em}(x)|\mu^-(p_1,r_1)\rangle$$

of the electromagnetic current for the scattering of an incoming muon $\mu^-(p_1,r_1)$ of momentum p_1 and 3rd component of spin r_1 to a muon $\mu^-(p_2,r_2)$ of momentum p_2 and 3rd component of spin r_2, in the classical limit of zero momentum transfer $q^2 = (p_2 - p_1)^2 \to 0$. In momentum space we obtain

$$\begin{aligned}\tilde{\mathcal{M}}(q;p) &= \int \mathrm{d}^4x \, \mathrm{e}^{-\mathrm{i}qx} \langle \mu^-(p_2,r_2)|j^\mu_{\rm em}(x)|\mu^-(p_1,r_1)\rangle \\ &= (2\pi)^4 \, \delta^{(4)}(q - p_2 + p_1) \, \langle \mu^-(p_2,r_2)|j^\mu_{\rm em}(0)|\mu^-(p_1,r_1)\rangle \,,\end{aligned}$$

proportional to the δ–function of four–momentum conservation. The T–matrix element is then given by

$$\langle \mu^-(p_2)|j^\mu_{\rm em}(0)|\mu^-(p_1)\rangle = (-\mathrm{i}e)\, \bar{u}(p_2) \Gamma^\mu(P,q) u(p_1) \,, \quad (P = p_1 + p_2) \,.$$

In QED it has a relativistically covariant decomposition of the form

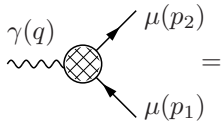

$$= (-\mathrm{i}e)\, \bar{u}(p_2) \left[\gamma^\mu F_{\rm E}(q^2) + \mathrm{i} \frac{\sigma^{\mu\nu} q_\nu}{2m_\mu} F_{\rm M}(q^2) \right] u(p_1) \,, \tag{17}$$

where $q = p_2 - p_1$ and $u(p)$ denote the Dirac spinors. $F_{\rm E}(q^2)$ is the electric charge or Dirac form factor and $F_{\rm M}(q^2)$ is the magnetic or Pauli form factor. Note that the matrix $\sigma^{\mu\nu} = \frac{\mathrm{i}}{2}[\gamma^\mu, \gamma^\nu]$ represents the spin 1/2 angular momentum tensor. In the static (classical) limit we have

$$F_{\rm E}(0) = 1 \;\; , \quad F_{\rm M}(0) = a_\mu \,, \tag{18}$$

where the first relation is the *charge renormalization condition* (in units of the physical positron charge e, which by definition is taken out as a factor), while the second relation is the finite prediction for a_μ, in terms of the form factor $F_{\rm M}$ the calculation of which will be described below. Instead of calculating the full vertex function $\Gamma_\mu(P,q)$ one can use the projection technique described in [90] and expand the vertex function to linear order in the external photon momentum q:

$$\Gamma_\mu(P,q) \simeq \Gamma_\mu(P,0) + q^\nu \frac{\partial}{\partial q^\nu} \, \Gamma_\mu(P,q)|_{q=0} \equiv V_\mu(p) + q^\nu \, T_{\nu\mu}(p) \,, \tag{19}$$

for fixed P. This allows us to simplify the calculation by working directly in the limit $q \to 0$ afterwards. Since a_μ does not depend on the direction of the muon momentum one can average over the direction of P which is orthogonal to q ($P \cdot q = 0$). As a master formula one finds

$$\begin{aligned} a_\mu = &\frac{1}{8\,(d-2)(d-1)\,m_\mu} \, \mathrm{Tr}\, \{(\not{p} + m_\mu)\,[\gamma^\mu, \gamma^\nu]\,(\not{p} + m_\mu)\, T_{\nu\mu}(p)\} \\ &+ \frac{1}{4\,(d-1)\,m_\mu^2} \, \mathrm{Tr}\, \left\{ \left[m_\mu^2\, \gamma^\mu - (d-1)\, m_\mu\, p^\mu - d\, \not{p}\, p^\mu \right] V_\mu(p) \right\}\Big|_{p^2 = m_\mu^2} \;\; , \end{aligned} \tag{20}$$

where $d = 4 - \varepsilon$ is the space-time dimension. In case of UV divergences the choice $\varepsilon > 0$ provides a dimensional regularization. The limit $\varepsilon \to 0$ is to be performed after renormalization. The amplitudes $V_\mu(p)$ and $T_{\nu\mu}(p)$ depend on one on–shell momentum $p = P/2$, only, and thus the problem reduces to the calculation of on–shell self–energy type diagrams as the external photon momentum now can be taken zero.

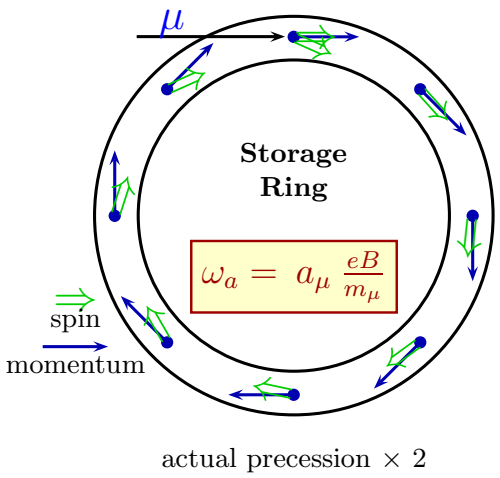

Fig. 3. Spin precession in the $g-2$ ring ($\sim 12^\circ$/circle).

Note that in higher orders the form factors in general aquire an imaginary part. One may therefore write an effective dipole moment Lagrangian with complex "coupling"

$$\mathcal{L}_{\rm eff}^{\rm DM} = -\frac{1}{2}\left\{\bar{\psi}\,\sigma^{\mu\nu}\left[D_\mu\,\frac{1+\gamma_5}{2} + D_\mu^*\,\frac{1-\gamma_5}{2}\right]\psi\right\}F_{\mu\nu} \tag{21}$$

with ψ the muon field and

$$\mathrm{Re}\,D_\mu = a_\mu\,\frac{e}{2m_\mu}\quad,\quad \mathrm{Im}\,D_\mu = d_\mu = \frac{\eta_\mu}{2}\,\frac{e}{2m_\mu}\,. \tag{22}$$

Thus the imaginary part of $F_{\rm M}(0)$ corresponds to an electric dipole moment. The latter is non–vanishing only if we have T violation. The existence of a relatively large EDM would also affect the extraction of a_μ. This will be discussed towards the end of the next section.

2. The Muon $g-2$ Experiments

2.1. *The Brookhaven Muon $g-2$ Experiment*

The measurement of a_μ in principle is simple. As illustrated in Fig. 3, when polarized muons travel on a circular orbit in a constant magnetic field, then a_μ is responsible for the *Larmor precession* of the direction of the spin of the muon, characterized by the angular frequency $\vec{\omega}_a$. Correspondingly, the principle of the BNL muon $g-2$ experiment involves the study of the orbital and spin motion of highly polarized muons in a magnetic storage ring. This method has been applied in the last CERN experiment [91] already. The key improvements of the BLN experiment include the very high intensity of the primary proton beam from the proton storage ring AGS (Alternating Gradient Synchrotron), the injection of muons instead of pions into the storage ring, and a super–ferric storage ring magnet [92] (see also the reviews [23,28,33,34,43]).

The muon $g-2$ experiment at Brookhaven works as illustrated in Fig. 4 [93,94,95]. Protons of energy 24 GeV from the AGS hit a target and produce pions. The pions are unstable and decay into muons plus a neutrino where the muons carry spin and thus a magnetic moment which is directed along the direction of the flight axis. The longitudinally polarized muons from pion decay are then injected into a uniform

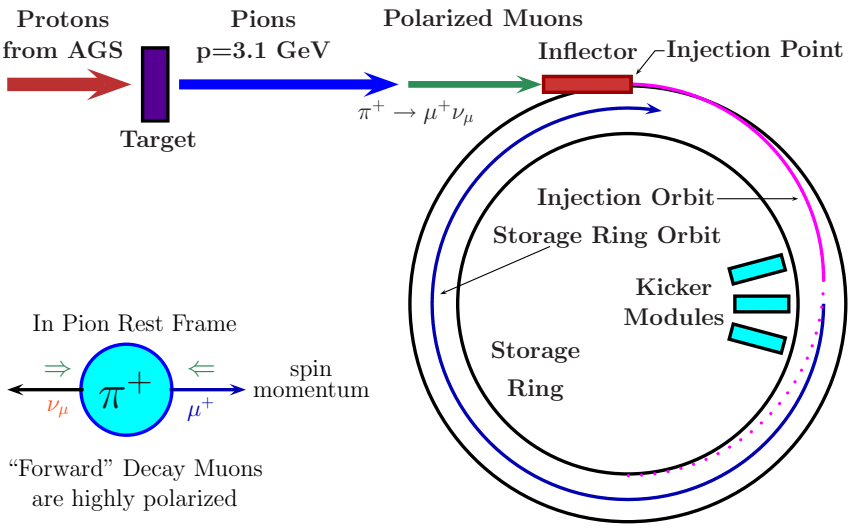

Fig. 4. The schematics of muon injection and storage in the $g-2$ ring.

magnetic field $\vec{B}$ where they travel in a circle. The ring [5] is a toroid–shaped structure with a diameter of 14 meters, the aperture of the beam pipe is 90 mm, the field is 1.45 Tesla and the momentum of the muon is $p_\mu = 3.094$ GeV. In the horizontal plane of the orbit the muons execute a relativistic cyclotron motion with angular frequency ω_c. By the motion of the muon magnetic moment in the homogeneous magnetic field the spin axis is changed in a particular way as described by the Larmor precession. After each circle the muon's spin axis changes by 12' (arc seconds), while the muon is traveling at the same momentum (see Fig. 3). The muon spin is precessing with angular frequency ω_s, which is slightly bigger than ω_c by the difference angular frequency $\omega_a = \omega_s - \omega_c$.

$$\omega_c = \frac{eB}{m_\mu \gamma}\,, \quad \omega_s = \frac{eB}{m_\mu \gamma} + a_\mu \frac{eB}{m_\mu}\,, \quad \omega_a = a_\mu \frac{eB}{m_\mu}\,, \tag{23}$$

where $\gamma = 1/\sqrt{1-v^2}$ is the relativistic Lorentz factor and v the muon velocity. In the experiment ω_a and B are measured. The muon mass m_μ is obtained from an independent experiment on muonium, which is a $(\mu^+ e^-)$ bound system. Note that if the muon would just have its Dirac magnetic moment $g = 2$ (tree level) the direction of the spin of the muon would not change at all.

In order to retain the muons in the ring an electrostatic focusing system is needed. Thus in addition to the magnetic field $\vec{B}$ an electric quadrupole field $\vec{E}$ in the plane normal to the particle orbit must be applied. This transversal electric field changes the angular frequency according to

$$\vec{\omega_a} = \frac{e}{m_\mu}\left(a_\mu \vec{B} - \left[a_\mu - \frac{1}{\gamma^2-1}\right]\,\vec{v}\times\vec{E}\right)\,. \tag{24}$$

This key formula for measuring a_μ was found by Bargmann, Michel and Telegdi in 1959 [70,96]. Interestingly, one has the possibility to choose γ such that $a_\mu - 1/(\gamma^2-1) = 0$, in which case ω_a becomes independent of $\vec{E}$. This is the so–called *magic* γ. When running at the corresponding magic energy, the muons are highly relativistic, the magic γ-factor being $\gamma = \sqrt{1+1/a_\mu} = 29.3$. The muons thus travel almost at the speed of light with energies of about $E_{\rm magic} = \gamma m_\mu \simeq 3.098$ GeV. This rather high energy, which is dictated by the requirement to minimize the precession frequency shift caused by the electric quadrupole superimposed upon the uniform magnetic field, also leads to a large time dilatation. The lifetime of a muon at rest is 2.19711 μs, while in the ring it is 64.435 μs (theory) [64.378 μs (experiment)]). Thus, with their lifetime being much larger than at rest, muons are circling in the ring many times before they decay into a positron

[5] A picture of the BNL muon storage ring may be found on the Muon $g-2$ Collaboration Web Page `http://www.g-2.bnl.gov/`

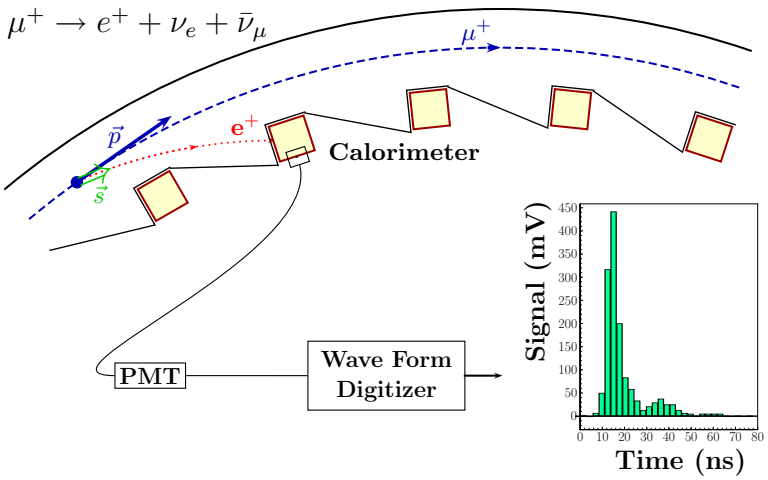

Fig. 5. Decay of μ^+ and detection of the emitted e^+ (PMT=Photomultiplier).

plus two neutrinos: $\mu^+ \to e^+ + \nu_e + \bar{\nu}_\mu$. In this decay we have the necessary strong correlation between the muon spin direction and the direction of emission of the positrons. The differential decay rate for the muon in the rest frame is given by Eq. (12) which may be written as

$$d\Gamma = N(E_e) \left(1 + \frac{1-2x_e}{3-2x_e} \cos\theta\right) d\Omega \,. \tag{25}$$

Again, E_e is the positron energy, x_e is E_e in units of the maximum energy $m_\mu/2$, $N(E_e)$ is a normalization factor and θ the angle between the positron momentum in the muon rest frame and the muon spin direction. The μ^+ decay spectrum is peaked strongly for small θ due to the non–vanishing coefficient of $\cos\theta$

$$A(E_e) \doteq \frac{1-2x_e}{3-2x_e} \,, \tag{26}$$

the asymmetry factor which reflects the *parity violation*.

The positron is emitted with high probability along the spin axis of the muon as illustrated in Fig. 5. The decay positrons are detected by 24 calorimeters evenly distributed inside the muon storage ring. These counters measure the positron energy and allow to determine the direction of the muon spin. A precession frequency dependent rate is obtained actually only if positrons above a certain energy are selected (forward decay positrons). The number of decay positrons with energy greater than E emitted at time t after muons are injected into the storage ring is given by

$$N(t) = N_0(E) \, \exp\left(\frac{-t}{\gamma\tau_\mu}\right) \, [1 + A(E) \, \sin(\omega_a t + \phi(E))] \,, \tag{27}$$

where $N_0(E)$ is a normalization factor, τ_μ the muon life time (in the muon rest frame), and $A(E)$ is the asymmetry factor for positrons of energy greater than E. Fig. 6 shows a typical example for the time structure detected in the BNL experiment. As expected the exponential decay law for the decaying muons is modulated by the $g-2$ angular frequency. In this way the angular frequency ω_a is neatly determined from the time distribution of the decay positrons observed with the electromagnetic calorimeters [12]–[16].

The second quantity which has to be measured very precisely in the experiment is the magnetic field. This is accomplished by *Nuclear Magnetic Resonance* (NMR) using a standard probe of H_2O [97]. This standard can be related to the magnetic moment of a free proton by

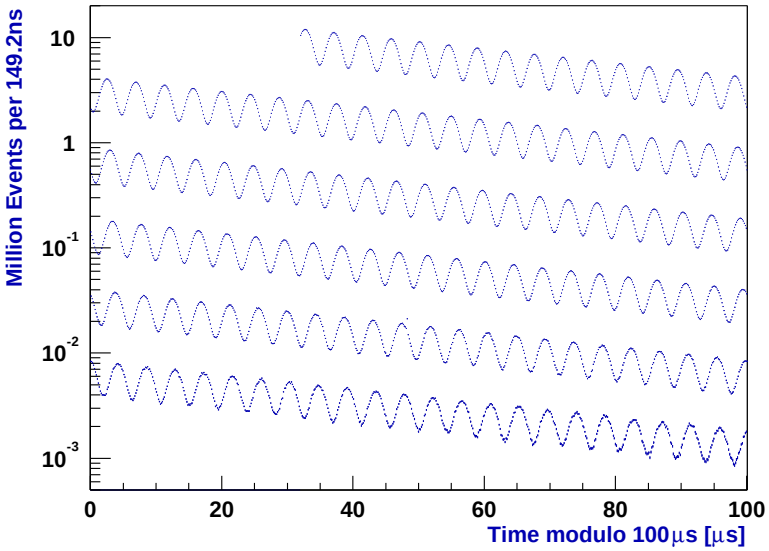

Fig. 6. Distribution of counts versus time for the 3.6 billion decays in the 2001 negative muon data–taking period [Courtesy of the E821 collaboration. Reprinted with permission from [92]. Copyright (2007) by the American Physical Society].

$$B = \frac{\omega_p}{2\mu_p} \,, \tag{28}$$

where ω_p is the Larmor spin precession angular velocity of a proton in water. Using ω_p and the frequency ω_a together with $\mu_\mu = (1 + a_\mu)\, e/(2m_\mu)$, one obtains

$$a_\mu = \frac{R}{\lambda - R} \quad \text{where} \quad R = \omega_a/\omega_p \quad \text{and} \quad \lambda = \mu_\mu/\mu_p \,. \tag{29}$$

The quantity λ shows up because the value of the muon mass m_μ is needed, and also because the B field measurement involves the proton mass m_p. Here the precision experiments on the microwave spectrum of ground state muonium $(\mu^+ e^-)$ [98] performed at LAMPF at Los Alamos provide the needed result. The measurements in combination with the theoretical prediction of the Muonium hyperfine splitting $\Delta\nu$ [99,100] (and references therein), allowed to extract the precise value

$$\lambda = \mu_\mu/\mu_p = 3.183\,345\,39(10)\ [30\ \text{ppb}] \,, \tag{30}$$

which is used by the E821 experiment to determine a_μ via Eq. (29).

Since the spin precession frequency can be measured very well, the precision at which $g-2$ can be measured is essentially determined by the possibility to manufacture a constant homogeneous magnetic field $\vec{B}$ and to determine its value very precisely. Important but easier to achieve is the tuning to the magic energy. Possible deviations may be corrected by adjusting the effective magnetic field appropriately.

Note that one of the reasons why the relativistic motion of the muons is so well understood is the fact that the orbital motion of charged particles in the storage ring may be investigated separately from the spin motion. The forces associated with the anomalous magnetic moment are very weak ($a_\mu \approx 1.16 \times 10^{-3}$) in comparison to the forces of the charge of the particle determining the orbital motion. While the static magnetic field $\vec{B}(r,z) = (0,0,B_0)$ causes the particles to move on a circle of radius $r_0 = \gamma m/(eB_0)$ the electric quadrupole field $\vec{E} = (E_r, E_\theta, E_z) = (\kappa x, 0, -\kappa z)$, (which produces a restoring force in the vertical direction and a repulsive force in the radial direction) leads to a superimposed oscillatory motion

$$x = A\, \cos(\sqrt{1-n}\,\omega_c\, t) \,,\ z = B\, \cos(\sqrt{n}\,\omega_c\, t) \,, \tag{31}$$

of the muons about the central beam (assumed to move along the y-axis) position. Here, $x = r - r_0$, κ a positive constant and $n = \frac{\kappa r_0}{\beta B_0}$ with $\beta = v$ is the field index. This motion is called *betatron oscillation*. The amplitudes depend on the initial condition of the particle trajectory. The betatron frequencies are $\omega_{y\mathrm{BO}} = \sqrt{n}\,\omega_c$ and $\omega_{x\mathrm{BO}} = \sqrt{1-n}\,\omega_c$ where $\omega_c = v/r_0$ is the cyclotron frequency.

The betatron motion also affects the anomalous magnetic precession Eq. (24), which holds for transversal magnetic field $\vec{v}\cdot\vec{B} = 0$. The latter, due to electrostatic focusing, is not accurately satisfied such that the more general formula

$$\vec{\omega}_a = -\frac{e}{m_\mu}\left\{a_\mu\,\vec{B} - a_\mu\,\left(\frac{\gamma}{\gamma+1}\right)\,(\vec{v}\cdot\vec{B})\,\vec{v} + \left(a_\mu - \frac{1}{\gamma^2-1}\right)\,\vec{E}\times\vec{v}\right\}, \tag{32}$$

has to be used as a starting point. Expanding about $\vec{v}\cdot\vec{B} = 0$ at the magic energy yields the *Pitch Correction* which for the BNL experiment amount to $C_P \simeq 0.3$ ppm. Similarly, the deviation from the magic energy (beam spread) requires a *Radial Electric Field Correction*, for the BNL experiment typically $C_E \simeq 0.5$ ppm. For more details on the machine and the basics of the beam dynamics we refer to [43,46].

A possible correction of the magnetic precession could be due to an electric dipole moment of the muon. If a large enough EDM

$$\vec{d}_e = \frac{\eta\,e}{2m_\mu}\vec{S} \tag{33}$$

would exist, where η is the dimensionless constant equivalent of magnetic moment g-factors, the applied electric field $\vec{E}$ (which is vanishing at the equilibrium beam position) and the motional electric field induced in the muon rest frame $\vec{E}^* = \gamma\,\vec{\beta}\times\vec{B}$ would add an extra precession of the spin with a component along $\vec{E}$ and one about an axis perpendicular to $\vec{B}$:

$$\vec{\omega}_a = \vec{\omega}_{a0} + \vec{\omega}_{\mathrm{EDM}} = \vec{\omega}_{a0} - \frac{\eta\,e}{2m_\mu}\,\left(\vec{E} + \vec{\beta}\times\vec{B}\right) \tag{34}$$

where $\vec{\omega}_{a0}$ denotes the would-be precession frequency for $\eta = 0$. The shift caused by a non-vanishing η is

$$\Delta\vec{\omega}_a = -2d_\mu\,\left(\vec{\beta}\times\vec{B}\right) - 2d_\mu\,\vec{E}$$

which, for $\beta \sim 1$ and $d_\mu\,\vec{E} \sim 0$, yields

$$\omega_a = B\,\sqrt{\left(\frac{e}{m_\mu}\,a_\mu\right)^2 + (2d_\mu)^2}\,. \tag{35}$$

The result is that the plane of precession in no longer horizontal but tilted at an angle

$$\delta \equiv \arctan\frac{\omega_{\mathrm{EDM}}}{\omega_{a0}} = \arctan\frac{\eta\,\beta}{2a_\mu} \simeq \frac{\eta}{2a_\mu} \tag{36}$$

and the precession frequency is increased by a factor

$$\omega_a = \omega_{a0}\,\sqrt{1+\delta^2}\,. \tag{37}$$

The tilt gives rise to an oscillating vertical component of the muon polarization and may be detected by recording separately the electrons which strike the counters above and below the mid–plane of the ring. This measurement has been performed in the last CERN experiment on $g-2$. The result $d_\mu = (3.7 \pm 3.4)\times 10^{-19}\,e\cdot\mathrm{cm}$ showed that it is negligibly small. The present experimental bound is $d_\mu < 2.7\times 10^{-19}\,e\cdot\mathrm{cm}$ while the SM estimate is $d_\mu \sim 3.2\times 10^{-25}\,e\cdot\mathrm{cm}$. One thus may safely assume d_μ to be too small to be able to affect the extraction of a_μ.

Table 1
Summary of CERN and E821 Results.

Experiment	Year	Polarity	$a_\mu \times 10^{10}$	Pre. [ppm]	Ref.
CERN I	1961	μ^+	11 450 000(220000)	4300	[101]
CERN II	1962-1968	μ^+	11 661 600(3100)	270	[102]
CERN III	1974-1976	μ^+	11 659 100(110)	10	[91]
CERN III	1975-1976	μ^-	11 659 360(120)	10	[91]
BNL	1997	μ^+	11 659 251(150)	13	[12]
BNL	1998	μ^+	11 659 191(59)	5	[13]
BNL	1999	μ^+	11 659 202(15)	1.3	[14]
BNL	2000	μ^+	11 659 204(9)	0.73	[15]
BNL	2001	μ^-	11 659 214(9)	0.72	[16]
	Average		11 659 208.0(6.3)	0.54	[92]

2.2. *Summary of Experimental Results*

Before the E821 experiment at Brookhaven presented their results in the years from 2001 to 2004, the last of a series of measurements of the anomalous g-factor at CERN was published about 30 years ago. At that time a_μ had been measured for muons of both charges in the Muon Storage Ring at CERN. The two results,

$$\begin{aligned} a_{\mu^-} &= 1165937(12) \times 10^{-9} \,, \\ a_{\mu^+} &= 1165911(11) \times 10^{-9} \,, \end{aligned} \tag{38}$$

are in good agreement with each other, and combine to give a mean

$$a_\mu = 1165924.0(8.5) \times 10^{-9} \quad [7 \text{ ppm}] \,, \tag{39}$$

which was very close to the theoretical prediction $1165921.0(8.3) \times 10^{-9}$ at that time. The measurements thus confirmed the remarkable QED calculation as well as a substantial hadronic photon vacuum polarization contribution, and served as a precise verification of the CPT theorem for muons. Measured in the experiments is the ratio of the muon precession frequency $\omega_a = \omega_s - \omega_c$ and the proton precession frequency from the magnetic field calibration ω_p: $R = \omega_a/\omega_p$ which together with the ratio of the magnetic moment of the muon to the one of the proton $\lambda = \mu_\mu/\mu_p$ determines the anomalous magnetic moment via Eq. (29). The CERN determination of a_μ was based on the value $\lambda = 3.1833437(23)$.

The BNL muon $g-2$ experiment has been able to improve and perfect the method of the last CERN experiments in several respects and was able to achieve an impressive 14–fold improvement in precision. The measurements are $R_{\mu^-} = 0.0037072083(26)$ and $R_{\mu^+} = 0.0037072048(25)$ the difference being $\Delta R = (3.5 \pm 3.4) \times 10^{-9}$. Together with $\lambda = 3.18334539(10)$ [103,104] one obtains the new values

$$\begin{aligned} a_{\mu^-} &= 11659214(8)(3) \times 10^{-10} \,, \\ a_{\mu^+} &= 11659204(7)(5) \times 10^{-10} \,. \end{aligned} \tag{40}$$

Assuming CPT symmetry, as valid in any QFT, and taking into account correlations between systematic errors between the various data sets, the new average $R = 0.0037072063(20)$ was obtained. The new average value is then given by [92]

$$a_\mu = 11659208.0(5.4)(3.3)[6.3] \times 10^{-10} \quad [0.54 \text{ ppm}] \,. \tag{41}$$

The two uncertainties given are the statistical and the systematic ones. The total error in square brackets follows by adding in quadrature the statistical and systematic errors. In Table 1 all results from CERN and E821 are collected. The new average is completely dominated by the BNL results. The individual

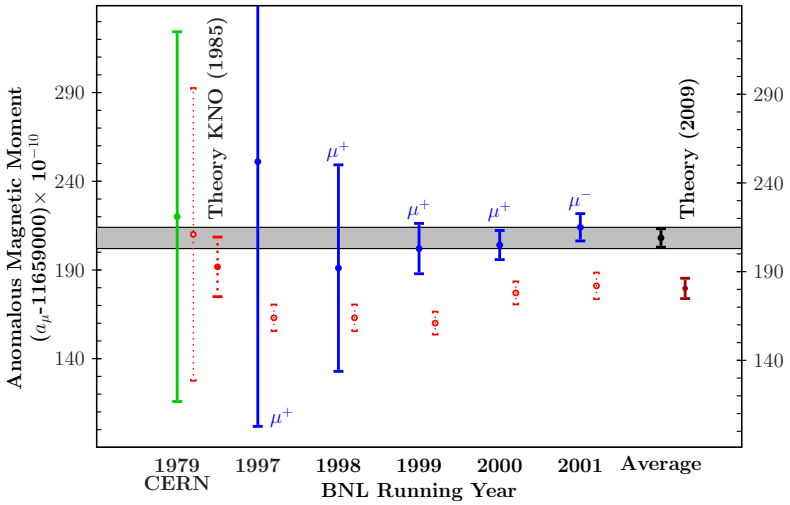

Fig. 7. Results for the individual E821 measurements, together with the new world average and the theoretical prediction. The CERN result is shown together with the theoretical prediction by Kinoshita et al. 1985, at about the time when the E821 project was proposed.The dotted vertical bars indicate the theory values quoted by the experiments.

measurements are shown also in Fig. 7. The comparison with the theoretical result including predictions from SM extensions will be discussed later in Sect. 7. In the following sections we first review the SM prediction of a_μ.

3. QED Prediction of $g-2$

Any precise theoretical prediction requires a precise knowledge of the fundamental parameters. In QED these are the fine structure constant α and the lepton masses. As the leading order result is $\frac{\alpha}{2\pi}$ and since we want to determine a_ℓ with very high precision, the most important basic parameter for calculating a_μ is the fine structure constant. Its most precise value is determined using of the electron anomalous magnetic moment

$$a_e^{\rm exp} = 0.001\,159\,652\,180\,73(28)[0.24\,{\rm ppb}]\ , \tag{42}$$

which very recently [105,106] has been obtained with extreme precision. Confronting the experimental value with the theoretical prediction as a series in α (see Sect. 3.2 below) determines [107,108,106]

$$\alpha^{-1}(a_e) = 137.035999084(51)[0.37\,{\rm ppb}]\ . \tag{43}$$

This new value has an uncertainty 20 times smaller than any preceding independent determination of α and we will use it throughout in the calculation of a_μ.

Starting at 2–loops, higher order corrections include contributions from lepton loops in which different leptons can circulate and results depend on the corresponding mass ratios. Whenever needed, we will use the following values for the muon–electron and muon–tau mass ratios, and lepton masses [37,38,103,104]

$$\begin{gathered} m_\mu/m_e = 206.768\,2838\,(54)\ ,\ m_\mu/m_\tau = 0.059\,4592\,(97)\ , \\ m_e = 0.510\,9989\,918(44){\rm MeV}\ ,\ m_\mu = 105.658\,3692\,(94){\rm MeV}\ ,\ m_\tau = 1776.99\,(29){\rm MeV}\ . \end{gathered} \tag{44}$$

The primary determination of the electron and muon masses come from measuring the ratio with respect to the mass of a nucleus and the masses are obtained in atomic mass units (amu). Therefore the ratios are known more precisely, than the numbers we get by inserting lepton masses given in MeV. In fact, the conversion factor to MeV is more uncertain than the mass of the electron and muon in amu.

Note that the mass–dependent contributions in fact differ for a_e, a_μ and a_τ, such that lepton universality is broken: $a_e \neq a_\mu \neq a_\tau$.

More SM parameters will be needed for the evaluation of weak and hadronic contributions. We have collected them in Appendix A together with known polylogarithmic functions needed for the representation of analytic results of the QED calculations.

Until recently the electron anomaly a_e and, until before the advent of the Brookhaven muon $g-2$ measurements, also a_μ were considered to provide the most clean and precise tests of QED. In fact the by far largest contribution to the anomalous magnetic moment is of pure QED origin, and with the new determination of a_e by the Harvard electron $g-2$ experiment [105,106] a_e together with its QED prediction [108] allows for the most precise determination of the electromagnetic fine structure constant. The dominance of just one type of interaction in the electromagnetic vertex of the leptons, historically, was very important for the development of QFT and QED, as it allowed to test QED as a model theory under simple unambiguous conditions. How important such experimental tests were we may learn from the fact that it took about 20 years from the invention of QED (Dirac 1928 [$g_e = 2$]) until the first reliable results could be established (Schwinger 1948 [$a_e^{(2)} = \alpha/2\pi$]) after a covariant formulation and renormalization was understood and settled in its main aspects.

When the precision of experiments improved, the QED part by itself became a big challenge for theorists, because higher order corrections are sizable, and as the order of perturbation theory increases, the complexity of the calculations grows dramatically. Thus experimental tests were able to check QED up to 7 digits in the prediction which requires to evaluate the perturbation expansion up to 5 terms (5 loops). The anomalous magnetic moment as a dimensionless quantity exhibits contributions which are just numbers expanded in powers of α, what one would get in QED with just one species of leptons, and contributions depending on the mass ratios if different leptons come into play. Thus taking into account all three leptons we obtain functions of the ratios of the lepton masses m_e, m_μ and m_τ. Considering a_μ, we can cast it into the following form [109,24]

$$a_\mu^{\rm QED} = A_1 + A_2(m_\mu/m_e) + A_2(m_\mu/m_\tau) + A_3(m_\mu/m_e, m_\mu/m_\tau)\ . \tag{45}$$

Here A_1 denotes the universal term common for all leptons. Also closed fermion loops contribute to this term provided the fermion is the muon (=external lepton). The term A_2 depends on one scale and gets contributions from diagrams with closed fermion loops where the fermion differs from the external one. Such contributions start at the two loop level: for the muon as the external lepton we have two possibilities: an additional electron–loop (light–in–heavy) $A_2(m_\mu/m_e)$ or an additional τ–loop (heavy–in–light) $A_2(m_\mu/m_\tau)$ two contributions of quite different character. The first produces large logarithms $\propto \ln(m_\mu/m_e)^2$ and accordingly large effects while the second, because of the *decoupling* of heavy particles in QED like theories [6], produces only small effects of order $\propto (m_\mu/m_\tau)^2$. The two–scale contribution requires a light as well as a heavy extra loop and hence starts at three loop order. We will discuss the different types of contributions in the following. Each of the terms is given in renormalized perturbation theory by an appropriate expansion in α:

$$\begin{aligned}
A_1 &= A_1^{(2)}\left(\frac{\alpha}{\pi}\right) + A_1^{(4)}\left(\frac{\alpha}{\pi}\right)^2 + A_1^{(6)}\left(\frac{\alpha}{\pi}\right)^3 + A_1^{(8)}\left(\frac{\alpha}{\pi}\right)^4 + A_1^{(10)}\left(\frac{\alpha}{\pi}\right)^5 + \cdots \\
A_2 &= \qquad\qquad A_2^{(4)}\left(\frac{\alpha}{\pi}\right)^2 + A_2^{(6)}\left(\frac{\alpha}{\pi}\right)^3 + A_2^{(8)}\left(\frac{\alpha}{\pi}\right)^4 + A_2^{(10)}\left(\frac{\alpha}{\pi}\right)^5 + \cdots \\
A_3 &= \qquad\qquad\qquad\qquad A_3^{(6)}\left(\frac{\alpha}{\pi}\right)^3 + A_3^{(8)}\left(\frac{\alpha}{\pi}\right)^4 + A_3^{(10)}\left(\frac{\alpha}{\pi}\right)^5 + \cdots
\end{aligned}$$

[6] The Appelquist-Carrazone decoupling–theorem [110] infers that in theories like QED or QCD, where couplings and masses are independent parameters of the Lagrangian, a heavy particle of mass M decouples from physics at lower scales E_0 as E_0/M for $M \to \infty$.

and later we will denote by

$$C_L = \sum_{k=1}^{3} A_k^{(2L)} \ , \tag{46}$$

the total L–loop coefficient of the $(\alpha/\pi)^L$ term. The present precision of the experimental result [16,92]

$$\delta a_\mu^{\rm exp} = 63 \times 10^{-11} \ , \tag{47}$$

as well as the future prospects of possible improvements [111], which are expected to be able to reach

$$\delta a_\mu^{\rm fin} \sim 10 \times 10^{-11} \ , \tag{48}$$

determine the precision at which we need the theoretical prediction. For the n–loop coefficients multiplying $(\alpha/\pi)^n$ the error Eq. (48) translates into the required accuracies: $\delta C_1 \sim 4 \times 10^{-8}$, $\delta C_2 \sim 1 \times 10^{-5}$, $\delta C_3 \sim 7 \times 10^{-3}$, $\delta C_4 \sim 3$ and $\delta C_5 \sim 1 \times 10^3$. To match the current accuracy one has to multiply all estimates with a factor 6, which is the experimental error in units of 10^{-10}.

3.1. *Universal Contributions*

• According to Eq. (70) the leading order contribution Fig. 8 may be written in the form (see below)

$$a_\ell^{(2)\ {\rm QED}} = \frac{\alpha}{\pi} \int_0^1 {\rm d}x \, (1-x) \ = \ \frac{\alpha}{\pi} \, \frac{1}{2} \ , \tag{49}$$

which is trivial to evaluate. This is the famous result of Schwinger from 1948 [52].

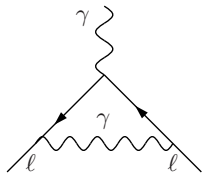

Fig. 8. The universal lowest order QED contribution to a_ℓ.

• At two loops in QED there are the 9 diagrams shown in Fig. 9 which contribute to a_μ. The first 6 diagrams, which have attached two virtual photons to the external muon string of lines contribute to the universal term. They form a gauge invariant subset of diagrams and yield the result

$$A_{1\ [1-6]}^{(4)} = -\frac{279}{144} + \frac{5\pi^2}{12} - \frac{\pi^2}{2} \ln 2 + \frac{3}{4} \zeta(3) \ .$$

The last 3 diagrams include photon *vacuum polarization* (vap / VP) due to the lepton loops. The one with the muon loop is also universal in the sense that it contributes to the mass independent correction

$$A_{1\ {\rm vap}}^{(4)}(m_\mu/m_\ell = 1) = \frac{119}{36} - \frac{\pi^2}{3} \ .$$

The complete "universal" part yields the coefficient $A_1^{(4)}$ calculated first by Petermann [112] and by Sommerfield [113] in 1957:

$$A_{1\ {\rm uni}}^{(4)} = \frac{197}{144} + \frac{\pi^2}{12} - \frac{\pi^2}{2} \ln 2 + \frac{3}{4} \zeta(3) = -0.328\ 478\ 965\ 579\ 193\ 78... \tag{50}$$

where $\zeta(n)$ is the Riemann ζ–function of argument n (see also [114]).

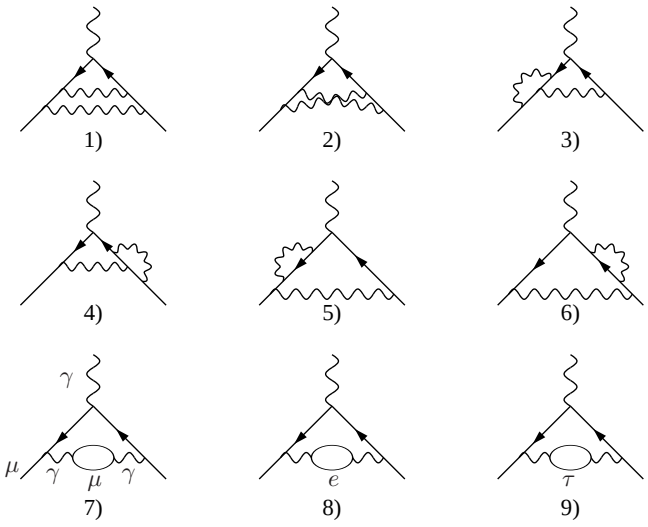

Fig. 9. Diagrams 1-7 represent the universal second order contribution to a_μ, diagram 8 yields the "light", diagram 9 the "heavy" mass dependent corrections.

• At three loops in QED there are the 72 diagrams shown in Fig. 10 contributing to $g-2$ of the muon. In closed fermion loops any of the SM fermions may circulate. The gauge invariant subset of 72 diagrams where all closed fermion loops are muon–loops yield the universal one–flavor QED contribution $A_{1\,\mathrm{uni}}^{(6)}$. This set has been calculated analytically mainly by Remiddi and his collaborators [115], and Laporta and Remiddi obtained the final result in 1996 after finding a trick to calculate the non–planar "triple cross" topology diagram 25) of Fig. 10 [116] (see also [117]). The result turned out to be surprisingly compact and reads

$$A_{1\,\mathrm{uni}}^{(6)} = \frac{28259}{5184} + \frac{17101}{810}\pi^2 - \frac{298}{9}\pi^2\ln 2 + \frac{139}{18}\zeta(3) + \frac{100}{3}\left\{\mathrm{Li}_4(\frac{1}{2}) + \frac{1}{24}\ln^4 2 - \frac{1}{24}\pi^2\ln^2 2\right\}$$
$$-\frac{239}{2160}\pi^4 + \frac{83}{72}\pi^2\zeta(3) - \frac{215}{24}\zeta(5) = 1.181\,241\,456\,587\ldots \qquad (51)$$

This famous analytical result largely confirmed an earlier numerical calculation by Kinoshita [117]. The constants needed for the evaluation of Eq. (51) are given in Eqs. (A.13) and (A.14).

The big advantage of the analytic result is that it allows a numerical evaluation at any desired precision. The direct numerical evaluation of the multidimensional Feynman integrals by Monte Carlo methods is always of limited precision and an improvement is always very expensive in computing power.

• At four loops there are 891 diagrams [373 have closed lepton loops (see Fig. 11), 518 without fermion loops=gauge invariant set Group V (see Fig. 12)] with common fermion lines. Their contribution has been calculated by numerical methods by Kinoshita and collaborators. The calculation of the 4–loop contribution to a_μ is a formidable task. Since the individual diagrams are much more complicated than the 3–loop ones, only a few have been calculated analytically so far [118]–[120]. In most cases one has to resort to numerical calculations. This approach has been developed and perfected over the past 25 years by Kinoshita and his collaborators [121]–[125] with the very recent recalculations and improvements [108,126,39]. As a result of the enduring heroic effort an improved answer has been obtained recently by Aoyama, Hayakawa, Kinoshita and Nio [108] who find

$$A_1^{(8)} = -1.9144(35) \qquad (52)$$

where the error is due to the Monte Carlo integration. This very recent result is correcting the one published before in [127] and shifting the coefficient of the $\left(\frac{\alpha}{\pi}\right)^4$ term by – 0.19 (10%). Some error in the cancellation of IR singular terms was found in calculating diagrams M_{18} ($-0.2207(210)$) and M_{16} ($+0.0274(235)$) in the

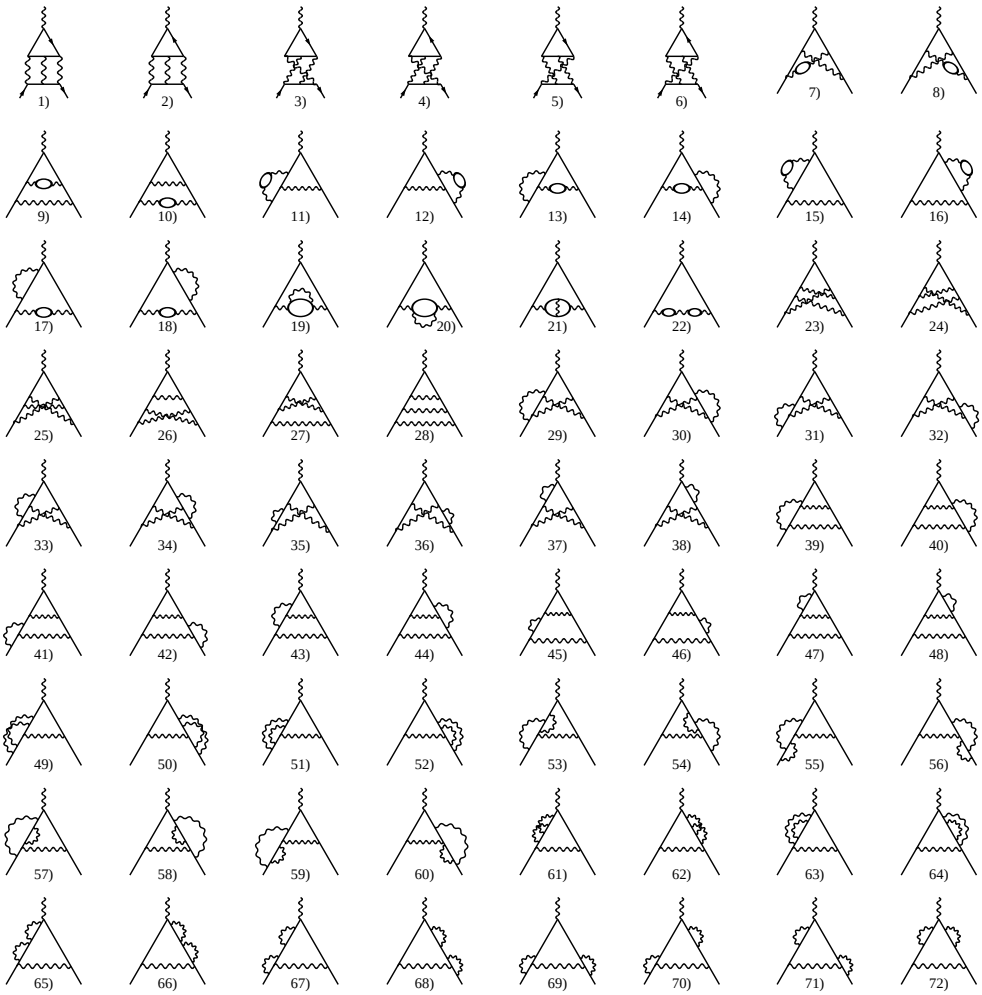

Fig. 10. The universal third order contribution to a_μ. All fermion loops here are muon–loops. Graphs 1) to 6) are the light–by—light scattering diagrams. Graphs 7) to 22) include photon vacuum polarization insertions. All non–universal contributions follow by replacing at least one muon in a closed loop by some other fermion.

set of diagrams Fig. 12. The latter 518 diagrams without fermion loops also are responsible for the largest part of the uncertainty in Eq. (52). Note that the universal $O(\alpha^4)$ contribution is sizable, about 6 standard deviations at current experimental accuracy, and a precise knowledge of this term is absolutely crucial for the comparison between theory and experiment.

• The universal 5–loop QED contribution is still largely unknown. Using the recipe proposed in Ref. [37], one obtains the following bound

$$A_1^{(10)} = 0.0(4.6)\ , \tag{53}$$

for the universal part as an estimate for the missing higher order terms.

As a result the universal QED contribution may be written as

$$a_\ell^{\rm uni} = 0.5\ \left(\frac{\alpha}{\pi}\right) - 0.328\,478\,965\,579\,193\,78\ldots\ \left(\frac{\alpha}{\pi}\right)^2 + 1.181\,241\,456\,587\ldots\ \left(\frac{\alpha}{\pi}\right)^3 - 1.9144(35)\ \left(\frac{\alpha}{\pi}\right)^4 + 0.0(4.6)\ \left(\frac{\alpha}{\pi}\right)^5$$

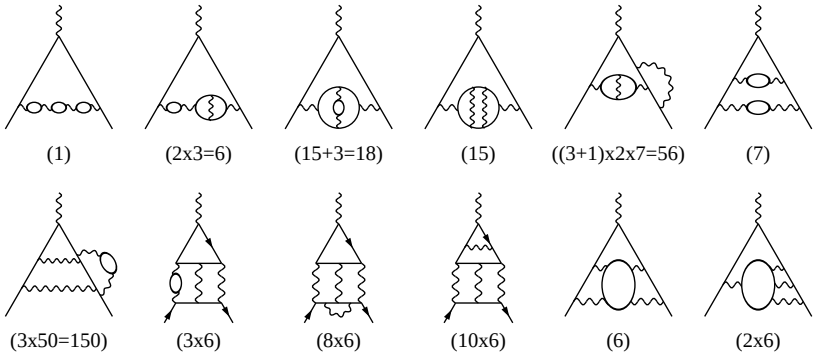

Fig. 11. Some typical eight order contributions to a_ℓ involving lepton loops. In brackets the number of diagrams of a given type if only muon loops are considered. The latter contribute to the universal part.

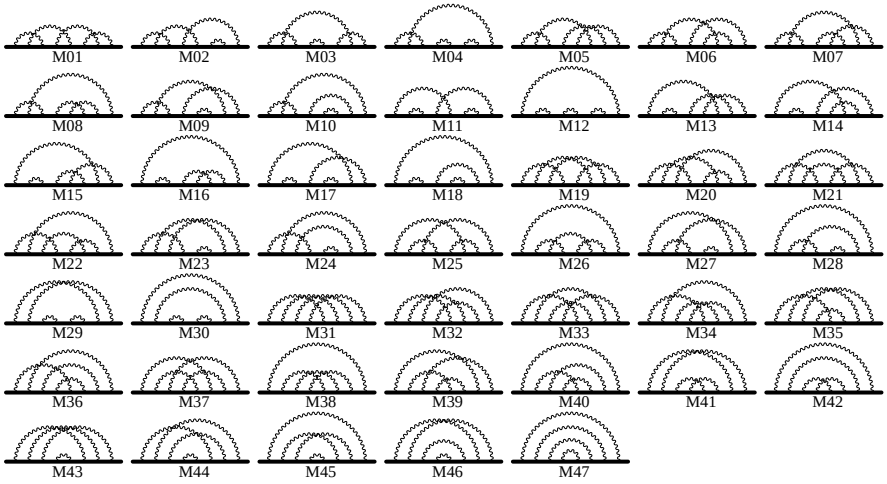

Fig. 12. 4-loop Group V diagrams. 47 self-energy-like diagrams of $M_{01} - M_{47}$ represent 518 vertex diagrams [by inserting the external photon vertex on the virtual muon lines in all possible ways]. Reprinted with permission from [108]. Copyright (2007) by the American Physical Society].

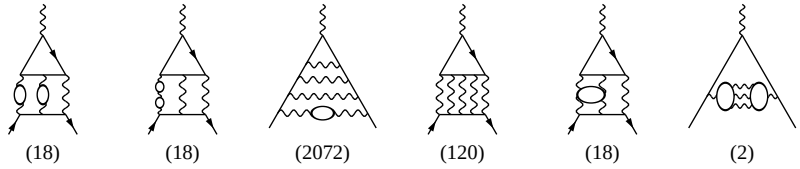

Fig. 13. Typical tenth order contributions to a_ℓ including fermion loops. In brackets the number of diagrams of the given type.

$$= 0.001\,159\,652\,176\,30(43)(10)(31)[54]\cdots \tag{54}$$

The three errors given are: the error from the uncertainty in α, given in Eq. (43), the numerical uncertainty of the α^4 coefficient and the error estimated for the missing higher order terms.

As we already know, the anomalous magnetic moment of a lepton is an effect of about 0.12%, $g_\ell/2 \simeq 1.00116\cdots$. It is remarkable that in spite of the fact that this observable is so small we know a_e and a_μ more precisely than most other precision observables. Note that the first term $a_\ell^{(2)} \simeq 0.00116141\cdots$ contributes the first three significant digits of the full result.

3.2. *Electron Anomalous Magnetic Moment and the Fine Structure Constant*

The universal terms given in Eq. (54) essentially determine the anomalous magnetic moment of the electron a_e and therefore allow a precise determination of the fine structure constant from the experimentally measured value for a_e by inverting the series in α. This is due to the fact that the effects from heavy leptons (muon, tau) in QED, from hadrons, the electroweak sector and potential new physics decouple as $(m_e/M)^2$, where M is some heavy lepton mass or a hadronic, weak or new physics scale.

The electron magnetic moment anomaly likely is the experimentally most precisely known quantity. Since recently, a new substantially improved result for a_e is available. It was obtained by Gabrielse et al. [105,106] in an experiment at Harvard University using a one–electron quantum cyclotron. The new results from 2006 and 2008 read

$$\begin{aligned} a_e^{\rm exp} &= 1.159\,652\,180\,85(76) \times 10^{-3}\,[.66\ {\rm ppb}]\,, \\ a_e^{\rm exp} &= 1.159\,652\,180\,73(28) \times 10^{-3}\,[.24\ {\rm ppb}]\,, \end{aligned} \tag{55}$$

the latter with an accuracy 15 times better than the earlier result

$$a_e^{\rm exp} = 1.159\,652\,1883(42) \times 10^{-3}\,[3.62\ {\rm ppb}]\,,$$

obtained by Dehmelt et al. at Washington University in 1987 [128,37]. The new value is shifting down a_e by 1.8 standard deviations.

The measurements of a_e not only played a key role in the history of precision tests of QED in particular, and of QFT concepts in general, today we may use the anomalous magnetic moment of the electron to get the most precise indirect measurement of the fine structure constant α. This possibility of course hangs on our ability to pin down the theoretical prediction with very high accuracy. Indeed a_e is much saver to predict reliably than a_μ. The reason is that non–perturbative hadronic effects as well as the sensitivity to unknown physics beyond the SM are suppressed by the large factor $m_\mu^2/m_e^2 \simeq 42\,753$ in comparison to a_μ. This suppression has to be put into perspective with the 2250 times higher precision with which we know a_e. We thus can say that effectively a_e is a factor 19 less sensitive to model dependent physics than a_μ.

The prediction is given by a perturbation expansion of the form (see also Eqs. (45), (46))

$$a_e^{\rm QED} = \sum_{n=1}^{N} C_n (\alpha/\pi)^n\ , \tag{56}$$

with terms up to five loops, $N = 5$, under consideration. The experimental precision of a_e requires the knowledge of the coefficients with accuracies $\delta C_2 \sim 1 \times 10^{-7}$, $\delta C_3 \sim 6 \times 10^{-5}$, $\delta C_4 \sim 2 \times 10^{-2}$ and $\delta C_5 \sim 10$. For what concerns the universal terms one may conclude by inspecting the convergence of Eq. (54) that one would expect the completely unknown coefficient C_5 to be $O(1)$ and hence negligible at present accuracy. In reality it is one of the main uncertainties, which is already accounted for in Eq. (54). Concerning the mass–dependent contributions, the situation for the electron is quite different from the muon. Since the electron is the lightest of the leptons a potentially large "light internal loop" contribution is absent. For a_e the muon is a heavy particle $m_\mu \gg m_e$ and its contribution is of the type "heavy internal loops" which is suppressed by an extra power of m_e^2/m_μ^2. In fact the μ–loops tend to decouple and therefore only yield small terms. Corrections due to internal μ–loops are suppressed as $O(2(\alpha/\pi)\,(m_e^2/m_\mu^2)) \simeq 1.1 \times 10^{-7}$ relative to the leading term and the τ–loops practically play no role at all. The fact that muons and tau leptons tend to decouple is also crucial for the unknown 5–loop contribution, since we can expect that corresponding contributions can be safely neglected.

The result may be written in the form

$$a_e^{\rm QED} = a_e^{\rm uni} + a_e(\mu) + a_e(\tau) + a_e(\mu,\tau)\ , \tag{57}$$

with the universal term given by Eq. (54) and

$$a_e(\mu) = 5.197\,386\,70(27) \times 10^{-7}\Big(\frac{\alpha}{\pi}\Big)^2 - 7.373\,941\,65(29) \times 10^{-6}\Big(\frac{\alpha}{\pi}\Big)^3 ,$$
$$a_e(\tau) = 1.83763(60) \times 10^{-9}\Big(\frac{\alpha}{\pi}\Big)^2 - 6.5819(19) \times 10^{-8}\Big(\frac{\alpha}{\pi}\Big)^3 ,$$
$$a_e(\mu,\tau) = 0.190945(62) \times 10^{-12}\Big(\frac{\alpha}{\pi}\Big)^3 .$$

As a result the perturbative expansion for the QED prediction of a_e is given by

$$a_e^{\rm QED} = \frac{\alpha}{2\pi} - 0.328\,478\,444\,002\,90(60)\left(\frac{\alpha}{\pi}\right)^2 + 1.181\,234\,016\,827(19)\left(\frac{\alpha}{\pi}\right)^3 - 1.9144(35)\left(\frac{\alpha}{\pi}\right)^4 + 0.0(4.6)\left(\frac{\alpha}{\pi}\right)^5 . \tag{58}$$

As mentioned before, the completely unknown universal 5–loop term $C_5 \simeq A_1^{(10)}$ has been estimated to be bounded by the last term. The missing 5–loop result represents the largest uncertainty in the prediction of a_e.

What is missing are the hadronic and weak contributions, which both are suppressed by the $(m_e/m_\mu)^2$ factor relative to a_μ. For a_e they are small [7] : $a_e^{\rm had} = 1.676(18)\times 10^{-12}$ and $a_e^{\rm weak} = 0.039\times 10^{-12}$, respectively (see the discussion of the corresponding contributions to a_μ and Sect. 6.3 below). The hadronic contribution now just starts to be significant, however, unlike in $a_\mu^{\rm had}$ for the muon, $a_e^{\rm had}$ is known with sufficient accuracy and is not the limiting factor here. The theory error is dominated by the missing 5–loop QED term. As a consequence a_e at this level of accuracy is theoretically well under control (almost a pure QED object) and therefore is an excellent observable for extracting α based on the SM prediction

$$a_e^{\rm SM} = a_e^{\rm QED}[\text{Eq. (58)}] + 1.715(18) \times 10^{-12}\ \text{(hadronic \& weak)} . \tag{59}$$

When we compare this result with the very recent extremely precise measurement of the electron anomalous magnetic moment [106] given by Eq. (42) we obtain

$$\alpha^{-1}(a_e) = 137.035999084(33)(12)(37)(2)[51] ,$$

which is the value Eq. (43) [106] given earlier. The first error is the experimental one of $a_e^{\rm exp}$, the second and third are the numerical uncertainties of the α^4 and α^5 terms, respectively. The last one is the hadronic uncertainty, which is completely negligible. The recent correction of the $O(\alpha^4)$ coefficient Eq. (52) (from $-1.7283(35)$ to $-1.9144(35)$) lead to a 7 σ shift in $\alpha(a_e)$. This is the most precise determination of α at present and we will use it for calculating a_μ.

Of course we still may use a_e for a precision test of QED. For a theoretical prediction of a_e we then have to adopt the best determinations of α which do not depend on a_e. They are [129,130]

$$\alpha^{-1}({\rm Cs}) = 137.03600000(110)[8.0\,{\rm ppb}] , \tag{60}$$
$$\alpha^{-1}({\rm Rb}) = 137.03599884(091)[6.7\,{\rm ppb}] , \tag{61}$$

and have been determined by atomic interferometry. In terms of $\alpha({\rm Cs})$ one gets $a_e = 0.00115965217299(930)$ which agrees well with the experimental value $a_e^{\rm exp} - a_e^{\rm the} = 7.74(9.30)\times 10^{-12}$; and similarly, using the value $\alpha({\rm Rb})$ the prediction is $a_e = 0.00115965218279(770)$, again in good agreement with experiment $a_e^{\rm exp} - a_e^{\rm the} = -2.06(7.70)\times 10^{-12}$. Errors are completely dominated by the uncertainties in α. The following Table 2 collects the typical contributions to a_e evaluated in terms of Eqs. (60,61).
Obviously an improvement of non–a_e determinations of α by a factor 20 would allow a much more stringent test of QED, and therefore would be very important. At present, assuming that $\left|\Delta a_e^{\text{New Physics}}\right| \simeq m_e^2/\Lambda^2$ where Λ approximates the scale of "New Physics", the agreement between $\alpha^{-1}(a_e)$ and $\alpha^{-1}({\rm Rb06})$ probes

[7] The total hadronic contribution to a_e is given by $a_e^{(4)}(\text{vap, had}) + a_e^{(6)}(\text{vap, had}) + a_e(\text{LbL, had}) \sim (1.860 \pm 0.015 - 0.223 \mp 0.002 + 0.039 \pm 0.013) \times 10^{-12}$ (see below).

Table 2
Contributions to $a_e(h/M)$ in units 10^{-6}. The three errors given in the universal contribution come from the experimental uncertainty in α, from the α^4 term and from the α^5 term, respectively.

contribution	$\alpha(h/M_{\rm Cs})$	$\alpha(h/M_{\rm Rb})$
universal	1159.652 16856(929)(10)(31)	1159.652 17836(769)(10)(31)
μ–loops	0.000 00271 (0)	0.000 00271 (0)
τ–loops	0.000 00001 (0)	0.000 00001 (0)
hadronic	0.000 00168 (2)	0.000 00168 (2)
weak	0.000 000039 (0)	0.000 000039 (0)
theory	1159.652 17299(930)	1159.652 18279(770)
experiment	1159.652 180 73 (28)	1159.652 180 73 (28)

the scale $\Lambda \lesssim O(250\ \text{GeV})$. To access the much more interesting range of $\Lambda \sim O(1\ \text{TeV})$ would also require a reliable estimate of the first significant digit of the 5–loop QED contribution, and an improved calculation of the 4–loop QED contribution to $a_e^{\rm SM}$.

3.3. *Mass Dependent Contributions*

Since fermions, as demanded by the SM [8], only interact via photons or other spin one gauge bosons, mass dependent corrections at first show up at the 2–loop level via photon vacuum polarization effects. At three loops light–by–light scattering loops show up, etc. As all fermions have different masses, the fermion-loops give rise to mass dependent effects, which were calculated at two loops in [131,132] (see also [133]–[137]), at three loops in [138]–[145], and at four loops in [118]–[120],[126]. For five loops only partial estimates exist [119,120],[146]–[151].

The leading mass dependent effects come from photon vacuum polarization, which leads to charge screening. Including a factor e^2 and considering the renormalized photon propagator (wave function renormalization factor Z_γ) we have

$$\mathrm{i}\, e^2\, D_\gamma^{'\mu\nu}(q) = \frac{-\mathrm{i}g^{\mu\nu}\, e^2\, Z_\gamma}{q^2\, \left(1+\Pi'_\gamma(q^2)\right)} + \text{ gauge terms } , \tag{62}$$

which in effect means that the charge has to be replaced by an energy-momentum scale dependent *running charge*

$$e^2 \to e^2(q^2) = \frac{e^2 Z_\gamma}{1+\Pi'_\gamma(q^2)} = \frac{e^2}{1+(\Pi'_\gamma(q^2)-\Pi'_\gamma(0))} , \tag{63}$$

where Z_γ is fixed to obtain the classical charge in the Thomson limit $q^2 \to 0$. In perturbation theory the lowest order diagram which contributes to $\Pi'_\gamma(q^2)$ is

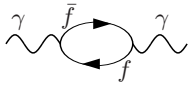

$$:= \quad -(q^2\, g^{\mu\nu} - q^\mu q^\nu)\, \Pi'_\gamma(q^2)$$

and describes the virtual creation and re-absorption of fermion pairs $\gamma^* \to e^+e^-, \mu^+\mu^-, \tau^+\tau^-, u\bar{u}, d\bar{d}, \cdots$(had) $\to \gamma^*$. The photon self–energy function may also be defined by the time-ordered correlator of two electromagnetic currents as

[8] Interactions are known to derive from a local gauge symmetry principle, which implies the structure of gauge couplings, which must be of vector (V) or axial–vector (A) type.

$$\mathrm{i}\,e^2 \int \mathrm{d}^4x\, \mathrm{e}^{\mathrm{i}qx} \langle 0|T j^\mu_{\rm em}(x) j^\nu_{\rm em}(0)|0\rangle = -(q^2\, g^{\mu\nu} - q^\mu q^\nu)\, \Pi'_\gamma(q^2)\ , \tag{64}$$

which is purely transversal by virtue of electromagnetic current conservation $\partial_\mu j^\mu_{\rm em}(x) = 0$.

In terms of the fine structure constant $\alpha = \frac{e^2}{4\pi}$ Eq. (63) reads

$$\alpha(q^2) = \frac{\alpha}{1 - \Delta\alpha(q^2)} \quad ; \quad \Delta\alpha(q^2) = -\mathrm{Re}\, \left(\Pi'_\gamma(q^2) - \Pi'_\gamma(0)\right)\ . \tag{65}$$

The various contributions to the shift in the fine structure constant come from the leptons (lep = e, μ and τ), the 5 light quarks (u, b, s, c, and b) and/or the corresponding hadrons (had). The top quark is too heavy to give a relevant contribution. The hadronic contributions will be considered later.

The renormalized photon self–energy is an analytic function and satisfies the dispersion relation (DR)

$$-\frac{\Pi'_{\gamma\,\rm ren}(k^2)}{k^2} = \int\limits_0^\infty \frac{\mathrm{d}s}{s}\, \frac{1}{\pi} \mathrm{Im}\, \Pi'_\gamma(s)\, \frac{1}{k^2 - s}\ . \tag{66}$$

Note that the only k dependence under the convolution integral shows up in the last factor. Thus, in a generic VP contribution

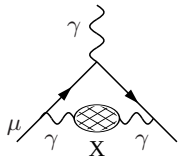

where the "blob" is the full photon propagator, including all kinds of contributions as predicted by the SM or beyond, the free photon propagator in the 1–loop vertex graph in the next higher order is replaced by

$$-\mathrm{i}g_{\mu\nu}/k^2 \to -\mathrm{i}g_{\mu\nu}/(k^2 - s)\ ,$$

which is the exchange of a photon of mass square s. This result then has to be convoluted with the imaginary part of the photon vacuum polarization. The calculation of the contribution from the massive photon proceeds exactly as in the massless case. Again $F_{\rm M}(0)$ most simply may be calculated using the projection method which allows to work at $q^2 = 0$. The result is [152,153]

$$a_\mu^{(2)\,\text{heavy}\,\gamma} \equiv \frac{\alpha}{\pi} K_\mu^{(2)}(s) = \frac{\alpha}{\pi} \int\limits_0^1 \mathrm{d}x\, \frac{x^2\,(1-x)}{x^2 + (s/m_\mu^2)(1-x)}\ , \tag{67}$$

which is the leading order contribution to a_μ from an exchange of a photon with square mass s. For $s = 0$ we get the known Schwinger result. Utilizing this result and Eq. (66), the contribution from the "blob" to $g-2$ reads

$$a_\mu^{(X)} = \frac{\alpha}{\pi^2} \int\limits_0^\infty \frac{\mathrm{d}s}{s}\, \mathrm{Im}\, \Pi_\gamma^{\prime(X)}(s)\, K_\mu^{(2)}(s)\ . \tag{68}$$

If we exchange integrations and evaluating the DR we arrive at [19]

$$\begin{aligned} a_\mu^{(X)} &= \frac{\alpha}{\pi} \int\limits_0^1 \mathrm{d}x\, (1-x) \int\limits_0^\infty \frac{\mathrm{d}s}{s}\, \frac{1}{\pi}\, \mathrm{Im}\, \Pi_\gamma^{\prime(X)}(s)\, \frac{x^2}{x^2 + (s/m_\mu^2)(1-x)} \\ &= \frac{\alpha}{\pi} \int\limits_0^1 \mathrm{d}x\, (1-x)\, \left[-\Pi_\gamma^{\prime(X)}(s_x)\right]\ , \text{ with } \ s_x = -\frac{x^2}{1-x}\, m_\mu^2\ . \end{aligned} \tag{69}$$

The last simple representation in terms of $\Pi_\gamma^{'(X)}(s_x)$ follows using

$$\frac{x^2}{x^2+(s/m_\mu^2)(1-x)} = -s_x\,\frac{1}{s-s_x}\;.$$

Formally, this means that we may replace the free photon propagator by the full transverse propagator in the 1–loop muon vertex [134]:

$$\begin{aligned} a_\mu^{(X),\mathrm{resummed}} &= \frac{\alpha}{\pi}\int\limits_0^1 \mathrm{d}x\,(1-x)\,\left(1-\Pi_{\gamma\,\mathrm{ren}}^{'(X)}(s_x)+(\Pi_{\gamma\,\mathrm{ren}}^{'(X)}(s_x))^2+\cdots\right) \\ &= \frac{\alpha}{\pi}\int\limits_0^1 \mathrm{d}x\,(1-x)\,\left(\frac{1}{1+\Pi_{\gamma\,\mathrm{ren}}^{'(X)}(s_x)}\right)\;. \end{aligned} \tag{70}$$

By Eq. (63) this is equivalent to the contribution of a free photon interacting with dressed charge (effective fine structure constant). However, since $\Pi'_{\gamma\,\mathrm{ren}}(k^2)$ is negative and grows logarithmically with k^2 the full photon propagator develops a so called *Landau pole* where the effective fine structure constant becomes infinite. Thus resumming the perturbation expansion under integrals produces a problem and one better resorts to the order by order approach, by expanding the full propagator into its geometrical progression. In this case Eq. (70) may be considered as a very useful bookkeeping device, collecting effects from different contributions and different orders.

The running of α caused by vacuum polarization effects is controlled by the renormalization group (RG). The latter systematically takes care of the terms enhanced by large short–distance logarithms of the type $\ln m_\mu/m_e$ in the case of a_μ. Since in QED one usually adopts an on shell renormalization scheme the RG for a_μ is actually the Callan-Symanzik (CS) equation [135], which in the limit $m_e \ll m_\mu$, i.e. neglecting power corrections in m_e/m_μ, takes the homogeneous form

$$\left(m_e\frac{\partial}{\partial m_e}+\beta(\alpha)\,\alpha\frac{\partial}{\partial\alpha}\right)\,a_\mu^{(\infty)}\left(\frac{m_\mu}{m_e},\alpha\right)=0\;,$$

where $a_\mu^{(\infty)}(\frac{m_\mu}{m_e},\alpha)$ is the corresponding asymptotic form of a_μ and $\beta(\alpha)$ is the QED β–function. The latter governs the charge screening of the electromagnetic charge. To leading order the charge is running according to

$$\alpha(\mu)=\frac{\alpha}{1-\frac{2}{3}\frac{\alpha}{\pi}\,\ln\frac{\mu}{m_e}}\simeq\alpha\,\left(1+\frac{2}{3}\frac{\alpha}{\pi}\,\ln\frac{\mu}{m_e}+\cdots\right)\;. \tag{71}$$

The solution of the CS equation amounts to replace α by the running fine structure constant $\alpha(m_\mu)$ in $a_\mu^{(\infty)}(\frac{m_\mu}{m_e},\alpha)$, which implies taking into account the leading logs of higher orders. If we replace in the 1–loop result $\alpha\to\alpha(m_\mu)$ we obtain

$$a_\mu=\frac{1}{2}\frac{\alpha}{\pi}\,(1+\frac{2}{3}\frac{\alpha}{\pi}\,\ln\frac{m_\mu}{m_e})\;, \tag{72}$$

which reproduces precisely the leading term of the 2–loop result given below. Since β is known to four loops [136] and also a_μ is known analytically at three loops, it is possible to obtain the important higher leading logs quite easily. For more elaborate RG estimates of contributions to $a_\mu^{(8)}$ and $a_\mu^{(10)}$ we refer to Ref. [119].

3.3.1. *2–loop Vacuum Polarization Insertions*

The leading mass dependent non–universal contribution is due to the last two diagrams of Fig. 9. The coefficient now is a function of the mass m_ℓ of the lepton forming the closed loop. For actually calculating the VP contributions the 1–loop photon vacuum polarization is needed. It is given by

$$\Pi'_{\gamma\,\mathrm{ren}}(q^2) = -\frac{\alpha}{\pi}\int\limits_0^1 \mathrm{d}z\; 2z\,(1-z)\;\ln(1-z\,(1-z)\,q^2/m_\ell^2)$$
$$= \frac{\alpha}{\pi}\int\limits_0^1 \mathrm{d}t\; t^2\,(1-t^2/3)\;\frac{1}{4m_\ell^2/q^2-(1-t^2)}\;, \tag{73}$$

and performing the integral yields

$$\Pi'_{\gamma\,\mathrm{ren}}(q^2) = -\frac{\alpha}{3\pi}\left\{\frac{8}{3}-\beta_\ell^2+\frac{1}{2}\beta_\ell\,(3-\beta_\ell^2)\;\ln\frac{\beta_\ell-1}{\beta_\ell+1}\right\}\;, \tag{74}$$

where $\beta_\ell = \sqrt{1-4m_\ell^2/q^2}$ is the lepton velocity. The imaginary part is given by the simple formula

$$\mathrm{Im}\;\Pi'_\gamma(q^2) = \frac{\alpha}{3}\left(1+\frac{2m_\ell^2}{q^2}\right)\;\beta_\ell\;. \tag{75}$$

For $q^2<0$ the amplitude $\Pi'_{\gamma\,\mathrm{ren}}(q^2)$ is negative definite and what is needed in Eq. (69) is $-\Pi_\gamma^{'(\ell)}(-\frac{x^2}{1-x}\,m_\mu^2)$ or Eq. (74) with $\beta_\ell = \sqrt{1+4\,x_\ell^2\,(1-x)/x^2}$, where $x_\ell = m_\ell/m_\mu$ and m_ℓ is the mass of the virtual lepton in the vacuum polarization subgraph.

Using the representation Eq. (69) together with Eq. (73) the VP insertion was computed in the late 1950s [131] for $m_\ell = m_e$ and neglecting terms of $O(m_e/m_\mu)$. Its exact expression was calculated in 1966 [132] and may be written in compact form as [35]

$$\begin{aligned}A_{2\,\mathrm{vap}}^{(4)}(1/x) =& -\frac{25}{36}-\frac{\ln x}{3}+x^2\,(4+3\ln x)+x^4\left[\frac{\pi^2}{3}-2\ln x\;\ln\left(\frac{1}{x}-x\right)-\mathrm{Li}_2(x^2)\right]\\ &+\frac{x}{2}\,(1-5x^2)\left[\frac{\pi^2}{2}-\ln x\;\ln\left(\frac{1-x}{1+x}\right)-\mathrm{Li}_2(x)+\mathrm{Li}_2(-x)\right]\\ =& -\frac{25}{36}-\frac{\ln x}{3}+x^2\,(4+3\ln x)+x^4\left[2\ln^2(x)-2\ln x\;\ln\left(x-\frac{1}{x}\right)+\mathrm{Li}_2(1/x^2)\right]\\ &+\frac{x}{2}\,(1-5x^2)\left[-\ln x\;\ln\left(\frac{x-1}{x+1}\right)+\mathrm{Li}_2(1/x)-\mathrm{Li}_2(-1/x)\right]\qquad (x>1)\;.\end{aligned} \tag{76}$$

The first form is valid for arbitrary x. For $x>1$ some of the logs as well as $\mathrm{Li}_2(x)$ develop a cut and a corresponding imaginary part like the one of $\ln(1-x)$. Therefore, for the numerical evaluation in terms of a series expansion, it is an advantage to rewrite the $\mathrm{Li}_2(x)$'s in terms of $\mathrm{Li}_2(1/x)$'s, according to Eq. (A.11), which leads to the second form.

There are two different regimes for the mass dependent effects, the light electron loops and the heavy tau loops [131,132]:

• **Light** internal masses give rise to potentially large logarithms of mass ratios which get singular in the limit $m_{\mathrm{light}}\to 0$

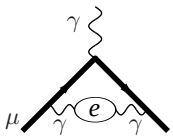

$$a_\mu^{(4)}(\mathrm{vap},e) = \left[\frac{1}{3}\ln\frac{m_\mu}{m_e}-\frac{25}{36}+O\left(\frac{m_e}{m_\mu}\right)\right]\;\left(\frac{\alpha}{\pi}\right)^2\;.$$

Here we have a typical result for a light field which produces a large logarithm $\ln\frac{m_\mu}{m_e}\simeq 5.3$, such that the first term ~ 2.095 is large relative to a typical constant second term -0.6944. Here the exact 2–loop result is

$$a_\mu^{(4)}(\mathrm{vap},e) \simeq 1.094\,258\,3111(84)\;\left(\frac{\alpha}{\pi}\right)^2 = 5.90406007(5)\times 10^{-6}\;. \tag{77}$$

The error is due to the uncertainty in the mass ratio (m_e/m_μ). The leading term as we have shown is due to the charge screening according to the RG.

For comparison we next consider the

• **equal** internal mass case, which yields the pure number

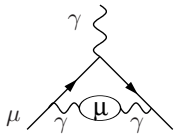

$$a_\mu^{(4)}(\text{vap},\mu) = \left[\frac{119}{36} - \frac{\pi^2}{3}\right] \left(\frac{\alpha}{\pi}\right)^2 ,$$

and is already included in the universal part Eq. (50). The result is typical for these kind of radiative correction calculations: a rational term of size 3.3055... and a transcendental π^2 term of very similar magnitude 3.2899... but of opposite sign largely cancel. The result is only 0.5% of the individual terms:

$$a_\mu^{(4)}(\text{vap},\mu) \simeq 0.015\,687\,4219 \left(\frac{\alpha}{\pi}\right)^2 = 8.464\,13320 \times 10^{-8} . \tag{78}$$

• **Heavy** internal masses decouple in the limit $m_{\text{heavy}} \to \infty$ and thus only yield small power corrections

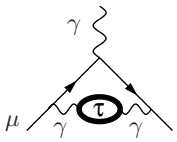

$$a_\mu^{(4)}(\text{vap},\tau) = \left[\frac{1}{45}\left(\frac{m_\mu}{m_\tau}\right)^2 + O\left(\frac{m_\mu^4}{m_\tau^4}\ln\frac{m_\tau}{m_\mu}\right)\right] \left(\frac{\alpha}{\pi}\right)^2 .$$

Here we have a typical "heavy physics" contributions, from a state of mass $M \gg m_\mu$, yielding a term proportional to m_μ^2/M^2. This means that besides the order in α there is an extra suppression factor, e.g. $O(\alpha^2) \to Q(\alpha^2 \frac{m_\mu^2}{M^2})$ in our case. To unveil new heavy states thus requires a corresponding high precision in theory and experiment. For the τ the contribution is relatively tiny

$$a_\mu^{(4)}(\text{vap},\tau) \simeq 0.000\,078\,064(25) \left(\frac{\alpha}{\pi}\right)^2 = 4.2120(13) \times 10^{-10} , \tag{79}$$

with the error from the mass ratio (m_μ/m_τ). Note that at the level of accuracy reached by the Brookhaven experiment (63×10^{-11}), the contribution is non–negligible. At the 2–loop level a $e-\tau$ mixed contribution is not possible, and hence $A_3^{(4)}(m_\mu/m_e, m_\mu/m_\tau) = 0$.

The complete 2–loop QED contribution from the diagrams displayed in Fig. 9 is given by

$$C_2 = A_{1\,\text{uni}}^{(4)} + A_{2\,\text{vap}}^{(4)}(m_\mu/m_e) + A_{2\,\text{vap}}^{(4)}(m_\mu/m_\tau) = 0.765\,857\,410\,(27) ,$$

and we have

$$a_\mu^{(4)\ \text{QED}} = 0.765\,857\,410\,(27) \left(\frac{\alpha}{\pi}\right)^2 \simeq 413217.620(14) \times 10^{-11} \tag{80}$$

for the complete 2–loop QED contribution to a_μ. The errors of $A_2^{(4)}(m_\mu/m_e)$ and $A_2^{(4)}(m_\mu/m_\tau)$ have been added in quadrature as the errors of the different measurements of the lepton masses may be treated as independent. The combined error $\delta C_2 = 2.7 \times 10^{-8}$ is negligible by the standards 1×10^{-5} estimated after Eq. (48).

3.3.2. *3–loop: Light-by-Light Scattering and Vacuum Polarization Insertions*

At three loops, in addition to photon vacuum polarization corrections, a new kind of contributions shows up exhibiting the so called *light–by–light scattering* (LbL) insertions: closed fermion loops with four photons attached. Note that the physical process $\gamma\gamma \to \gamma\gamma$ of light–by–light scattering involves real on–shell photons. There are 6 diagrams which follow from the first one in Fig. 14, by permutation of the photon vertices on the external muon line, plus the ones obtained by reversing the direction of the fermion loop. Remember

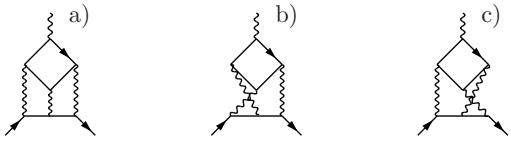

Fig. 14. Light–by–light scattering insertions in the electromagnetic vertex.

that closed fermion loops with three photons vanish by Furry's theorem. Again, besides the equal mass case $m_{\rm loop} = m_\mu$ there are two different regimes for electron and tau loops [142,143], respectively:
• **Light** internal masses also in this case give rise to potentially large logarithms of mass ratios which get singular in the limit $m_{\rm light} \to 0$

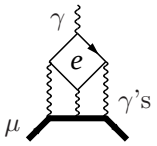

$$a_\mu^{(6)}({\rm lbl},e) = \left[\frac{2}{3}\pi^2 \ln\frac{m_\mu}{m_e} + \frac{59}{270}\pi^4 - 3\,\zeta(3) - \frac{10}{3}\pi^2 + \frac{2}{3} + O\left(\frac{m_e}{m_\mu}\ln\frac{m_\mu}{m_e}\right)\right]\left(\frac{\alpha}{\pi}\right)^3 .$$

This again is a light loop which yields an unexpectedly large contribution

$$a_\mu^{(6)}({\rm lbl},e) \simeq 20.947\,924\,89(16)\left(\frac{\alpha}{\pi}\right)^3 = 2.625\,351\,02(2)\times 10^{-7}\,, \tag{81}$$

with the error from the (m_e/m_μ) mass ratio. Historically, it was calculated first numerically by Aldins et al. [69], after a 1.7 σ discrepancy with the CERN measurement [67] in 1968 showed up.

Again, for comparison we also consider the
• **equal** internal masses case, which yields a pure number

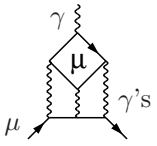

$$a_\mu^{(6)}({\rm lbl},\mu) = \left[\frac{5}{6}\,\zeta(5) - \frac{5}{18}\,\pi^2\,\zeta(3) - \frac{41}{540}\pi^4 - \frac{2}{3}\pi^2\ln^2 2 + \frac{2}{3}\ln^4 2 + 16a_4 - \frac{4}{3}\,\zeta(3) - 24\pi^2\ln 2 + \frac{931}{54}\pi^2 + \frac{5}{9}\right]\left(\frac{\alpha}{\pi}\right)^3 ,$$

and has been included in the universal part Eq. (51) already. The constant a_4 is defined in Eq. (A.14). The single scale QED contribution is much smaller

$$a_\mu^{(6)}({\rm lbl},\mu) \simeq 0.371005293\left(\frac{\alpha}{\pi}\right)^3 = 4.64971652\times 10^{-9}\,, \tag{82}$$

but is still a substantial contributions at the required level of accuracy.
• **Heavy** internal masses again decouple in the limit $m_{\rm heavy} \to \infty$ and thus only yield small power corrections

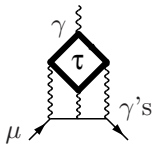

$$a_\mu^{(6)}({\rm lbl},\tau) = \left[\left[\frac{3}{2}\,\zeta(3) - \frac{19}{16}\right]\left(\frac{m_\mu}{m_\tau}\right)^2 + O\left(\frac{m_\mu^4}{m_\tau^4}\ln^2\frac{m_\tau}{m_\mu}\right)\right]\left(\frac{\alpha}{\pi}\right)^3 .$$

Numerically we obtain

$$a_\mu^{(6)}({\rm lbl},\tau) \simeq 0.002\,142\,83(69)\left(\frac{\alpha}{\pi}\right)^3 = 2.685\,56(86)\times 10^{-11}\,. \tag{83}$$

This contribution could play a role for a next generation precision experiment only. The error indicated is from the (m_μ/m_τ) mass ratio.

All other corrections follow from Fig. 10 by replacing at least one muon in a loop by another lepton or quark. The corresponding mass dependent corrections are of particular interest because the light electron

loops yield contributions which are enhanced by large logarithms. Results for $A_2^{(6)}$ have been obtained in [138,139,141,142,143], for $A_3^{(6)}$ in [140,137,144,145,120]. For the light–by–light contribution, graphs 1) to 6) of Fig. 10, the exact analytic result is known [142], but only the much simpler asymptotic expansions have been published. At present the following series expansions are sufficient to match the requirement of the precision needed: for electron LbL loops we have

$$\begin{aligned}
A_{2\,\mathrm{lbl}}^{(6)}(m_\mu/m_e) &= \frac{2}{3}\pi^2 \ln\frac{m_\mu}{m_e} + \frac{59}{270}\pi^4 - 3\zeta(3) - \frac{10}{3}\pi^2 + \frac{2}{3} \\
&+ \left(\frac{m_e}{m_\mu}\right) \left[\frac{4}{3}\pi^2 \ln\frac{m_\mu}{m_e} - \frac{196}{3}\pi^2 \ln 2 + \frac{424}{9}\pi^2\right] \\
&+ \left(\frac{m_e}{m_\mu}\right)^2 \left[-\frac{2}{3}\ln^3\frac{m_\mu}{m_e} + \left(\frac{\pi^2}{9} - \frac{20}{3}\right) \ln^2\frac{m_\mu}{m_e} - \left(\frac{16}{135}\pi^4 + 4\zeta(3) - \frac{32}{9}\pi^2 + \frac{61}{3}\right) \ln\frac{m_\mu}{m_e} \right. \\
&\qquad \left. + \frac{4}{3}\pi^2\zeta(3) - \frac{61}{270}\pi^4 + 3\,\zeta(3) + \frac{25}{18}\pi^2 - \frac{283}{12}\right] \\
&+ \left(\frac{m_e}{m_\mu}\right)^3 \left[\frac{10}{9}\pi^2 \ln\frac{m_\mu}{m_e} - \frac{11}{9}\pi^2\right] \\
&+ \left(\frac{m_e}{m_\mu}\right)^4 \left[\frac{7}{9}\ln^3\frac{m_\mu}{m_e} + \frac{41}{18}\ln^2\frac{m_\mu}{m_e} + \left(\frac{13}{9}\pi^2 + \frac{517}{108}\right)\ln\frac{m_\mu}{m_e} + \frac{1}{2}\zeta(3) + \frac{191}{216}\pi^2 + \frac{13283}{2592}\right] \\
&\qquad + O\left((m_e/m_\mu)^5\right) = 20.947\,924\,89(16)\,, \qquad (84)
\end{aligned}$$

where here and in the following we use m_e/m_μ as given in Eq. (44). The leading term in the (m_e/m_μ) expansion turns out to be surprisingly large. It has been calculated first in [154]. Prior to the exact calculation in [142] good numerical estimates 20.9471(29) [155] and 20.9469(18) [156] have been available. For τ LbL loops one obtains

$$\begin{aligned}
A_{2\,\mathrm{lbl}}^{(6)}(m_\mu/m_\tau) &= \frac{m_\mu^2}{m_\tau^2}\left[\frac{3}{2}\zeta_3 - \frac{19}{16}\right] \\
&+ \frac{m_\mu^4}{m_\tau^4}\left[\frac{13}{18}\zeta_3 - \frac{161}{1620}\zeta_2 - \frac{831931}{972000} - \frac{161}{3240}L^2 - \frac{16189}{97200}L\right] \\
&+ \frac{m_\mu^6}{m_\tau^6}\left[\frac{17}{36}\zeta_3 - \frac{13}{224}\zeta_2 - \frac{1840256147}{3556224000} - \frac{4381}{120960}L^2 - \frac{24761}{317520}L\right] \\
&+ \frac{m_\mu^8}{m_\tau^8}\left[\frac{7}{20}\zeta_3 - \frac{2047}{54000}\zeta_2 - \frac{453410778211}{1200225600000} - \frac{5207}{189000}L^2 - \frac{41940853}{952560000}L\right] \\
&+ \frac{m_\mu^{10}}{m_\tau^{10}}\left[\frac{5}{18}\zeta_3 - \frac{1187}{44550}\zeta_2 - \frac{86251554753071}{287550049248000} - \frac{328337}{14968800}L^2 - \frac{640572781}{23051952000}L\right] \\
&+ O\left((m_\mu/m_\tau)^{12}\right) = 0.002\,142\,833(691)\,, \qquad (85)
\end{aligned}$$

where $L = \ln(m_\tau^2/m_\mu^2)$, $\zeta_2 = \zeta(2) = \pi^2/6$ and $\zeta_3 = \zeta(3)$. The expansion given in [142] in place of the exact formula has been extended in [143] with the result presented here.

Vacuum polarization insertions contributing to $a^{(6)}$ may origin from one or two internal closed fermion loops. The vacuum polarization insertions into photon lines again yield mass dependent effects if one or two of the μ loops of the universal contributions are replaced by an electron or a τ. Here we first give the numerical results for the coefficients of $\left(\frac{\alpha}{\pi}\right)^3$ [141,144,145]:

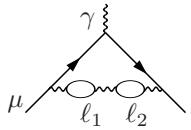

$$\begin{aligned}
A_\mu^{(6)}(\mathrm{vap}, e) &= 1.920\,455\,130(33)\,, \\
A_\mu^{(6)}(\mathrm{vap}, \tau) &= -0.001\,782\,33(48)\,, \\
A_\mu^{(6)}(\mathrm{vap}, e, \tau) &= 0.000\,527\,66(17)\,.
\end{aligned}$$

Again the exact results are available [141] but the following much simpler asymptotic expansions are adequate at present precision: for electron loops replacing muon loops in Fig. 10 one finds

$$
\begin{aligned}
A_{2\,\mathrm{vap}}^{(6)}(m_\mu/m_e) = {} & \frac{2}{9}\ln^2\frac{m_\mu}{m_e} + \left(\zeta(3) - \frac{2}{3}\pi^2\ln 2 + \frac{1}{9}\pi^2 + \frac{31}{27}\right)\ln\frac{m_\mu}{m_e} \\
& + \frac{11}{216}\pi^4 - \frac{2}{9}\pi^2\ln^2 2 - \frac{8}{3}a_4 - \frac{1}{9}\ln^4 2 - 3\zeta(3) + \frac{5}{3}\pi^2\ln 2 - \frac{25}{18}\pi^2 + \frac{1075}{216} \\
& + \left(\frac{m_e}{m_\mu}\right)\left[-\frac{13}{18}\pi^3 - \frac{16}{9}\pi^2\ln 2 + \frac{3199}{1080}\pi^2\right] \\
& + \left(\frac{m_e}{m_\mu}\right)^2\left[\frac{10}{3}\ln^2\frac{m_\mu}{m_e} - \frac{11}{9}\ln\frac{m_\mu}{m_e} - \frac{14}{3}\pi^2\ln 2 - 2\zeta(3) + \frac{49}{12}\pi^2 - \frac{131}{54}\right] \\
& + \left(\frac{m_e}{m_\mu}\right)^3\left[\frac{4}{3}\pi^2\ln\frac{m_\mu}{m_e} + \frac{35}{12}\pi^3 - \frac{16}{3}\pi^2\ln 2 - \frac{5771}{1080}\pi^2\right] \\
& + \left(\frac{m_e}{m_\mu}\right)^4\left[-\frac{25}{9}\ln^3\left(\frac{m_\mu}{m_e}\right) - \frac{1369}{180}\ln^2\left(\frac{m_\mu}{m_e}\right) + \left(-2\zeta(3) + 4\pi^2\ln 2 - \frac{269}{144}\pi^2 - \frac{7496}{675}\right)\ln\frac{m_\mu}{m_e}\right. \\
& - \frac{43}{108}\pi^4 + \frac{8}{9}\pi^2\ln^2 2 + \frac{80}{3}a_4 + \frac{10}{9}\ln^4 2 + \frac{411}{32}\zeta(3) + \frac{89}{48}\pi^2\ln 2 - \frac{1061}{864}\pi^2 \\
& \left. - \frac{274511}{54000}\right] + O\left((m_e/m_\mu)^5\right) = 1.920\,455\,130(33)\,. \qquad (86)
\end{aligned}
$$

The leading and finite terms were first given in [157], the correct (m_e/m_μ) terms have been given in [140]. In contrast to the LbL contribution the leading logs of the VP contribution may be obtained relatively easy by renormalization group considerations using the running fine structure constant [135,158]. In place of the known but lengthy exact result only the expansion shown was presented in [141]. Despite the existence of large leading logs the VP contribution is an order of magnitude smaller than the one from the LbL graphs. Replacing muon loops in Fig. 10 by tau loops in all possible ways one obtains

$$
\begin{aligned}
A_{2\,\mathrm{vap}}^{(6)}(m_\mu/m_\tau) = {} & \left(\frac{m_\mu}{m_\tau}\right)^2\left[-\frac{23}{135}\ln\frac{m_\tau}{m_\mu} - \frac{2}{45}\pi^2 + \frac{10117}{24300}\right] \\
& + \left(\frac{m_\mu}{m_\tau}\right)^4\left[\frac{19}{2520}\ln^2\frac{m_\tau}{m_\mu} - \frac{14233}{132300}\ln\frac{m_\tau}{m_\mu} + \frac{49}{768}\zeta(3) - \frac{11}{945}\pi^2 + \frac{2976691}{296352000}\right] \\
& + \left(\frac{m_\mu}{m_\tau}\right)^6\left[\frac{47}{3150}\ln^2\frac{m_\tau}{m_\mu} - \frac{805489}{11907000}\ln\frac{m_\tau}{m_\mu} + \frac{119}{1920}\zeta(3) - \frac{128}{14175}\pi^2 + \frac{102108163}{30005640000}\right] \\
& + O\left((m_\mu/m_\tau)^8\right) = -0.001\,782\,327(484)\,. \qquad (87)
\end{aligned}
$$

Also in this case, in place of exact result obtained in [141] only the expansion shown was given in the paper. As has been cross checked recently against the exact results in [35], all the expansions presented are sufficient for numerical evaluations at the present level of accuracy.

Starting at three loops, a contribution to $A_3(m_\mu/m_e, m_\mu/m_\tau)$, depending on two mass ratios, shows up. The relevant term is due to diagram 22) of Fig. 10 with one fermion loop an electron–loop and the other a τ–loop. According to Eq. (70) we may write

$$
a_\mu^{(6)}(\mathrm{vap}, e, \tau)\Big|_{\mathrm{dia\ 22)}} = \frac{\alpha}{\pi}\int_0^1 dx(1-x)\ 2\ \left[-\Pi'^{\,e}_{\gamma\,\mathrm{ren}}\left(\frac{-x^2}{1-x}m_\mu^2\right)\right]\left[-\Pi'^{\,\tau}_{\gamma\,\mathrm{ren}}\left(\frac{-x^2}{1-x}m_\mu^2\right)\right], \qquad (88)
$$

which together with Eq. (73) leads to a three–fold integral representation. However, since $\Pi'^{\,\ell}_{\gamma\,\mathrm{ren}}$ given by Eq. (73) is analytically known, Eq. (88) represents a 1–dimensional integral. It has been calculated as an expansion in the two mass ratios in [140,144] and was extended to $O((m_\mu^2/m_\tau^2)^5)$ recently in [145]. The result reads

$$
\begin{aligned}
A_{3\,\mathrm{vap}}^{(6)}(m_\mu/m_e, m_\mu/m_\tau) = {} & \left(\frac{m_\mu^2}{m_\tau^2}\right)\left[\frac{2}{135}\ln\frac{m_\mu^2}{m_e^2} - \frac{1}{135}\right] \\
& + \left(\frac{m_\mu^2}{m_\tau^2}\right)^2\left[-\frac{1}{420}\ln\frac{m_\tau^2}{m_\mu^2}\ln\frac{m_\tau^2\ m_\mu^2}{m_e^4} - \frac{37}{22050}\ln\frac{m_\tau^2}{m_e^2} + \frac{1}{504}\ln\frac{m_\mu^2}{m_e^2} + \frac{\pi^2}{630} - \frac{229213}{12348000}\right] \\
& + \left(\frac{m_\mu^2}{m_\tau^2}\right)^3\left[-\frac{2}{945}\ln\frac{m_\tau^2}{m_\mu^2}\ln\frac{m_\tau^2\ m_\mu^2}{m_e^4} - \frac{199}{297675}\ln\frac{m_\tau^2}{m_e^2} - \frac{1}{4725}\ln\frac{m_\mu^2}{m_e^2} + \frac{4\pi^2}{2835} - \frac{1102961}{75014100}\right] \\
& + \left(\frac{m_\mu^2}{m_\tau^2}\right)^4\left[-\frac{1}{594}\ln\frac{m_\tau^2}{m_\mu^2}\ln\frac{m_\tau^2\ m_\mu^2}{m_e^4} - \frac{391}{2058210}\ln\frac{m_\tau^2}{m_e^2} - \frac{19}{31185}\ln\frac{m_\mu^2}{m_e^2} + \frac{\pi^2}{891} - \frac{161030983}{14263395300}\right] \\
& + \frac{2}{15}\frac{m_e^2}{m_\tau^2} - \frac{4\pi^2}{45}\frac{m_e^3}{m_\tau^2 m_\mu} + \mathcal{O}\left[\left(\frac{m_\mu^2}{m_\tau^2}\right)^5\ln\frac{m_\tau^2}{m_\mu^2}\ln\frac{m_\tau^2\ m_\mu^2}{m_e^4}\right] + \mathcal{O}\left(\frac{m_e^2}{m_\tau^2}\frac{m_\mu^2}{m_\tau^2}\right) \\
= {} & 0.00052766(17)\,. \qquad (89)
\end{aligned}
$$

The result is in agreement with the numerical evaluation [141]. The τ–lepton mass uncertainty determines the error. The leading–logarithmic term of this expansion corresponds to simply replacing $\alpha(q^2 = 0)$ by $\alpha(m_\mu^2)$ in the 2–loop diagram with a τ loop. The last term, with odd powers of m_e and m_μ, has been included although it is not relevant numerically. It illustrates typical contributions of the eikonal expansion, the only source of terms non–analytical in masses squared.

With Eqs. (51) and (84) to (89) the complete 3–loop QED contribution to a_μ is now known analytically, either in form of a series expansion or exact. The mass dependent terms may be summarized as follows:

$$
\begin{aligned}
A_2^{(6)}(m_\mu/m_e) &= 22.868\,380\,02(20), \\
A_2^{(6)}(m_\mu/m_\tau) &= \ 0.000\,360\,51(21), \\
A_{3\,\mathrm{vap}}^{(6)}(m_\mu/m_e, m_\mu/m_\tau) &= \ 0.000\,527\,66(17).
\end{aligned} \qquad (90)
$$

As already mentioned above, the $A_2^{(6)}(m_\mu/m_e)$ contribution is surprisingly large and predominantly from light–by–light scattering via an electron loop. The importance of this term was discovered in [69], improved by numerical calculation in [24] and calculated analytically in [142]. Adding up the relevant terms we have

$$C_3 = 24.050\,509\,64\,(46)$$

or

$$a_\mu^{(6)\ \mathrm{QED}} = 24.050\,509\,64\,(46)\,\left(\frac{\alpha}{\pi}\right)^3 \simeq 30141.902(1)\times 10^{-11} \qquad (91)$$

as a result for the complete 3–loop QED contribution to a_μ. We have combined the first two errors of Eq. (90) in quadrature and the last linearly, as the latter depends on the same errors in the mass ratios.

3.3.3. *4–loop: Light Lepton Insertions*

Also at four loops, the light internal electron loops, included in $A_2^{(8)}(m_\mu/m_e)$, give the by far largest contribution. Here 469 diagrams contribute which may be divided into four gauge invariant (g-i) groups:

Group I: 49 diagrams obtained from the 1–loop muon vertex by inserting 1–, 2– and 3–loop lepton VP subdiagrams, i.e., the internal photon line of Fig. 8 is replaced by the full propagator at three loops. The group is subdivided into four g-i subclasses I(a), I(b), I(c) and I(d) as illustrated in Fig. 15. Results for this group have been obtained by numerical and analytic methods [126,118]. The numerical result [126]

$$A_{2\,I}^{(8)} = 16.720\,359\,(20)\ ,$$

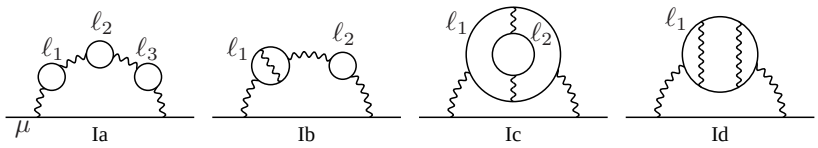

Fig. 15. Typical diagrams of subgroups Ia (7 diagrams), Ib (18 diagrams), Ic (9 diagrams) and Id (15 diagrams). The lepton lines represent fermions propagating in an external magnetic field. ℓ_i denote VP insertions.

has been obtained by using simple integral representations.
Group II: 90 diagrams generated from the 2–loop muon vertex by inserting 1–loop and/or 2–loop lepton VP subdiagrams as shown in Fig. 16. As for the previous case, results for this group have been obtained by

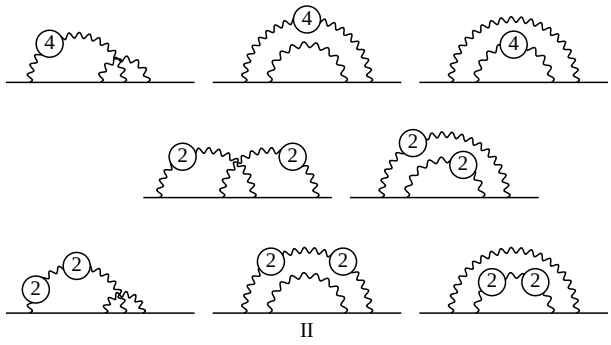

Fig. 16. Typical diagrams of group II (90 diagrams). The lepton lines as in Fig. 15. 2 and 4, respectively, indicate second (1–loop subdiagrams) and fourth (2–loop subdiagrams) order lepton–loops.

numerical and analytic methods [126,118]. The result here is [126]

$$A_{2\,II}^{(8)} = -16.674\,591\,(68)\ .$$

Group III: 150 diagrams generated from the 3–loop muon vertex Fig. 10 by inserting one 1–loop electron VP subdiagrams in each internal photon line in all possible ways. Examples are given in Fig. 17. This is a

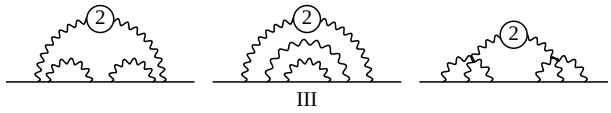

Fig. 17. Typical diagrams of group III (150 diagrams). The lepton lines as in Fig. 15.

group which has been calculated numerically only. The result found in [126] reads

$$A_{2\,III}^{(8)} = 10.793\,43\,(414)\ .$$

Group IV: 180 diagrams with muon vertex containing LbL subgraphs decorated with additional radiative corrections. This group is subdivided as shown in Fig. 18 into *g-i* subsets IV(a), IV(b), IV(c) and IV(d). The calculation of the corresponding contribution is at the limit of present possibilities. The result has been evaluated by two independent methods in [126] and reads

$$A_{2\,IV}^{(8)} = 121.8431\,(59)\ .$$

The sum of the results from the different groups thus reads

$$A_2^{(8)}(m_\mu/m_e) = 132.6823(72)\ . \tag{92}$$

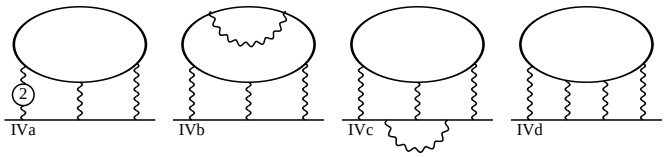

Fig. 18. Typical diagrams of subgroups IVa (54 diagrams), IVb (60 diagrams), IVc (48 diagrams) and IVd (18 diagrams). The lepton lines as in Fig. 15.

A small contribution to $A_3^{(8)}$ comes from the diagrams which depend on 3 masses. There are 102 diagrams containing two or three closed loops of VP and/or LbL type, defined above as the classes I (30 diagrams), II (36 diagrams) and IV (36 diagrams). The results found in [126] read

$$\begin{aligned} A_{3I}^{(8)}(m_\mu/m_e, m_\mu/m_\tau) &= 0.007\,630\,(01)\,, \\ A_{3II}^{(8)}(m_\mu/m_e, m_\mu/m_\tau) &= -0.053\,818\,(37)\,, \\ A_{3IV}^{(8)}(m_\mu/m_e, m_\mu/m_\tau) &= 0.083\,782\,(75)\,, \end{aligned} \tag{93}$$

and are adding up to the value

$$A_3^{(8)}(m_\mu/m_e, m_\mu/m_\tau) = 0.037\,594\,(83)\,. \tag{94}$$

A rough estimate of the τ–loops contribution performed in [126] yields

$$A_2^{(8)}(m_\mu/m_\tau) = 0.005(3)\,. \tag{95}$$

Note that all mass dependent as well as the mass independent $O(\alpha^4)$ QED contributions to a_μ have been recalculated by different methods by Kinoshita and collaborators [126,127,108]. There is also some progress in analytic calculations [159]. Adding the $A^{(8)}$ terms discussed above we obtain

$$C_4 = 130.8105(85)\,,$$

which yields

$$a_\mu^{(8)\ \mathrm{QED}} = 130.810\,5\,(85)\,\left(\frac{\alpha}{\pi}\right)^4 \simeq 380.807(25)\times 10^{-11}\,, \tag{96}$$

the result for the complete 4–loop QED contribution to a_μ.

3.3.4. *5–loop and Summary of QED Contributions*

Also at five loops electron loop insertions are the leading contributions (see Fig. 13). Here the number of diagrams is 9080, a very discouraging number as Kinoshita [39] remarks. This contribution originally was evaluated using renormalization group (RG) arguments in [24,146]. The new estimate by Kinoshita and Nio [39,148] is

$$A_2^{(10)}(m_\mu/m_e) = 663(20), \tag{97}$$

and was obtained by numerically evaluating all Feynman diagrams, which are known or likely to be enhanced. The error estimate should cover all remaining subleading contributions. The number in Eq. (97) was subsequently cross–checked by Kataev [149]. A very recent calculation from the class of leading tenth order contributions (singlet (SI) VP insertion diagrams which includes the last diagram of Fig. 13 with two electron LbL loops) yields $A_2^{(10)}(m_\mu/m_e) = -1.26344(14)$ [150]. This result has been reproduced at the 3% level by an asymptotic expansion in [151], where also the much larger 4–loop non-singlet (NS) VP insertion with electron loops has been calculated: $A_2^{(10),\mathrm{as}}(m_\mu/m_e) = 63.481_{\mathrm{NS}} - 1.21429_{\mathrm{SI}} = 62.2667$. Since

the leading terms are included in Eq. (97) already and subleading terms are unknown in general, we will stay with the above result in the following.

Thus, taking into account Eq. (53), we arrive at

$$C_5 \sim 663.0(20.0)(4.6)$$

or

$$a_\mu^{(10)\ \mathrm{QED}} \sim 663(20)(4.6)\ \left(\frac{\alpha}{\pi}\right)^5 \simeq 4.483(135)(31) \times 10^{-11} \tag{98}$$

as an estimate of the 5–loop QED contribution.

In Table 3 we collect the results of the QED calculations. In spite of the fact that the expansion coefficients C_i multiplying $(\alpha/\pi)^i$ grow rapidly with the order, the convergence of the perturbative expansion of a_μ^{QED} is good. This suggests that the perturbative truncation error is well under control at the present level of accuracy.

Table 3
The QED contributions to a_μ.

C_i		$a_\mu^{(2i)\ \mathrm{QED}} \times 10^{11}$	
C_1	0.5	$a^{(2)}$	116140973.289(43)
C_2	0.765 857 410 (27)	$a^{(4)}$	413217.620(14)
C_3	24.050 509 64 (46)	$a^{(6)}$	30141.902(1)
C_4	130.8105(85)	$a^{(8)}$	380.807(25)
C_5	663.0(20.0)(4.6)	$a^{(10)}$	4.483(135)(31)

The universal QED terms have been given in Eq. (54) and together with the mass dependent QED terms of the 3 flavors (e, μ, τ) we obtain

$$a_\mu^{\mathrm{QED}} = 116\,584\,718.104(.044)(.015)(.025)(.139)[.148] \times 10^{-11}\ . \tag{99}$$

The errors are given by the uncertainties in α_{input}, in the mass ratios, the numerical error on α^4 terms and the guessed uncertainty of the α^5 contribution, respectively.

Now we have to address the question what happens beyond QED. What is measured in an experiment includes effects from the real world and we have to include the contributions from all known particles and interactions such that from a possible deviation between theory and experiment we may get a hint of the yet unknown physics.

4. Hadronic Vacuum Polarization Corrections

On a perturbative level we may obtain the hadronic vacuum polarization contribution by replacing internal lepton loops in the QED VP contributions by quark loops, adapting charge, color multiplicity and the masses accordingly. Since quarks are, however, confined inside hadrons, a quark mass cannot be defined in the same natural way as a lepton mass and quark mass values depend in various ways on the physical circumstances. Moreover, the running strong coupling "constant" $\alpha_s(s)$ becomes large at low energies $E = \sqrt{s}$. Therefore perturbative QCD (pQCD) fails to "converge" in any practical sense in this region and pQCD may only be trusted above about 2 GeV and away from thresholds and resonances. The low energy structure of QCD with confinement and the spontaneous breaking of chiral symmetry in the chiral limit (on a Lagrangian level characterized by vanishing (current) quark masses) is completely beyond the scope of pQCD. Low energy QCD is characterized by its typical spectrum of low lying hadronic states, the pseudoscalar pions, the Kaons and the η as quasi Goldstone bosons (true ones in the chiral limit), the pseudoscalar singlet η', the spin-1

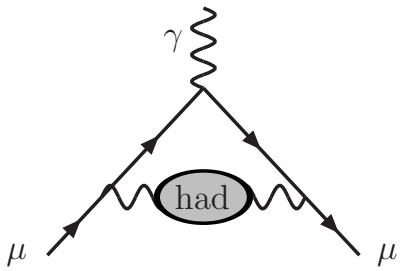

Fig. 19. Leading hadronic contribution to $g-2$.

vector bosons ρ, ω, ϕ and by the order parameters of chiral symmetry breaking, like the quark condensates $\langle\bar{q}q\rangle \neq 0$ $(q = u, d, s)$. For the calculation of the hadronic contributions $a_\mu^{\rm had}$ to the $g-2$ of the muon, baryons like proton and neutron do not play a big role.

Quarks contribute to the electromagnetic current according to their charge

$$j_{\rm em}^{\mu\,{\rm had}} = \sum_c \left(\frac{2}{3}\bar{u}_c\gamma^\mu u_c - \frac{1}{3}\bar{d}_c\gamma^\mu d_c - \frac{1}{3}\bar{s}_c\gamma^\mu s_c + \frac{2}{3}\bar{c}_c\gamma^\mu c_c - \frac{1}{3}\bar{b}_c\gamma^\mu b_c + \frac{2}{3}\bar{t}_c\gamma^\mu t_c \right) . \tag{100}$$

The hadronic electromagnetic current $j_{\rm em}^{\mu\,{\rm had}}$ is a color singlet and hence includes a sum over colors indexed by c. Its contribution to the electromagnetic current correlator Eq. (64) defines $\Pi_\gamma^{'\,{\rm had}}(s)$, which enters the calculation of the leading order hadronic contribution to $a_\mu^{\rm had}$, diagrammatically given by Fig. 19.

Perturbative QCD fails to be a reliable tool for estimating $a_\mu^{\rm had}$ and known approaches to low energy QCD like chiral perturbation theory as well as extensions of it which incorporate spin-1 bosons or lattice QCD are far from being able to make precise predictions. We therefore have to resort to a semi-phenomenological approach using dispersion relations together with the optical theorem and experimental data.

The basic relations are

– analyticity (deriving from causality), which allows to write the DR

$$\Pi'_\gamma(k^2) - \Pi'_\gamma(0) = \frac{k^2}{\pi}\int_0^\infty {\rm d}s\, \frac{{\rm Im}\Pi'_\gamma(s)}{s\,(s-k^2-{\rm i}\varepsilon)} \ . \tag{101}$$

– optical theorem (deriving from unitarity), which relates the imaginary part of the vacuum polarization amplitude to the total cross section in e^+e^-–annihilation

$${\rm Im}\Pi'_\gamma(s) = \frac{s}{4\pi\alpha(s)}\,\sigma_{\rm tot}(e^+e^- \to \text{anything}) := \frac{\alpha(s)}{3}\,R(s)\,, \tag{102}$$

with

$$R(s) = \sigma_{\rm tot}/\frac{4\pi\alpha(s)^2}{3s} \ . \tag{103}$$

The normalization factor is the point cross section (tree level) $\sigma_{\mu\mu}(e^+e^- \to \gamma^* \to \mu^+\mu^-)$ in the limit $s \gg 4m_\mu^2$. We obtain the hadronic contribution if we restrict "anything" to hadrons. The complementary leptonic part may be calculated reliable in perturbation theory and the production of a lepton pair at lowest order is given by

$$R_\ell(s) = \sqrt{1-\frac{4m_\ell^2}{s}}\left(1+\frac{2m_\ell^2}{s}\right) \ , \quad (\ell = e, \mu, \tau), \tag{104}$$

which may be read off from the imaginary part given in Eq. (75). This result provides an alternative way to calculate the renormalized vacuum polarization function Eq. (73), namely, via the DR Eq. (66) which now takes the form

$$\Pi'^{\ell}_{\gamma\,\mathrm{ren}}(q^2) = \frac{\alpha q^2}{3\pi} \int\limits_{4m_\ell^2}^{\infty} \mathrm{d}s\, \frac{R_\ell(s)}{s(s-q^2-\mathrm{i}\varepsilon)}\,, \tag{105}$$

yielding the vacuum polarization due to a lepton–loop.

In contrast to the leptonic part, the hadronic contribution cannot be calculated analytically as a perturbative series, but it can be expressed in terms of the cross section of the reaction $e^+e^- \to$ hadrons, which is known from experiments. Via

$$R_{\mathrm{had}}(s) = \sigma(e^+e^- \to \mathrm{hadrons}) / \frac{4\pi\alpha(s)^2}{3s}\,, \tag{106}$$

we obtain the relevant hadronic vacuum polarization

$$\Pi'^{\mathrm{had}}_{\gamma\,\mathrm{ren}}(q^2) = \frac{\alpha q^2}{3\pi} \int\limits_{4m_\pi^2}^{\infty} \mathrm{d}s\, \frac{R_{\mathrm{had}}(s)}{s(s-q^2-\mathrm{i}\varepsilon)}\,. \tag{107}$$

At low energies, where the dominating final state consists of two charged pions[9], the cross section is given by the square of the electromagnetic form factor of the pion $F_\pi^{(0)}(s)$ (effective $\pi^+\pi^-\gamma$ vertex undressed from VP effects, see below),

$$R_{\mathrm{had}}(s) = \frac{1}{4}\left(1-\frac{4m_\pi^2}{s}\right)^{\frac{3}{2}} |F_\pi^{(0)}(s)|^2 \quad , \qquad 4\,m_\pi^2 < s < 9\,m_\pi^2 \quad , \tag{108}$$

which directly follows from the corresponding imaginary part

$$\mathrm{Im}\,\Pi'^{\,(\pi)}_{\gamma}(q^2) = \frac{\alpha}{12}\,(1-4m_\pi^2/s)^{3/2}$$

of a pion loop in the photon vacuum polarization. At $s = 0$ we have $F_\pi^{(0)}(0) = 1$, i.e., $F_\pi^{(0)}(0)$ measures the classical pion charge in units of e. For point–like pions we would have $F_\pi^{(0)}(s) \equiv 1$. There are three differences between the pionic loop integral and those belonging to the lepton loops:
– the masses are different
– the spins are different
– the pion is composite – the Standard Model leptons are elementary
The compositeness manifests itself in the occurrence of the form factor $F_\pi(s)$, which generates an enhancement: at the ρ peak, $|F_\pi(s)|^2$ reaches values of about 45, while the quark parton model would give about 7. The remaining difference in the expressions for the quantities $R_\ell(s)$ and $R_{\mathrm{had}}(s)$ in Eqs. (104) and (108), respectively, originates in the fact that the leptons carry spin $\frac{1}{2}$, while the spin of the pion vanishes. Near threshold, the angular momentum barrier suppresses the function $R_{\mathrm{had}}(s)$ by three powers of momentum, while $R_\ell(s)$ is proportional to the first power. The suppression largely compensates the enhancement by the form factor – by far the most important property is the mass, which sets the relevant scale.

4.1. *Lowest Order Vacuum Polarization Contribution*

Using Eq. (68) together with Eq. (102), the $O(\alpha^2)$ contributions to a_μ^{had} may be directly evaluated in terms of $R_{\mathrm{had}}(s)$ defined in Eq. (106). More precisely we may write

$$a_\mu^{(4)}(\mathrm{vap,\,had}) = \left(\frac{\alpha m_\mu}{3\pi}\right)^2 \left(\int\limits_{m_{\pi^0}^2}^{E_{\mathrm{cut}}^2} \mathrm{d}s\, \frac{R_{\mathrm{had}}^{\mathrm{data}}(s)\,\hat{K}(s)}{s^2} + \int\limits_{E_{\mathrm{cut}}^2}^{\infty} \mathrm{d}s\, \frac{R_{\mathrm{had}}^{\mathrm{pQCD}}(s)\,\hat{K}(s)}{s^2} \right), \tag{109}$$

[9] A much smaller contribution is due to $\gamma^* \to \pi^0\gamma$, the hadronic final state with the lowest threshold $s > m_{\pi^0}^2$.

with a cut $E_{\rm cut}$ in the energy, separating the non–perturbative part to be evaluated from the data and the perturbative high energy tail to be calculated using pQCD. The kernel $K(s)$ is represented by Eq. (67) discarding the factor α/π. This integral can be performed analytically. Written in terms of the variable

$$x = \frac{1-\beta_\mu}{1+\beta_\mu}\ , \quad \beta_\mu = \sqrt{1-4m_\mu^2/s},$$

the result reads [10] [153]

$$K(s) = \frac{x^2}{2}\,(2-x^2) + \frac{(1+x^2)(1+x)^2}{x^2}\left(\ln(1+x) - x + \frac{x^2}{2}\right) + \frac{(1+x)}{(1-x)}\,x^2\ln(x)\ . \tag{111}$$

We have written the integral Eq. (109) in terms of the rescaled function

$$\hat{K}(s) = \frac{3s}{m_\mu^2}K(s), \tag{112}$$

which is only slowly varying in the range of integration. It increases monotonically from 0.63... at the $\pi\pi$ threshold $s = 4m_\pi^2$ to 1 at $s = \infty$. The graph is shown in Fig. 20.

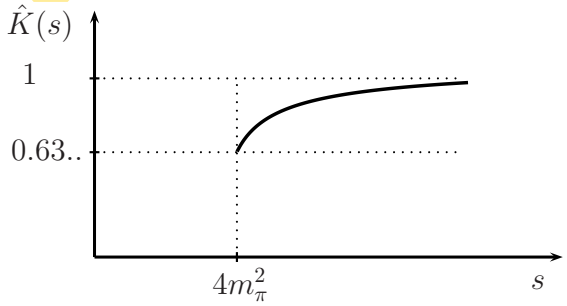

Fig. 20. Graph of weight function $\hat{K}(s)$ of the $g-2$ dispersion integral.

Note the $1/s^2$–enhancement of contributions from low energies in a_μ. Thus the $g-2$ kernel gives very high weight to the low energy range, in particular to the lowest lying resonance, the ρ^0. Thus, this $1/E^4$ magnification of the low energy region by the a_μ kernel–function together with the existence of the pronounced ρ^0 resonance in the $\pi^+\pi^-$ cross–section are responsible for the fact that pion pair production $e^+e^- \to \pi^+\pi^-$ gives the by far largest contribution to $a_\mu^{\rm had}$. The ρ is the lowest lying vector–meson resonance and shows up in $\pi^+\pi^- \to \rho^0$ at $m_\rho \sim 770$ MeV. This dominance of the low energy hadronic cross–section by a single simple two–body channel is good luck for a precise determination of a_μ, although a very precise determination of the $\pi^+\pi^-$ cross–section is a rather difficult task. The experimental data for the low energy region are shown in Fig. 21. Below about 810 MeV $\sigma_{\rm tot}^{\rm had}(s) \simeq \sigma_{\pi\pi}(s)$ to a good approximation but at increasing energies more and more channels open and "measurements of R" get more difficult. In the light sector of u, d, s quarks, besides the ρ there is the ω, which is mixing with the ρ, and the ϕ resonance, essentially a $\bar{s}s$ bound system. In the charm region we have the pronounced $\bar{c}c$–resonances, the $J/\psi_{1S}, \psi_{2S}, \cdots$ resonance series and in the bottom region the $\bar{b}b$–resonances $\Upsilon_{1S}, \Upsilon_{2S}, \cdots$. Many of the resonances are very narrow as indicated in Fig. 22.

A collection of e^+e^-–data at energies > 1 GeV is shown in Fig. 22 [160]. The compilation is an up–to–date version of earlier ones [83],[161]-[167] by different groups. For detailed references and comments on the data

[10] The representation Eq. (111) of $K(s)$ is valid for the muon (or electron) where we have $s > 4m_\mu^2$ in the domain of integration $s > 4m_\pi^2$, and x is real, and $0 \le x \le 1$. For the τ Eq. (111) applies for $s > 4m_\tau^2$. In the region $4m_\pi^2 < s < 4m_\tau^2$, where $0 < r = s/m_\tau^2 < 4$, we may use the form

$$K(s) = \tfrac{1}{2} - r + \tfrac{1}{2}r\,(r-2)\,\ln(r) - \left(1 - 2r + \tfrac{1}{2}r^2\right)\,\varphi/w, \tag{110}$$

with $w = \sqrt{4/r-1}$ and $\varphi = 2\arctan(w)$.

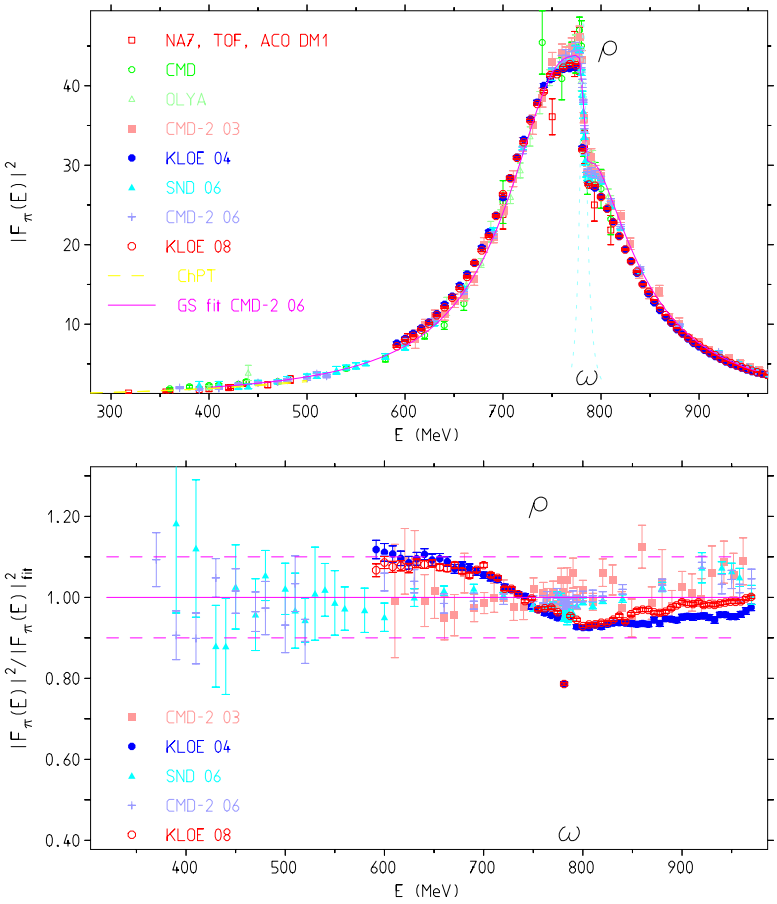

Fig. 21. The dominating low energy domain is given by the channel $e^+e^- \to \pi^+\pi^-$ which exhibits the ρ–resonance. The $\rho-\omega$ mixing, due to isospin breaking by $m_u \neq m_d$, is distorting the ideal Breit-Wigner resonance shape of the ρ. The ratio $|F_\pi(E)|^2/|F_\pi(E)|^2_{\rm fit}$ shows the fairly good compatibility of the newer measurements relative to a CMD-2 fit. Dashed horizontal lines mark ± 10%.

we refer to [83] and the more recent experimental publications by MD-1 [168], BES [84], CMD-2 [85,169], KLOE [86,170], SND [171], BaBar [172] and [173]. A list of experiments and references till 2003 is given in [167], where the available data are collected.

For the evaluation of the basic integral Eq. (109) we take $R(s)$ data up to $\sqrt{s} = E_{cut} = 5.2$ GeV and for the Υ resonance–region between 9.46 and 13 GeV and apply perturbative QCD from 5.2 to 9.46 GeV and for the high energy tail above 13 GeV. The result obtained is [174] (update including [170])

$$a_\mu^{(4)}(\text{vap, had}) = (690.30 \pm 5.26)[(692.37 \pm 5.58)] \times 10^{-10} \tag{113}$$

and is based on a direct integration of all relevant e^+e^-–data available [11] . In braces the value before including the new KLOE result [170].

Note that the different data sets shown in Fig. 21 exhibit systematic deviations in the distribution which are not yet understood. In contrast, the $a_\mu^{\rm had}$ integrals in general are in good agreement [12] . A very recent *preliminary* precision measurement of the $e^+e^- \to \pi^+\pi^-(\gamma)$ cross section with the ISR method by BaBar [175]

[11] The corresponding contribution to a_e reads $a_e^{(4)}(\text{vap, had}) = (1.860 \pm 0.015) \times 10^{-12}$. Since the kernel Eq. (112) of the integral Eq. (109) also depends on the lepton mass, the result does not scale with $(m_e/m_\mu)^2$ but is about 15% larger.

[12] In the common KLOE energy range (591.6,969.5) MeV individual contributions for $a_\mu^{(4)}$(vap, had) based on the latest [2004/2008] data are: 387.20(0.50)(3.30) [KLOE], 392.64(1.87)(3.14) [CMD-2] and 390.47(1.34)(5.08) [SND].

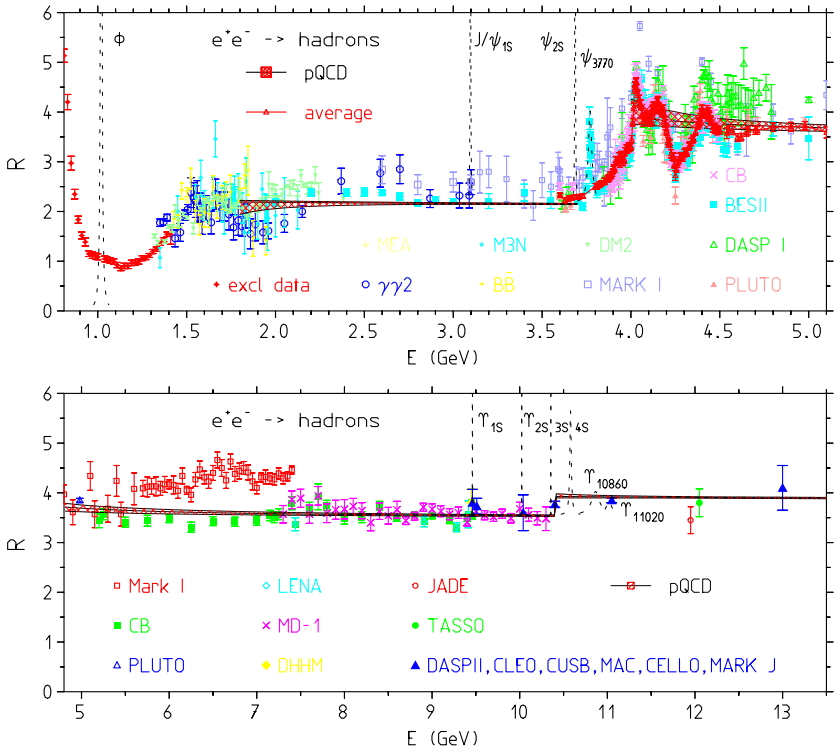

Fig. 22. Experimental results for $R_\gamma^{\rm had}(s)$ in the range 1 GeV $< E = \sqrt{s} <$ 13 GeV, obtained at the various e^+e^- storage rings. The perturbative quark–antiquark production cross–section is also displayed (pQCD). Parameters: $\alpha_s(M_Z) = 0.118 \pm 0.003$, $M_c = 1.6 \pm 0.15$ GeV, $M_b = 4.75 \pm 0.2$ GeV and the $\overline{\rm MS}$ scale varied in the range $\mu \in (\sqrt{s}/2, 2\sqrt{s})$.

once more reveals large (in comparison with the claimed experimental errors) discrepancies with respect to previous results. The integrated result yields a shift $\delta a_\mu^{\rm had}(\pi\pi) \simeq +13.5 \times 10^{-10}$ and seems to be in much better agreement with corresponding results obtained from the τ spectral–functions (see below), however, the spectrum is much steeper (-10% at 0.5 GeV up to +10% at 1 GeV) than the one from ALEPH, for example. The new e^+e^-–based result agrees better (at $\pm$ 5% level) with the more recent Belle τ results. We will say more about the possibility to use τ data for the calculation of $a_\mu^{\rm had}$, below.

For the e^+e^-–based result (113), the size of contributions and squared errors from different energy regions are illustrated in Fig. 23.

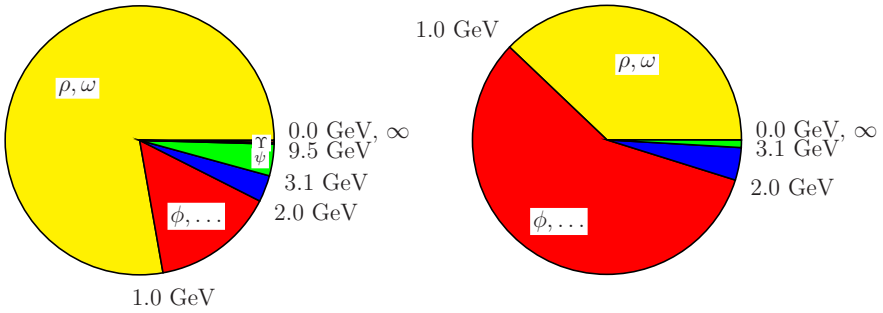

Fig. 23. The distribution of contributions (left) and errors (right) in % for $a_\mu^{(4)}$(vap, had) from different energy regions. The error of a contribution i shown is $\delta_{i\,\rm tot}^2 / \sum_i \delta_{i\,\rm tot}^2$ in %. The total error combines statistical and systematic errors in quadrature.

Some other recent evaluations are collected in Table 4. Differences in errors come about mainly by utilizing more "theory–driven" concepts : use of selected data sets only, extended use of perturbative QCD in place

Table 4
Some recent evaluations of $a_\mu^{(4)}$(vap, had).

$a_\mu^{(4)}$(vap, had) $\times 10^{10}$	data	Ref.
696.3[7.2]	e^+e^-	[177]
711.0[5.8]	$e^+e^- + \tau$	[177]
694.8[8.6]	e^+e^-	[178]
684.6[6.4]	e^+e^- TH	[179]
699.6[8.9]	e^+e^-	[180]
692.4[6.4]	e^+e^-	[181]

$a_\mu^{(4)}$(vap, had) $\times 10^{10}$	data	Ref.
693.5[5.9]	e^+e^-	[182]
701.8[5.8]	$e^+e^- + \tau$	[182]
690.9[4.4]	e^+e^{-**}	[183]
689.4[4.6]	e^+e^{-**}	[184]
692.1[5.6]	e^+e^{-**}	[160]
690.3[5.3]	e^+e^{-**}	[174]

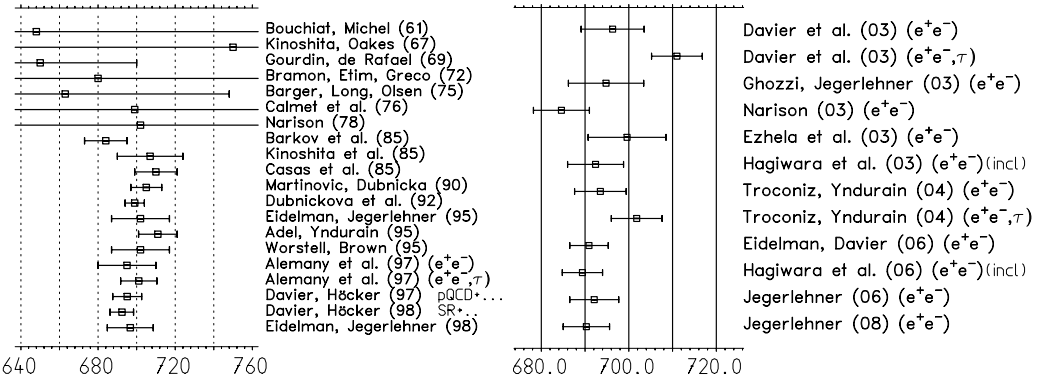

Fig. 24. History of evaluations before 2000 (left) [73]–[76],[185]–[188],[79]–[81],[189,190,83], [161]–[166], and some more recent ones (right) [177]–[184], [160,174]; $(e^+e^-) = e^+e^-$–data based, (e^+e^-,τ) = in addition include data from τ spectral functions (see Sect. 4.1.2).

of data [assuming local duality], sum rule methods, low energy effective methods [176]. The last four (**) results include the recent data from SND, CMD-2, and BaBar. The last update also includes the most recent data from BaBar [173] and KLOE [170].

There have been many independent evaluations of $a_\mu^{(4)}$(vap, had) in the past [13] and some of the more recent ones are listed in Table 4. Fig. 24 gives a fairly complete history of the evaluations based on e^+e^-–data.

Before we will continue with a discussion of the higher order hadronic contributions, we first present additional details about what precisely goes into the DR Eq. (109) and briefly discuss some issues concerning the determination of the required hadronic cross–sections.

4.1.1. *Dispersion Relations and Hadronic e^+e^-–Annihilation Cross Sections*

To leading order in α, the hadronic "blob" in Fig. 19 has to be identified with the photon self–energy function $\Pi_\gamma^{\prime\,\mathrm{had}}(s)$. The latter we may relate to the cross–section $e^+e^- \to$ hadrons by means of the DR Eq. (101) which derives from the correspondence Fig. 25 based on unitarity (optical theorem) and causality (analyticity), as elaborated earlier. Note that $\Pi_\gamma^{\prime\,\mathrm{had}}(q^2)$ is a one particle irreducible (1PI) object, represented by diagrams which cannot be cut into two disconnected parts by cutting a single photon line. At low energies the imaginary part is related to intermediate hadronic states like $\pi^0\gamma, \rho, \omega, \phi, \cdots, \pi\pi, 3\pi, 4\pi, \cdots, \pi\pi\gamma, , \cdots, KK, KK\pi\cdots$ which in the DR correspond to the states produced in e^+e^-–annihilation via a virtual photon. At least one hadron plus any strong, electromagnetic or weak interaction contribution counts.

[13] The method how to calculate hadronic vacuum polarization effects in terms of hadronic cross–sections was developed long time ago by Cabibbo and Gatto [72]. First estimations were performed in [73]–[76],[185,188]. As cross–section measurements made further progress much more precise estimates became possible in the mid 80's [79]–[81]. A more detailed analysis based on a complete up–to–date collection of data followed about 10 years later [83].

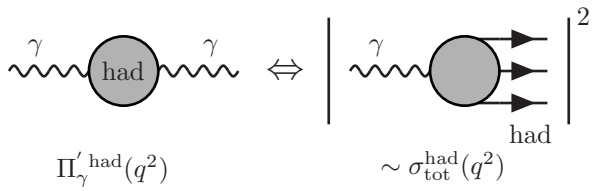

Fig. 25. Optical theorem for the hadronic contribution to the photon propagator.

e^+e^-–data in principle may be used up to energies where $\gamma - Z$ interference comes into play above about 40 GeV.

Experimentally, what is determined is of the form

$$R^{\mathrm{exp}}_{\mathrm{had}}(s) = \frac{N_{\mathrm{had}}\,(1+\delta_{\mathrm{RC}})}{N_{\mathrm{norm}}\,\varepsilon}\,\frac{\sigma_{\mathrm{norm}}(s)}{\sigma_{\mu\mu,\,0}(s)}\,,$$

where N_{had} is the number of observed hadronic events, N_{norm} is the number of observed normalizing events, ε is the detector efficiency–acceptance product of hadronic events while δ_{RC} are radiative corrections to hadron production. $\sigma_{\mathrm{norm}}(s)$ is the physical cross–section for normalizing events, including all radiative corrections integrated over the acceptance used for the luminosity measurement, and $\sigma_{\mu\mu,\,0}(s) = 4\pi\alpha^2/3s$ is the normalization. This also shows that a precise measurement of $R(s)$ requires precise knowledge of the relevant radiative corrections.

Radiation effects may be used to measure $\sigma_{\mathrm{had}}(s')$ at all energies $\sqrt{s'}$ lower than the fixed energy $\sqrt{s}$ at which an accelerator is running [191]. This is possible due to initial state radiation (ISR), which can lead to huge effects for kinematical reasons. The relevant *radiative return* (RR) mechanism is illustrated in Fig. 26: in the radiative process $e^+e^- \to \pi^+\pi^-\gamma$, photon radiation from the initial state reduces the invariant mass from s to $s' = s\,(1-k)$ of the produced final state, where k is the fraction of energy carried away by the photon radiated from the initial state. Such RR cross-section measurements are particularly interesting for machines running on–resonance like the ϕ– and B–factories, which have enhanced event rates as they are running on top of a peak [192,193,194]. The first dedicated RR experiment has been performed by KLOE at DAΦNE/Frascati, by measuring the $\pi^+\pi^-$ cross–section [86,170] (see Fig. 21 and Refs. [195,196]).

Results for exclusive multi–hadron production channels from BaBar play an important role in the energy range between 1.4 to 2 GeV. In fact new data became available for most of the channels of the exclusive measurements in this region. In contrast the inclusive measurements date back to the early 1980's and show much larger uncertainties.

It is important to note that what we need in the DR is the 1PI "blob" which by itself is not what is measured, i.e. it is not a physical observable. In reality the virtual photon lines attached to the hadronic "blob" are dressed photons (full photon propagators which include all possible radiative corrections) and in order to obtain the 1PI part one has to undress the cross section by amputation of the full photon lines. The $e^+e^- \to$ hadrons transition amplitude is proportional to e^2 from the $e^+e^-\gamma^*$ and the $\gamma^* q\bar{q}$ (hadrons) vertices

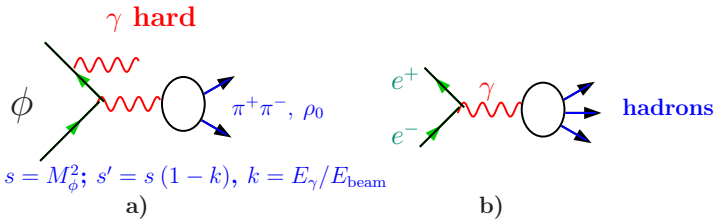

Fig. 26. a) Principle of the radiative return determination of the $\pi^+\pi^-$ cross–section by KLOE at the ϕ–factory DAΦNE. At the B–factory at SLAC, using the same mechanism, BaBar has measured many other channels at higher energies. b) Standard measurement of σ_{had} in an energy scan, by tuning the beam energy.

which in the cross section appears in quadrature $\propto e^4$ or α^2. Due to the running of the electromagnetic charge the physical (dressed) cross section is $\propto \alpha^2(s)$. Undressing requires to replace the running $\alpha(s)$ by the classical α:

$$\sigma_{\rm tot}^{(0)}(e^+e^- \to \text{hadrons}) = \sigma_{\rm tot}(e^+e^- \to \text{hadrons}) \left(\frac{\alpha}{\alpha(s)}\right)^2 \tag{114}$$

and, using Eq. (101) we obtain

$$\Pi'_\gamma(k^2) - \Pi'_\gamma(0) = \frac{k^2}{4\pi^2\alpha} \int\limits_0^\infty \mathrm{d}s \, \frac{\sigma_{\rm tot}^{(0)}(e^+e^- \to \text{hadrons})}{(s - k^2 - \mathrm{i}\varepsilon)} \quad . \tag{115}$$

It should be stressed that using the physical cross section in the DR gives a nonsensical result. In order to get the photon propagator we have to subtract in any case the effective charge from the external $e^+e^-\gamma$ vertex at the correct scale. Thus if we would use

$$\frac{k^2}{4\pi^2\alpha} \int\limits_0^\infty \mathrm{d}s \, \frac{\sigma_{\rm tot}(e^+e^- \to \text{hadrons})}{(s - k^2 - \mathrm{i}\varepsilon)}$$

we would be double counting the VP effects. In contrast with the linearly in $\alpha/\alpha(s)$ rescaled cross–section

$$\frac{k^2}{4\pi^2} \int\limits_0^\infty \mathrm{d}s \, \frac{1}{\alpha(s)} \frac{\sigma_{\rm tot}(e^+e^- \to \text{hadrons})}{(s - k^2 - \mathrm{i}\varepsilon)} \,, \tag{116}$$

we obtain the hadronic shift Eq. (70) for the full photon propagator.

Since what we need is the hadronic blob, in processes as displayed in Fig. 26, it is evident that a precise extraction of the desired object requires a subtraction of all radiative corrections not subsummed in the blob. Thus besides the VP effects, in particular, the initial state radiation (ISR) has to be subtracted. It is well known that photon radiation leads to infrared (IR) singularities if not virtual and real (soft) radiation are included on the same footing (Bloch-Nordsieck prescription). Thereby soft photon radiation has to be included at least up to energies $0 < E < E_{\rm cut}$ where $E_{\rm cut}$ is the detection threshold of the detector utilized. Any charged particle cross–section measurement requires some detector dependent cuts in photon phase space and the detector dependent radiation effects must be subtracted in order to obtain a detector independent meaningful physics cross–section. Besides the ISR there is final state radiation (FSR) as well as initial–final state interference effects, where the latter to leading order drop out in total cross sections for C symmetric cuts. While ISR from the e^+e^- initial state it calculable in QED to any desired order of precision, the calculation of the FSR for hadronic final states is not fully under control. In addition, experimentally it is not possible to distinguish ISR from FSR photons. Fortunately the most important channel contributing to $a_\mu^{(4)}$(vap, had) is the two–body $\pi^+\pi^-$ one and FSR usually is calculated in scalar QED (sQED) which however is appropriate only for relatively soft photons which see the pions as point particles. In fact a generalized version of sQED is applied where the point form–factor $F_\pi^{\rm point} = 1$ is replaced by the experimentally determined pion form–factor $F_\pi(s)$. The FSR contribution will be discussed in Sect. 4.2. On the level of the quarks the leading order FSR contribution would be given by the diagrams 19) to 21) of Fig. 10 and corresponds to the inclusion of the final state radiation correction of $R(s)$. The Kinoshita-Lee-Nauenberg (KLN) theorem infers that these fully inclusive corrections are not enhanced by any logarithms. This also infers that the model dependence of the FSR contribution is at worst moderate. For a more detailed discussion see Refs. [197]–[201] and references therein.

4.1.2. *Hadronic τ-Decays and Isospin Violations*

In principle, the $I = 1$ iso–vector part of $e^+e^- \to$ hadrons can be obtained in an alternative way by using the precise vector spectral functions from hadronic τ–decays $\tau \to \nu_\tau +$ hadrons which are related by an

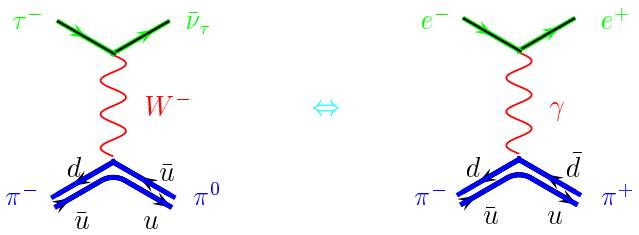

Fig. 27. τ–decay vs. e^+e^-–annihilation: the involved hadronic matrix–elements $\langle \text{out } \pi^+\pi^-|j_\mu^{I=1}(0)|0\rangle$ and $\langle \text{out } \pi^0\pi^-|J^-_{V\mu}(0)|0\rangle$ are related by isospin.

isospin rotation [202,163], like $\pi^0\pi^- \to \pi^+\pi^-$, as illustrated in Fig. 27 for the most relevant 2π channel. After isospin violating corrections, due to photon radiation and the mass splitting $m_d - m_u \neq 0$, have been applied, there remains an unexpectedly large discrepancy between the e^+e^-- and the τ-based determinations of a_μ [177], as may be seen in Table 4. Possible explanations are so far unaccounted isospin breaking [178] and/or experimental problems with the data. For example, FSR corrections in the charged current τ–channel are expected to be more model dependent than in the neutral e^+e^-–channel as they exhibit a much larger short distance sensitivity. Since the e^+e^--data are more directly related to what is required in the dispersion integral, one usually advocates to use the e^+e^- data only in the evaluation of $a_\mu^{(4)}(\text{vap, had})$.

Precise τ–spectral functions became available in 1997ff from ALEPH, OPAL and CLEO [203]–[205] and the idea to use the τ spectral data to improve the evaluation of the hadronic contributions a_μ^{had} was pioneered by Alemany, Davier and Höcker [163]. More recently an new measurement was presented by Belle [206]. Data sets for $|F_\pi|^2$ are displayed in Fig. 28. Taking into account the τ–data increases the contribution to a_μ^{had} by 2 σ (see Table 4 and Fig. 24). The unexpectedly large discrepancy between isospin rotated τ–data, corrected for isospin violations, and the direct e^+e^-–data remains one of the unsolved problems. This on the one hand means that doubts continue to exist that low energy hadronic cross–sections are sufficiently well under control, on the other hand a solution of the problem would contribute to reduce hadronic errors on $g-2$ predictions further.

For the dominating 2π channel, the precise relation we are talking about may be derived by comparing the relevant lowest order diagrams Fig. 27, which for the e^+e^- case translates into

$$\sigma_{\pi\pi}^{(0)} \equiv \sigma_0(e^+e^- \to \pi^+\pi^-) = \frac{4\pi\alpha^2}{s}\, v_0(s) \tag{117}$$

and for the τ case into

$$\frac{1}{\Gamma}\frac{d\Gamma}{ds}(\tau^- \to \pi^-\pi^0\nu_\tau) = \frac{6|V_{ud}|^2 S_{EW}}{m_\tau^2}\frac{B(\tau^- \to \nu_\tau\, e^-\,\bar{\nu}_e)}{B(\tau^- \to \nu_\tau\,\pi^-\pi^0)}\left(1-\frac{s}{m_\tau^2}\right)\left(1+\frac{2s}{m_\tau^2}\right) v_-(s), \tag{118}$$

where $|V_{ud}| = 0.9746 \pm 0.0006$ [103] denotes the CKM weak mixing matrix element and $S_{\text{EW}} = 1.0198 \pm 0.0006$ accounts for electroweak radiative corrections [208]–[212],[177]. The spectral functions are obtained from the corresponding invariant mass distributions. The $B(i)$'s are branching ratios, $B(\tau^- \to \nu_\tau\, e^-\,\bar{\nu}_e) = (17.810 \pm 0.039)\%$, $B(\tau^- \to \nu_\tau\,\pi^-\pi^0) = (25.471 \pm 0.129)\%$. SU(2) symmetry (CVC) would imply

$$v_-(s) = v_0(s) \quad . \tag{119}$$

The spectral functions $v_i(s)$ are related to the pion form factors $F_\pi^i(s)$ by

$$v_i(s) = \frac{\beta_i^3(s)}{12}|F_\pi^i(s)|^2 \quad ; \quad (i = 0, -), \tag{120}$$

where $\beta_i(s)$ is the pion velocity. The difference in phase space of the pion pairs gives rise to the relative factor $\beta^3_{\pi^-\pi^0}/\beta^3_{\pi^-\pi^+}$.

Before a precise comparison via Eq. (119) is possible all kinds of isospin breaking effects have to be taken into account. For the $\pi\pi$ channel the most relevant corrections have been investigated in [212,213]. The corrected version of Eq. (119) may be written in the form

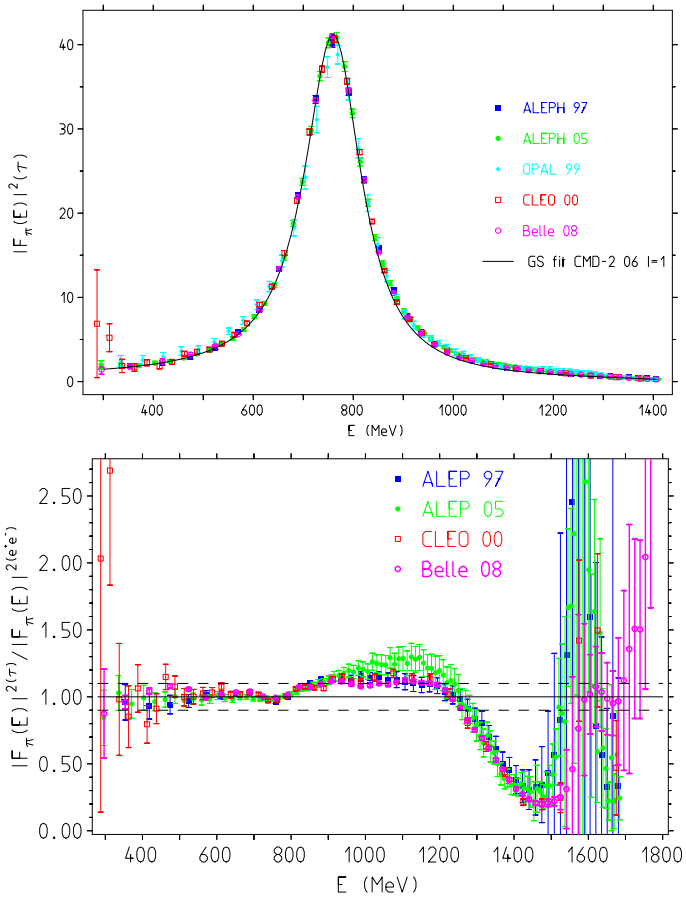

Fig. 28. Modulus square of the $I = 1$ pion form factor extracted from $\tau^{\pm} \to \nu_\tau \pi^{\pm} \pi^0$ which shows the $\rho^{\pm}$–resonance. The ratio $|F_\pi(E)|^2(\tau)/|F_\pi(E)|^2_{\rm fit}(e^+e^-[I=1])$ illustrates the missing consistency of the τ–data relative to a CMD-2 fit. Dashed horizontal lines mark ± 10% (see also [206,207]). Note that the reference fit line represents the e^+e^- data only below about 1 GeV (see Fig. 21). At higher energies data for $e^+e^- \to \pi^+\pi^-$ are rather poor, but old Orsay DM2 data as well as the new preliminary BaBar radiative return data [175] also exhibit the dip at 1.5 GeV, i.e. our "normalization" above 1 GeV is to be considered as arbitrary.

$$\sigma^{(0)}_{\pi\pi} = \left[\frac{K_\sigma(s)}{K_\Gamma(s)}\right] \frac{d\Gamma_{\pi\pi[\gamma]}}{ds} \times \frac{R_{\rm IB}(s)}{S_{\rm EW}}, \tag{121}$$

with

$$K_\Gamma(s) = \frac{G_F^2\,|V_{ud}|^2\,m_\tau^3}{384\pi^3}\left(1-\frac{s}{m_\tau^2}\right)^2\left(1+2\,\frac{s}{m_\tau^2}\right);\; K_\sigma(s) = \frac{\pi\alpha^2}{3s},$$

and the isospin breaking correction

$$R_{\rm IB}(s) = \frac{1}{G_{\rm EM}(s)}\,\frac{\beta^3_{\pi^-\pi^+}}{\beta^3_{\pi^-\pi^0}}\,\left|\frac{F_V(s)}{f_+(s)}\right|^2 \tag{122}$$

includes the QED corrections to $\tau^- \to \nu_\tau \pi^- \pi^0$ decay with virtual plus real soft and hard photon radiation integrated over all phase space.

Originating from Eq. (120), $\beta^3_{\pi^-\pi^+}/\beta^3_{\pi^-\pi^0}$ is a phase space correction due to the $\pi^{\pm} - \pi^0$ mass difference. $F_V(s) = F^0_\pi(s)$ is the neutral current (NC) vector form factor, which exhibits besides the $I = 1$ part an $I = 0$ contribution. The latter $\rho - \omega$ mixing term is due to the SU(2) breaking by the $m_d - m_u$ mass difference. Finally, $f_+(s) = F^-_\pi$ is the charged current (CC) $I = 1$ vector form factor. One of the leading

isospin breaking effects is the $\rho-\omega$ mixing correction included in $|F_V(s)|^2$. The form–factor corrections, in principle, also should include the electromagnetic shifts in the masses and the widths of the ρ's[14]. Up to this last mentioned effect, discussed in [178] (also see [214]), which was considered to be negligible in earlier isospin breaking estimates, all the corrections were applied in [177] but were not able to eliminate the observed discrepancy between $v_-(s)$ and $v_0(s)$. The deviation is starting at the peak of the ρ and is increasing with energy to about 10-20%. More precisely, Fig. 28 shows a good agreement below about 800 MeV, a 10% enhancement between 800 and 1200 MeV and a pronounced dip around 1500 MeV. The trend shown by the ALEPH 97 and CLEO data is clearly stressed by the new Belle measurement [206]. The Belle data differ substantially from the ALEPH 05 data, however, which lie higher by more than 10% in the intermediate range [+20% relative to e^+e^-].

We should mention here once more that photon radiation by hadrons is poorly understood theoretically. The commonly accepted recipe is to treat radiative corrections of the pions by scalar QED, except for the short distance (SD) logarithm proportional to $\ln M_W/m_\pi$ which is replaced by the quark parton model result and included in $S_{\rm EW}$ by convention. This SD log is present only in the weak charged current transition $W^{+*}\to\pi^+\pi^0\,(\gamma)$, while in the charge neutral electromagnetic current transition $\gamma^*\to\pi^+\pi^-\,(\gamma)$ this kind of leading log is absent. In any case there is an uncertainty in the correction of the isospin violations by virtual and real photon radiation which is hard to quantify. We also should stress that the possible isospin breaking resonance parameter shifts, like Δm_ρ and $\Delta\Gamma_\rho$, so far have not been determined unambiguously. Note, however, that the new Belle results [206] precisely confirm the earlier observed shifts in mass and width of the ρ [215,178], which could be part of the source of additional isospin violations.

A reason for the τ vs e^+e^- discrepancy could be the way (incoherent) the pure $I=1$ part (given by τ–data) is combined with the missing $I=0$ contribution (approximately separated out from the e^+e^--data). What is needed and what is measured in e^+e^- is the interference $|A_1(s)+A_0(s)|^2$ which in any case must be smaller than $|A_1(s)|^2+|A_0(s)|^2$. In any case, one has to keep in mind that isospin breaking can only have two origins: the m_u-m_d mass difference and electromagnetic effects and the latter require a small **positive** mass difference $m_{\rho^\pm}-m_{\rho^0}\sim 1$ MeV and similar for ρ' and ρ''. In fact, a fit of the data for the ρ yields a factor of 2 larger result, which maybe is a problem. It should be noted that the fits including several masses, widths and mixings are not very stable. In Ref. [216] effects of the ρ–ω–ϕ mixing on the dipion mass spectrum in e^+e^-–annihilation and τ–decay were analyzed within the HLS effective model and it was suggested that they could explain the observed isospin breakings. As a possibility one also may consider the case that the τ–data based evaluation of $a_\mu^{\rm had}$ is the more reliable one. The integrated data in the range $m_\pi-1.8$ GeV after applying known isospin violation corrections is given by

– Belle (τ) [206]

$$a_\mu^{\pi\pi}=(523.5\pm 1.5(\exp)\pm 2.6(\mathrm{Br})\pm 2.5(\mathrm{iso}))\times 10^{-10}\,, \tag{123}$$

– ALEPH, CLEO, OPAL (τ) [177]

$$a_\mu^{\pi\pi}=(520.1\pm 2.4(\exp)\pm 2.7(\mathrm{Br})\pm 2.5(\mathrm{iso}))\times 10^{-10}\,, \tag{124}$$

which compares to

– CMD2, SND (e^+e^-) [183]

$$a_\mu^{\pi\pi}=(504.6\pm 3.1(\exp)\pm 0.9(\mathrm{rad}))\times 10^{-10}\,, \tag{125}$$

where errors are the experimental ones (exp), from the normalizing branching fraction (Br), from isospin breaking corrections (iso) and from radiative corrections (rad). Including τ data shifts the theoretical prediction by $\delta a_\mu^{\rm had}\simeq +17.9\times 10^{-10}$ thus would improve the agreement between theory and experiment for a_μ

[14] Because of the strong resonance enhancement, especially in the ρ region, a small isospin breaking shift in mass and width between ρ^0 and $\rho^\pm$, typically $\Delta m_\rho=m_{\rho^\pm}-m_{\rho^0}\sim 2.5$ MeV and $\Delta\Gamma_\rho=\Gamma_{\rho^\pm}-\Gamma_{\rho^0}\sim 1.5$ MeV and similar shifts for the higher resonances ρ', ρ'' and the mixing amplitudes of these states, causes a large effect in the tails by the kinematical shift this implies.

to the 1.2 σ level, see Sect. 7. However, using the τ–data would also increase the "gap" between a too low value of indirect Higgs mass determinations in comparison with the known direct lower bound. This does certainly not support the idea that the τ–data based evaluation is more likely to be the correct choice [217].

4.1.3. *Perturbative QCD Contributions*

The high energy tail of the basic dispersion integral Eq. (109) can safely be calculated in pQCD because of the *asymptotic freedom* of QCD. The latter property infers that the effective strong interaction constant $\alpha_s(s)$ gets weaker the higher the energy scale $E = \sqrt{s}$, and we may calculate the hadronic current correlators in perturbation theory as a power series in α_s/π. The object of interest is

$$\rho(s) = \frac{1}{\pi}\mathrm{Im}\,\Pi'_\gamma(s)\;;\;\; \Pi^{\mu\nu}_\gamma(q) = (q^\mu q^\nu - q^2 g^{\mu\nu})\,\Pi'_\gamma(q^2):$$  . (126)

The QCD perturbation expansion diagrammatically is given by

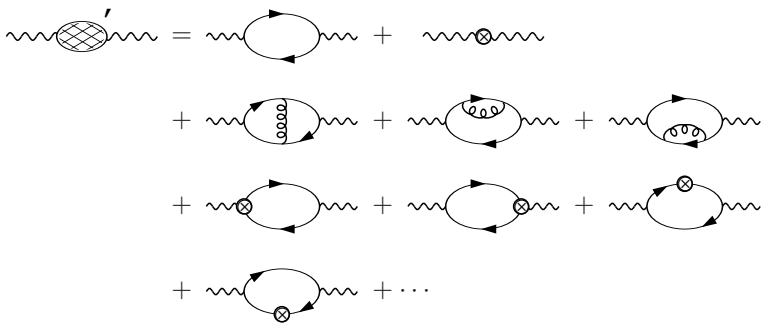

Lines ~~~ show external photons, ⟶ propagating quarks/antiquarks and ∿∿∿ propagating gluons. The vertices ⊗ are marking renormalization counter term insertions. They correspond to subtraction terms which render the divergent integrals finite.

Perturbative vacuum polarization effects were first discussed by Dirac [218] in QED (for photons and electrons in place of gluons and quarks) and finally unambiguously calculated at the 1–loop level by Schwinger [219] and Feynman [220]. Soon later Jost and Luttinger [221] presented the first 2–loop calculation.

In zeroth order in the strong coupling α_s we have

$2\,\mathrm{Im}$ 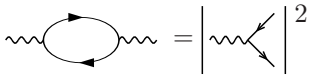

which is proportional to the the free quark–antiquark production cross–section [222] in the so called *Quark Parton Model*, describing quarks with the strong interactions turned off. Because of asymptotic freedom this picture should be a good approximation asymptotically in the high energy limit of QCD. In pQCD, of course, we only can calculate the $q\bar{q}$ ($q = u, d, s, \cdots$) production cross–section and not the physical hadron production cross–section $\sigma_{\mathrm{tot}}(e^+e^- \to \gamma^* \to \mathrm{hadrons})$ itself. In this case the R function corresponding to Eq. (106) is defined by

$$R(s)^{\mathrm{pert}} \doteq \frac{\sigma_{\mathrm{tot}}(e^+e^- \to \gamma^* \to \sum_q q\bar{q},\, q\bar{q}g, \cdots)}{\frac{4\pi\alpha^2}{3s}} = \frac{12\pi^2}{e^2}\rho(s)^{\mathrm{pert}}\,, \tag{127}$$

which for sufficiently large s can be calculated perturbatively. The result is given by [223,224,225,226]

$$R(s)^{\mathrm{pert}} = N_c \sum_q Q_q^2\,\frac{v_q}{2}\,\left(3 - v_q^2\right)\,\Theta(s - 4m_q^2)\left\{1 + ac_1(v_q) + a^2c_2 + a^3c_3 + a^4c_4\cdots\right\}, \tag{128}$$

where $a = \alpha_s(s)/\pi$ and, assuming $4m_q^2 \ll s$, i.e. in the massless approximation

$$
\begin{aligned}
c_1 &= 1, \\
c_2 &= C_2(R)\,\left[-\frac{3}{32}\,C_2(R) - \frac{3}{4}\beta_0\,\zeta(3) - \frac{33}{48}\,N_q + \frac{123}{32}\,N_c\right] \\
&= \frac{365}{24} - \frac{11}{12}\,N_q - \beta_0\,\zeta(3) \simeq 1.9857 - 0.1153\,N_q, \\
c_3 &= -6.6368 - 1.2002\,N_q - 0.0052\,N_q^2 - 1.2395\,(\sum_q Q_q)^2/(3\sum_q Q_q^2), \\
c_4 &= -0.010\,N_q^3 \,+\, 1.88\,N_q^2 \,-\, 34.4\,N_q \,+\, 135.8 - \pi^2\beta_0^2\left(1.9857 - 0.1153\,N_q + \frac{5\beta_1}{6\beta_0}\right),
\end{aligned}
$$

in the $\overline{\rm MS}$ scheme. $N_q = \sum_{q:4m_q^2\le s} 1$ is the number of active quark flavors. The mass dependent threshold factor in front of the curly brackets in Eq. (128) is a function of the velocity $v_q = \left(1 - \frac{4m_q^2}{s}\right)^{1/2}$ and the exact mass dependence of the first correction term

$$
c_1(v_q) = \frac{2\pi^2}{3v_q} - (3+v_q)\left(\frac{\pi^2}{6} - \frac{1}{4}\right)
$$

is singular (Coulomb singularity due to soft gluon final state interaction) at threshold. The singular terms exponentiate [227]:

$$
\begin{aligned}
1 + x &\to \frac{2x}{1-{\rm e}^{-2x}}\;;\;\; x = \frac{2\pi\alpha_s}{3\beta}\,, \\
\left(1 + c_1(v_q)\,\frac{\alpha_s}{\pi} + \cdots\right) &\to \left(1 + c_1(v_q)\,\frac{\alpha_s}{\pi} - \frac{2\pi\alpha_s}{3v_q}\right)\,\frac{4\pi\alpha_s}{3v_q}\,\frac{1}{1-\exp\left\{-\frac{4\pi\alpha_s}{3v_q}\right\}}\,.
\end{aligned}
$$

In the ranges where we apply pQCD the strength of the coupling is still substantial. This requires renormalization group improvement of perturbative predictions. Thus, as usual, the coupling α_s and the masses m_q have to be understood as running parameters:

$$
R\left(\frac{m_{0q}^2}{s_0}, \alpha_s(s_0)\right) = R\left(\frac{m_q^2(\mu^2)}{s}, \alpha_s(\mu^2)\right)\;;\;\; \mu = \sqrt{s},
$$

where $\sqrt{s_0}$ is a reference energy. Mass effects are important once one approaches a threshold from the perturbatively save region sufficiently far above the thresholds. They have been calculated up to three loops by Chetyrkin, Kühn and collaborators [228] and have been implemented in the FORTRAN routine `RHAD` by Harlander and Steinhauser [229].

Where can we trust the perturbative result? In the complex s–plane, perturbative QCD is supposed to work best in the deep Euclidean region away from the physical region characterized by a cut along the positive real axis for $s > s_0 = 4m^2$ where m is the mass of the lightest particles which can be pair–produced. Fortunately, the physical region to a large extent is accessible to pQCD as well provided the energy scale is sufficiently large and one looks for the appropriate observable.

The imaginary part corresponds to the jump of the vacuum polarization function $\Pi'(q^2)$ across the cut. On the cut we have the thresholds of the physical states, with lowest lying channels: $\pi^+\pi^-$, $\pi^0\pi^+\pi^-$, $\cdots$ and resonances ρ, ω, ϕ, $J/\psi\cdots$, $\Upsilon\cdots$, $\cdots$. QCD is confining the quarks inside hadrons. In any case the quarks *hadronize*, a non–perturbative phenomenon which is poorly understood in detail. Neither the physical *thresholds* nor the *resonances* are obtained with perturbation theory! In particular, the perturbative quark–pair thresholds in Eq. (128) do not nearly approximate the physical thresholds for the low energy region below about 2 GeV. At higher energies pQCD works sufficiently far away from thresholds and resonances, i.e. in regions where $R(s)$ is a slowly varying function. Fig. 22 shows the e^+e^-–data together with the

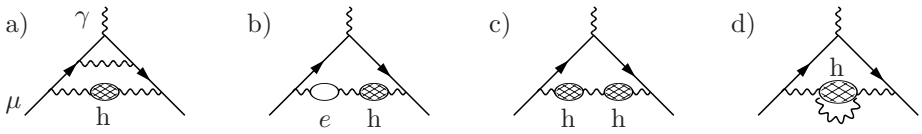

Fig. 29. Hadronic higher order VP contributions: a)-c) involving LO vacuum polarization, d) involving HO vacuum polarization (FSR of hadrons).

perturbative QCD prediction. Less problematic is the space–like (Euclidean) region $-q^2 \to \infty$, since it is away from thresholds and resonances.

The time–like quantity $R(s)$ intrinsically is non-perturbative and exhibits bound states, resonances, instanton effects (η') and in particular the hadronization of the quarks. In applying pQCD to describe real physical cross–sections of hadro–production one needs a "rule" which bridges the asymptotic freedom regime with the confinement regime, since the hadronization of the colored partons produced in the hard kicks into color singlet hadrons eludes a quantitative understanding. The rule is referred to as *quark hadron duality* [15] [231,232], which states that for large s the average non–perturbative hadron cross–section equals the perturbative quark cross–section:

$$\overline{\sigma(e^+e^- \to \text{hadrons})}(s) \simeq \sum\nolimits_q \sigma(e^+e^- \to q\bar{q}, q\bar{q}g, \cdots)(s) \ , \tag{129}$$

where the averaging extends from the hadron production threshold up to s–values which must lie sufficiently far above the quark–pair production threshold (global duality). Qualitatively, such a behavior is visible in the data Fig. 22 above about 2 GeV between the different flavor thresholds sufficiently above the lower threshold. A glance at the region from 4 to 5 GeV gives a good flavor of duality at work. Note however that for precise reliable predictions it has not yet been possible to quantify the accuracy of the duality conjecture. A quantitative check would require much more precise cross–section measurements than the ones available today. Ideally, one should attempt to reach the accuracy of pQCD predictions. In addition, in dispersion integrals the cross–sections are weighted by different s–dependent kernels, while the duality statement is claimed to hold for weight unity. One procedure definitely is contradicting duality reasonings: to "take pQCD plus resonances" or to "take pQCD where $R(s)$ is smooth and data in the complementary ranges". Also adjusting the normalization of experimental data to conform with pQCD within energy intervals (assuming local duality) has no solid foundation. Nevertheless, the application of pQCD in the regions advocated in [229] seems to be on fairly solid ground on a phenomenological level. A more conservative use of pQCD is possible by going to the Euclidean region and applying the Adler function [233] method as proposed in Refs. [234,165,235]. As mentioned earlier, the low energy structure of QCD also exhibits non–perturbative quark condensates. The latter also yield contributions to $R(s)$, which for large energies are calculable by the operator product expansion of the current correlator Eq. (64) [236]. The corresponding $\langle m_q\bar{q}q\rangle/s^2$ power corrections in fact are small at energies where pQCD applies [234,82] and hence not a problem in our context.

4.2. *Higher Order Hadronic Vacuum Polarization Corrections*

At order $O(\alpha^3)$ there are several classes of hadronic VP contributions with typical diagrams shown in Fig. 29. They have been estimated first in [187]. Classes (a) to (c) involve leading hadronic VP insertions and may be treated using DRs together with experimental e^+e^-–annihilation data. Class (d) involves leading QED corrections of the charged hadrons and correspond to the inclusion of hadronic final state radiation (FSR).

The $O(\alpha^3)$ hadronic contributions from classes (a), (b) and (c) may be evaluated without particular problems as described in the following.

[15] Quark–hadron duality was first observed phenomenologically for the structure function in deep inelastic electron–proton scattering [230].

At the 3–loop level all diagrams of Fig. 10 which involve closed muon–loops are contributing to the hadronic corrections when at least one muon–loop is replaced by a quark–loop dressed by strong interactions mediated by virtual gluons.
Class (a) consists of a subset of 12 diagrams of Fig. 10: diagrams 7) to 18) plus 2 diagrams obtained from diagram 22) by replacing one muon–loop by a hadronic "bubble", and yields a contribution of the type

$$a_\mu^{(6)[(a)]} = \left(\frac{\alpha}{\pi}\right)^3 \frac{2}{3} \int\limits_{4m_\pi^2}^{\infty} \frac{\mathrm{d}s}{s}\, R(s)\, K^{[(a)]}\left(s/m_\mu^2\right), \tag{130}$$

where $K^{[(a)]}(s/m_\mu^2)$ is a QED function which was obtained analytically by Barbieri and Remiddi [90]. The kernel function is the contribution to a_μ of the 14 two–loop diagrams obtained from diagrams 1) to 7) of Fig. 9 by replacing one of the two photons by a "heavy photon" of mass $\sqrt{s}$. The convolution Eq. (130) then provides the insertion of a photon self–energy part into the photon line represented by the "heavy photon" according to the method outlined after Eq. (66). While the exact expressions are given in [90] some sufficiently precise handy approximations have been given by Krause [237] in form of an expansion up to fourth order in m^2/s which reads

$$\begin{aligned} K^{[(a)]}(s/m^2) = \frac{m^2}{s}\Bigg\{ & \left[\frac{223}{54} - 2\zeta(2) - \frac{23}{36}\ln\frac{s}{m^2}\right] \\ & + \frac{m^2}{s}\left[\frac{8785}{1152} - \frac{37}{8}\zeta(2) - \frac{367}{216}\ln\frac{s}{m^2} + \frac{19}{144}\ln^2\frac{s}{m^2}\right] \\ & + \frac{m^4}{s^2}\left[\frac{13072841}{432000} - \frac{883}{40}\zeta(2) - \frac{10079}{3600}\ln\frac{s}{m^2} + \frac{141}{80}\ln^2\frac{s}{m^2}\right] \\ & + \frac{m^6}{s^3}\left[\frac{2034703}{16000} - \frac{3903}{40}\zeta(2) - \frac{6517}{1800}\ln\frac{s}{m^2} + \frac{961}{80}\ln^2\frac{s}{m^2}\right]\Bigg\}\,. \end{aligned} \tag{131}$$

Here m is the mass of the external lepton, $m = m_\mu$ in our case. The expanded approximation is more practical for the evaluation of the dispersion integral, because it is numerically more stable in general.
Class (b) consists of 2 diagrams only, obtained from diagram 22) of Fig. 10, and one may write this contribution in the form

$$a_\mu^{(6)[(b)]} = \left(\frac{\alpha}{\pi}\right)^3 \frac{2}{3} \int\limits_{4m_\pi^2}^{\infty} \frac{\mathrm{d}s}{s} R(s)\, K^{[(b)]}(s/m_\mu^2), \tag{132}$$

with

$$K^{[(b)]}(s/m_\mu^2) = \int\limits_0^1 \mathrm{d}x\, \frac{x^2\,(1-x)}{x^2 + (1-x)\,s/m_\mu^2} \left[-\hat{\Pi}_\gamma^{'\,e}\left(-\frac{x^2}{1-x}\frac{m_\mu^2}{m_e^2}\right)\right], \tag{133}$$

where we have set $\Pi^{'} = \frac{\alpha}{\pi}\hat{\Pi}^{'}$. Using Eq. (74) with $z = -\frac{x^2}{1-x}\frac{m_\mu^2}{m_e^2}$, we have

$$\hat{\Pi}_\gamma^{'\,e}(z) = \frac{8}{9} - \frac{\beta^2}{3} + \left(\frac{1}{2} - \frac{\beta^2}{6}\right)\beta \ln\frac{\beta-1}{\beta+1} \quad \text{with} \quad \beta = \sqrt{1 + 4\frac{1-x}{x^2}\frac{m_e^2}{m_\mu^2}}\,.$$

Here the kernel function is the contribution to a_μ of the 2 two–loop diagrams obtained from diagram 8) of Fig. 9 by replacing one of the two photons by a "heavy photon" of mass $\sqrt{s}$.

In diagram b) $m_f^2/m^2 = (m_e/m_\mu)^2$ is very small and one may expand β in terms of this small parameter. The expansion of Eq. (133) to fifth order in m^2/s and to first order in m_f^2/m^2 is given by

$$
\begin{aligned}
K^{[(b)]}(s) = \frac{m^2}{s}\Bigg\{ & \left(-\frac{1}{18}+\frac{1}{9}\ln\frac{m^2}{m_f^2}\right) \\
& +\frac{m^2}{s}\left(-\frac{55}{48}+\frac{\pi^2}{18}+\frac{5}{9}\ln\frac{s}{m_f^2}+\frac{5}{36}\ln\frac{m^2}{m_f^2}-\frac{1}{6}\ln^2\frac{s}{m_f^2}+\frac{1}{6}\ln^2\frac{m^2}{m_f^2}\right) \\
& +\frac{m^4}{s^2}\left(-\frac{11299}{1800}+\frac{\pi^2}{3}+\frac{10}{3}\ln\frac{s}{m_f^2}-\frac{1}{10}\ln\frac{m^2}{m_f^2}-\ln^2\frac{s}{m_f^2}+\ln^2\frac{m^2}{m_f^2}\right) \\
& -\frac{m^6}{s^3}\left(\frac{6419}{225}-\frac{14}{9}\pi^2+\frac{76}{45}\ln\frac{m^2}{m_f^2}-\frac{14}{3}\ln^2\frac{m^2}{m_f^2}-\frac{140}{9}\ln\frac{s}{m_f^2}+\frac{14}{3}\ln^2\frac{s}{m_f^2}\right) \\
& -\frac{m^8}{s^4}\left(\frac{53350}{441}-\frac{20}{3}\pi^2+\frac{592}{63}\ln\frac{m^2}{m_f^2}-20\ln^2\frac{m^2}{m_f^2}-\frac{200}{3}\ln\frac{s}{m_f^2}+20\ln^2\frac{s}{m_f^2}\right)\Bigg\} \\
& +\frac{m_f^2}{m^2}\left[\frac{m^2}{s}-\frac{2}{3}\frac{m^4}{s^2}-\frac{m^6}{s^3}\left(-2\ln\frac{s}{m^2}+\frac{25}{6}\right)-\frac{m^8}{s^4}\left(-12\ln\frac{s}{m^2}+\frac{97}{5}\right)\right. \\
& \left. -\frac{m^{10}}{s^5}\left(-56\ln\frac{s}{m^2}+\frac{416}{5}\right)\right] . \qquad (134)
\end{aligned}
$$

If we neglect terms $\mathcal{O}(\frac{m_f^2}{m^2})$ the x–integration in Eq. (133) may be performed analytically with the result [237]

$$
\begin{aligned}
K^{[(b)]}(s) = & -\left(\frac{5}{9}+\frac{1}{3}\ln\frac{m_f^2}{m^2}\right)\times\Bigg\{\frac{1}{2}-(x_1+x_2) \\
& +\frac{1}{x_1-x_2}\left[x_1^2(x_1-1)\ln\left(\frac{-x_1}{1-x_1}\right)-x_2^2(x_2-1)\ln\left(\frac{-x_2}{1-x_2}\right)\right]\Bigg\}-\frac{5}{12} \\
& +\frac{1}{3}(x_1+x_2)+\frac{1}{3(x_1-x_2)}\left\{x_1^2(1-x_1)\left[\mathrm{Li}_2\left(\frac{1}{x_1}\right)-\frac{1}{2}\ln^2\left(\frac{-x_1}{1-x_1}\right)\right]\right. \\
& \left. -x_2^2(1-x_2)\left[\mathrm{Li}_2\left(\frac{1}{x_2}\right)-\frac{1}{2}\ln^2\left(\frac{-x_2}{1-x_2}\right)\right]\right\} , \qquad (135)
\end{aligned}
$$

with $x_{1,2}=\frac{1}{2}(b\pm\sqrt{b^2-4b})$ and $b=s/m^2$.
Class (c) includes the double hadronic VP insertion, which is given by

$$
a_\mu^{(6)[(c)]} = \left(\frac{\alpha}{\pi}\right)^3\frac{1}{9}\int\limits_{4m_\pi^2}^{\infty}\frac{\mathrm{d}s}{s}\frac{\mathrm{d}s'}{s'}R(s)\,R(s')\,K^{[(c)]}(s,s'), \qquad (136)
$$

where

$$
K^{[(c)]}(s,s') = \int\limits_0^1 \mathrm{d}x\,\frac{x^4\,(1-x)}{[x^2+(1-x)\,s/m_\mu^2][x^2+(1-x)\,s'/m_\mu^2]} .
$$

This integral may be performed analytically. Setting $b=s/m^2$ and $c=s'/m^2$ one obtains for $b\neq c$

$$
\begin{aligned}
K^{[(c)]}(s,s') = & \frac{1}{2}-b-c-\frac{(2-b)\,b^2\,\ln(b)}{2\,(b-c)}-\frac{b^2\,\left(2-4\,b+b^2\right)\,\ln(\frac{b+\sqrt{-(4-b)\,b}}{b-\sqrt{-(4-b)\,b}})}{2\,(b-c)\,\sqrt{-(4-b)\,b}} \\
& -\frac{(-2+c)\,c^2\,\ln(c)}{2\,(b-c)}+\frac{c^2\,\left(2-4\,c+c^2\right)\,\ln(\frac{c+\sqrt{-(4-c)\,c}}{c-\sqrt{-(4-c)\,c}})}{2\,(b-c)\,\sqrt{-(4-c)\,c}} , \qquad (137)
\end{aligned}
$$

Table 5
Higher order contributions from diagrams a) - c) (in units 10^{-11}). Note that errors between contributions a) and b) are 100% anticorrelated, and the contribution c) is suppressed. The error of $a_\mu^{(6)}$(vap, had) is also close to 100% anticorrelated to the one of the leading term $a_\mu^{(4)}$(vap, had).

$a_\mu^{(6)[(a)]}$	$a_\mu^{(6)[(b)]}$	$a_\mu^{(6)[(c)]}$	$a_\mu^{(6)}$(vap, had)	Ref.
-199(4)	107(3)	2.3(0.6)	-90(5)	[79]
-211(5)	107(2)	2.7(0.1)	-101(6)	[237]
-209(4)	106(2)	2.7(1.0)	-100(5)	[163]
-207.3(1.9)	106.0(0.9)	3.4(0.1)	-98(1)	[181,184]
-207.5(2.0)	104.2(0.9)	3.0(0.1)	-100.3 (1.1)	[160]

and for $b = c$

$$K^{[(c)]}(s,s') = \frac{1}{2} - 2\,c + \frac{c}{2}\,(-2 + c - 4\,\ln(c) + 3\,c\,\ln(c)) + \frac{c\,\left(-2 + 4\,c - c^2\right)}{2(-4+c)} + \frac{c\,\left(12 - 42\,c + 22\,c^2 - 3\,c^3\right)\,\ln(\frac{c+\sqrt{(-4+c)\,c}}{c-\sqrt{(-4+c)\,c}})}{2\,(-4+c)\,\sqrt{(-4+c)\,c}}\,. \tag{138}$$

Results obtained by different groups, for so far unaccounted higher order vacuum polarization effects, are collected in Table 5. We will adopt the estimate [16]

$$a_\mu^{(6)}(\text{vap, had}) = (-100.3 \pm 1.1)\,\times 10^{-11} \tag{139}$$

obtained with the compilation [160].

Class (d) exhibits 3 diagrams (diagrams 19) to 21) of Fig. 10 and corresponds to the leading hadronic contribution with $R(s)$ corrected for final state radiation. We thus may write this correction by replacing

$$R(s) \to R(s)\,\eta(s)\,\frac{\alpha}{\pi} \tag{140}$$

in the basic integral Eq. (109). This correction is particularly important for the dominating two pion channel for which $\eta(s)$ may be calculated in scalar QED. The result reads [238,239]

$$\begin{aligned}\eta(s) = \frac{1+\beta_\pi^2}{\beta_\pi}\Bigg\{ & 4\mathrm{Li}_2\left(\frac{1-\beta_\pi}{1+\beta_\pi}\right) + 2\mathrm{Li}_2\left(-\frac{1-\beta_\pi}{1+\beta_\pi}\right) \\ & -3\log\left(\frac{2}{1+\beta_\pi}\right)\,\log\left(\frac{1+\beta_\pi}{1-\beta_\pi}\right) - 2\log(\beta_\pi)\,\log\left(\frac{1+\beta_\pi}{1-\beta_\pi}\right)\Bigg\} \\ & -3\log\left(\frac{4}{1-\beta_\pi^2}\right) - 4\log(\beta_\pi) \\ & +\frac{1}{\beta_\pi^3}\left[\frac{5}{4}(1+\beta_\pi^2)^2 - 2\right]\,\log\left(\frac{1+\beta_\pi}{1-\beta_\pi}\right) + \frac{3}{2}\frac{1+\beta_\pi^2}{\beta_\pi^2}\,,\end{aligned} \tag{141}$$

and provides a good measure for the dependence of the FSR on the pion mass. Neglecting the pion mass is obviously equivalent to taking the high energy limit $\eta(s \to \infty) = 3$. As sQED treats the pions as point–like particles the hard part of the spectrum, where photons couple to quarks rather than to the hadron,

[16] Our evaluation of the contribution to a_e is $a_e^{(6)}(\text{vap, had}) = (-0.223 \pm 0.002) \times 10^{-12}$. The result is dominated by the diagram Fig. 29a) which now includes the electron loop, while diagram b) includes the muon loop and is suppressed by a factor $(m_e/m_\mu)^2$. A similar suppression factor applies for the other diagrams (see also [237]).

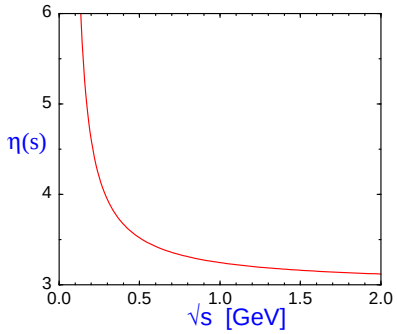

Fig. 30. The FSR correction factor $\eta(s)$ as a function of the c.m. energy $\sqrt{s}$.

is certainly not taken into account properly. Since we are not able to unambiguously calculate radiation from strongly bound systems one should focus much more on direct measurements of the spectrum [201]. In Fig. 30 the sQED correction $\eta(s)$ is plotted as a function of the center of mass energy. We observe that for energies below 1 GeV the pion mass leads to a considerable enhancement of the FSR corrections. Regarding the desired precision, ignoring the pion mass would therefore lead to wrong results. As usual, close to the threshold of charged particle production the Coulomb force between the two final state particles leads to substantial corrections. In this limit ($s \simeq 4m_\pi^2$) the factor $\eta(s)$ becomes singular [$\eta(s) \to \pi^2/2\beta_\pi$] which means that the $O(\alpha)$ result for the FSR correction cannot be trusted anymore. Fortunately, the singular terms are known to all orders of perturbation theory and can be resummed. In fact the leading terms exponentiate and one obtains [238]:

$$R^{(\gamma)}(s) = R(s) \left(1 + \eta(s)\frac{\alpha}{\pi} - \frac{\pi\alpha}{2\beta_\pi}\right) \frac{\pi\alpha}{\beta_\pi} \times \left[1 - \exp\left(-\frac{\pi\alpha}{\beta_\pi}\right)\right]^{-1} \quad . \tag{142}$$

While only the exponentiated correction yields the correct answer close to the threshold, the deviation from the non–exponentiated one is below 1 % above $\sqrt{s} = 0.3$ GeV. The $O(\alpha)$ $\pi^+\pi^-\gamma$ correction calculated in sQED yields

$$\delta^\gamma a_\mu^{(4)}(\text{vap, had}) = a_\mu^{(6)[(d)]} = (38.6 \pm 1.0) \times 10^{-11} \ , \tag{143}$$

as a contribution to a_μ. Here, we added a guesstimated error which of course is not the true model error, the latter remaining unknown [17]. In the inclusive region above typically 2 GeV, the FRS corrections are well represented by the inclusive photon emission from quarks. However, since in inclusive measurements experiments commonly do not subtract FSR, the latter is included already in the data and no additional contribution has to be taken into account. In more recent analyses this contribution is usually included as the $\pi^+\pi^-\gamma$ channel in the leading hadronic VP contribution, in particular in the value given in Eq. (113) .

5. Hadronic Light-by-Light Scattering Contribution

The most problematic set of hadronic corrections are those related to hadronic light–by–light scattering, which for the first time show up at order $O(\alpha^3)$ via the diagrams of Fig. 31. We already know from the leptonic counterpart Fig. 14 that such contributions can be dramatically enhanced and thus represent an important contribution which has to be evaluated carefully. The problem is that even for real–photon light–by–light scattering, perturbation theory is far from being able to describe reality, as the reader may convince himself by a glance at Fig. 32, showing sharp spikes of π^0, η and η' production, while pQCD predicts a smooth

[17] One could expect that due to $\gamma - \rho^0$ mixing (VMD type models [240], see below) the sQED contribution gets substantially reduced. However, due to the low scales $\sim m_\mu, m_\pi$ involved here, in relation to M_ρ, the photons essentially behave classically in this case. Also, the bulk of the VP contribution at these low scales comes from the neutral ρ^0–exchange, while the FSR is due to the dissociated charged $\pi^+\pi^-$ intermediate state as assumed in sQED. Fig. 30 shows that the main contribution comes from very low energies.

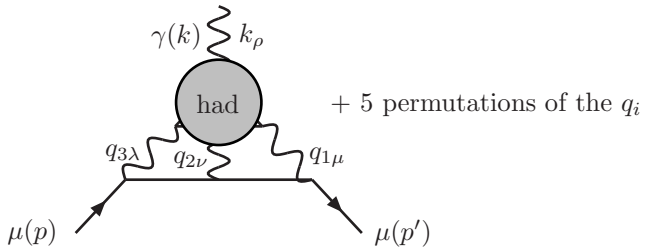

Fig. 31. Assignment of momenta for the calculation of the hadronic contribution of the light–by–light scattering to the muon electromagnetic vertex.

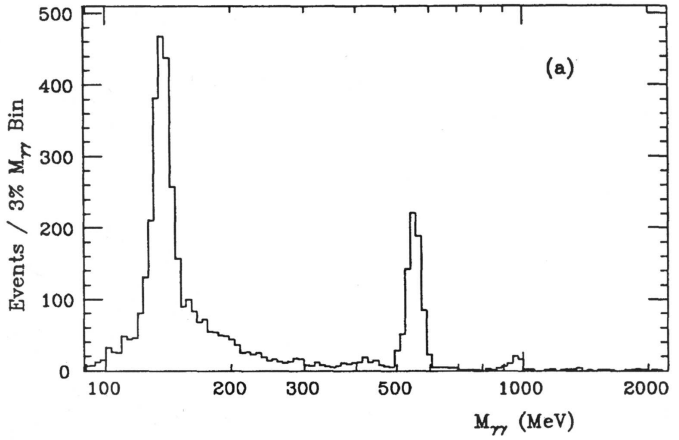

Fig. 32. The invariant $\gamma\gamma$ mass spectrum obtained with the Crystal Ball detector [241]. The three spikes seen represent the $\gamma\gamma \to$ pseudoscalar (PS) $\to \gamma\gamma$ excitations: PS=π^0, η, η'.

continuum (see Fig. 33).

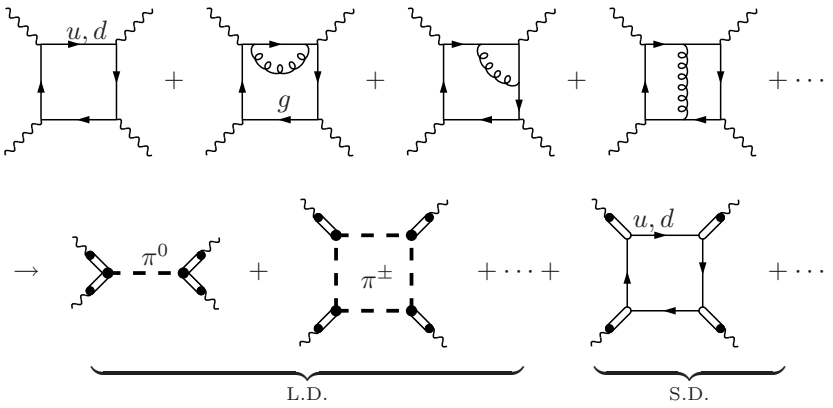

Fig. 33. Hadronic light–by–light scattering is dominated by π^0–exchange in the odd parity channel, pion loops etc. at long distances (L.D.) and quark loops including hard gluonic corrections at short distances (S.D.). The photons in the effective theory couple to hadrons via $\gamma - \rho^0$ mixing.

As a contribution to the anomalous magnetic moment three of the four photons in Fig. 31 are virtual and to be integrated over all four–momentum space, such that a direct experimental input for the non–perturbative dressed four–photon correlator is not available. In this case one has to resort to the low energy effective descriptions of QCD like *chiral perturbation theory* (CHPT) extended to include vector–mesons. Note that early evaluations assumed that the main contribution to hadronic light-by-light scattering comes

from momentum regions around the muon mass. It was later observed in Refs. [242,243] that the higher momentum region, around $500-1000$ MeV, also gives important contributions. Therefore, hadronic resonances beyond the Goldstone bosons of CHPT need to be considered as well. The Resonance Lagrangian Approach (RLA) is realizing vector–meson dominance model (VMD) ideas in accord with the low energy structure of QCD [88]. Other effective theories are the extended Nambu-Jona-Lasinio (ENJL) model [243] (see also [244]) or the very similar hidden local symmetry (HLS) model [242,245]; approaches more or less accepted as a framework for the evaluation of the hadronic LbL effects. The amazing fact is that the interactions involved in the hadronic LbL scattering process are the parity conserving QED and QCD interactions while the process is dominated by the parity odd pseudoscalar meson–exchanges. This means that the effective $\pi^0\gamma\gamma$ interaction vertex exhibits the parity violating γ_5 coupling, which of course in $\gamma\gamma \to \pi^0 \to \gamma\gamma$ must appear twice (an even number of times). The process indeed is induced by the parity odd $O(p^4)$ Wess-Zumino-Witten (WZW) effective Lagrangian term [246,247]

$$\mathcal{L}^{(4)}_{\rm WZW} = \frac{\alpha}{\pi}\frac{N_c}{12F_\pi}\left(\pi^0 + \frac{1}{\sqrt{3}}\,\eta_8 + 2\sqrt{\frac{2}{3}}\,\eta_0\right)\,\tilde{F}_{\mu\nu}F^{\mu\nu}\,. \tag{144}$$

The latter reproduces the ABJ anomaly [248] on the level of the hadrons. π^0 is the neutral pion field, F_π the pion decay constant ($F_\pi = 92.4\,$MeV). The pseudoscalars η_8, η_0 are mixing into the physical states η, η'. However, the constant WZW form factor yields a divergent result, applying a cut–off Λ one obtains the leading term

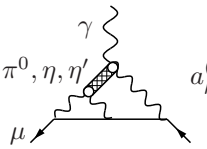

$$a_\mu^{(6)}({\rm lbl},\pi^0) = \left[\frac{N_c^2}{48\pi^2}\frac{m_\mu^2}{F_\pi^2}\,\ln^2\frac{\Lambda}{m_\mu} + \cdots\right]\left(\frac{\alpha}{\pi}\right)^3,$$

with an universal coefficient $\mathcal{C} = N_c^2 m_\mu^2/(48\pi^2 F_\pi^2)$ [17,249]; in the VMD dressed cases M_V represents the cut–off $\Lambda \to M_V$ if $M_V \to \infty$ [18] . For the case of π^0-exchange, a two-dimensional integral representation for $a_\mu^{{\rm LbL};\pi^0}$ has been derived in Ref. [17] (in terms of the moduli of the Euclidean loop momenta $|Q_1|$ and $|Q_2|$) for a certain class of form factors including the VMD dressed case. The universal weight functions multiplying the model-dependent form factors clearly show the relevance of momenta of order $500-1000$ MeV.

A new quality of the problem encountered here is the fact that the integrand depends on 3 invariants q_1^2, q_2^2, q_3^2, where $q_3 = -(q_1+q_2)$. In contrast, the hadronic VP correlator, or the VVA triangle with an external zero momentum vertex (which enters the electroweak contribution, see Sect. 6), only depends on a single invariant q^2. In the latter case, the invariant amplitudes (form factors) may be separated into a low energy part $q^2 \le \Lambda^2$ (soft) where the low energy effective description applies and a high energy part $q^2 > \Lambda^2$ (hard) where pQCD works. In multi–scale problems, however, there are mixed soft–hard regions, where no answer is available in general, unless we have data to constrain the amplitudes in such regions. In our case, only the soft region $q_1^2, q_2^2, q_3^2 \le \Lambda^2$ and the hard region $q_1^2, q_2^2, q_3^2 > \Lambda^2$ are under control of either the low energy effective field theory (EFT) and of pQCD, respectively. In the other domains operator product expansions and/or soft versus hard factorization "theorems" à la Brodsky-Farrar [250] may be applied.

Another problem of the RLA is that the low energy effective theory is non–renormalizable and thus has unphysical UV behavior, while QCD is renormalizable and has the correct UV behavior (but unphysical IR behavior). As a consequence of the mismatch of the functional dependence on the cut–off, one cannot match the two pieces in a satisfactory manner and one obtains a cut–off dependent prediction. Unfortunately, the cut–off dependence of the sum is not small even if one varies the cut–off only within "reasonable" boundaries around about 1 or 2 GeV, say. Of course the resulting uncertainty just reflects the model dependence and so to say parametrizes our ignorance. An estimate of the real model dependence is difficult as long as we are not knowing the true solution of the problem. In CHPT and its extensions, the low energy constants

[18] Since the leading term is divergent and requires UV subtraction, we expect this term to drop from the physical result, unless a physical cut–off tames the integral, like the physical ρ in effective theories which implement the VMD mechanism.

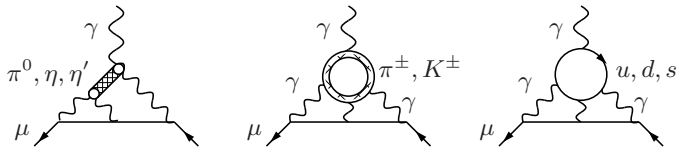

(a) [L.D.] (b) [L.D.] (c) [S.D.]

Fig. 34. Hadronic light–by–light scattering diagrams in a low energy effective model description. Diagrams (a) and (b) represent the long distance [L.D.] contributions at momenta $p \leq \Lambda$, diagram (c) involving a quark loop which yields the leading short distance [S.D.] part at momenta $p \geq \Lambda$ with $\Lambda \sim 1$ to 2 GeV an UV cut–off. Internal photon lines are dressed by $\rho - \gamma$ mixing.

Table 6
Orders with respect to $1/N_c$ and chiral expansion of typical leading contributions shown in Fig. 34.

Diagram	$1/N_c$ expansion	p expansion	type
Fig. 34(a)	N_c	p^6	π^0, η, η' exchange
Fig. 34(a)	N_c	p^8	a_1, ρ, ω exchange
Fig. 34(b)	1	p^4	meson loops ($\pi^\pm$, $K^\pm$)
Fig. 34(c)	N_c	p^8	quark loops

parametrizing the effective Lagrangian are accounting for the appropriate S.D. behavior, usually. Some groups however prefer an alternative approach based on the fact that the weakly coupled large–N_c QCD, i.e., $SU(N_c)$ for $N_c \to \infty$ under the constraint $\alpha_s N_c$=constant, is theoretically better known than true QCD with $N_c = 3$. It is thus tempting to approximate QCD as an expansion in $1/N_c$ [251,252,253].

Of course, also applying a large–N_c expansion one has to respect the low energy properties of QCD as encoded by CHPT. In CHPT the effective Lagrangian has an overall factor N_c, while the U matrix, exhibiting the pseudoscalar fields, is N_c independent. Each additional meson field has a $1/F_\pi \propto 1/\sqrt{N_c}$. In the context of CHPT the $1/N_c$ expansion thus is equivalent to a semiclassical expansion. The chiral Lagrangian can be used at tree level, and loop effects are suppressed by powers of $1/N_c$. Note, however, that for instance the low-energy constants L_i which appear at order p^4 in the chiral Lagrangian have different weights in the N_c counting.

The various hadronic LbL contributions in the effective theory are shown in Fig. 34 and the corresponding $1/N_c$ and chiral $O(p)$ counting is given in Table 6 [244]. Note that the chiral counting refers to the contribution to the 4-point function $\langle VVVV \rangle$ and not to a_μ itself. Based on this classification it was argued in Ref. [244] that the (constituent) quark-loop represents the irreducible part of the 4-point function and should be included as a separate contribution (although maybe with dressed couplings of the constituent quarks to the photons, which arises naturally in the ENJL model employed in Ref. [244]), in addition to the exchanges or loops of resonances. Within the CHPT approach, this irreducible part can be viewed as a local counterterm contribution $\bar{\psi}\sigma^{\mu\nu}\psi F_{\mu\nu}$ to a_μ. In particular, it was argued in Ref. [244] that the (constituent) quark-loop should not be used as a substitute for the hadronic contributions (exchanges and loops with resonances), as was done in earlier evaluations of the hadronic light-by-light scattering contribution to $g-2$ in Refs. [187,79].

Based on refined effective field theory models, two major efforts in evaluating the full $a_\mu^{\rm LbL}$ contribution were made by Hayakawa, Kinoshita and Sanda (HKS 1995) [242], Bijnens, Pallante and Prades (BPP 1995) [243] and Hayakawa and Kinoshita (HK 1998) [245] (see also Kinoshita, Nizic and Okamoto (KNO 1985) [79]). Although the details of the calculations are quite different, which results in a different splitting of various contributions, the results are in good agreement and essentially given by the π^0-pole contribution, which was taken with the wrong sign, however. In order to eliminate the cut–off dependence in separating L.D. and S.D. physics, more recently it became favorable to use quark–hadron duality, as it holds in the large N_c limit of QCD [251,252], for modeling of the hadronic amplitudes [244]. The infinite series of narrow vector states known to show up in the large N_c limit is then approximated by a suitable lowest meson dominance (LMD) ansatz [254], assumed to be saturated by known low lying physical states of appropriate quantum

numbers. This approach was adopted in a reanalysis by Knecht and Nyffeler (KN 2001) [17,249], in which they discovered a sign mistake in the dominant π^0, η, η' exchange contribution (see also [255,256]), which changed the central value by $+167 \times 10^{-11}$, a 2.8 σ shift, and which reduced a larger discrepancy between theory and experiment. More recently Melnikov and Vainshtein (MV 2004) [257] found additional problems in previous calculations, this time in the short distance constraints (QCD/OPE) used in matching the high energy behavior of the effective models used for the π^0, η, η' exchange contribution. Most evaluations have adopted the pion-pole approximation which, however, violates four-momentum conservation at the external $\pi^0\gamma^*\gamma$ vertex, if used too naively, as pointed out in Refs. [257,44,46]. In the following we will attempt an evaluation which avoids such manifest inconsistencies. Maybe some of the confusion in the recent literature was caused by the fact that the distinction between off-shell and on-shell (pion-pole) form factors was not made properly.

Let us start now with a setup of what one has to calculate actually. We will closely follow Ref. [17] in the following. The hadronic light–by–light scattering contribution to the electromagnetic vertex is represented by the diagram Fig. 31. According to the diagram, a complete discussion of the hadronic light–by–light contributions involves the full rank–four hadronic vacuum polarization tensor

$$\Pi_{\mu\nu\lambda\rho}(q_1, q_2, q_3) = \int \mathrm{d}^4x_1\, \mathrm{d}^4x_2\, \mathrm{d}^4x_3\, \mathrm{e}^{\,\mathrm{i}\,(q_1x_1+q_2x_2+q_3x_3)}\, \langle\, 0 \,|\, T\{j_\mu(x_1)j_\nu(x_2)j_\lambda(x_3)j_\rho(0)\} \,|\, 0\,\rangle\,. \tag{145}$$

The external photon momentum k is incoming, the q_i's of the virtual photons are outgoing from the hadronic "blob". Here $j_\mu(x) \equiv (\bar\psi \hat Q \gamma_\mu \psi)(x)$ ($\bar\psi = (\bar u, \bar d, \bar s)$, $\hat Q = \mathrm{diag}(2,-1,-1)/3$ the charge matrix) denotes the light quark part of the electromagnetic current. Since $j_\mu(x)$ is conserved, the tensor $\Pi_{\mu\nu\lambda\rho}(q_1, q_2, q_3)$ satisfies the Ward-Takahashi identities $\{q_1^\mu; q_2^\nu; q_3^\lambda; k^\rho\}\Pi_{\mu\nu\lambda\rho}(q_1, q_2, q_3) = 0$, with $k = (q_1 + q_2 + q_3)$ which implies

$$\Pi_{\mu\nu\lambda\rho}(q_1, q_2, k - q_1 - q_2) = -k^\sigma(\partial/\partial k^\rho)\, \Pi_{\mu\nu\lambda\sigma}(q_1, q_2, k - q_1 - q_2)\,, \tag{146}$$

and thus tells us that the object of interest is linear in k when we go to the static limit $k^\mu \to 0$ in which the anomalous magnetic moment is defined. As a consequence the electromagnetic vertex amplitude takes the form $\Pi_\rho(p', p) = k^\sigma \Pi_{\rho\sigma}(p', p)$ and the hadronic light–by–light contribution to the muon anomalous magnetic moment is given by (see also [157])

$$F_{\mathrm{M}}(0) \,=\, \frac{1}{48 m_\mu}\, \mathrm{Tr}\, \{(\not p + m_\mu)[\gamma^\rho, \gamma^\sigma](\not p + m_\mu)\Pi_{\rho\sigma}(p, p)\}\,. \tag{147}$$

The required vertex tensor amplitude is determined by

$$\begin{aligned}\Pi_{\rho\sigma}(p', p) = -\mathrm{i}e^6 \int & \frac{\mathrm{d}^4q_1}{(2\pi)^4} \frac{\mathrm{d}^4q_2}{(2\pi)^4} \frac{1}{q_1^2\, q_2^2\, (q_1 + q_2 - k)^2} \frac{1}{(p' - q_1)^2 - m_\mu^2} \frac{1}{(p - q_1 - q_2)^2 - m_\mu^2} \\ & \times\; \gamma^\mu\, (\not p' - \not q_1 + m_\mu)\, \gamma^\nu\, (\not p - \not q_1 - \not q_2 + m_\mu)\, \gamma^\lambda \\ & \times\; \frac{\partial}{\partial k^\rho}\, \Pi_{\mu\nu\lambda\sigma}(q_1, q_2, k - q_1 - q_2)\,,\end{aligned} \tag{148}$$

where now $k = 0$ such that $p' = p$ and $q_3 = -(q_1 + q_2)$. After performing the trace (see below) we have what we actually need to calculate. The integral to be performed is 8 dimensional. Thereof 3 integrations can be done analytically. In general, one has to deal with a 5 dimensional non–trivial integration over 3 angles and 2 moduli.

The hadronic tensor $\Pi_{\mu\nu\lambda\sigma}(q_1, q_2, k - q_1 - q_2)$ in Eq. (145) or (148) is a very complicated object, because it has an unexpectedly complex structure as we will see, in no way comparable with the leptonic counterpart. The general covariant decomposition involves 138 Lorentz structures of which 32 can contribute to $g-2$ [243]. Fortunately, this tensor is dominated by the pseudoscalar exchanges $\pi^0, \eta, \eta', ...$ (see Fig. 32), described by the WZW effective Lagrangian (144) at lowest order in the chiral expansion. This fact rises hope that a half–way reliable estimate should be possible. Generally, the perturbative QCD expansion only is useful to evaluate the short distance tail, while the dominant long distance part must be evaluated using some low energy effective model which includes the pseudoscalar Goldstone bosons as well as the vector mesons as shown in Fig. 33.

5.1. *Pseudoscalar–exchange Contribution*

Here we discuss the dominating hadronic contributions which are due to the neutral pseudoscalar–exchange diagrams shown in Fig. 35.

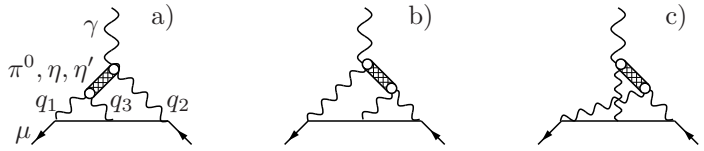

Fig. 35. Leading hadronic light–by–light scattering diagrams. In accord with Eq. (151), here all photon momenta are chosen incoming to the pion transition form factors. Internal photon lines are dressed by $\rho-\gamma$ mixing.

We first concentrate on the exchange of the neutral pion. The key object which enters the Feynman diagrams is the **off-shell** $\pi^0\gamma\gamma$ form factor $\mathcal{F}_{\pi^{0*}\gamma^*\gamma^*}((q_1+q_2)^2,q_1^2,q_2^2)$ which is defined, up to small mixing effects with the states η and η', via the Green's function $\langle VVP\rangle$ in QCD

$$\begin{aligned}&\int \mathrm{d}^4x\,\mathrm{d}^4y\,\mathrm{e}^{\mathrm{i}(q_1\cdot x+q_2\cdot y)}\,\langle\,0|T\{j_\mu(x)j_\nu(y)P^3(0)\}|0\rangle\\&=\varepsilon_{\mu\nu\alpha\beta}\,q_1^\alpha q_2^\beta\,\frac{\mathrm{i}\langle\overline{\psi}\psi\rangle}{F_\pi}\,\frac{\mathrm{i}}{(q_1+q_2)^2-m_\pi^2}\,\mathcal{F}_{\pi^{0*}\gamma^*\gamma^*}((q_1+q_2)^2,q_1^2,q_2^2)\,,\end{aligned}\tag{149}$$

where $P^3=\bar{\psi}i\gamma_5\frac{\lambda^3}{2}\psi=\left(\bar{u}i\gamma_5u-\bar{d}i\gamma_5d\right)/2$. Note that we denote by $\langle\overline{\psi}\psi\rangle$ the **single flavor** bilinear quark condensate. The form factor is of course Bose symmetric $\mathcal{F}_{\pi^{0*}\gamma^*\gamma^*}((q_1+q_2)^2,q_1^2,q_2^2)=\mathcal{F}_{\pi^{0*}\gamma^*\gamma^*}((q_1+q_2)^2,q_2^2,q_1^2)$, as the two photons are indistinguishable. We will later also use the following notation

$$\begin{aligned}\mathcal{A}_{\mu\nu}(\pi^0\to\gamma^*\gamma^*)&=\mathrm{i}\int\mathrm{d}^4x\,\mathrm{e}^{\mathrm{i}q\cdot x}\langle\,0|T\{j_\mu(x)j_\nu(0)\}|\pi^0(p)\rangle\\&=\varepsilon_{\mu\nu\alpha\beta}\,q^\alpha p^\beta\,\mathcal{F}_{\pi^0\gamma^*\gamma^*}(m_\pi^2,q^2,(p-q)^2)\,,\end{aligned}\tag{150}$$

where now the pion is on-shell, but the photons are in general off-shell.

We would like to stress that the identification of the pion-exchange contribution in the full hadronic light-by-light scattering amplitude in $g-2$ according to Fig. 35 only makes sense, if the pion is on-shell (or nearly on-shell). If one is (far) off the mass shell of the exchanged particle (here the pion), it is not possible to separate different contributions to the $g-2$, unless one uses some particular model where for instance elementary pions can propagate. In this sense, only the result for the pion-pole contribution to $g-2$ with on-shell form factors is model-independent. On the other hand, the pion-pole contribution is only a part of the full result, since in general the form factors will enter the calculation with off-shell momenta. Although the contribution in a particular channel will then be model-dependent, the sum of all off-shell contributions in all channels will again lead, at least in principle, to a model-independent result.

Apart from the $\pi^0\gamma\gamma$ form factor everything is known and may be worked out (see e.g. [17]) with the result

$$\begin{aligned}a_\mu^{\mathrm{LbL};\pi^0}=-e^6\int\frac{d^4q_1}{(2\pi)^4}\frac{d^4q_2}{(2\pi)^4}\,&\frac{1}{q_1^2q_2^2(q_1+q_2)^2[(p+q_1)^2-m_\mu^2][(p-q_2)^2-m_\mu^2]}\\&\times\left[\frac{\mathcal{F}_{\pi^{0*}\gamma^*\gamma^*}(q_2^2,q_1^2,q_3^2)\;\mathcal{F}_{\pi^{0*}\gamma^*\gamma}(q_2^2,q_2^2,0)}{q_2^2-m_\pi^2}\;T_1(q_1,q_2;p)\right.\\&\left.+\;\frac{\mathcal{F}_{\pi^{0*}\gamma^*\gamma^*}(q_3^2,q_1^2,q_2^2)\;\mathcal{F}_{\pi^{0*}\gamma^*\gamma}(q_3^2,q_3^2,0)}{q_3^2-m_\pi^2}\;T_2(q_1,q_2;p)\right],\end{aligned}\tag{151}$$

with

$$
\begin{aligned}
T_1(q_1,q_2;p) &= \frac{16}{3}\,(p\cdot q_1)\,(p\cdot q_2)\,(q_1\cdot q_2)\;-\;\frac{16}{3}\,(p\cdot q_2)^2\,q_1^2 \\
&\quad -\frac{8}{3}\,(p\cdot q_1)\,(q_1\cdot q_2)\,q_2^2\;+\;8(p\cdot q_2)\,q_1^2\,q_2^2\;-\;\frac{16}{3}(p\cdot q_2)\,(q_1\cdot q_2)^2 \\
&\quad +\frac{16}{3}\,m_\mu^2\,q_1^2\,q_2^2\;-\;\frac{16}{3}\,m_\mu^2\,(q_1\cdot q_2)^2\,, \\
T_2(q_1,q_2;p) &= \frac{16}{3}\,(p\cdot q_1)\,(p\cdot q_2)\,(q_1\cdot q_2)\;-\;\frac{16}{3}\,(p\cdot q_1)^2\,q_2^2 \\
&\quad +\frac{8}{3}\,(p\cdot q_1)\,(q_1\cdot q_2)\,q_2^2\;+\;\frac{8}{3}\,(p\cdot q_1)\,q_1^2\,q_2^2 \\
&\quad +\frac{8}{3}\,m_\mu^2\,q_1^2\,q_2^2\;-\;\frac{8}{3}\,m_\mu^2\,(q_1\cdot q_2)^2\,.
\end{aligned}
\tag{152}
$$

The first and the second graphs in Fig. 35 give rise to identical contributions, leading to the term with T_1, whereas the third graph gives the contribution involving T_2. The factor T_2 has been symmetrized with respect to the exchange $q_1 \leftrightarrow -q_2$. Note that now the external photon has zero four-momentum ($k^\mu = 0$) such that $q_3 = -(q_1+q_2)$.

The result in Eq. (151) does not depend on the direction of the muon momentum vector p such that we may average in Euclidean space over the directions $\hat{P}$:

$$
\langle\cdots\rangle = \frac{1}{2\pi^2}\int \mathrm{d}\Omega(\hat{P})\,\cdots \tag{153}
$$

using the technique of Gegenbauer polynomials (hyperspherical approach), see Ref. [258]. Since all p dependent terms are independent of the pseudoscalar form factors one may perform the integrations in general. After reducing numerators of the amplitudes T_i against the denominators of the propagators one is left with the following integrals ($(4) \equiv (P+Q_1)^2 + m_\mu^2$ and $(5) \equiv (P-Q_2)^2 + m_\mu^2$ with $P^2 = -m_\mu^2$)

$$
\begin{aligned}
\langle\frac{1}{(4)}\frac{1}{(5)}\rangle &= \frac{1}{m_\mu^2 R_{12}}\arctan\left(\frac{zx}{1-zt}\right), \\
\langle(P\cdot Q_1)\,\frac{1}{(5)}\rangle &= -\,(Q_1\cdot Q_2)\,\frac{(1-R_{m2})^2}{8m_\mu^2}, \\
\langle(P\cdot Q_2)\frac{1}{(4)}\rangle &= \;\;(Q_1\cdot Q_2)\,\frac{(1-R_{m1})^2}{8m_\mu^2}, \\
\langle\frac{1}{(4)}\rangle &= -\,\frac{1-R_{m1}}{2m_\mu^2}, \\
\langle\frac{1}{(5)}\rangle &= -\,\frac{1-R_{m2}}{2m_\mu^2},
\end{aligned}
\tag{154}
$$

where $R_{mi} = \sqrt{1+4m_\mu^2/Q_i^2}$ and $(Q_1\cdot Q_2) = Q_1\,Q_2\,t$ with $t = \cos\theta$, θ the angle between the two Euclidean four–vectors Q_1 and Q_2. Denoting $x = \sqrt{1-t^2}$, we have $R_{12} = Q_1\,Q_2\,x$ and

$$
z = \frac{Q_1 Q_2}{4m_\mu^2}\,(1-R_{m1})\,(1-R_{m2})\;.
$$

We have thus eliminated all momentum dependences up to the three which also show up in the hadronic form factors Q_1^2, Q_2^2, and Q_3^2 or equivalently on $(Q_1\cdot Q_2) = Q_1 Q_2\cos\theta$ and end up with a 3–dimensional integral over $Q_1 = |Q_1|$, $Q_2 = |Q_2|$ and $t = \cos\theta$:

$$
a_\mu^{\mathrm{LbL};\pi^0} = -\frac{2\alpha^3}{3\pi^2}\int\limits_0^\infty \mathrm{d}Q_1\mathrm{d}Q_2\int\limits_{-1}^{+1}\mathrm{d}t\,\sqrt{1-t^2}\,Q_1^3\,Q_2^3\;\left[F_1\,P_6\,I_1(Q_1,Q_2,t) + F_2\,P_7\,I_2(Q_1,Q_2,t)\right], \tag{155}
$$

where $P_6 = 1/(Q_2^2 + m_\pi^2)$, and $P_7 = 1/(Q_3^2 + m_\pi^2)$ denote the Euclidean single particle exchange propagators. The integration kernels I_1 and I_2, which factorize from the dependence on the hadronic form-factors in F_1 and F_2, are given by

$$\begin{aligned}
I_1(Q_1,Q_2,t) = X(Q_1,Q_2,t) \Big(& 8\,P_1\,P_2\,(Q_1\cdot Q_2) \\
& -2\,P_1\,P_3\,(Q_2^4/m_\mu^2 - 2\,Q_2^2) - 2\,P_1\,(2 - Q_2^2/m_\mu^2 + 2\,(Q_1\cdot Q_2)\,/m_\mu^2) \\
& +4\,P_2\,P_3\,Q_1^2 - 4\,P_2 - 2\,P_3\,(4 + Q_1^2/m_\mu^2 - 2\,Q_2^2/m_\mu^2) + 2/m_\mu^2 \Big) \\
& -2\,P_1\,P_2\,(1 + (1-R_{m1})\,(Q_1\cdot Q_2)\,/m_\mu^2) \\
& +P_1\,P_3\,(2 - (1-R_{m1})\,Q_2^2/m_\mu^2) + P_1\,(1-R_{m1})/m_\mu^2 \\
& +P_2\,P_3\,(2 + (1-R_{m1})^2\,(Q_1\cdot Q_2)\,/m_\mu^2) + 3\,P_3\,(1-R_{m1})/m_\mu^2, \\
I_2(Q_1,Q_2,t) = X(Q_1,Q_2,t) \Big(& 4\,P_1\,P_2\,(Q_1\cdot Q_2) \\
& +2\,P_1\,P_3\,Q_2^2 - 2\,P_1 + 2\,P_2\,P_3\,Q_1^2 - 2\,P_2 - 4P_3 - 4/m_\mu^2 \Big) \\
& -2\,P_1\,P_2 - 3\,P_1\,(1-R_{m2})/(2m_\mu^2) - 3\,P_2\,(1-R_{m1})/(2m_\mu^2) \\
& +P_1\,P_3\,(2 + 3\,(1-R_{m2})\,Q_2^2/(2m_\mu^2) + (1-R_{m2})^2\,(Q_1\cdot Q_2)\,/(2m_\mu^2)) \\
& +P_2\,P_3\,(2 + 3\,(1-R_{m1})\,Q_1^2/(2m_\mu^2) + (1-R_{m1})^2\,(Q_1\cdot Q_2)\,/(2m_\mu^2)) \\
& -P_3\,(2 - R_{m1} - R_{m2})/(2m_\mu^2),
\end{aligned} \tag{156}$$

where we used the notation $P_1 = 1/Q_1^2$, $P_2 = 1/Q_2^2$, and $P_3 = 1/Q_3^2$ for the Euclidean propagators and introduced the auxiliary function

$$X(Q_1,Q_2,t) = \frac{1}{Q_1 Q_2\,x}\arctan\left(\frac{zx}{1-zt}\right)\,, \tag{157}$$

which has the following asymptotic expansion for small x, near the forward and backward points:

$$X(Q_1,Q_2,t) = \frac{1}{Q_1 Q_2}\,\begin{cases} \frac{z}{1-z}\left(1 + \frac{1}{6}\frac{z\,(z-3)}{(1-z)^2}\,x^2\right) + O\left(x^3\right) & \text{for } t > 0 \\ \frac{z}{1+z}\left(1 + \frac{1}{6}\frac{z\,(z+3)}{(1+z)^2}x^2\right) + O\left(x^3\right) & \text{for } t < 0 \end{cases}\,.$$

Equation (155) provides the general set up for studying any type of single particle exchange contribution as a 3–dimensional integral representation. The non-perturbative factors according to Eq. (151) are given by

$$\begin{aligned}
F_1 &= \mathcal{F}_{\pi^{0*}\gamma^*\gamma^*}(-Q_2^2,-Q_1^2,-Q_3^2)\;\mathcal{F}_{\pi^{0*}\gamma^*\gamma}(-Q_2^2,-Q_2^2,0)\,, \\
F_2 &= \mathcal{F}_{\pi^{0*}\gamma^*\gamma^*}(-Q_3^2,-Q_1^2,-Q_2^2)\;\mathcal{F}_{\pi^{0*}\gamma^*\gamma}(-Q_3^2,-Q_3^2,0),
\end{aligned} \tag{158}$$

and will be considered next. Note that F_2 is symmetric under the exchange $Q_1 \leftrightarrow Q_2$. We used this property to write $I_2(Q_1,Q_2,t)$ in Eq. (156) in a symmetric way.

5.1.1. *The $\pi^0\gamma\gamma$ Transition Form Factor: Experimental and Theoretical Constraints*

Above we have formally reduced the problem of calculating the π^0–exchange contribution diagrams in Fig. 35 to the problem of calculating the integral Eq. (155). The non–perturbative aspect is now confined in the form–factor function $\mathcal{F}_{\pi^{0*}\gamma^*\gamma^*}(q_3^2,q_1^2,q_2^2)$ defined in Eq. (149), which is largely unknown. For the time being we have to use one of the hadronic models mentioned above together with pQCD as a constraint on the high energy asymptotic behavior. Fortunately some experimental data are also available. The con-

stant $\mathcal{F}_{\pi^0\gamma\gamma}(m_\pi^2,0,0)$ is well determined by the $\pi^0\to\gamma\gamma$ decay rate. The on–shell transition amplitude in the chiral limit follows from the WZW–Lagrangian Eq. (144), and is given by

$$M_{\pi^0\gamma\gamma} = -e^2\,\mathcal{F}_{\pi^0\gamma\gamma}(0,0,0) = \frac{e^2 N_c}{12\pi^2 F_\pi} = \frac{\alpha}{\pi F_\pi} \approx 0.025\ \text{GeV}^{-1}\,, \tag{159}$$

and with $F_\pi \sim 92.4$ MeV and quark color number $N_c = 3$, rather accurately predicts the experimental result

$$|M^{\rm exp}_{\pi^0\gamma\gamma}| = \sqrt{64\pi\Gamma_{\pi^0\gamma\gamma}/m_\pi^3} = 0.025 \pm 0.001\ \text{GeV}^{-1}\,. \tag{160}$$

Note that the amplitude $M_{\pi^0\gamma\gamma}$, defined to be finite in the chiral limit, in terms of the conventional amplitude $\mathcal{M}_{\pi^0\gamma\gamma} = -e^2\,\mathcal{A}_{\mu\nu}(\pi^0\to\gamma\gamma)\,\varepsilon^{*\mu}(q_1,\lambda_1)\,\varepsilon^{*\nu}(q_2,\lambda_2)$ follows (up to a phase) via $\sum_{\lambda_1,\lambda_2}\left|\mathcal{M}_{\pi^0\gamma\gamma}\right|^2 = \frac{m_\pi^4}{2}|M_{\pi^0\gamma\gamma}|^2$.

Additional experimental information is available for $\mathcal{F}_{\pi^0\gamma^*\gamma}(m_\pi^2,-Q^2,0)$ coming from experiments $e^+e^-\to e^+e^-\pi^0$. Note that the production of an on–shell pion at large $-q_1^2 = Q^2$ is only possible if the real photon is highly energetic, i.e., $q_2^0 = |\vec{q}_2|$ large. This is different from the $g-2$ kinematical situation at the external photon vertex, where the external photon has zero four–momentum. By four–momentum conservation thus only $\mathcal{F}_{\pi^{0*}\gamma^*\gamma}(-Q^2,-Q^2,0)$ and **not** $\mathcal{F}_{\pi^{0*}\gamma^*\gamma}(m_\pi^2,-Q^2,0)$ can enter at the **external** vertex.

For the **internal** vertex both photons are virtual, and luckily, experimental data on $\mathcal{F}_{\pi^0\gamma^*\gamma}(m_\pi^2,-Q^2,0)$ is available from CELLO [259] and CLEO [260], which provides a crucial constraint on this form factor. Fortunately, this constrains the border domain of **one** of the problematic mixed soft–hard regions at the **internal** vertex. Experiments fairly well confirm the Brodsky-Lepage [261] evaluation of the large Q^2 behavior

$$\lim_{Q^2\to\infty}\ \mathcal{F}_{\pi^0\gamma^*\gamma}(m_\pi^2,-Q^2,0) \sim -\frac{2F_\pi}{Q^2}. \tag{161}$$

In this approach the transition form factor is represented as a convolution of a hard scattering amplitude (HSA) and the soft non–perturbative meson wave function and the asymptotic behavior follows from a pQCD calculation of the HSA. Together with the constraint from π^0 decay, $\lim_{Q^2\to 0}\ \mathcal{F}_{\pi^0\gamma^*\gamma}(m_\pi^2,-Q^2,0) = \frac{-1}{4\pi^2 F_\pi}$, an interpolating formula

$$\mathcal{F}_{\pi^0\gamma^*\gamma}(m_\pi^2,-Q^2,0) \simeq \frac{-1}{4\pi^2 F_\pi}\frac{1}{1+(Q^2/8\pi^2F_\pi^2)} \tag{162}$$

was proposed, which in fact gives an acceptable fit to the data. Refinements of form factor calculations/models were discussed and compared with the data in [260] (see also [262,263,264,265]).

Apart from these experimental constraints, any satisfactory model for the off-shell form factor $\mathcal{F}_{\pi^{0*}\gamma^*\gamma^*}((q_1+q_2)^2,q_1^2,q_2^2)$ should match at large momentum with short-distance constraints from QCD that can be calculated using the OPE. In Ref. [266] the short-distance properties for the three-point function $\langle VVP\rangle$ in Eq. (149) in the chiral limit and assuming octet symmetry have been worked out in detail (see also Ref. [267] for earlier partial results). At least for the pion the chiral limit should be a not too bad approximation [19], however, for the η and, in particular, for the non-Goldstone boson η' further analysis will be necessary.

It is important to notice that the Green's function $\langle VVP\rangle$ is an order parameter of chiral symmetry. Therefore, it vanishes to all orders in perturbative QCD in the chiral limit, so that the behavior at short distances is smoother than expected from naive power counting arguments. Two limits are of interest. In the first case, the two momenta become simultaneously large, which in position space describes the situation where the space-time arguments of all the three operators tend towards the same point at the same rate. To leading order and up to corrections of order $\mathcal{O}(\alpha_s)$ one obtains the following behavior for the form factor [20]

$$\lim_{\lambda\to\infty}\ \mathcal{F}_{\pi^{0*}\gamma^*\gamma^*}((\lambda q_1+\lambda q_2)^2,(\lambda q_1)^2,(\lambda q_2)^2) = \frac{F_0}{3}\,\frac{1}{\lambda^2}\,\frac{q_1^2+q_2^2+(q_1+q_2)^2}{q_1^2 q_2^2} + \mathcal{O}\left(\frac{1}{\lambda^4}\right)\,. \tag{163}$$

[19] As pointed out in Ref. [268], the integrals in Eq. (151) are infrared safe for $m_\pi \to 0$. This can also be seen within the EFT approach to light-by-light scattering proposed in Refs. [249,256] to be discussed later in Sect. 5.3.

[20] In the chiral limit, the relation between the off-shell form factor and the single invariant function $\mathcal{H}_V$ which appears in $\langle VVP\rangle$ is given by $\mathcal{F}_{\pi^{0*}\gamma^*\gamma^*}((q_1+q_2)^2,q_1^2,q_2^2) = -(2/3)(F_0/\langle\overline{\psi}\psi\rangle_0)(q_1+q_2)^2\mathcal{H}_V(q_1^2,q_2^2,(q_1+q_2)^2)$, see Ref. [266] for details.

The second situation of interest corresponds to the case where the relative distance between only two of the three operators in $\langle VVP\rangle$ becomes small. It so happens that the corresponding behaviors in momentum space involve, apart from the correlator $\langle AP\rangle$ which, in the chiral limit, is saturated by the single-pion intermediate state,

$$\int d^4x e^{ip\cdot x}\langle 0|T\{A_\mu^a(x)P^b(0)\}|0\rangle = \delta^{ab}\langle\overline{\psi}\psi\rangle_0\,\frac{p_\mu}{p^2}\,, \tag{164}$$

(we denote by $\langle\overline{\psi}\psi\rangle_0$ the **single flavor** bilinear quark condensate in the chiral limit) the two-point function $\langle VT\rangle$ of the vector current and the antisymmetric tensor density,

$$\delta^{ab}(\Pi_{\rm VT})_{\mu\rho\sigma}(p) \,=\, \int d^4x e^{ip\cdot x}\langle 0|T\{V_\mu^a(x)(\overline{\psi}\,\sigma_{\rho\sigma}\frac{\lambda^b}{2}\,\psi)(0)\}|0\rangle\,, \tag{165}$$

with $\sigma_{\rho\sigma} = \frac{i}{2}[\gamma_\rho,\gamma_\sigma]$ (the similar correlator between the axial current and the tensor density vanishes as a consequence of invariance under charge conjugation). Conservation of the vector current and invariance under parity then give

$$(\Pi_{\rm VT})_{\mu\rho\sigma}(p) \,=\, (p_\rho\eta_{\mu\sigma} - p_\sigma\eta_{\mu\rho})\,\Pi_{\rm VT}(p^2)\,. \tag{166}$$

The leading short-distance behavior of this two-point function is given by (see also [269])

$$\lim_{\lambda\to\infty}\Pi_{\rm VT}((\lambda p)^2) \,=\, -\,\frac{1}{\lambda^2}\,\frac{\langle\overline{\psi}\psi\rangle_0}{p^2} \,+\, \mathcal{O}\left(\frac{1}{\lambda^4}\right)\,. \tag{167}$$

The short-distance behavior of the form factor then reads

$$\lim_{\lambda\to\infty}\mathcal{F}_{\pi^{0*}\gamma^*\gamma^*}(q_2^2,(\lambda q_1)^2,(q_2-\lambda q_1)^2) = \frac{2F_0}{3}\frac{1}{\lambda^2}\frac{1}{q_1^2} + \mathcal{O}\left(\frac{1}{\lambda^3}\right)\,, \tag{168}$$

when the space-time arguments of the two vector currents in $\langle VVP\rangle$ approach each other and

$$\lim_{\lambda\to\infty}\mathcal{F}_{\pi^{0*}\gamma^*\gamma^*}((\lambda q_1+q_2)^2,(\lambda q_1)^2,q_2^2) = -\frac{2}{3}\frac{F_0}{\langle\overline{\psi}\psi\rangle_0}\Pi_{\rm VT}(q_2^2) + \mathcal{O}\left(\frac{1}{\lambda}\right)\,, \tag{169}$$

when the space-time argument of one of the vector currents approaches the one of the pseudoscalar density.

In particular, at the external vertex in light-by-light scattering in Eq. (151), the following limit is relevant [270]

$$\lim_{\lambda\to\infty}\mathcal{F}_{\pi^{0*}\gamma^*\gamma}((\lambda q_1)^2,(\lambda q_1)^2,0) = -\frac{2}{3}\frac{F_0}{\langle\overline{\psi}\psi\rangle_0}\Pi_{\rm VT}(0) + \mathcal{O}\left(\frac{1}{\lambda}\right)\,. \tag{170}$$

Note that there is no fall-off in this limit, unless $\Pi_{\rm VT}(0)$ vanishes. As pointed out in Ref. [271], the value of $\Pi_{\rm VT}(p^2)$ at zero momentum is related to the quark condensate magnetic susceptibility χ of QCD in the presence of a constant external electromagnetic field, introduced in Ref. [272]

$$\langle 0|\bar{q}\sigma_{\mu\nu}q|0\rangle_F = e\,e_q\,\chi\,\langle\overline{\psi}\psi\rangle_0\,F_{\mu\nu}, \tag{171}$$

with $e_u = 2/3$ and $e_d = -1/3$. With our definition of $\Pi_{\rm VT}$ in Eq. (165) one then obtains the relation (see also Ref. [273])

$$\Pi_{\rm VT}(0) = -\frac{\langle\overline{\psi}\psi\rangle_0}{2}\chi. \tag{172}$$

Unfortunately there is no agreement in the literature what the actual value of χ should be. In comparing different results one has to keep in mind that χ actually depends on the renormalization scale μ. In Ref. [272] the estimate $\chi(\mu = 0.5\ \text{GeV}) = -(8.16^{+2.95}_{-1.91})\ \text{GeV}^{-2}$ was given in a QCD sum rule evaluation of nucleon magnetic moments. This value was confirmed by the recent reanalysis [274] which yields $\chi = -(8.5\pm$

1.0) GeV^{-2}. A similar value $\chi = -N_c/(4\pi^2 F_\pi^2) = -8.9$ GeV^{-2} was obtained by Vainshtein [275]. From the explicit expression of χ it is not immediately clear what should be the relevant scale μ. Since pion dominance was used in the matching with the OPE below some higher states, it was argued in Ref. [275] that the normalization point is probably rather low, $\mu \sim 0.5$ GeV. Calculations within the instanton liquid model yield $\chi^{\rm ILM}(\mu \sim 0.5 - 0.6 \text{ GeV}) = -4.32$ GeV^{-2} [276], where the scale is set by the inverse average instanton size ρ^{-1}. The value of $\chi\langle\overline{\psi}\psi\rangle_0 = 42$ MeV at the same scale obtained in Ref. [276] agrees roughly with the result $35 - 40$ MeV from Ref. [277] derived in the same model. On the other hand, assuming that $\Pi_{\rm VT}(q^2)$ is well described by the multiplet of the lowest-lying vector mesons (LMD) and satisfies the OPE constraint from Eq. (167), leads to the ansatz [278,271,266]

$$\Pi_{\rm VT}^{\rm LMD}(q^2) \,=\, -\,\langle\overline{\psi}\psi\rangle_0\,\frac{1}{q^2 - M_V^2}\,. \tag{173}$$

Using Eq. (172) then leads to the estimate $\chi^{\rm LMD} = -2/M_V^2 = -3.3$ GeV^{-2} [278]. Again, it is not obvious at which scale this relation holds. In analogy to estimates of low-energy constants in chiral Lagrangians [88], it might be at $\mu = M_V$. This LMD estimate was soon afterwards improved by taking into account higher resonance states (ρ', ρ'') in the framework of QCD sum rules, with the results $\chi(0.5 \text{ GeV}) = -(5.7 \pm 0.6)$ GeV^{-2} [271] and $\chi(1 \text{ GeV}) = -(4.4 \pm 0.4)$ GeV^{-2} [279]. A more recent analysis [280] yields, however, a smaller absolute value $\chi(1 \text{ GeV}) = -(3.15 \pm 0.30)$ GeV^{-2}, close to the original LMD estimate. For a quantitative comparison of all these estimates for χ we would have to run them to a common scale, for instance 1 GeV, which can obviously not be done within perturbation theory starting from such low scales as $\mu = 0.5$ GeV. [21] Finally, even if the RG running could be performed non-perturbatively, it is not clear what would be the relevant scale μ in the context of hadronic light-by-light scattering.

Further important information on the (on-shell) pion form factor in Eq. (150) has been obtained in Ref. [282] based on higher-twist terms in the OPE and worked out in [283]. We consider the $\pi^0 \to \gamma\gamma$ transition amplitude Eq. (150) with $j_\mu = \frac{2}{3}\bar{u}\gamma_\mu u - \frac{1}{3}\bar{d}\gamma_\mu d$ the relevant part of the electromagnetic current. In the chiral limit, the first two terms of $\mathcal{F}_{\pi^0\gamma^*\gamma^*}(0, -Q^2, -Q^2)$ for large Euclidean momentum $Q^2 \to \infty$ read [282]

$$\mathcal{A}^{\mu\nu}(\pi^0 \to \gamma^*\gamma^*) = \mathrm{i}\frac{1}{3}\,\varepsilon^{\mu\nu\alpha\beta}\langle\,0|\frac{q_\alpha}{q^2}\,j_{5\beta}^{(3)} - \frac{8}{9}\frac{q_\alpha}{q^4}\,\tilde{j}_\beta^{(3)}|\pi^0(p)\rangle, \tag{174}$$

where $j_{5\mu}^{(3)} = \bar{\psi}\lambda^3\gamma_\mu\gamma_5\psi$ and $\tilde{j}_\mu^{(3)} = g_s\,\bar{\psi}\lambda^3\gamma^\rho\,T^a\tilde{G}^a_{\rho\mu}\psi$. The matrix elements are parametrized as follows: $\langle\,0|j_{5\mu}^{(3)}(0)|\pi^0(p)\rangle = 2\mathrm{i}\,F_0 p_\mu$ and $\langle\,0|\tilde{j}_\mu^{(3)}(0)|\pi^0(p)\rangle = -2\mathrm{i}\,F_0 p_\mu\,\delta^2$. For the pion form factor this implies

$$\frac{\mathcal{F}_{\pi^0\gamma^*\gamma^*}(0, -Q^2, -Q^2)}{\mathcal{F}_{\pi^0\gamma\gamma}(0,0,0)} = \frac{8}{3}\pi^2 F_0^2\left\{\frac{1}{Q^2} - \frac{8}{9}\frac{\delta^2}{Q^4} + \cdots\right\} \tag{175}$$

and the sum rule estimate performed in [283] yields $\delta^2 = (0.2 \pm 0.02)$ GeV^2.

5.1.2. *Hadronic Light-by-light Scattering and the Triangle Anomaly*

In this subsection we present the additional QCD short-distance constraints which have been derived by Melnikov and Vainshtein in Ref. [257], closely following their notations. The light-by-light scattering amplitude is written as follows

$$\begin{aligned}\mathcal{M} &= \alpha^2 N_c \mathrm{Tr}[\hat{Q}^4]\,\mathcal{A} = \alpha^2 N_c \mathrm{Tr}[\hat{Q}^4]\,\mathcal{A}_{\mu_1\mu_2\mu_3\gamma\delta}\,\epsilon_1^{\mu_1}\epsilon_2^{\mu_2}\epsilon_3^{\mu_3}\,f^{\gamma\delta} \\ &= -e^3\int d^4x d^4y e^{-iq_1x - iq_2y}\,\epsilon_1^{\mu_1}\epsilon_2^{\mu_2}\epsilon_3^{\mu_3}\,\langle 0|T\{j_{\mu_1}(x)j_{\mu_2}(y)j_{\mu_3}(0)\}|\gamma\rangle,\end{aligned} \tag{176}$$

[21] A further complication arises in comparisons with papers from the early 1980's because not only $\mu = 0.5$ GeV was frequently used, but also 1-loop running with a low $\Lambda_{\rm QCD}^{n_f=3} = 100 - 150$ MeV, whereas more recent estimates yield $\Lambda_{\overline{\rm MS}}^{n_f=3} = 346$ MeV (at 4-loop) [281].

with the photon momenta q_i (incoming, $\sum q_i = 0$) and the photon polarization vectors ϵ_i. The first three photons are virtual, while the fourth one represents the external magnetic field and can be regarded as a real photon with vanishingly small momentum q_4. The field strength tensor of the external soft photon is denoted by $f^{\gamma\delta} = q_4^\gamma \epsilon_4^\delta - q_4^\delta \epsilon_4^\gamma$. Since for a_μ only terms linear in q_4 are needed, see Eq. (146), one can set $q_4 = 0$ in the amplitude $\mathcal{A}_{\mu_1\mu_2\mu_3\gamma\delta}$.

The authors Ref. [257] then consider the momentum region $q_1^2 \approx q_2^2 \gg q_3^2$, with the well-known OPE result (see also Eq. (174))

$$i\int d^4x d^4y e^{-iq_1x-iq_2y} T\{j_{\mu_1}(x) j_{\mu_2}(y)\} = \int d^4z e^{-i(q_1+q_2)z} \frac{2i}{\hat{q}^2} \varepsilon_{\mu_1\mu_2\delta\rho}\, \hat{q}^\delta j_5^\rho(z) + \ldots, \tag{177}$$

where $j_5^\rho = \overline{\psi}\hat{Q}^2\gamma^\rho\gamma_5\psi$ is the axial current and $\hat{q} = (q_1 - q_2)/2 \approx q_1 \approx -q_2$. Only the leading term for large Euclidean $\hat{q}$ has been retained in the OPE. The momentum $q_1 + q_2 = -q_3$ flowing through j_5^ρ is assumed to much smaller than $\hat{q}$. In this way the matrix element in Eq. (176) can be related in the particular kinematical limit $q_1^2 \approx q_2^2 \gg q_3^2$ to the amplitude

$$T^{(a)}_{\mu_3\rho} = i\int d^4z e^{iq_3z}\, \langle 0|T\{j^{(a)}_{5\rho}(z) j_{\mu_3}(0)\}|\gamma\rangle, \tag{178}$$

if the current j_5^ρ is expressed as a linear combination of the isovector, $j_{5\rho}^{(3)} = \overline{\psi}\lambda_3\gamma_\rho\gamma_5\psi$, hypercharge $j_{5\rho}^{(8)} = \overline{\psi}\lambda_8\gamma_\rho\gamma_5\psi$, and the $SU(3)$ singlet, $j_{5\rho}^{(0)} = \overline{\psi}\gamma_\rho\gamma_5\psi$, currents. The amplitude $T^{(a)}_{\mu_3\rho}$ involves the axial current $j^{(a)}_{5\rho}$ and two electromagnetic currents, one with momentum q_3 and the other one (the external magnetic field) with vanishing momentum. The triangle amplitude for such kinematics was studied in Ref. [275], see also Refs. [284,285,286]. It was found that $T^{(a)}_{\mu_3\rho}$ can be written in terms of two independent functions $w^{(a)}_{L,T}(q_3^2)$

$$T^{(a)}_{\mu_3\rho} = -\frac{ieN_c\mathrm{Tr}[\lambda_a\hat{Q}^2]}{4\pi^2}\left\{w_L^{(a)}(q_3^2) q_{3\rho} q_3^\sigma \tilde{f}_{\sigma\mu_3} + w_T^{(a)}(q_3^2)\left(-q_3^2\tilde{f}_{\mu_3\rho} + q_{3\mu_3}q_3^\sigma\tilde{f}_{\sigma\rho} - q_{3\rho}q_3^\sigma\tilde{f}_{\sigma\mu_3}\right)\right\}, \tag{179}$$

where $\tilde{f}_{\sigma\mu_3} = \frac{1}{2}\epsilon_{\sigma\mu_3\alpha\beta}f^{\alpha\beta}$. The first (second) amplitude is related to the longitudinal (transversal) part of the axial current, respectively. In terms of hadrons, the invariant function $w_{L(T)}$ describes the exchanges of the pseudoscalar (axial vector) mesons.

In perturbation theory these invariant functions are completely fixed by the ABJ anomaly and one obtains for massless quarks from the triangle diagram

$$w_L^{(a)}(q^2) = 2w_T^{(a)}(q^2) = -\frac{2}{q^2}. \tag{180}$$

In the chiral limit, the result for $w_L^{(3,8)}$ is exact to all orders in perturbation theory [287] and there are also no nonperturbative contributions [288]. As shown in Ref. [275], in the chiral limit, the relation (180) is true to all orders, however, $w_T^{(3,8)}$ receives nonperturbative corrections. The poles in $w_L^{(3,8)}$ at $q^2 = 0$ are identified with the poles of the Goldstone bosons, π^0 in $w_L^{(3)}$ and η in $w_L^{(8)}$.

For $q_1^2 \approx q_2^2 \gg q_3^2$, one can therefore write the hadronic light-by-light scattering amplitude as follows

$$\mathcal{A}_{\mu_1\mu_2\mu_3\gamma\delta}f^{\gamma\delta} = \frac{8}{\hat{q}^2}\epsilon_{\mu_1\mu_2\delta\rho}\hat{q}^\delta \sum_{a=3,8,0} W^{(a)}\left\{w_L^{(a)}(q_3^2) q_3^\rho q_3^\sigma \tilde{f}_{\sigma\mu_3}\right.$$
$$\left. + w_T^{(a)}(q_3^2)\left(-q_3^2\tilde{f}^\rho{}_{\mu_3} + q_{3\mu_3}q_3^\sigma\tilde{f}^\rho{}_\sigma - q_3^\rho q_3^\sigma\tilde{f}_{\sigma\mu_3}\right)\right\} + \ldots, \tag{181}$$

where the weights $W^{(a)}$ are given by $W^{(3)} = \frac{1}{4}$, $W^{(8)} = \frac{1}{12}$ and $W^{(0)} = \frac{2}{3}$.

The expression in Eq. (181) is then extrapolated to arbitrary values of q_1^2, q_2^2 by writing $\mathcal{A} = \mathcal{A}_{\rm PS} + \mathcal{A}_{AV} +$ permutations, with the ansatz [22]

[22] From now on we only consider the pseudoscalar exchanges and use Euclidean space notation as in Ref. [257].

$$\mathcal{A}_{\rm PS} = \sum_{a=3,8,0} W^{(a)}\, \phi_L^{(a)}(q_1^2,q_2^2)\, w_L^{(a)}(q_3^2)\, (f_2^{\mu\nu}\, \tilde{f}_1^{\nu\mu})(\tilde{f}^{\rho\sigma}\, f_3^{\sigma\rho}), \tag{182}$$

where $f_i^{\mu\nu} = q_i^\mu \epsilon_i^\nu - q_i^\nu \epsilon_i^\mu$ denote the field strength tensors. The form factors $\phi_L^{(a)}(q_1^2,q_2^2)$ account for the dependence of the amplitude on $q_{1,2}^2$, i.e. the internal interaction vertex in a_μ with two virtual photons, whereas the meson propagator and the external interaction vertex form the triangle amplitude described by the functions $w_L^{(a)}(q_3^2)$.

For the pion one obtains, outside the chiral limit,

$$w_L^{(3)}(q_3^2) = \frac{2}{q_3^2 + m_\pi^2}, \tag{183}$$

whereas the ABJ anomaly fixes $\phi_L^{(3)}(0,0) = N_c/(4\pi^2 F_\pi^2)$. Defining the $\pi^0\gamma^*\gamma^*$ form factor as follows $F_{\pi^0\gamma^*\gamma^*}(q_1^2,q_2^2) = \phi_L^{(3)}(q_1^2,q_2^2)/\phi_L^{(3)}(0,0)$, one finally obtains the result

$$\mathcal{A}_{\pi^0} = -\frac{N_c W^{(3)}}{2\pi^2 F_\pi^2}\, \frac{F_{\pi^0\gamma^*\gamma^*}(q_1^2,q_2^2)}{q_3^2+m_\pi^2}\, (f_2^{\mu\nu}\, \tilde{f}_1^{\nu\mu})(\tilde{f}^{\rho\sigma}\, f_3^{\sigma\rho}) + \text{permutations}. \tag{184}$$

By relating the $\langle VVV|\gamma\rangle$ matrix element to the triangle amplitude $\langle AV|\gamma\rangle$, in particular to the invariant function $w_L^{(3)}(q_3^2)$, Melnikov and Vainshtein deduce that no form factor $F_{\pi^0\gamma^*\gamma}(q_3^2,0)$ should be used at the external vertex, but only a constant factor, see Eq. (184). They rightly point out that such a form factor violates momentum conservation at the external vertex and criticize the procedure adopted in earlier works [243,242,245,17]. However, it is obvious from their expressions (reproduced above), that they only consider the on-shell pion form factor $\mathcal{F}_{\pi^0\gamma^*\gamma^*}(q_1^2,q_2^2) \equiv \mathcal{F}_{\pi^0\gamma^*\gamma^*}(m_\pi^2,q_1^2,q_2^2)$ (e.g. at the internal vertex) and not the off-shell pion form factor $\mathcal{F}_{\pi^{0*}\gamma^*\gamma^*}(q_3^2,q_1^2,q_2^2)$. Therefore, contrary to the claim in their paper, they only consider the **pion-pole** contribution to hadronic light-by-light scattering. Actually, also a second argument by Melnikov and Vainshtein in favor of a constant form factor at the external vertex was based on the use of on-shell form factors. Since $\mathcal{F}_{\pi^0\gamma^*\gamma}(q_3^2,0) \equiv \mathcal{F}_{\pi^0\gamma^*\gamma}(m_\pi^2,q_3^2,0) \sim 1/q_3^2$, for large q_3^2, according to Brodsky-Lepage, the use of a (non-constant) on-shell form factor at the external vertex would lead to an overall $1/q_3^4$ behavior which contradicts Eq. (184).

Translated into our notation employed in Eq. (151), Refs. [17,289] and maybe also earlier works, considered, e.g. for the first diagram of Fig. 35, the form factors in the pion-pole approximation

$$\mathcal{F}_{\pi^0\gamma^*\gamma^*}(m_\pi^2,q_1^2,q_3^2)\, \cdot \mathcal{F}_{\pi^0\gamma^*\gamma}(m_\pi^2,q_2^2,0)\,. \tag{185}$$

Although pole–dominance might be expected to give a reasonable approximation, it is not correct as it was used in those references. The point is that the form factor sitting at the external photon vertex in the pole approximation [read $\mathcal{F}_{\pi^0\gamma^*\gamma}(m_\pi^2,q_2^2,0)$] for $q_2^2 \neq m_\pi^2$ violates four–momentum conservation $k^\mu = 0$ [257,44,46]. The latter requires $\mathcal{F}_{\pi^{0*}\gamma^*\gamma}(q_2^2,q_2^2,0)$. In order to avoid this inconsistency, Melnikov and Vainshtein proposed to use

$$\mathcal{F}_{\pi^0\gamma^*\gamma^*}(m_\pi^2,q_1^2,q_3^2)\, \cdot \mathcal{F}_{\pi^0\gamma\gamma}(m_\pi^2,m_\pi^2,0)\,, \tag{186}$$

i.e. a constant (WZW) form factor at the external vertex. The absence of a form factor at the external vertex in the pion-pole approximation follows automatically, if one carefully considers the momentum dependence of the form factor. This procedure is also consistent with any quantum field theoretical framework for hadronic light-by-light scattering, for instance, if one uses a (resonance) Lagrangian to derive the form factors, and where a different treatment of the internal and external vertex (apart from the kinematics) is not possible. On the other hand, taking the diagram more literally, would require

$$\mathcal{F}_{\pi^{0*}\gamma^*\gamma^*}(q_2^2,q_1^2,q_3^2)\, \cdot \mathcal{F}_{\pi^{0*}\gamma^*\gamma}(q_2^2,q_2^2,0)\,, \tag{187}$$

as the more appropriate amplitude, see Eq. (151). In fact, we advocate the consistent use of off-shell form factors on both vertices as explained earlier. As will be shown in more detail in Sect. 5.1.4, the use of appropriate off-shell form factors within the framework of large-N_c QCD **does** lead to a short-distance

behavior which qualitatively agrees with the OPE constraints which were derived in Ref. [257] albeit with a different constant $c_{\rm MV} = -0.274$ vs. $c_{\rm JN} = -0.092$ (factor 3 lower). [23]

5.1.3. *The $\pi^0\gamma\gamma$ Transition Form Factor in different Models*

After the presentation of the experimental and theoretical constraints we now turn to some of the ansätze for the $\pi^0\gamma\gamma$ form factor, which have been used in the literature to evaluate the pion-exchange (or pion-pole) contribution and which are based on or are motivated by different models for low-energy hadrons. All these ansätze have certain drawbacks, thus leading to different results with inherent model-dependent uncertainties which are difficult to estimate.

The simplest model is the constant WZW form factor (recall that $q_3 = -(q_1 + q_2)$)

$$\mathcal{F}^{\rm WZW}_{\pi^{0*}\gamma^*\gamma^*}(q_3^2, q_1^2, q_2^2) = -\frac{N_c}{12\pi^2 F_\pi}\,, \tag{188}$$

which leads, however, to a divergent result in the integral in Eq. (151) [24], since there is no damping at high energies. One can use some momentum cutoff around $1-2$ GeV, but this procedure is completely arbitrary. Nevertheless, the WZW form factor serves as a physical normalization to the $\pi^0 \to \gamma\gamma$ decay rate and all models satisfy the constraint

$$\mathcal{F}_{\pi^0\gamma\gamma}(m_\pi^2, 0, 0) = \mathcal{F}^{\rm WZW}_{\pi^0\gamma\gamma}(m_\pi^2, 0, 0) = -\frac{N_c}{12\pi^2 F_\pi}. \tag{189}$$

One way to implement a damping at high momentum is the VMD prescription ($\gamma-\rho$ mixing) which works reasonably well in many applications to low-energy hadronic physics. It follows automatically in the HLS model which was used in Refs. [242,245] to evaluate the full hadronic light-by-light scattering contribution. The HLS models implements VMD in a consistent way, respecting chiral symmetry and electromagnetic gauge invariance. It leads to the form factor

$$\mathcal{F}^{\rm VMD}_{\pi^{0*}\gamma^*\gamma^*}(q_3^2, q_1^2, q_2^2) = -\frac{N_c}{12\pi^2 F_\pi}\frac{M_V^2}{(q_1^2 - M_V^2)}\frac{M_V^2}{(q_2^2 - M_V^2)}\,. \tag{190}$$

Note that the on- and off-shell VMD form factors are identical, since they do not depend on the momentum q_3^2 which flows through the pion-leg. The problem with the VMD form factor is that the damping is now too strong as it behaves like $\mathcal{F}_{\pi^0\gamma^*\gamma^*}(m_\pi^2, -Q^2, -Q^2) \sim 1/Q^4$, instead of $\sim 1/Q^2$ deduced from the OPE, see Eq. (168).

Another model for the form factor $\mathcal{F}_{\pi^{0*}\gamma^*\gamma^*}$ which was for instance used in Refs. [242,245,290] is the constituent quark model (CQM). The off-shell form factor is given by a quark triangular loop

$$\begin{aligned} F^{\rm CQM}_{\pi^{0*}\gamma^*\gamma^*}(q^2, p_1^2, p_2^2) &= 2M_q^2\, C_0(M_q, M_q, M_q; q^2, p_1^2, p_2^2) \\ &\equiv \int [{\rm d}\alpha]\, \frac{2M_q^2}{M_q^2 - \alpha_2\alpha_3 p_1^2 - \alpha_3\alpha_1 p_2^2 - \alpha_1\alpha_2 q^2}\,, \end{aligned} \tag{191}$$

where $[{\rm d}\alpha] = {\rm d}\alpha_1{\rm d}\alpha_2{\rm d}\alpha_3\,\delta(1-\alpha_1-\alpha_2-\alpha_3)$ and M_q is a constituent quark mass ($q = u, d, s$). For $p_1^2 = p_2^2 = q^2 = 0$ we obtain $F^{\rm CQM}_{\pi^{0*}\gamma^*\gamma^*}(0,0,0) = 1$, which is the proper ABJ anomaly. Note the symmetry of C_0 under permutations of the arguments (p_1^2, p_2^2, q^2). For large p_1^2 at $p_2^2 \sim 0$, $q^2 \sim 0$ or $p_1^2 \sim p_2^2$ at $q^2 \sim 0$ the asymptotic behavior is given by

$$F^{\rm CQM}_{\pi^0\gamma^*\gamma}(0, p_1^2, 0) \sim r\,\ln^2 r\,, \quad F^{\rm CQM}_{\pi^0\gamma^*\gamma^*}(0, p_1^2, p_1^2) \sim 2\,r\,\ln r, \tag{192}$$

[23] The large momentum behavior of the full light-by-light scattering amplitude for other momentum regions was also derived in Ref. [257] by evaluating exactly the massless quark loop. Although the ansatz with a constant form factor at the external vertex in Eq. (184) does not satisfy all of these constraints, it was argued in Ref. [257] that the effects of these other short-distance constraints on the final numerical result is negligible.

[24] Actually, the contribution involving the term T_2 in Eq. (151) is finite even for a constant form factor, see Refs. [245,17]. The numerical value is in fact always much smaller, less than 5%, than the results obtained for the part with T_1 with more realistic form factors.

where $r = \frac{M_q^2}{-p_1^2}$. The same behavior follows for $q^2 \sim p_1^2$ at $p_2^2 \sim 0$. Note that in all cases we have the same power behavior $\sim 1/p_i^2$ modulo logarithms. However, also this model has some drawbacks. It is possible to reproduce the correct OPE behavior (up to the logarithmic factors) by choosing the constituent quark mass as $M_q = 2\pi F_\pi/\sqrt{N_c} \sim 335$ MeV, which is close to $M_u = M_d = 300$ MeV often used in the literature. However, the same mass leads to a coefficient in the Brodsky-Lepage limit, which is too small by a factor of 6. Fitting instead the Brodsky-Lepage behavior would lead to the unrealistic value $M_q = \sqrt{24}\pi F_\pi/\sqrt{N_c} \sim 820$ MeV. In general, the description of the data with the CQM form factor is rather poor, since the $\log^2$ in Eq. (192) is distorting the power law for the values of p_1^2 probed in the experiment, see Ref. [245]. Furthermore, the permutation symmetry of the arguments in $F^{\rm CQM}_{\pi^{0*}\gamma^*\gamma^*}(q_3^2, q_1^2, q_2^2)$ is not based on any symmetry of the original QCD Green's function $\langle VVP\rangle$ in Eq. (149). Therefore there is also a damping in the other OPE limit studied above, $F^{\rm CQM}_{\pi^{0*}\gamma^*\gamma}(q^2, q^2, 0) \sim 1/q^2$, which does not agree with the result from Eq. (170), unless $\Pi_{\rm VT}(0) = 0$. The vanishing of $\Pi_{\rm VT}(0)$ contradicts, however, the relation between $\Pi_{\rm VT}(0)$ and the magnetic susceptibility χ in Eq. (172). Finally, it was argued in Ref. [244] that maybe one has to dress the coupling of the photons to the constituent quarks à la VMD which leads to a further damping at high momenta. Of course, all of this is very model dependent. A more complicated ansatz for the form factor, based on the nonlocal chiral quark model, was employed recently in Ref. [291] to evaluate the pion-exchange contribution. See that paper and references therein for a description of the model and the explicit expression for the form factor.

In Ref. [243] the ENJL model was used to evaluate the pseudoscalar exchange diagrams. This calculation was cross-checked in Ref. [242] by using a simplified version where the momentum dependence of some parameters, like F_π, M_ρ, was neglected. The off-shell form factor $\mathcal{F}_{\pi^{0*}\gamma^*\gamma^*}$ in the ENJL model is essentially given by a CQM-like form factor, see Ref. [243] and references therein for more details. In the ENJL model the dressing of the coupling of the constituent quarks to the photon arises automatically via the summation of chains of quark bubble diagrams. As for the CQM form factor, not all QCD short-distance constraints are fulfilled in the ENJL model. In general, the ENJL model is only valid up to some cutoff of order $800 - 1200$ MeV. Therefore, in Ref. [243] a modified version of the ENJL form factor was finally used for the numerical evaluation of the pion-exchange contribution. In this way some of the short-distance constraints could be satisfied, in particular to reproduce the Brodsky-Lepage behavior (161) and the experimental data for the on-shell form factor $\mathcal{F}_{\pi^0\gamma^*\gamma}(m_\pi^2, -Q^2, 0)$.

The results for the form factor $\mathcal{F}_{\pi^{0*}\gamma^*\gamma^*}$ obtained in different low energy effective hadronic models as usual do not satisfy all the large momentum asymptotics required by QCD. Using these form factors in loops thus leads to cut–off dependent results, where the cut–off is to be varied between reasonable values ($\sim 1 - 2$ GeV) which enlarges the model error of such estimates. Nevertheless it should be stressed that such approaches are perfectly legitimate and the uncertainties just reflect the lack of precise understanding of this kind of non-perturbative physics.

In order to eliminate (or at least reduce) this cut–off dependence, other models for $\mathcal{F}_{\pi^{0*}\gamma^*\gamma^*}$ were proposed later in Ref. [266] and then applied to hadronic light-by-light scattering in Ref. [17]. These models are based on the large–N_c picture of QCD, where, in leading order in N_c, an (infinite) tower of narrow resonances contributes in each channel of a particular Green's function. The low-energy and short-distance behavior of these Green's functions is then matched with results from QCD, using CHPT and the OPE, respectively. Based on the experience gained in many examples of low-energy hadronic physics, and from the use of dispersion relations and spectral representations for two-point functions, it is then assumed that with a minimal number of resonances in a given channel one can get a reasonable good description of the QCD Green's function in the real world. Often only the lowest lying resonance is considered, lowest meson dominance, LMD, as a generalization of vector meson dominance VMD. Note that it might not always be possible to satisfy **all** short-distance constraints, in particular from the high-energy behavior of form factors, if only a **finite number** of resonances is included, see Ref. [292]. Ideally, the matching with the QCD constraints and other informations, e.g. from decays of resonances, then determines all the free parameters in these minimal hadronic ansätze (MHA).

In this spirit, on-shell $\mathcal{F}_{\pi^0\gamma^*\gamma^*}(m_\pi^2, q_1^2, q_2^2)$ and off-shell form factors $\mathcal{F}_{\pi^{0*}\gamma^*\gamma^*}(q_3^2, q_1^2, q_2^2)$ were constructed in Ref. [266] which contain either the lowest lying multiplet of vector resonances (LMD) or two multiplets, the ρ and the ρ' (LMD+V). Both ansätze fulfill **all** the OPE constraints from Eqs. (163), (168) and (169),

however, the LMD ansatz does **not** reproduce the Brodsky-Lepage behavior from Eq. (161). Instead it behaves like $\mathcal{F}^{\rm LMD}_{\pi^0\gamma^*\gamma^*}(m_\pi^2,-Q^2,0)\sim$ const. The $1/Q^2$ fall-off can be achieved with the LMD+V ansatz with a certain choice of the free parameters (for more details see below). The on-shell form factors where later used in Ref. [17] to evaluate the pion-pole contribution, see also Ref. [289]. However, as mentioned earlier, taking on-shell form factors at both vertices violates four-momentum conservation.

5.1.4. *New Evaluation of the Pseudoscalar-exchange Contribution*

As stressed above, we advocate to use consistently dressed off-shell form factors at both vertices, using for our new numerical evaluation of the pion-exchange contribution the LMD+V **off-shell** form factor [266]

$$\begin{aligned}\mathcal{F}^{\rm LMD+V}_{\pi^{0*}\gamma^*\gamma^*}(p_\pi^2,q_1^2,q_2^2)&=\frac{F_\pi}{3}\,\frac{\mathcal{P}(q_1^2,q_2^2,p_\pi^2)}{\mathcal{Q}(q_1^2,q_2^2)},\\ \mathcal{P}(q_1^2,q_2^2,p_\pi^2)&=q_1^2\,q_2^2\,(q_1^2+q_2^2+p_\pi^2)+h_1\,(q_1^2+q_2^2)^2+h_2\,q_1^2\,q_2^2+h_3\,(q_1^2+q_2^2)\,p_\pi^2+h_4\,p_\pi^4\\ &\quad+h_5\,(q_1^2+q_2^2)+h_6\,p_\pi^2+h_7,\\ \mathcal{Q}(q_1^2,q_2^2)&=(q_1^2-M_{V_1}^2)\,(q_1^2-M_{V_2}^2)\,(q_2^2-M_{V_1}^2)\,(q_2^2-M_{V_2}^2),\end{aligned}\tag{193}$$

with $p_\pi^2\equiv(q_1+q_2)^2$.

We would like to point out that using the off-shell LMD+V form factor at the external vertex leads to a short-distance behavior which qualitatively agrees with the OPE constraints derived by Melnikov and Vainsthein in Ref. [257]. As a matter of fact, taking first $q_1^2\sim q_2^2\gg q_3^2$ and then q_3^2 large, one obtains, together with the pion propagator in Eq. (151), an overall $1/q_3^2$ behavior for the pion-exchange contribution, as expected from Eq. (184), since, according to Eq. (170), $\mathcal{F}^{\rm LMD+V}_{\pi^{0*}\gamma^*\gamma}(q_3^2,q_3^2,0)\sim$ const for large q_3^2. This also qualitatively agrees with the $1/q_3^2$ fall-off obtained for the quark-box diagram in light-by-light scattering derived in Ref. [257].

Before we can apply the above form–factor we have to pin down as far as possible the additional parameters h_i, which come in when the pion is far off-shell. A detailed analysis of these constraints, as well as a new calculation of the π^0–exchange contribution based on the off-shell LMD+V form factor, has been performed recently by one of the authors (A.N.) [270] and we closely follow the discussion presented there.

The constants h_i in the ansatz for $\mathcal{F}^{\rm LMD+V}_{\pi^{0*}\gamma^*\gamma^*}$ in Eq. (193) are determined as follows. The normalization with the WZW form factor in Eq. (189) yields $h_7=-N_cM_{V_1}^4M_{V_2}^4/(4\pi^2F_\pi^2)-h_6m_\pi^2-h_4m_\pi^4$. Note that in Refs. [266,17] the small corrections proportional to the pion mass were dropped, assuming that the h_i are of order $1-10$ in appropriate units of GeV. The Brodsky-Lepage behavior Eq. (161) can be reproduced by choosing $h_1=0$ GeV^2. Furthermore, in Ref. [266] a fit to the CLEO data for the on-shell form factor $\mathcal{F}^{\rm LMD+V}_{\pi^0\gamma^*\gamma}(m_\pi^2,-Q^2,0)$ was performed, with the result $h_5=6.93\pm0.26$ GeV$^4-h_3m_\pi^2$. Again, the correction proportional to the pion mass was omitted in Refs. [266,17]. As pointed out in Ref. [257], the constant h_2 can be obtained from the higher-twist corrections in the OPE. Comparing with Eq. (175) yields the result $h_2=-4\,(M_{V_1}^2+M_{V_2}^2)+(16/9)\,\delta^2\simeq-10.63$ GeV^2, where we used $M_{V_1}=M_\rho=775.49$ MeV and $M_{V_2}=M_{\rho'}=1.465$ GeV [293].

Within the LMD+V framework, the vector-tensor two-point function discussed earlier reads [266]

$$\Pi^{\rm LMD+V}_{\rm VT}(p^2)=-\,\langle\overline{\psi}\psi\rangle_0\,\frac{p^2+c_{\rm VT}}{(p^2-M_{V_1}^2)(p^2-M_{V_2}^2)}\,,\tag{194}$$

$$c_{\rm VT}=\frac{M_{V_1}^2M_{V_2}^2\chi}{2},\tag{195}$$

where we fixed the constant $c_{\rm VT}$ using Eq. (172). As shown in Ref. [266] the OPE from Eq. (169) for $\mathcal{F}^{\rm LMD+V}_{\pi^{0*}\gamma^*\gamma^*}$ leads to the relation

$$h_1+h_3+h_4=2c_{\rm VT}.\tag{196}$$

As noted above, the value of the magnetic susceptibility $\chi(\mu)$ and the relevant scale μ are not precisely known. Adopting the estimate presented in Ref. [270] we will use $\chi=-(3.3\pm1.1)$ GeV^{-2} in our numerical

evaluation, which implies the constraint $h_3+h_4 = -(4.3\pm1.4)$ GeV^2. We will vary h_3 in the range ±10 GeV^2 and determine h_4 from Eq. (196) and vice versa.

The coefficient h_6 is undetermined as well. Direct phenomenological constraints are not available. Model estimates within the resonance Lagrangian and/or large-N_c inspired approaches are given in [270]. In accordance with these estimates we will vary h_6 in the range 5 ± 5 GeV^4.

Of course, the uncertainties of the values of the undetermined parameters h_3, h_4 and h_6 and of the magnetic susceptibility $\chi(\mu)$ are a drawback when using the off-shell LMD+V form factor and will limit the precision of the final result. Before presenting our estimate we note that as a check we have reproduced with our 3-dimensional integral representation for $a_\mu^{\mathrm{LbL};\pi^0}$ in Eq. (155) the results for various form factors obtained earlier in the literature, e.g. $a_{\mu;\mathrm{VMD}}^{\mathrm{LbL};\pi^0} = 57 \times 10^{-11}$ with the value for $M_\rho = 775.49$ MeV given above.

The results for $a_\mu^{\mathrm{LbL};\pi^0}$ for some selected values of χ, h_3, h_4 and h_6, varied in the ranges discussed above, with fixed $h_1 = 0$ GeV^2, $h_2 = -10.63$ GeV^2 and $h_5 = 6.93$ GeV$^4 - h_3 m_\pi^2$ are collected in Table 7.

Table 7
Results for $a_\mu^{\mathrm{LbL};\pi^0} \times 10^{11}$ obtained with the off-shell LMD+V form factor for some selected values of $\chi, h_3[h_4]$ (imposing the constraint (196) with $h_1 = 0$ GeV^2) and h_6. The values of the other model parameters are given in the text.

		$h_6 = 0$ GeV^4	$h_6 = 5$ GeV^4	$h_6 = 10$ GeV^4
$\chi = -4.4$ GeV^{-2}	$h_{3[4]} = -10$ GeV^2	69.8 [66.9]	75.7 [72.5]	81.9 [78.4]
	$h_{3[4]} = 0$ GeV^2	67.8 [68.9]	73.4 [74.7]	79.4 [80.8]
	$h_{3[4]} = 10$ GeV^2	65.8 [71.0]	71.2 [76.9]	77.0 [83.3]
$\chi = -3.3$ GeV^{-2}	$h_{3[4]} = -10$ GeV^2	68.4 [65.3]	74.1 [70.7]	80.2 [76.5]
	$h_{3[4]} = 0$ GeV^2	66.4 [67.3]	71.9 [72.8]	77.8 [78.8]
	$h_{3[4]} = 10$ GeV^2	64.5 [69.2]	69.7 [75.0]	75.4 [81.2]
$\chi = -2.2$ GeV^{-2}	$h_{3[4]} = -10$ GeV^2	67.1 [63.8]	72.7 [69.0]	78.7 [74.7]
	$h_{3[4]} = 0$ GeV^2	65.2 [65.7]	70.5 [71.1]	76.3 [77.0]
	$h_{3[4]} = 10$ GeV^2	63.3 [67.6]	68.4 [73.3]	74.0 [79.3]

Varying χ in the range $-(3.3 \pm 1.1)$ GeV^{-2} changes the result for $a_\mu^{\mathrm{LbL};\pi^0}$ by at most $\pm2.1 \times 10^{-11}$. The uncertainty in h_6 affects the result by up to $\pm6.4 \times 10^{-11}$. The variation of $a_\mu^{\mathrm{LbL};\pi^0}$ with h_3 (with h_4 determined from the constraint in Eq. (196) with $h_1 = 0$ GeV^2 or vice versa) is much smaller, at most $\pm2.5 \times 10^{-11}$. The variation of h_5 by ±0.26 GeV^4 only leads to changes of $\pm0.6 \times 10^{-11}$ in the final result.

Within the scanned region, we obtain a minimal value of $a_\mu^{\mathrm{LbL};\pi^0} = 63.3 \times 10^{-11}$ for $\chi = -2.2$ GeV^{-2}, $h_3 = 10$ GeV^2, $h_6 = 0$ GeV^4 and a maximum of $a_\mu^{\mathrm{LbL};\pi^0} = 83.3 \times 10^{-11}$ for $\chi = -4.4$ GeV^{-2}, $h_4 = 10$ GeV^2, $h_6 = 10$ GeV^4. In the absence of more information on the precise values of the constants h_3, h_4 and h_6, we take the average of the results obtained with $h_6 = 5$ GeV^4 for $h_3 = 0$ GeV^2, i.e. 71.9×10^{-11}, and for $h_4 = 0$ GeV^2, i.e. 72.8×10^{-11}, as our central value, 72.3×10^{-11}. To estimate the error, we add all the uncertainties from the variations of χ, h_3 (or h_4), h_5 and h_6 linearly to cover the full range of values obtained with our scan of parameters. Note that the uncertainties of χ and the coefficients h_3, h_4 and h_6 do not follow a Gaussian distribution. In this way we obtain our final estimate [270] (see also [174])

$$a_\mu^{\mathrm{LbL};\pi^0} = (72 \pm 12) \times 10^{-11}. \tag{197}$$

Unless one can pin down the ranges of χ and h_6 more precisely, we get a larger error than previous estimates based e.g. on the on-shell LMD+V form factor (which has less free parameters). We would like to stress that although the central value of our result in Eq. (197) is rather close to $a_\mu^{\mathrm{LbL};\pi^0} = (76.5 \pm 6.7) \times 10^{-11}$ given by Melnikov and Vainshtein [257],[25] this is **pure coincidence**. We have used off-shell LMD+V form factors

[25] Actually, using the on-shell LMD+V form factor at the internal vertex with $h_2 = -10$ GeV^2 and $h_5 = 6.93$ GeV^4 and a constant WZW form factor at the external vertex, we obtain 79.8×10^{-11}, close to the value 79.6×10^{-11} given in Ref. [41] and 79.7×10^{-11} in Ref. [291].

at both vertices, whereas Melnikov and Vainshtein evaluated the **pion-pole** contribution using the on-shell LMD+V form factor at the internal vertex and the constant WZW form factor at the external vertex.[26]

As far as the contribution to a_μ from the exchanges of the other light pseudoscalars, η and η', is concerned, it is not so straightforward to apply the above analysis within the LMD+V framework to these resonances. In particular, the short-distance analysis in Ref. [266] was performed in the chiral limit and assumed octet symmetry. For the η the effect of nonzero quark masses has definitely to be taken into account. Furthermore, the η' has a large admixture from the singlet state and the gluonic contribution to the axial anomaly will play an important role. We therefore resort to a simplified approach which was also adopted in other recent works [242,245,243,17,257] and take the VMD form factor Eq. (190), normalized to the experimental decay width $\Gamma(\mathrm{P}\to\gamma\gamma)$, $\mathrm{P}=\eta,\eta'$. We can fix the normalization by adjusting the pseudoscalar decay constant. Using the latest values $\Gamma(\eta\to\gamma\gamma)=0.510\pm0.026$ keV and $\Gamma(\eta'\to\gamma\gamma)=4.30\pm0.15$ keV from Ref. [293], one obtains $F_{\eta,\mathrm{eff}}=93.0$ MeV with $m_\eta=547.853$ MeV and $F_{\eta',\mathrm{eff}}=74.0$ MeV with $m_{\eta'}=957.66$ MeV. We have seen above that the pion exchange contribution evaluated with off-shell form factors is not far from the pion-pole contribution. Of course, only a more detailed analysis will show, whether this approximation works well for η and η'. It should also be kept in mind that the VMD form factor has a too strong damping for large momenta. From the experience with the pion contribution, it seems, however, more important to have a good description of the relevant form factors at small and intermediate energies below 1 GeV, e.g., by reproducing the slope of the form factor $\mathcal{F}_{\mathrm{P}\gamma^*\gamma}(m_\mathrm{P}^2,-Q^2,0)$, at the origin. The CLEO Collaboration [260] has made a fit of the (on-shell) form factors $\mathcal{F}_{\eta\gamma^*\gamma}(m_\eta^2,-Q^2,0)$ and $\mathcal{F}_{\eta'\gamma^*\gamma}(m_{\eta'}^2,-Q^2,0)$ using an interpolating formula similar to Eq. (162) with an adjustable vector meson mass Λ_P. Taking their values $\Lambda_\eta=774\pm29$ MeV or $\Lambda_{\eta'}=859\pm28$ MeV as the vector meson mass M_V in the expression of the VMD form factor in Eq. (190), we get $a_\mu^{\mathrm{LbL};\eta}=(14.5\pm4.8)\times10^{-11}$ and $a_\mu^{\mathrm{LbL};\eta'}=(12.5\pm4.2)\times10^{-11}$, where we assumed a relative error of 33%. Note that these values are somewhat smaller than $a_\mu^{\mathrm{LbL};\eta-\mathrm{pole}}=18\times10^{-11}$ and $a_\mu^{\mathrm{LbL};\eta'-\mathrm{pole}}=18\times10^{-11}$ given in Ref. [257], where the constant WZW form factor was used at the external vertex. Adding up all contributions from the pseudoscalars, we finally obtain the estimate

$$a_\mu^{\mathrm{LbL;PS}}=(99\pm16)\times10^{-11}\,, \tag{198}$$

given in [270] (see also [174]).

5.2. *Summary of the Light-by-Light Scattering Results*

We are now ready to summarize the results obtained by the different groups for the hadronic light-by-light scattering contribution. A comparison of the different results also sheds light on the difficulties and the model dependencies in the theoretical estimations achieved so far. Very recently, a joint effort to summarize the results obtained by various groups has been presented by Prades, de Rafael and Vainshtein [PdRV] [294]. The values advocated by them are included in our tables.

Pseudoscalar exchanges

According to Table 6 the diagram Fig. 34(a) with the exchange of pseudoscalars yields the most important contribution in the large-N_c counting, but requires a model for the $\mathcal{F}_{\pi^{0*}\gamma^*\gamma^*}$ form factor for its evaluation. Although it is subleading in the chiral expansion in comparison to the loop with charged pions and Kaons

[26] Note that at the external vertex

$$\frac{3}{F_\pi}\,\mathcal{F}^{\mathrm{LMD+V}}_{\pi^{0*}\gamma^*\gamma}(q_1^2,q_1^2,0)\overset{q_1^2\to\infty}{\to}\frac{h_1+h_3+h_4}{M_{V_1}^2M_{V_2}^2}=\frac{2c_\mathrm{VT}}{M_{V_1}^2M_{V_2}^2}=\chi\,,$$

while $\mathcal{F}^{\mathrm{VVA\ triangle}}_{\pi^{0*}\gamma^*\gamma}(q_1^2,q_1^2,0)|_{m_q=0}=\mathcal{F}^{\mathrm{WZW}}_{\pi^0\gamma\gamma}(0,0,0)=\mathcal{F}^{\mathrm{LMD+V}}_{\pi^0\gamma\gamma}(0,0,0)$ utilized in Ref. [257] means

$$\frac{3}{F_\pi}\,\mathcal{F}^{\mathrm{LMD+V}}_{\pi^0\gamma\gamma}(0,0,0)=\frac{h_7}{M_{V_1}^4M_{V_2}^4}=-\frac{N_c}{4\pi^2F_\pi^2}\simeq-8.9\ \mathrm{GeV}^{-2}\,,$$

i.e. with Vainshtein's [275] value of χ we would precisely satisfy the Melnikov-Vainshtein [257] short-distance constraint.

(Fig. 34(b)), it turns out that this is the numerically dominating contribution, see the numbers collected in Table 8. The dominance of the pseudoscalar exchange contributions in view of Fig. 32 after all is an experimental fact.

Table 8
Results for the π^0, η and η' exchange contributions.

Model for $\mathcal{F}_{P^*\gamma^*\gamma^*}$	$a_\mu(\pi^0) \times 10^{11}$	$a_\mu(\pi^0, \eta, \eta') \times 10^{11}$
Point coupling	$+\infty$	$+\infty$
ENJL (modified) [BPP] [243,41]	59(9)	85(13)
VMD / HLS [HKS,HK] [242,245]	57(4)	83(6)
nonlocal χQM (off-shell) [291]	65(2)	–
LMD+V [KN] (on-shell, $h_2 = 0$ GeV^2) [17]	58(10)	83(12)
LMD+V [KN] (on-shell, $h_2 = -10$ GeV^2) [17]	63(10)	88(12)
LMD+V [MV] (on-shell, constant FF at external vertex) [257]	77(7)	114(10)
LMD+V [PdRV] (on-shell, constant FF at external vertex) [294]	–	114(13)
LMD+V [N] (off-shell, $\chi = -(3.3 \pm 1.1)$ GeV$^{-2}, h_6 = (5 \pm 5)$ GeV^4) [270]	72(12)	99(16)

BPP [243] work within the context of the ENJL model, however, they take the model only seriously for scales below a few hundred MeV. At higher momenta, they modify the corresponding ENJL form factor with VMD dressing or consider a pure VMD form factor. In particular, they try to find a phenomenological parametrization that interpolates between the ENJL form factor, which works well below 0.5 GeV, and the measured (on-shell) form factor $\mathcal{F}_{\pi^0\gamma^*\gamma}(m_\pi^2, -Q^2, 0)$ for Euclidean momenta above 0.5 GeV and with its asymptotic behavior predicted by QCD (Brodsky-Lepage). The results for η and η' are obtained by using a VMD form factor normalized to the experimental decay rate P $\to \gamma\gamma$ and rescaled with the ENJL result for π^0. HKS, HK [242,245] work with the HLS model which leads to a VMD form factor, but also studied the effects of various other kinds of form factors: (dressed) CQM, ENJL-like[27], mixed versions. At the end, they choose a VMD model where the normalization is fixed by the experimental two-photon decay width. Furthermore, the rather small error estimate is derived from fitting the (on-shell) form factor $\mathcal{F}_{P\gamma^*\gamma}(m_P^2, -Q^2, 0)$ to the available data. This procedure might, however, underestimate the intrinsic model dependence, in particular, for off-shell values of the form factor. In Ref. [291] off-shell form factors were used at both vertices, following the suggestion in Ref. [44]. These authors use the nonlocal chiral quark model which shows a strong, exponential suppression for large pion virtualities. This is very different from what is observed in all the other models. Finally, we note that all the LMD+V estimates in Table 8 only apply to the pion. For the η and η' a VMD form factor is used, normalized to the experimental decay width.

Axial-vector and scalar exchanges

Next in Table 6 are the exchanges of other resonances, like axial-vectors and scalars in a diagram analogous to Fig. 34(a). They are also leading in N_c, but of higher order in the chiral counting, compared to the pseudoscalars. The results for the axial-vector contribution are collected in Table 9 and those for the scalars in Table 10. Since the masses of these resonances are higher[28] in comparison with the pseudoscalars, in particular the π^0, the corresponding suppression by the propagator leads in general to smaller results, unless the coupling to photons is extraordinary large.

In Ref. [257] it was argued that again a constant form factor should be used at the external vertex to reproduce QCD short-distance constraints, similarly to the procedure adopted for the pseudoscalars in the same reference. Using a simple VMD ansatz they also derive the first term in a series expansion in powers of

[27] By ENJL-like we denote the fact that the authors of Refs. [242,245] took for a cross-check of the evaluation in Ref. [243], the expressions for the form factor in the ENJL model, however, they neglected the momentum dependence of f_π, M_V and the parameter g_A in this model.
[28] Apart from the contribution of a potentially light, broad σ-meson $f_0(600)$.

Table 9
Results for the axial-vector (a_1, f_1 and f_1') exchange contributions.

Model for $\mathcal{F}_{A^*\gamma^*\gamma^*}$	$a_\mu(a_1) \times 10^{11}$	$a_\mu(a_1, f_1, f_1') \times 10^{11}$
ENJL-VMD [BPP] (nonet symmetry) [243]	2.5(1.0)	–
ENJL-like [HKS,HK] (nonet symmetry) [242,245]	1.7(1.7)	–
LMD [MV] (ideal mixing) [257]	5.7	22(5)
LMD [PdRV] [294]	–	15(10)

m_μ/M, where M denotes the axial-vector mass (assuming nonet-symmetry were they are all treated as equal as done in Refs. [243,242,245]). They observe that the result strongly depends on the exact choice of this mass, e.g. with $M = M_\rho$ they obtain 28×10^{-11}. The results shown in Table 9 have been obtained by using a more sophisticated ansatz for the form factor at the external vertex which was first proposed in Ref. [284]. Note that the form factor now includes a dressing with respect to the one off-shell photon at the external vertex. In this way they treat the resonances a_0, f_1, f_1' separately. Since the dressing leads to lower effective axial-vector masses and since the states f_0 and f_0' have an enhanced coupling to photons (similarly to η and η'), the final result is a factor of 10 larger than those obtained earlier in Refs. [243,242,245]. The result for the sum of all resonances in Ref. [257] does not depend too much on the value of the mixing angle between f_0 and f_0' (treating f_1 as pure octet and f_1' as pure $SU(3)$ singlet, they obtain the result 17×10^{-11}). We think the procedure adopted in Ref. [257] is an important improvement over Refs. [243,242,245] and we will therefore take the result for the axial-vectors from that reference for our final estimate for the full hadronic light-by-light scattering contribution below, despite the fact that only on-shell form factors have been used in Ref. [257]. As we argued above for the pseudoscalar exchanges, we think that one should use consistently off-shell form factors at the internal and the external vertex.

Table 10
Results for the scalar exchange contributions.

Model for $\mathcal{F}_{S^*\gamma^*\gamma^*}$	$a_\mu(\text{scalars}) \times 10^{11}$
Point coupling	$-\infty$
ENJL[BPP] [243,41]	-7(2)
ENJL[PdRV] [294]	-7(7)

The contribution from scalar resonances with masses around 1 GeV was first studied in Ref. [79], but found to be negligible (0.1×10^{-11}), compared to the dominating π^0 exchange contribution. Within the ENJL model used in Ref. [243], this scalar exchange contribution is related via Ward identities to the (constituent) quark loop. In fact, Ref. [245] argued that the effect of the exchange of (broad) scalar resonances below several hundred MeV might already be included in the sum of the (dressed) quark loop and the dressed pion and Kaon loop. Such a potential double-counting is definitely an issue for the broad sigma meson $f_0(600)$. Furthermore there is some ongoing debate in the literature, see the PDG [104] and references therein, whether the scalar resonances $f_0(980)$ and $a_0(980)$ are two-quark or four-quark states (meson molecules).

The parameters of the ENJL model used in Ref. [243] have been determined in Refs. [295,296,297]. In particular, in [295] a fit was performed to various low-energy observables and resonance parameters, among them a scalar multiplet with mass $M_S = 983$ MeV. However, with those fitted parameters, the ENJL model actually predicts a rather low mass of $M_S^{\text{ENJL}} = 620$ MeV. This would then correspond more to the light sigma meson $f_0(600)$. We note that within a very simple model of a scalar meson S coupled to photons via a term $S\, F_{\mu\nu} F^{\mu\nu}$, together with a simple VMD-dressing, there arises again a leading $\log^2$ term for $M_\rho \to \infty$. If the coupling in the above Lagrangian is the same as for the π^0 in the WZW term, i.e. $\alpha N_c/(12\pi F_\pi)$, then the coefficient of the log-square term is identical to the universal coefficient found for the pion, except for the negative sign, see Ref. [255]. The question is whether the usually broad scalar resonances can really be

described by such a simple resonance Lagrangian which works best in the large-N_c limit, i.e. for very narrow states.

Charged pion and Kaon loops

Third in Table 6 are the charged pion- and Kaon-loops Fig. 34(b) which yield the leading contribution in chiral counting, but are subleading in N_c. The results are given in Table 11.

Table 11
Results for the (dressed) $\pi^\pm, K^\pm$ loops.

Model $\pi^+\pi^-\gamma^*(\gamma^*)$	$a_\mu(\pi^\pm)\times 10^{11}$	$a_\mu(\pi^\pm, K^\pm)\times 10^{11}$
Point coupling (sQED)	−45.3	−49.8
VMD [KNO, HKS] [79,242]	−16	–
full VMD [BPP] [243]	−18(13)	−19(13)
HLS [HKS,HK] [242,245]	−4.45	−4.5(8.1)
[MV] [257]	–	0(10)
full VMD [PdRV] [294]	–	−19(19)

The result without dressing (scalar QED) is finite, see the EFT analysis discussed in Sect. 5.3, in contrast to the pseudoscalar exchanges. There was some debate between the authors of Refs. [242,245] (using the HLS model) and [243] (using full VMD), on how the dressing of the point vertex has to be implemented without violating gauge and chiral invariance. This explains the numerical difference between the two evaluations. The difference of the two values also indicates the potential model dependence of the result. The most important fact, however, is that the dressing leads to a rather huge suppression of the final result compared to the undressed case, so that the final result is much smaller than the one obtained for the pseudoscalars. This effect was studied for the HLS model in Ref. [257], in an expansion in $(m_\pi/M_\rho)^2$ and $\delta = (m_\mu - m_\pi)/m_\pi$, with the result ($L = \ln(M_\rho/m_\pi)$)

$$\begin{aligned} a_\mu^{\mathrm{LbL};\pi^\pm} &= \left(\frac{\alpha}{\pi}\right)^3 \sum_{i=0}^{\infty} f_i(\delta, L) \left(\frac{m_\pi^2}{M_\rho^2}\right)^i = \left(\frac{\alpha}{\pi}\right)^3 (-0.0058) \\ &= (-46.37 + 35.46 + 10.98 - 4.70 - 0.3 + \ldots) \times 10^{-11} = -4.9(3) \times 10^{-11}, \end{aligned} \tag{199}$$

where the functions $f_i(\delta, L)$ have been calculated for $i = 0, \ldots, 4$ in Ref. [257] and are explicitly given for $i = 0, 1, 2$ there. The subsequent terms in the last line correspond to the terms in the expansion in the first line. As one can see, there occurs a large cancellation between the first three terms in the series and the expansion converges only very slowly. The main reason is that typical momenta in the loop integral are of order $\mu = 4m_\pi \approx 550$ MeV and the effective expansion parameter is μ/M_ρ. The authors of Ref. [257] took this as an indication that the final result is very likely suppressed, but also very model dependent and that the chiral expansion looses its predictive power. The pion and Kaon loop contribution is then only one among many potential contributions of $\mathcal{O}(1)$ in N_c and they lump all of these into the guesstimate $a_\mu^{\mathrm{LbL};N_c^0} = (0 \pm 10) \times 10^{-11}$. However, since this estimate does not even cover the explicit, although model-dependent, results for the pion and Kaon loops given in Refs. [243,242], we think this procedure is not very appropriate.

Dressed quark loop

Finally, the last entry in Table 6 is the (constituent) quark loop Fig. 34(c) which appears as short-distance complement of the ENJL and HLS low-energy effective models used in Refs. [243,242,245]. It is again leading order in N_c and of the same chiral order as the axial-vector and scalar exchanges in $\langle VVV \rangle$. As argued in Ref. [244] such a quark-loop can be interpreted as an irreducible contribution to the 4-point function and should be added to the other contributions, although a dressing of the coupling of the constituent quarks

with the photons might occur. According to quark-hadron duality, the (constituent) quark loop also models the contribution to a_μ from the exchanges and loops of heavier resonances, like $\pi', a_0', f_0', p, n, \ldots$ which have not been included explicitly so far. It also "absorbs" the remaining cutoff dependences of the low-energy effective models. This is even true for the modeling of the pion-exchange contribution within the large N_c inspired approach (LMD+V), since not all QCD short-distance constraints in the 4-point function $\langle VVVV \rangle$ are reproduced with those ansätze. Some estimates for the (dressed) constituent quark loop are given in Table 12.

Table 12
Results for the (dressed) quark loops.

Model	$a_\mu(\text{quarks}) \times 10^{11}$
Point coupling	62(3)
VMD [HKS, HK] [242,245]	9.7(11.1)
ENJL + bare heavy quark [BPP] [243]	21(3)
Bare c-quark only [PdRV] [294]	2.3

We observe again a large, very model-dependent effect of the dressing of the photons. HKS, HK [242,245] used a simple VMD-dressing for the coupling of the photons to the constituent quarks as it happens for instance in the ENJL model. On the other hand, BPP [243] employed the ENJL model up to some cutoff μ and then added a bare quark loop with a constituent quark mass $M_Q = \mu$. The latter contribution simulates the high-momentum component of the quark loop, which is non-negligible. The sum of these two contributions is rather stable for $\mu = 0.7, 1, 2$ and 4 GeV and gives the value quoted in Table 12. A value of 2×10^{-11} for the c-quark loop is included by BPP [243], but not by HKS [242,245].

Summary

The totals of all contributions to hadronic light-by-light scattering reported in the most recent estimations are shown in Table 13. We have also included some "guesstimates" for the total value. Note that the number $a_\mu^{\text{LbL;had}} = (80 \pm 40) \times 10^{-11}$ written in the fourth column in Table 13 under the heading KN was actually not given in Ref. [17], but represents estimates used mainly by the Marseille group before the appearance of the paper by MV [257]. Furthermore, we have included in the sixth column the estimate $a_\mu^{\text{LbL;had}} = (110 \pm 40) \times 10^{-11}$ given recently in Refs. [298,41,43]. Note that PdRV [294] (seventh column) do not include the dressed light quark loops as a separate contribution. They assume them to be already covered by using the short-distance constraint from MV [257] on the pseudoscalar-pole contribution. PdRV add, however, a small contribution from the bare c-quark loop.

Table 13
Summary of the most recent results for the various contributions to $a_\mu^{\text{LbL;had}} \times 10^{11}$. The last column is our estimate based on our new evaluation for the pseudoscalars and some of the other results.

Contribution	BPP	HKS	KN	MV	BP	PdRV	N/JN
π^0, η, η'	85±13	82.7±6.4	83±12	114±10	–	114±13	99±16
π, K loops	−19±13	−4.5±8.1	–	–	–	−19±19	−19±13
π, K loops + other subleading in N_c	–	–	–	0±10	–	–	–
axial vectors	2.5±1.0	1.7±1.7	–	22± 5	–	15±10	22± 5
scalars	−6.8±2.0	–	–	–	–	−7± 7	−7± 2
quark loops	21± 3	9.7±11.1	–	–	–	2.3	21± 3
total	83±32	89.6±15.4	80±40	136±25	110±40	105±26	116±39

As one can see from Table 13, the different models used by various groups lead to slightly different results for the individual contributions. The final result [29]

$$a_\mu^{\rm LbL;had} = (116 \pm 39) \times 10^{-11} \tag{200}$$

for the hadronic light-by-light scattering contribution is dominated by the pseudoscalar exchange contribution, which we have recalculated from scratch and beyond the pion-pole approximation which has been used frequently. The other contributions are smaller, but not negligible [243,41]. Furthermore, they cancel out to some extent. Since the variation of the results for these individual contributions reflects our inherent ignorance of strong interaction physics in hadronic light-by-light scattering, it has become customary to take the difference between those values as an indication of the model uncertainty and to add the errors in Table 13 linearly (note, however, that PdRV [294] add the errors in quadrature). Maybe this error estimate is too conservative. For instance, the sum of the dressed pion and Kaon loops and the dressed quark loops is almost identical for the two evaluations by BPP [243] and HKS [242,245] using different models. But maybe this is a pure numerical coincidence, since these contributions have a different counting in N_c and p^2, see Table 6. Unless one can obtain for instance a more precise and reliable determination of the pion-loop contribution, it will be difficult to claim that we really control this kind of hadronic physics. At the moment, one cannot argue that either the ENJL / full VMD model employed by BPP or the HLS model used by HSK is superior compared to the other approach.

We also want to stress again that the identification of individual contributions in hadronic light-by-light scattering (like pion-exchange or the pion loop) is model dependent as soon as one uses off-shell form factors. Keeping this caveat in mind, we think that some progress has been made in recent years in understanding the pseudoscalar and axial-vector exchange contributions, following Refs. [17,257,41] and our new evaluation for the pseudoscalar-exchange contribution in Sect. 5.1.4. Also the effective field theory analysis of Refs. [249,256], which yields the leading log terms in the pion exchange contribution, agrees roughly with the numerical values obtained with different models, although the EFT approach cannot give a precise number in the end, see Sect. 5.3. Apart from the numerical differences between BPP and HKS for the dressed pion loop and the dressed quark loop, there is the issue of the scalar exchange contribution, see also the discussion above. We think that a priori such a contribution is likely to be there and the numerical value given in Ref. [243] looks reasonable, therefore we have included it in our final estimate. In view of the relatively large contribution of the axial-vector mesons with masses around 1300 MeV, it should finally be kept in mind that other states in that mass region could also contribute significantly to the final result. It is not clear at present, whether all of these contributions are appropriately modeled by the dressed quark loop. We will discuss some prospects for improving the estimate of the hadronic light-by-light scattering contribution to a_μ and for reducing its theoretical error in Sect. 8.

5.3. *An Effective Field Theory Approach to Hadronic Light-by-Light Scattering*

In Ref. [249] an EFT approach to hadronic light-by-light scattering was presented based on an effective Lagrangian that describes the physics of the Standard Model well below 1 GeV. It includes photons, light leptons, and the pseudoscalar mesons and obeys chiral symmetry and $U(1)$ gauge invariance.

The leading contribution to $a_\mu^{\rm LbL;had}$, of order [30] p^6, is given by a finite loop of charged pions, see Fig. 34(b), however, with point-like electromagnetic vertices, i.e. without the dressing of the photons (scalar QED). The

[29] For the electron we obtain $a_e^{\rm LbL;\pi^0} = (2.98 \pm 0.34) \times 10^{-14}$ with the off-shell LMD+V form factor. This number supersedes the value given in Ref. [17]. Note that the naive rescaling $a_e^{\rm LbL;\pi^0}({\rm rescaled}) = (m_e/m_\mu)^2 a_\mu^{\rm LbL;\pi^0} = 1.7 \times 10^{-14}$ yields a value which is almost a factor 2 too small. Estimates for the other pseudoscalars are $(0.49 \pm 0.16) \times 10^{-14}[\eta]$ and $(0.39 \pm 0.13) \times 10^{-14}[\eta']$. Since the other contributions are smaller and/or largely cancel, we arrive at an estimate $a_e^{\rm LbL;had} \sim (3.9 \pm 1.3) \times 10^{-14}$, where we assumed a relative error of 33% to be conservative.

[30] Note that here we count directly the chiral order of the contribution to a_μ, in contrast to the counting used in Table 6 and Ref. [244]. In the EFT approach of Ref [249], the chiral power counting is generalized by treating e, m and fermion bilinears as order p.

numerical value is $a_{\mu;\mathrm{sQED}}^{\mathrm{LbL}}(\pi^\pm, K^\pm\text{−loops}) \simeq -48\times 10^{-11}$. Since this contribution involves a loop of hadrons, it is subleading in the large-N_c expansion, see Table 6.

At order p^8 and at leading order in N_c, we encounter the divergent pion-pole contribution, diagrams (a) and (b) of Fig. 36, involving two WZW vertices. The diagram (c) is actually finite. The divergences

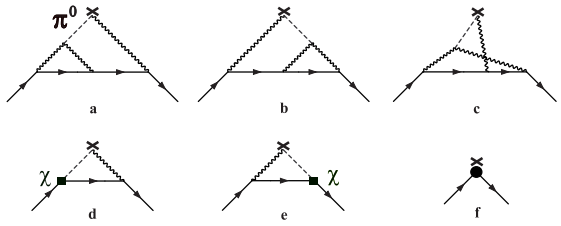

Fig. 36. The graphs contributing to $a_\mu^{\mathrm{LbyL};\pi^0}$ at lowest order in the effective field theory.

of the triangular subgraphs in the diagrams (a) and (b) are removed by inserting the counterterm χ from the Lagrangian[31] $\mathcal{L}^{(6)} = (\alpha^2/4\pi^2 F_\pi)\ \chi\ \overline{\psi}\gamma_\mu\gamma_5\psi\,\partial^\mu\pi^0 + \cdots$, leading to the one-loop diagrams (d) and (e). Finally, there is an overall divergence of the two-loop diagrams (a) and (b) that is removed by a magnetic moment type counterterm, diagram (f). Since the EFT involves such a local contribution, we will not be able to give a precise numerical prediction for $a_\mu^{\mathrm{LbL;had}}$. Nevertheless, it is interesting to consider the leading and next-to-leading logarithms that are in addition enhanced by a factor N_c and which can be calculated using the renormalization group [249]. The EFT and large-N_c analysis tells us that

$$a_\mu^{\mathrm{LbL;had}} = \left(\frac{\alpha}{\pi}\right)^3 \left\{ f\left(\frac{m_{\pi^\pm}}{m_\mu}, \frac{m_{K^\pm}}{m_\mu}\right) + N_c \left(\frac{m_\mu^2}{16\pi^2 F_\pi^2}\frac{N_c}{3}\right)\left[\ln^2\frac{\mu_0}{m_\mu} + c_1 \ln\frac{\mu_0}{m_\mu} + c_0\right] \right.$$
$$\left. + \mathcal{O}\left(\frac{m_\mu^2}{\mu_0^2}\times \log\text{'s}\right) + \mathcal{O}\left(\frac{m_\mu^4}{\mu_0^4} N_c \times \log\text{'s}\right)\right\}, \tag{201}$$

where $f(m_{\pi^\pm}/m_\mu, m_{K^\pm}/m_\mu) = -0.038$ represents the charged pion and Kaon-loop that is formally of order one in the chiral and N_c counting and μ_0 denotes some hadronic scale, e.g. M_ρ. The coefficient $\mathcal{C} = (N_c^2 m_\mu^2)/(48\pi^2 F_\pi^2) \simeq 0.025$ for $N_c = 3$ of the $\log^2$ term is universal [17,249] and of order N_c, since $F_\pi = \mathcal{O}(\sqrt{N_c})$.

Unfortunately, although the logarithm is sizeable, $\ln(M_\rho/m_\mu) \simeq 1.98$, in $a_\mu^{\mathrm{LbL;had}}$ there occurs a cancellation between the log-square and the log-term. In Ref. [299] the result for the VMD form factor for large M_ρ was fitted to an expression as given in Eq. (201), with the outcome (taking only the diagrams in Fig. 34(a) and (b) into account, which diverge for $M_\rho \to \infty$)

$$a_{\mu;\mathrm{VMD}}^{\mathrm{LbL};\pi^0} \doteq \left(\frac{\alpha}{\pi}\right)^3 \mathcal{C}\ \left[\ln^2\frac{M_\rho}{m_\mu} + c_1 \ln\frac{M_\rho}{m_\mu} + c_0\right]$$
$$\stackrel{\mathrm{Fit}}{=} \left(\frac{\alpha}{\pi}\right)^3 \mathcal{C}\ \ [3.94 - 3.30 + 1.08] = [123 - 103 + 34]\times 10^{-11} = 54\times 10^{-11}\,. \tag{202}$$

This behavior is confirmed by the analytical result derived in Ref. [255] in terms of a series expansion in $\delta = (m_\pi^2 - m_\mu^2)/m_\mu^2$ and m_μ^2/M_ρ^2. Collecting all terms proportional to log-square and log, separately, one obtains $a_{\mu;\mathrm{VMD}}^{\mathrm{LbL};\pi^0} = [136 - 112 + 30]\times 10^{-11} = 54\times 10^{-11}$. Note that the coefficient of $\ln^2(M_\rho/m_\mu)$ in the expansion given in Ref. [255] also contains corrections of order m_μ^2/M_ρ^2, which are not included in the universal term proportional to $\mathcal{C}$ in Eq. (201). This cancellation between the different logarithmically enhanced contributions is also visible in Ref. [256]. In that paper the remaining parts of c_1 have been calculated: $c_1 = -2\chi(\mu_0)/3 + 0.237 = -0.93^{+0.67}_{-0.83}$, with our conventions for χ and $\chi(M_\rho)_{\mathrm{exp}} = 1.75^{+1.25}_{-1.00}$ [300].

[31] The low-energy constant χ in this effective Lagrangian should not be confused with the magnetic susceptibility discussed earlier.

Finally, the EFT analysis shows that the modeling of hadronic light-by-light scattering by a constituent quark loop, as suggested in Refs. [301,302] (see also [303]), is not consistent with QCD.[32] The latter has a priori nothing to do with the full "quark loop" in QCD which is dual to the corresponding contribution in terms of hadronic degrees of freedom. Equation (201) tells us that at leading order in N_c any model of QCD has to show the behavior $a_\mu^{\rm LbL;had} \sim (\alpha/\pi)^3 N_c [N_c m_\mu^2/(48\pi^2 F_\pi^2)] \ln^2 \Lambda$, with a universal coefficient, if one sends the cutoff Λ to infinity. From the analytical result given in Ref. [142], one obtains the result $a_\mu^{\rm LbL;CQM} \sim (\alpha/\pi)^3 N_c (m_\mu^2/M_Q^2) + \ldots$, for $M_Q \gg m_\mu$, if we interpret the constituent quark mass M_Q as a hadronic cutoff. Even though one may argue that $N_c/(48\pi^2 F_\pi^2)$ can be replaced by $1/M_Q^2$, the log-square term is not correctly reproduced with this model. Therefore, the constituent quark model (CQM) cannot serve as a reliable description for the dominant contribution to $a_\mu^{\rm LbL;had}$, in particular, its sign. Note that the contribution of the quark-loop (within the CQM) to a_μ starts at order p^8, i.e. it is of the same chiral order as the pseudoscalar-exchanges and not $\mathcal{O}(p^2)$ higher as suggested by the counting in Table 6 based on Ref. [244].

6. Electroweak Corrections

The contribution of weak virtual processes to $g-2$ has been of interest long before one was actually able to unambiguously calculate them and before they were playing a role in a comparison with the experiment. After the renormalizability of the electroweak SM had been established by 't Hooft in 1971 [304] it was possible to make convincing predictions for a_μ beyond QED [305]. The sensitivity of the last CERN experiment was far from being able to check the prediction and the weak contribution actually was one of the motivations to think about a new muon $g-2$ experiment. The test of the weak contribution is actually one of the milestones achieved by the Brookhaven experiment E821. The weak contribution now is almost three standard deviations, and without it the deviation between theory and experiment would be at the 6 σ level.

6.1. *1-loop Contribution*

The leading weak contribution diagrams are shown in Fig. 37 in the unitary gauge. As a_μ is a physical observable one can calculate it directly in the non-renormalizable unitary gauge. In the latter only physical particles are present and diagrams exhibiting Higgs ghosts and Faddeev-Popov ghosts are absent. The first diagram of Fig. 37 might be of particular interest as it exhibits a triple gauge vertex. The coupling of the photon to the charged W boson is of course dictated by electromagnetic gauge invariance.

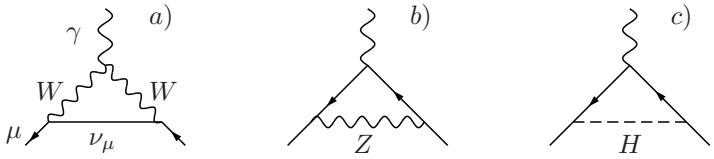

Fig. 37. The leading weak contributions to a_μ; diagrams in the physical unitary gauge.

In the approximation where tiny terms $O(m_\mu^2/M_{W,Z}^2)$ are neglected, the gauge boson contributions are given by [305]

$$a_\mu^{(2)\,\rm EW}(W) = \frac{\sqrt{2} G_\mu m_\mu^2}{16\pi^2}\,\frac{10}{3} \simeq +388.70(0)\times 10^{-11}\,,$$
$$a_\mu^{(2)\,\rm EW}(Z) = \frac{\sqrt{2} G_\mu m_\mu^2}{16\pi^2}\,\frac{(-1+4\,s_W^2)^2-5}{3} \simeq -193.89(2)\times 10^{-11}\,. \qquad (203)$$

For the Higgs exchange one finds

[32] In any case, any kind of quark loop fails to explain the observation reproduced in Fig. 32, which requires an effective description in terms of hadrons as illustrated in Fig. 33.

$$a_\mu^{(2)\,\mathrm{EW}}(H) = \frac{\sqrt{2}G_\mu m_\mu^2}{4\pi^2}\int\limits_0^1 dy\,\frac{(2-y)\,y^2}{y^2+(1-y)(m_H/m_\mu)^2}$$
$$\simeq \frac{\sqrt{2}G_\mu m_\mu^2}{4\pi^2}\begin{cases}\dfrac{m_\mu^2}{m_H^2}\,\ln\dfrac{m_H^2}{m_\mu^2} & \text{for} \quad m_H \gg m_\mu \\ \dfrac{3}{2} & \text{for} \quad m_H \ll m_\mu\end{cases}$$
$$\leq 5\times 10^{-14} \quad \text{for} \quad m_H \geq 114\ \text{GeV}\,, \tag{204}$$

and taking into account the LEP bound Eq. (A.4), this is a negligible contribution. Using the SM parameters given in Eqs. (A.1) and (A.2) we obtain

$$a_\mu^{(2)\,\mathrm{EW}} = (194.82 \pm 0.02)\times 10^{-11}\,, \tag{205}$$

where the error is due to the uncertainty in s_W^2.

6.2. *2-loop Contribution*

Typical electroweak 2–loop corrections are the electromagnetic corrections of the 1–loop diagrams Fig. 37 (part of the bosonic corrections) or fermionic loop insertions as shown in Fig. 38. All these corrections are proportional to

$$\mathcal{K}_2 = \frac{\sqrt{2}G_\mu\, m_\mu^2}{16\pi^2}\,\frac{\alpha}{\pi} \simeq 2.70866237\times 10^{-12}\,. \tag{206}$$

A first incomplete calculation was presented by Kukhto, Kuraev, Schiller and Silagadze [306] in 1992. Corrections found turned out to be enhanced by very large logarithms $\ln M_Z/m_f$, which mainly come from fermion triangular–loops like in Fig. 38a. Note that due to Furry's theorem in QED loops with three photons attached do not contribute and the $\gamma\gamma\gamma$–amplitude vanishes. This is different if the parity violating weak interactions come into play. Contributions from the two orientations of the closed fermion loops do not cancel and the $\gamma\gamma Z$, γZZ and γWW amplitudes do not vanish. In fact in the γWW triangle charge conservation only allows one orientation of the fermion loop.

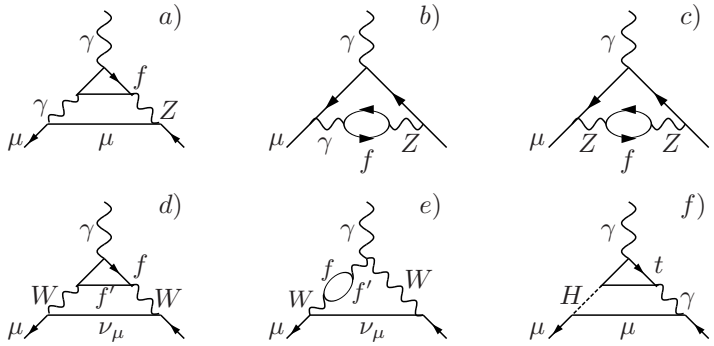

Fig. 38. Electroweak two–loop diagrams exhibiting fermion loops in the unitary gauge, $f = (\nu_e, \nu_\mu, \nu_\tau,)\, e, \mu, \tau, u, c, t, d, s, b$ with weak doublet partners $f' = (e, \mu, \tau,)\, \nu_e, \nu_\mu, \nu_\tau, d, s, b, u, c, t$. The neutrinos (in brackets) do not couple directly to the photon and hence are absent in the triangular subgraphs.

Diagrams a) and b), with an internal photon, appear enhanced by a large logarithm. While contributions from diagram b) mediated by $\gamma - Z$–mixing are suppressed by small vector coupling coefficients [33] $(1-4\,s_W^2) \sim 0.1$ (quark loops) or $(1-4\,s_W^2)^2 \sim 0.01$ (lepton loops), the individual triangle fermion loops contributing to the $\gamma\gamma Z$–vertex of diagram a) lead to un-suppressed corrections

[33] The $Zf\bar{f}$ vector and axial–vector neutral current (NC) coupling coefficients are given by

$$a_\mu^{(4)\,\mathrm{EW}}([f]) \simeq \mathcal{K}_2\, 2T_{3f} N_{cf} Q_f^2 \left[3\ln\frac{M_Z^2}{m_{f'}^2} + C_f\right], \tag{207}$$

in which $m_{f'} = m_\mu$ if $m_f \le m_\mu$ and $m_{f'} = m_f$ if $m_f > m_\mu$ and

$$C_f = \begin{cases} 5/2 & \text{for } m_f < m_\mu\,, \\ 11/6 - 8/9\,\pi^2 & \text{for } m_f = m_\mu\,, \\ -6 & \text{for } m_f > m_\mu\,. \end{cases}$$

The individual fermion f contribution is proportional to $N_{cf}Q_f^2 a_f$. This is the coefficient of the triangular subdiagram which exhibits the Adler-Bell-Jackiw (ABJ) or VVA anomaly [248], which must cancel if all fermions are included [307]. As we know, the *anomaly cancellation* enforces the known lepton–quark family structure of the SM. In [306] only lepton loops were taken into account and thus terms due to the quarks of similar size and structure were missed. The anomaly cancellation condition of the SM reads

$$\sum\nolimits_f N_{cf} Q_f^2 a_f = 0\,, \tag{208}$$

and hence the leading short distance logarithms proportional to $\ln M_Z$ are expected to cancel as well. This has been checked to happen on the level of the quark parton model (QPM) for the 1st and 2nd fermion family [308,309,310].

Assuming that we may use the not very well defined *constituent quark masses* from Eq. (A.8) with $M_u, M_d > m_\mu$, the QPM result for the first family reads [309]

$$a_\mu^{(4)\,\mathrm{EW}}([e,u,d])_{\mathrm{QPM}} \simeq -\mathcal{K}_2 \left[\ln\frac{M_u^8}{m_\mu^6 M_d^2} + \frac{17}{2}\right] \simeq -4.00\times 10^{-11}, \tag{209}$$

for the second family, with $M_s, M_c > m_\mu$, we obtain

$$a_\mu^{(4)\,\mathrm{EW}}([\mu,c,s])_{\mathrm{QPM}} \simeq -\mathcal{K}_2 \left[\ln\frac{M_c^8}{m_\mu^6 M_s^2} + \frac{47}{6} - \frac{8\pi^2}{9}\right] \simeq -4.65\times 10^{-11}\,. \tag{210}$$

For the heavy quarks of the third family perturbation theory is applicable and the straight forward calculation yields the result [311,308,309,312]

$$\begin{aligned} a_\mu^{(4)\,\mathrm{EW}}([\tau,b,t]) &= -\mathcal{K}_2 \left[\frac{8}{3}\ln\frac{m_t^2}{M_Z^2} - \frac{2}{9}\frac{M_Z^2}{m_t^2}\left(\ln\frac{m_t^2}{M_Z^2} + \frac{5}{3}\right) + \ln\frac{M_Z^2}{m_b^2} + 3\ln\frac{M_Z^2}{m_\tau^2} - \frac{8}{3} + \;\cdots\;\right] \\ &\simeq -\mathcal{K}_2 \times 30.3(3) \simeq -8.21(10)\times 10^{-11}\,. \end{aligned} \tag{211}$$

Terms of order m_μ^2/m_τ^2, m_b^2/M_Z^2, M_Z^4/m_t^4 are small and have been neglected.

While the QPM results presented above, indeed confirmed the complete cancellation of the $\ln M_Z$ terms for the 1st and 2nd family, in the third family, with the given mass hierarchy, the corresponding terms $\ln M_Z/m_\tau$ and $\ln M_Z/m_b$ remain unbalanced as m_t is larger than M_Z as first pointed out in Ref. [311].

We want to stress that the fermionic loops with light-quarks (u,d,s) in Fig. 38 are only meant as a symbolic representation of another, genuinely non-perturbative hadronic contribution to the muon $g-2$, similar to the hadronic vacuum polarization and the hadronic light-by-light scattering contributions considered earlier. Below we will discuss the more and more sophisticated approaches that have been used over the years in the literature to control these hadronic uncertainties, going beyond the naive QPM shown in Fig. 38.

Improving on the constituent quark model used above, one can also look at the $Z\gamma\gamma$ contribution in Fig. 38a) from a purely hadronic point of view, using chiral perturbation theory (CHPT) as the low-energy

---

$v_f = T_{3f} - 2Q_f\, s_W^2\,, \quad a_f = T_{3f}\,,$

where T_{3f} is the weak isospin $(\pm\frac{1}{2})$ of the fermion f.

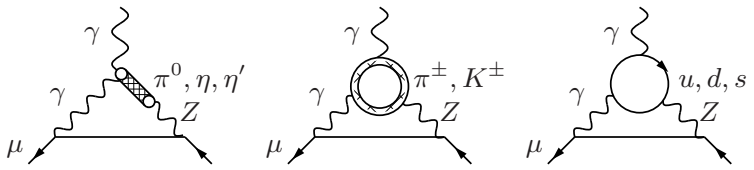

(a) [L.D.] (b) [L.D.] (c) [S.D.]

Fig. 39. The two leading EFT diagrams (L.D.) and the QPM diagram (S.D.). The charged pion loop is subleading in N_c and will be discarded.

effective field (EFT) theory of QCD. This approach was proposed in Ref. [308] and the corresponding Feynman diagrams are shown in Fig. 39(a) and (b). To lowest order in the chiral expansion, the hadronic $Z\gamma\gamma$ interaction is dominated by the pseudoscalar meson (the quasi Goldstone bosons) exchange. The corresponding effective couplings are given by

$$\mathcal{L}^{(2)} = -\frac{e}{2\sin\Theta_W\cos\Theta_W} F_\pi \partial_\mu \left(\pi^0 + \frac{1}{\sqrt{3}}\,\eta_8 - \frac{1}{\sqrt{6}}\,\eta_0\right) Z^\mu \,, \tag{212}$$

which is the relevant part of the $O(p^2)$ chiral effective Lagrangian, and the effective $O(p^4)$ WZW Lagrangian Eq. (144).

The $[u,d,s]$ contribution is obtained with a long distance (L.D.) part ($E < M_\Lambda$) evaluated in the EFT and a short distance (S.D.) part ($E > M_\Lambda$) from Fig. 39(c) evaluated in the QPM. The cut–off for matching L.D. and S.D. part typically is $M_\Lambda = m_P \sim 1$ GeV to $M_\Lambda = M_\tau \sim 2$ GeV. The diagrams from Fig. 39, together with their crossed versions in the unitary gauge, yield, in the chiral limit and up to terms suppressed by m_μ^2/M_Λ^2 ,[34]

$$a_\mu^{(4)\,\mathrm{EW}}([u,d,s]; p < M_\Lambda)_{\mathrm{EFT}} = \mathcal{K}_2 \left[\frac{4}{3}\ln\frac{M_\Lambda^2}{m_\mu^2} + \frac{2}{3}\right] \simeq 2.10 \times 10^{-11} \,,$$
$$a_\mu^{(4)\,\mathrm{EW}}([u,d,s]; p > M_\Lambda)_{\mathrm{QPM}} = \mathcal{K}_2 \left[2\ln\frac{M_Z^2}{M_\Lambda^2}\right] \simeq 4.45 \times 10^{-11} \,.$$

In Sect. 6.2.1 below, we will learn that the last diagram of Fig. 39 in fact takes into account the leading term of Eq. (221) which is protected by Vainshtein's relation Eq. (219).

Above a divergent term has been dropped, as the latter cancels against corresponding terms from the complementary contributions from e, μ and c fermion–loops. Including the finite contributions from e, μ and c :

$$a_\mu^{(4)\,\mathrm{EW}}([e,\mu,c])_{QPM} = -\mathcal{K}_2 \left[6\ln\frac{M_Z^2}{m_\mu^2} - 4\ln\frac{M_Z^2}{M_c^2} + \frac{37}{3} - \frac{8}{9}\pi^2\right]$$
$$\simeq -\mathcal{K}_2 \times 51.83 \simeq -14.04 \times 10^{-11} \,,$$

the complete answer for the 1st plus 2nd family reads [308]

$$a_\mu^{(4)\,\mathrm{EW}}\left(\begin{bmatrix} e,u,d \\ \mu,c,s \end{bmatrix}\right) = -\mathcal{K}_2 \left[\frac{14}{3}\ln\frac{M_\Lambda^2}{m_\mu^2} - 4\ln\frac{M_\Lambda^2}{M_c^2} + \frac{35}{3} - \frac{8}{9}\pi^2\right]$$

[34] The simplest way to implement the cut–off M_Λ of the low energy effective field theory is to write for the Z–propagator

$$\frac{1}{M_Z^2+Q^2} = \underbrace{\frac{1}{M_\Lambda^2+Q^2}}_{EFT} + \underbrace{\frac{1}{M_Z^2+Q^2} - \frac{1}{M_\Lambda^2+Q^2}}_{QPM}$$

and by using the QPM for the second term. The first term corresponds to Eq. (20) of [308], later corrected in the constant term. In the first term M_Z is replaced by M_Λ, in the second term constant terms drop out in the difference as the quark masses in any case have values far below the cut–offs M_Λ and M_Z . For the actual calculation we may use Eq. (217) below.

$$\simeq -\mathcal{K}_2 \times 27.58(46) \simeq -7.47(13) \times 10^{-11} \,. \tag{213}$$

In Eq. (213) the error comes from varying the cut–off M_Λ between 1 GeV and 2 GeV. Below about 1 GeV, the calculation within the EFT can be trusted, above 2 GeV we can use pQCD. Fortunately the result is not very sensitive to the choice of the cut–off. Nevertheless, the mismatch of the cut–off dependencies of the L.D. and the S.D. parts is a problem and gives raise to worries about the reliability of the estimate. Therefore, a refined treatment of these effects is discussed in the following, beginning with a consideration of the general structure of these contributions.

6.2.1. *Hadronic Effects in Weak Loops and the Triangle Anomaly*

In order to discuss the contribution from VVA triangle fermions loops, following [284], one has to consider the $Z^*\gamma\gamma^*$ amplitude

$$T_{\nu\lambda} = \mathrm{i}\int \mathrm{d}^4x\, \mathrm{e}^{\mathrm{i}qx}\langle 0|T\{j_\nu(x)\, j_{5\lambda}(0)\}|\gamma(k)\rangle \,, \tag{214}$$

which we need for small k up to quadratic terms. The corresponding covariant decomposition

$$T_{\nu\lambda} = -\frac{\mathrm{i}\, e}{4\pi^2}\, \Big[w_T(q^2)\,(-q^2\tilde{f}_{\nu\lambda} + q_\nu q^\alpha \tilde{f}_{\alpha\lambda} - q_\lambda q^\alpha \tilde{f}_{\alpha\nu}) + w_L(q^2)\, q_\lambda q^\alpha \tilde{f}_{\alpha\nu}\Big] \,, \tag{215}$$

exhibits two terms, a transversal amplitude w_T and a longitudinal one w_L, with respect to the axial current index λ.

The $g-2$ contribution $a_\mu^{(4)\,\mathrm{EW}}([f])_{\mathrm{VVA}}$ of a fermion f in the $Z^*\gamma\gamma^*$ amplitude, in the unitary gauge with Z propagator $\mathrm{i}\,(-g_{\mu\nu} + q_\mu q_\nu/M_Z^2)/(q^2 - M_Z^2)$, is given by [35]

$$\begin{aligned} a_\mu^{(4)\,\mathrm{EW}}([f])_{\mathrm{VVA}} &= \mathcal{K}_2 \;\mathrm{i}\int \mathrm{d}^4q\, \frac{1}{q^2+2qp}\left[\frac{1}{3}\left(1+\frac{2(qp)^2}{q^2m_\mu^2}\right)\left(w_L - \frac{M_Z^2}{M_Z^2-q^2}\, w_T\right) + \frac{M_Z^2}{M_Z^2-q^2}\, w_T\right] \\ &= \mathcal{K}_2 \int_0^{\Lambda^2} \mathrm{d}Q^2\, \frac{1}{6}\, \frac{Q^2}{m_\mu^2}\Big\{ w_L(Q^2)\, \left((Q^2/m_\mu^2 - 2)\,(1-R_m) + 2\right) \\ &\qquad - w_T(Q^2)\, \frac{M_Z^2}{M_Z^2+Q^2}\, \left((Q^2/m_\mu^2 + 4)\,(1-R_m) + 2\right)\Big\} \,, \end{aligned} \tag{216}$$

in terms of the two scalar amplitudes $w_{L,T}(q^2)$. Λ is a cutoff to be taken to ∞ at the end, after summing over a family. We have performed a Wick rotation to Euclidean space with $Q^2 = -q^2$ and $R_m = \sqrt{1+4m_\mu^2/Q^2}$. For leading estimates we may expand in $m_\mu^2/Q^2 \ll 1$. For contributions from the heavier states it is sufficient to set $p = 0$ except in the phase space where it would produce an IR singularity. Including the leading corrections the result takes the simple form

$$\begin{aligned} a_\mu^{(4)\,\mathrm{EW}}([f])_{\mathrm{VVA}} \simeq \mathcal{K}_2 \int_{m_\mu^2}^{\Lambda^2} \mathrm{d}Q^2 \Big\{ & w_L(Q^2)\, \left(1 - \frac{4}{3}\, m_\mu^2/Q^2 + \cdots\right) \\ & + w_T(Q^2)\, \frac{M_Z^2}{M_Z^2+Q^2}\, \left(1 - \frac{2}{3}\, m_\mu^2/Q^2 + \cdots\right)\Big\} \,. \end{aligned} \tag{217}$$

Interestingly, the Adler-Bardeen non–renormalization theorem valid for the anomalous amplitude w_L in full QCD (considering the quarks $q = u, d, s, c, b, t$ only):

[35] Since the result does not depend on the direction of the external muon momentum p we may average over the 4-dimensional Euclidean sphere which yields the exact 1–dimensional integral representation given.

$$w_L(Q^2)\big|_{m=0} = w_L^{1-\text{loop}}(Q^2)\Big|_{m=0} = \sum_q (2T_q Q_q^2)\,\frac{2N_c}{Q^2}\,, \tag{218}$$

carries over to the perturbative part of the transversal amplitude. In fact, Vainshtein [275] has shown that in the chiral limit the relation

$$w_T(Q^2)_{\text{pQCD}}\big|_{m=0} = \frac{1}{2}\,w_L(Q^2)\big|_{m=0} \tag{219}$$

is valid actually to all orders of perturbative QCD in the kinematical limit relevant for the $g-2$ contribution. This means that in the chiral limit the perturbative QPM result for w_T is exact in pQCD. This looks puzzling, since in low energy effective QCD, which specifies the non–perturbative strong interaction dynamics, this kind of term seems to be absent. The non–renormalization theorem has been proven independently in [286] and was extended to the full off–shell triangle amplitude to 2–loops in [313]. Note that corrections to Vainshtein's relation Eq. (219) must be of non–perturbative origin.

A simple heuristic proof of Vainshtein's theorem proceeds by first looking at the imaginary part of Eq. (214) and the covariant decomposition Eq. (215). In accordance with the Cutkosky rules the imaginary part of an amplitude is always more convergent than the amplitude itself. The imaginary part of the one–loop result is finite and one does not need a regularization to calculate it unambiguously. In particular, it allows us to use anti–commuting γ_5 to move it from the axial vertex $\gamma_\lambda\gamma_5$ to the vector vertex γ_ν. In the limit $m_f = 0$, this involves anti–commuting γ_5 with an even number of γ–matrices, no matter how many gluons are attached to the quark line joining the two vertices. As a result $\text{Im}\,T_{\nu\lambda}$ must be symmetric under $\nu \leftrightarrow \lambda,\ q \leftrightarrow -q$:

$$\text{Im}\,\Big[w_T(q^2)\,(-q^2\tilde{f}_{\nu\lambda} + q_\nu q^\alpha \tilde{f}_{\alpha\lambda} - q_\lambda q^\alpha \tilde{f}_{\alpha\nu}) + w_L(q^2)\,q_\lambda q^\alpha \tilde{f}_{\alpha\nu}\Big] \propto q_\nu q^\alpha \tilde{f}_{\alpha\lambda} + q_\lambda q^\alpha \tilde{f}_{\alpha\nu}\,,$$

which, on the r.h.s., requires that $q^2 = 0$, to get rid of the antisymmetric term proportional to $\tilde{f}_{\nu\lambda}$, and that w_T is proportional to w_L: $w_L = c\,w_T$; the symmetry follows when $c = 2$. Thus the absence of an antisymmetric part is possible only if

$$2\,\text{Im}\,w_T(q^2) = \text{Im}\,w_L(q^2) = \text{constant}\ \times\ \delta(q^2)\,, \tag{220}$$

where the constant is fixed to be $2\pi \cdot 2T_{3f}N_{cf}Q_f^2$ by the exact form of w_L. Both w_L and w_T are analytic functions which fall off sufficiently fast at large q^2 such that they satisfy convergent DRs

$$w_{T,L}(q^2) = \frac{1}{\pi}\int_0^\infty \text{d}s \frac{\text{Im}\,w_{T,L}(s)}{s-q^2}\,,$$

which together with Eq. (220) implies Eq. (219). According to the Adler-Bardeen non–renormalization theorem and by the topological nature of the anomaly (see [247]), w_L given by Eq. (218) is exact beyond perturbation theory. Vainshtein's non–renormalization theorem for w_T in the chiral limit implies

$$w_T(q^2) = \frac{2T_{3f}N_{cf}Q_f^2}{Q^2} + \text{non}-\text{perturbative corrections}\,. \tag{221}$$

Coming back to the calculation of Eq. (217), we observe that the contribution from w_L for individual fermions is logarithmically divergent, but it completely drops for a complete family due to the vanishing anomaly cancellation coefficient. The contribution from w_T is convergent for individual fermions due to the damping by the Z propagator. In fact it is the leading $1/Q^2$ term of the w_T amplitude which produces the $\ln\frac{M_Z}{m}$ terms. However, the coefficient is the same as the one for the anomalous term and thus for each complete family also the $\ln M_Z$ terms must drop out. Since the leading perturbative contributions have to cancel the non-perturbative contributions to w_T which are not constraint by the anomaly cancellation condition require special attention. Non-perturbative effects are accessible in a systematic manner via the OPE.

6.2.2. *Non–perturbative Effects via the OPE*

In order to study further the matrix element Eq. (214) we need to look at the OPE of the two currents

$$\hat{T}_{\nu\lambda} = \mathrm{i}\int \mathrm{d}^4x\, \mathrm{e}^{\mathrm{i}qx}\, T\{j_\nu(x)\, j_{5\lambda}(0)\} = \sum_i c^i_{\nu\lambda\alpha_1\ldots\alpha_i}(q)\, \mathcal{O}_i^{\alpha_1\ldots\alpha_i}\ ,$$

where the operators $\mathcal{O}$ are local operators constructed from the light fields, the photon, light quarks and gluon fields. The operator matrix elements describe the non–perturbative long range strong interaction features while the perturbatively calculable Wilson coefficients c^i encode the short distance properties. We are concerned with the matrix element

$$T_{\nu\lambda} = \langle 0|\hat{T}_{\nu\lambda}|\gamma(k)\rangle = \sum_i c^i_{\nu\lambda\alpha_1\ldots\alpha_i}(q)\, \langle 0|\mathcal{O}_i^{\alpha_1\ldots\alpha_i}|\gamma(k)\rangle \tag{222}$$

in the classical limit $k \to 0$. The leading contribution is linear in $\tilde{f}_{\alpha\beta}$ the dual of $f_{\alpha\beta} = k_\alpha\varepsilon_\beta - k_\beta\varepsilon_\alpha$. Therefore, only those operators contribute which have the structure of an antisymmetric tensor

$$\langle 0|\mathcal{O}_i^{\alpha\beta}|\gamma(k)\rangle = -\mathrm{i}\,\frac{1}{4\pi^2}\kappa_i \tilde{f}^{\alpha\beta}\ . \tag{223}$$

The constants κ_i depend on the renormalization scale μ. Given the tensor structure Eq. (215), the operators contributing to $T_{\nu\lambda}$ are of the form

$$T_{\nu\lambda} = \sum_i \left\{c^i_T(q^2)\,(-q^2\mathcal{O}^i_{\nu\lambda} + q_\nu q^\alpha \mathcal{O}^i_{\alpha\lambda} - q_\lambda q^\alpha \mathcal{O}^i_{\alpha\nu}) + c^i_L(q^2)\, q_\lambda q^\alpha \mathcal{O}^i_{\alpha\nu}\right\}\ . \tag{224}$$

Consequently, we may write

$$w_{T,L}(q^2) = \sum_i c^i_{T,L}(q^2,\mu^2)\,\kappa_i(\mu^2)\ . \tag{225}$$

In this expansion for large $Q^2 = -q^2$ the relevance of the terms is determined by the dimension of the operators, the low dimensional ones being the most relevant, unless they vanish or are suppressed by small coefficients due to exact or approximate symmetries, like chiral symmetry. The functions we expand are analytic in the q^2–plane and the asymptotic expansion for large Q^2 is a formal power series in $1/Q^2$ up to logarithms. This implies that operators of odd dimension produce terms proportional to the mass m_f of the light fermion field from which the operator is constructed. Thus, in the chiral limit only antisymmetric operators of *even* dimensions contribute.

In the following discussion of the different terms we will include the factors T_{3f} at the $Z^\lambda j_{5\lambda}(0)$ vertex (axial current coefficient), Q_f at the $A^\nu j_\nu(x)$ vertex (vector current coefficient) and the color multiplicity factor N_{cf}. An additional factor Q_f (coupling to the external photon) comes in via the matrix elements κ_i of fermion operators $\bar{\psi}_f\cdots\psi_f$. Coefficients κ_i which go with helicity flip operators $\bar{\psi}_{fR}\cdots\psi_{fL}$ or $\bar{\psi}_{fL}\cdots\psi_{fR}$ are proportional to m_f.

The leading operator is of dimension $d_\mathcal{O} = 2$ and corresponds to the parity odd dual electromagnetic field strength tensor

$$\mathcal{O}_F^{\alpha\beta} = \frac{1}{4\pi^2}\tilde{F}^{\alpha\beta} = \frac{1}{4\pi^2}\varepsilon^{\alpha\beta\rho\sigma}\partial_\rho A_\sigma\ .$$

The normalization here is chosen such that $\kappa_F = 1$ and hence $w^F_{L,T} = c^F_{L,T}$. The coefficient for this leading term is given by the one–loop triangle diagram and yields

$$c^F_L[f] = 2c^F_T[f] = \frac{4T_{3f}N_{cf}Q_f^2}{Q^2}\ \left[1 - \frac{2m_f^2}{Q^2}\ \ln\frac{Q^2}{\mu^2} + O(\frac{m_f^4}{Q^4})\right]\ . \tag{226}$$

Again, the leading $1/Q^2$ term cancels family–wise by quark–lepton duality. We know that in the chiral limit this is the only contribution to w_L.

The next to leading term is the $d_{\mathcal{O}} = 3$ operator given by

$$\mathcal{O}_f^{\alpha\beta} = -\mathrm{i}\bar{f}\sigma^{\alpha\beta}\gamma_5 f \equiv \frac{1}{2}\varepsilon^{\alpha\beta\rho\sigma}\bar{f}\sigma^{\rho\sigma} f \ .$$

Such helicity flip operators only contribute if chiral symmetry is broken and the coefficients must be of the form $c^f \propto m_f/Q^4$. The coefficients are determined by tree level Compton scattering type diagrams and again contribute equally to both amplitudes

$$c_L^f[f] = 2c_T^f[f] = \frac{8T_{3f}Q_f m_f}{Q^4} \ .$$

For the sake of illustration, not taking into account soft strong interaction effects, we may calculate the soft photon quark matrix element in the QPM. The result is UV divergent and in the $\overline{\mathrm{MS}}$ scheme given by

$$\kappa_f = -Q_f\, N_{cf}\, m_f\, \ln\frac{\mu^2}{m_f^2} \ .$$

When inserted in the $d_{\mathcal{O}} = 3$ contribution to w_T one gets

$$\Delta^{(d_{\mathcal{O}}=3)} w_L = 2\Delta^{(d_{\mathcal{O}}=3)} w_T = \frac{8}{Q^4}\sum_f T_{3f}\, Q_f\, m_f\, \kappa_f$$

and thus recovers precisely the $1/Q^4$ term of Eq. (226). While this illustrated the use of the OPE we have just reproduced the pQCD result. However, in contrast to the leading $1/Q^2$ term which is not modified by soft gluon interactions, i.e., $\kappa_F = 1$ is exact, the physical κ_f cannot be obtained from pQCD. So far it is an unknown constant, in fact it is proportional to the magnetic susceptibility χ of QCD [272], which we have discussed in Sect. 5.1.1 before. Here again, the spontaneous breakdown of the chiral symmetry plays a key role. It implies the existence of the quark condensates $\langle\bar{\psi}\psi\rangle_0 \neq 0$, which are non–vanishing in the chiral limit [36] . Now, unlike in perturbation theory, κ_f need not be proportional to m_f. In fact it is proportional to $\langle\bar{\psi}\psi\rangle_0$. As the condensate is of dimensionality 3, another quantity must enter carrying dimension of a mass and which is finite in the chiral limit. In the u, d quark sector this is either the pion decay constant F_0 or the ρ mass M_{ρ^0}. Since κ_f is given by the matrix element Eq. (223) it must be proportional to $N_{cf}Q_f$ such that

$$\kappa_f = N_{cf}Q_f\frac{\langle\bar{\psi}_f\psi_f\rangle_0}{F_0^2}$$

and hence [312,275]

$$\Delta^{(d_{\mathcal{O}}=3)}\, w_L = 2\,\Delta^{(d_{\mathcal{O}}=3)}\, w_T = \frac{8}{Q^4}\sum_f N_{cf}T_{3f}\, Q_f^2\, m_f\, \frac{\langle\bar{\psi}_f\psi_f\rangle_0}{F_0^2} \ . \tag{227}$$

The overall normalization is chosen such that it reproduces the expansion of the non–perturbative modification of w_L, which becomes proportional to the pion propagator beyond the chiral limit:

$$w_L = \frac{2}{Q^2 + m_\pi^2} = \frac{2}{Q^2} - \frac{2m_\pi^2}{Q^4} + \cdots$$

We will come back to that point below.

All operators of $d_{\mathcal{O}} = 4$ yield terms suppressed by the light quark masses as m_f^2/Q^4 and vanish in the chiral limit. Similarly the dimension $d_{\mathcal{O}} = 5$ operators are contributing to the $1/Q^6$ coefficient but require

[36] Typically they take values $\langle\bar{\psi}\psi\rangle_0 \simeq -(240\ \mathrm{MeV})^3$

a factor m_f and thus again are suppressed due to close-by chiral symmetry.

Interestingly the dimension $d_{\mathcal{O}} = 6$ operators play a more important role. There is a term which is proportional to the quark condensates and behaves like $1/Q^6$ and which gives a non–vanishing contribution in the chiral limit. Such terms only contribute to the transversal amplitude, and using estimates presented in [254] one obtains

$$\Delta^{(d_{\mathcal{O}}=6)}\, w_T(Q^2)_{\rm NP} \simeq -\frac{16}{9}\pi^2\, \frac{2}{F_0^2}\, \frac{\alpha_s}{\pi} \frac{\langle\bar\psi\psi\rangle^2}{Q^6}\ , \tag{228}$$

for large enough Q^2, the ρ mass being the typical scale. This NP contribution breaks the degeneracy $w_T(Q^2) = \frac{1}{2} w_L(Q^2)$ which holds for the perturbative part only.
As a result the consequences of the OPE for the light quarks u, d and s in the chiral limit may be summarized in the relations [284]:

$$\begin{aligned} w_L[u,d]_{m_{u,d}=0} &= -3\, w_L[s]_{m_s=0} = \frac{2}{Q^2}\ , \\ w_T[u,d]_{m_{u,d}=0} &= -3\, w_T[s]_{m_s=0} = \frac{1}{Q^2} - \frac{32\pi\alpha_s}{9\, Q^6}\, \frac{\langle\bar\psi\psi\rangle_0^2}{F_\pi^2} + O(Q^{-8})\ . \end{aligned} \tag{229}$$

The condensates are fixed essentially by the Gell-Mann-Oakes-Renner (GOR) relations

$$\begin{aligned} (m_u + m_d)\, \langle\bar\psi\psi\rangle_0 &= -F_0^2 m_\pi^2\ , \\ m_s \langle\bar\psi\psi\rangle_0 &\simeq -F_0^2 M_K^2\ , \end{aligned}$$

and the last term of Eq. (229) numerically estimates to

$$w_T(Q^2)_{\rm NP} \sim -\alpha_s\, (0.772\ {\rm GeV})^4/Q^6\ ,$$

i.e., the scale is close to the ρ mass.

As a result non–perturbative corrections to the leading π^0, η, η' exchange contributions in w_L require the inclusion of vector–meson exchanges which contribute to w_T. More precisely, for the transversal function the intermediate states have to be 1^+ mesons with isospin 1 and 0 or 1^- mesons with isospin 1. The lightest ones are ρ, ω and a_1. They are massive also in the chiral limit.

In principle, the incorporation of vector–mesons, like the ρ, in accordance with the basic symmetries is possible using the Resonance Lagrangian Approach (RLA) [88], an extended form of CHPT. Like in the light-by-light scattering case discussed before, the more recent analyses are modeling the hadronic amplitudes [244] in the spirit of large N_c QCD [251,252] where quark–hadron duality becomes exact. The infinite series of narrow vector states known to show up in the large N_c limit is then approximated by a suitable lowest meson dominance (LMD), i.e., amplitudes are assumed to be saturated by known low lying physical states of appropriate quantum numbers. This approach was adopted in an analysis by the Marseille group [312]. An analysis which takes into account the complete structure Eq. (229) was finalized in [284]. In the narrow width approximation one may write the ansatz

$${\rm Im}\, w_T = \pi \sum\nolimits_i g_i\, \delta(s - m_i^2)\ , \tag{230}$$

where the weight factors g_i satisfy

$$\sum\nolimits_i g_i = 1\ ,\ \ \sum\nolimits_i g_i m_i^2 = 0\ , \tag{231}$$

in order to reproduce Eq. (229) in the chiral limit. Corrections which show up beyond the chiral limit may be implemented by modifying the second constraint such that they match the coefficients of the corresponding terms in the OPE.

While for leptons we have the amplitude

$$w_L[\ell] = -\frac{2}{Q^2}\ ,\ (\ell = e,\mu,\tau)\ ,$$

the hadronic counterparts get modified by strong interaction effects as mentioned: a sufficient number of states with appropriate weight factors has to be included in order to be able to satisfy the S.D. constraints, obtained via the OPE. Since the Z does not have fixed parity both vector and axial vector states couple (see Fig. 39a). For the 1st family π^0, $\rho(770)$ and $a_1(1260)$ are taken into account

$$\begin{aligned} w_L[u,d] &= \frac{2}{Q^2+m_\pi^2} \simeq 2\,\left(\frac{1}{Q^2} - \frac{m_\pi^2}{Q^4} + \cdots\right)\ , \\ w_T[u,d] &= \frac{1}{M_{a_1}^2 - M_\rho^2}\left[\frac{M_{a_1}^2 - m_\pi^2}{Q^2+M_\rho^2} - \frac{M_\rho^2 - m_\pi^2}{Q^2+M_{a_1}^2}\right] \simeq \left(\frac{1}{Q^2} - \frac{m_\pi^2}{Q^4} + \cdots\right)\ , \end{aligned} \tag{232}$$

for the 2nd family $\eta'(960)$, $\eta(550)$, $\phi(1020)$ and $f_1(1420)$ are included

$$\begin{aligned} w_L[s] &= -\frac{2}{3}\left[\frac{2}{Q^2+M_{\eta'}^2} - \frac{1}{Q^2+m_\eta^2}\right] \simeq -\frac{2}{3}\left(\frac{1}{Q^2} - \frac{\tilde{M}_\eta^2}{Q^4} + \cdots\right)\ , \\ w_T[s] &= -\frac{1}{3}\frac{1}{M_{f_1}^2 - M_\phi^2}\left[\frac{M_{f_1}^2 - m_\eta^2}{Q^2+M_\phi^2} - \frac{M_\phi^2 - m_\eta^2}{Q^2+M_{f_1}^2}\right] \simeq -\frac{1}{3}\left(\frac{1}{Q^2} - \frac{m_\eta^2}{Q^4} + \cdots\right)\ , \end{aligned} \tag{233}$$

with $\tilde{M}_\eta^2 = 2M_{\eta'}^2 - m_\eta^2$. The expanded forms allow for a direct comparison with the structure of the OPE and reveal that the residues of the poles have been chosen correctly.

While the contributions to a_μ from the heavier states may be calculated using the simplified integral Eq. (217), for the leading π^0 contribution we have to use Eq. (216), which also works for $m_\pi \sim m_\mu$. The results obtained for the 1st family reads [284] [37]

$$a_\mu^{(4)\,\mathrm{EW}}([e,u,d]) \simeq -\mathcal{K}_2\left\{\frac{1}{3}\left(r_\pi\,(r_\pi+2)\,\sqrt{\frac{4}{r_\pi}-1}\left[\arcsin\left(1-\frac{r_\pi}{2}\right)+\frac{\pi}{2}\right]\right.\right.$$

[37] Up to the common factor $\mathcal{K}_2$ for pseudoscalar exchanges like $w_L(Q^2) = 1/(Q^2+m_\pi^2) - 1/(Q^2+M_Z^2)$ (Pauli-Villars regulated) one obtains the exact result

$$F_L(x) = \frac{1}{6}\left(x\,(x+2)\,f(x) - x^2\ln x + 2x + 3\right) - \ln\frac{m_\mu^2}{M_Z^2}\ ,$$

where

$$f(x) = \begin{cases} -\sqrt{4/x-1}\,\left(\arcsin\left(1-\frac{x}{2}\right)+\frac{\pi}{2}\right) & \text{for } x<4 \quad (x=x_\pi)\ , \\ \sqrt{1-4/x}\,\ln\left(-2/(x\sqrt{1-4/x}-x+2)\right) & \text{for } x>4 \quad (x=x_\eta)\ , \end{cases}$$

with $x_\pi = m_\pi^2/m_\mu^2$, $x_\eta = m_\eta^2/m_\mu^2$ etc. and M_Z as a cut-off. For vector exchanges like $w_T(Q^2) = 1/(Q^2+M_\rho^2)$ one obtains

$$F_T(m_\mu^2/M_\rho^2) = -\ln\frac{M_\rho^2}{M_Z^2} - \frac{2}{3}\,\frac{m_\mu^2}{M_\rho^2}\,\ln\left(\frac{M_\rho^2}{m_\mu^2}+1\right) + O\left(\left(m_\mu^2/M_\rho^2\right)^2\right)\ .$$

Up to terms $O(m_\mu^2/M_Z^2)$ the result reads

$$\begin{aligned} F_T(\frac{1}{x_\rho}) = \frac{1}{6}\Big\{ &(x_\rho^2 - 6\,x_\rho)\,\ln x_\rho - 2\,x_\rho - 6\,\ln a + 9 - x_\rho\,r_\rho\,\ln(-2/(r_\rho - x_\rho + 2)) \\ &-r_\rho\,\ln((x_\rho^4 - r_\rho\,(x_\rho^3 - 6\,x_\rho^2 + 10\,x_\rho - 4) - 8\,x_\rho^3 + 20\,x_\rho^2 - 16\,x_\rho + 2)/2)\Big\}\ , \end{aligned}$$

with $x_\rho = M_\rho^2/m_\mu^2$, $r_\rho = \sqrt{x_\rho^2 - 4x_\rho}$ and $a = m_\mu^2/M_Z^2$.

$$+r_\pi^2 \ln r_\pi - 2r_\pi - 3\Big) + \ln\frac{M_\rho^2}{m_\mu^2} - \frac{M_\rho^2}{M_{a_1}^2 - M_\rho^2}\ln\frac{M_{a_1}^2}{M_\rho^2} + \frac{5}{2}\Big\}$$
$$\simeq -\mathcal{K}_2 \times 8.49(74) = -2.30(20)\times 10^{-11}\,, \tag{234}$$

with $r_\pi = m_\pi^2/m_\mu^2$. This may be compared with the QPM result Eq. (209), which is about a factor of two larger and once more illustrates the problem of perturbative calculations in the light quark sector. For the 2nd family after adding the μ and the perturbative charm contribution one obtains

$$a_\mu^{(4)\,\mathrm{EW}}([\mu,c,s]) \simeq -\mathcal{K}_2 \left[\frac{2}{3}\ln\frac{M_\phi^2}{M_{\eta'}^2} - \frac{2}{3}\ln\frac{M_{\eta'}^2}{m_\eta^2}\right.$$
$$\left. + \frac{1}{3}\frac{M_\phi^2 - m_\eta^2}{M_{f_1}^2 - M_\phi^2}\ln\frac{M_{f_1}^2}{M_\phi^2} + 4\ln\frac{M_c^2}{M_\phi^2} + 3\ln\frac{M_\phi^2}{m_\mu^2} - \frac{8\pi^2}{9} + \frac{59}{6}\right]$$
$$\simeq -\mathcal{K}_2 \times 17.25(1.10) \simeq -4.67(30)\times 10^{-11}\,, \tag{235}$$

which yields a result close to the one obtained with the QPM Eq. (210). For the 2nd family the QPM estimate works better due to the fact that the non–perturbative light s–quark contribution is suppressed by a factor four relative to the c due to the different charge.

Altogether, for the 1st plus 2nd family, the large N_c QCD inspired LMD result is

$$a_\mu^{(4)\,\mathrm{EW}}\left(\begin{bmatrix} e,u,d \\ \mu,c,s \end{bmatrix}\right)_{\mathrm{LMD}} \simeq -\mathcal{K}_2 \times 25.74 \simeq -6.97\times 10^{-11}\,, \tag{236}$$

and turns out to be rather close to the very crude estimate Eq. (213) based on separating L.D. and S.D. by a cut–off in the range 1 to 2 GeV.

Note that numerically the differences of the different estimates (QPM, EFT, large N_c) are not substantial. Following [284], we adopt the specific forms discussed last in the following.

6.2.3. *Residual Fermion–Loop Effects*

So far unaccounted are sub–leading contributions which come from diagrams $c), d), e)$ and $f)$ in Fig. 38. They have been calculated in [309,310] with the result

$$a_{\mu\,\mathrm{NLL}}^{(4)\,\mathrm{EW}} = -\mathcal{K}_2\left\{\frac{1}{2s_W^2}\left[\frac{5}{8}\frac{m_t^2}{M_W^2} + \ln\frac{m_t^2}{M_W^2} + \frac{7}{3}\right] + \Delta C^{tH}\right\}$$
$$\simeq -4.15(11)\times 10^{-11} - (1.1^{-0.1}_{+1.4})\times 10^{-11}\,, \tag{237}$$

where ΔC^{tH} is the coefficient from diagram $f)$

$$\Delta C^{tH} = \begin{cases} \frac{16}{9}\ln\frac{m_t^2}{m_H^2} + \frac{104}{27} & m_H \ll m_t\,, \\ \frac{32}{3}\left(1 - \frac{1}{\sqrt{3}}\mathrm{Cl}_2\left(\pi/3\right)\right) & m_H = m_t\,, \\ \frac{m_t^2}{m_H^2}\left(8 + \frac{8}{9}\pi^2 + \frac{8}{3}\left(\ln\frac{m_H^2}{m_t^2} - 1\right)^2\right) & m_H \gg m_t\,, \end{cases}$$

with typical values $\Delta C^{tH} = (5.84, 4.14, 5.66)$ contributing to Eq. (237) by $(-1.58, -1.12, -1.53)\times 10^{-11}$, respectively, for $m_H = (100, m_t, 300)$ GeV. The first term in Eq. (237) is for $\Delta C^{tH} = 0$, the second is the ΔC^{tH} contribution for $m_H = m_t$ with uncertainty corresponding to the range $m_H = 100$ GeV to $m_H = 300$ GeV.

6.2.4. *Bosonic Contributions*

In approximate form, the full electroweak bosonic corrections have been calculated by Czarnecki, Krause and Marciano in 1995 [314]. At two loops, in the linear 't Hooft gauge, including fermion loops, there are 1678 diagrams to be considered, and the many mass scales involved complicate the exact calculation considerably. The calculation [314] has been performed by asymptotic expansions in $(m_\mu/M_V)^2$ and $(M_V/m_H)^2$, where $M_V = M_W$ or M_Z and $m_H \gg M_V$. The heavy mass expansion of course substantially simplifies the calculation. As a further approximation an expansion in the NC vector couplings was used. The latter are suppressed like $(1-4\,s_W^2) \sim 0.1$ for quarks and $(1-4\,s_W^2)^2 \sim 0.01$ for leptons. As a result a two–loop electroweak correction

$$a_\mu^{(4)\,\mathrm{EW}}(\mathrm{bosonic}) = \mathcal{K}_2 \left(\sum_{i=-1}^{2} \left[a_{2i}\,(s_W^2)^i + \frac{M_W^2}{m_H^2} b_{2i}\,(s_W^2)^i \right] + O(s_W^6) \right)$$
$$\simeq -21.4^{+4.3}_{-1.0} \times 10^{-11} \tag{238}$$

was found for $M_W = 80.392$ GeV ($s_W^2 = 1 - M_W^2/M_Z^2$) and $m_H = 250$ GeV ranging between $m_H = 100$ GeV and $m_H = 500$ GeV. The expansion coefficients are given in [314]. The on mass–shell renormalization prescription has been used and the one–loop contributions in Eq. (203) were parametrized in terms of the muon decay constant G_μ. This means that part of the two–loop bosonic corrections have been absorbed into the lowest order result. For the lower Higgs masses the heavy Higgs mass expansion is not accurate and an exact calculation has been performed by Heinemeyer, Stöckinger and Weiglein [315] and by Gribouk and Czarnecki [316]. The result has the form

$$a_\mu^{(4)\,\mathrm{EW}}(\mathrm{bosonic}) = \mathcal{K}_2 \left(c_L^{\mathrm{bos},2L} \ln \frac{m_\mu^2}{M_W^2} + c_0^{\mathrm{bos},2L} \right) , \tag{239}$$

where the coefficient of the large logarithm $\ln \frac{m_\mu^2}{M_W^2} \sim -13.27$ is given by the simple expression

$$c_L^{\mathrm{bos},2L} = \frac{1}{18}[107 + 23\,(1-4s_W^2)^2] \sim 5.96\,.$$

While the leading term is simple, the Higgs mass dependent function $c_0^{\mathrm{bos},2L}$ in its exact analytic form is rather unwieldy and therefore has not been published. The numerical result of [315] was confirmed in [316]. The 2nd Ref. also presents a number of semi–analytic intermediate results which give more insight into the calculation. Considering a Higgs mass range $m_H = 50$ GeV to $m_H = 500$ GeV, say, one may expand the

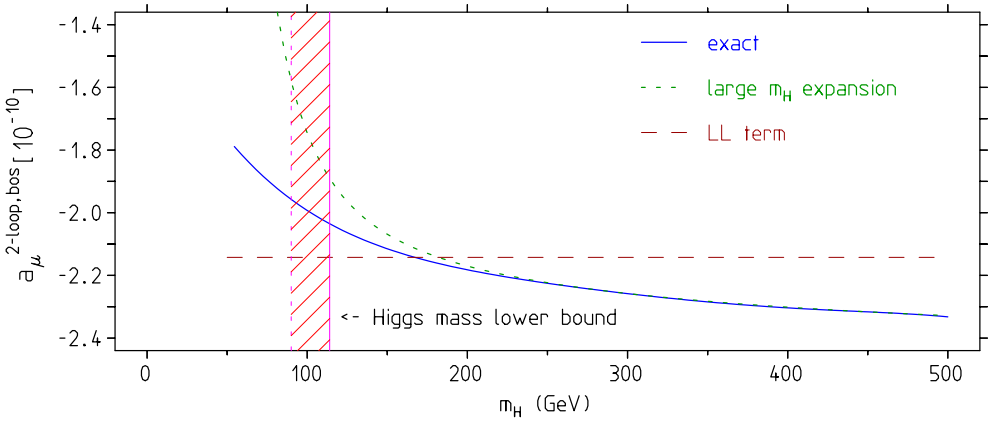

Fig. 40. Exact result for the bosonic correction vs. the asymptotic expansion Eq. (238) minus a correction 0.88×10^{-11} and the LL approximation (first term of Eq. (239)).

result as a function of the unknown Higgs mass in terms of Tschebycheff polynomials defined on the interval

Table 14
Summary of weak 2–loop effects in units 10^{-11}. Fermion triangle loops: 1st, 2nd and 3rd family LO, fermion loops NLL and bosonic loops (with equation numbers).

$[eud]$ LO Eq. (234)	$[\mu sc]$ LO Eq. (235)	$[\tau bt]$ LO Eq. (211)	NLL Eq. (237)	bosonic Eq. (241)
-2.30±0.2	-4.67±0.3	-8.21±0.1	$-5.3^{+0.1}_{-1.4}$	$-21.6^{+1.5}_{-1.0}$

[-1,1]. A suitable variable is $x = (2m_H - 550\ \text{GeV})/(450\ \text{GeV})$ and with the polynomials $t_1 = 1\ ,\ \ t_2 = x\ ,\ \ t_{i+2} = 2xt_{i+1} - t_i\ ,\ \ i = 1, \cdots, 4$, we may approximate Eq. (239) in the given range by

$$a_\mu^{(4)\,\mathrm{EW}}(\text{bosonic}) \simeq \sum_{i=1}^{6} a_i\, t_i(x) \times 10^{-10}\ , \tag{240}$$

with the coefficients given by $a_1 = 80.0483$, $a_2 = 8.4526$, $a_3 = -3.3912$, $a_4 = 1.4024$, $a_5 = -0.5420$ and $a_6 = 0.2227$. The result is shown in Fig. 40, which may be translated into

$$a_\mu^{(4)\,\mathrm{EW}}(\text{bosonic}) = (-21.56^{+1.49}_{-1.05}) \times 10^{-11}\ , \tag{241}$$

and applies for $m_H = 100$ GeV to $m_H = 300$ GeV. The central value is obtained for $m_H = m_t$. Note that the exact result exhibits a much more moderate Higgs mass dependence at lower Higgs masses. This also implies that the uncertainty caused by the unknown Higgs mass is reduced considerably.

Summary of the Results for the Weak Contributions

As a rough estimate the perturbative 2–loop leading logs may be summarized in compact form by [314,308,309], [310,284]

$$\begin{aligned} a_{\mu\,\mathrm{LL}}^{(4)\,\mathrm{EW}} = -\mathcal{K}_2 \Bigg\{ & \left[\frac{215}{9} + \frac{31}{9}(1 - 4s_W^2)^2\right] \ln\frac{M_Z}{m_\mu} \\ & - \sum_{f\in F} N_f Q_f \left[12\, T_f^3\, Q_f - \frac{8}{9}\left(T_f^3 - 2Q_f s_W^2\right)\left(1 - 4s_W^2\right)\right] \ln\frac{M_Z}{m_f} \Bigg\}\ . \end{aligned} \tag{242}$$

Electron and muon loops as well as non–fermionic loops produce the $\ln(M_Z/m_\mu)$ terms in this expression (the first line) while the sum runs over $F = \tau, u, d, s, c, b$. The logarithm $\ln(M_Z/m_f)$ in the sum implies that the fermion mass m_f is larger than m_μ. For the light quarks, such as u, d and s, whose current masses are very small, m_f has a meaning of an effective hadronic constituent mass. In this approximation $a_{\mu\,\mathrm{LL}}^{(4)\,\mathrm{EW}} \simeq -36.72 \times 10^{-11}$, which is to be compared with the full estimate Eq. (243), below. Note that the $(1 - 4s_W^2)$ suppressed LL terms from photonic corrections to diagram Fig. 37b [23/9 of the 31/9] and Fig. 38b [for e and μ 2× 4/9 and corresponding terms (2nd term) in the sum over $f \in F$] only account a negligible contribution -31.54×10^{-13}. The un-suppressed LL terms from Fig. 38a [2× 54/9 of the 215/9 for e and μ plus the corresponding terms (1st term) in the sum $f \in F$] in the above expression cancel for the 1st and 2nd fermion family. What survives are the terms due to the virtual photon corrections (bosonic) of the 1–loop diagrams Fig. 37a,b [120/9(W) - 13/9(Z) of the 215/9] and the incomplete cancellation in the 3rd fermion family resulting as a consequence of the mass separation pattern $m_\tau, M_b \ll M_Z \ll m_t$, relative to the effective cut–off M_Z.

The hadronic effects required a much more careful study which takes into account the true structure of low energy QCD and as leading logs largely cancel a careful study of the full 2–loop corrections was necessary. The various weak contributions are collected in Table 14 and add up to the total weak 2–loop contribution

$$a_\mu^{(4)\,\mathrm{EW}} \simeq (-42.08 \pm 1.5[m_H, m_t] \pm 1.0[\text{had}]) \times 10^{-11}\ . \tag{243}$$

The high value -40.98 corresponds to low $m_H = 100$ GeV, the central value to $m_H = m_t$ and the minimum -43.47 to a high $m_H = 300$ GeV (see Eq. (A.4)).

Three–loop effects were studied by RG methods first in [310]. The result

$$a_{\mu\,\mathrm{LL}}^{(6)\,\mathrm{EW}} \simeq (0.4 \pm 0.2) \times 10^{-11} \tag{244}$$

was later confirmed by [284]. The error estimates uncalculated 3–loop contributions.

By adding up Eqs. (205), (243) and (244) we find the result [38]

$$a_\mu^{\rm EW} = (153.2 \pm 1.0[\rm had] \pm 1.5[m_H, m_t, 3-loop]) \times 10^{-11} \,, \tag{245}$$

based on [284,315,316].

6.3. *2–loop electroweak contributions to a_e*

The dominant electroweak 1–loop contributions Eq. (203) scale with high precision with an overall factor $x_{(e\mu)} = (m_e/m_\mu)^2$, up to terms which are suppressed with higher powers up to logarithms, like the contribution from the Higgs Eq. (204). Thus

$$a_e^{(2)\,\rm EW} = x_{(e\mu)}\, a_\mu^{(2)\,\rm EW} = 45.57(0) \times 10^{-15} \,.$$

At two loops various contributions do not scale in this simple way [306,309,314]. We therefore present a set of modified formulae, which allow us to calculate $a_e^{(4)\,\rm EW}$. Apart from the overall factor

$$\mathcal{K}_2 \to x_{(e\mu)} \mathcal{K}_2 \simeq 6.3355894 \times 10^{-17} \,, \tag{246}$$

the logarithmically enhanced as well as some constant terms change according to Eq. (207), adapted for the electron. We only present those terms which do not scale trivially. The QPM results Eqs. (209) and (210) are modified to

$$a_e^{(4)\,\rm EW}([e,u,d])_{\rm QPM} \simeq -\mathcal{K}_2 \left[\ln \frac{M_u^8}{m_e^6 M_d^2} + \frac{47}{6} - \frac{8\pi^2}{9}\right] \simeq -2.36 \times 10^{-15}, \tag{247}$$

$$a_e^{(4)\,\rm EW}([\mu,c,s])_{\rm QPM} \simeq -\mathcal{K}_2 \left[\ln \frac{M_c^8}{m_\mu^6 M_s^2}\right] \simeq -1.15 \times 10^{-15} \,, \tag{248}$$

for the 1st and 2nd family, respectively. The EFT/QPM estimates used in Eq. (213) now read

$$a_e^{(4)\,\rm EW}([u,d,s]; p < M_\Lambda)_{\rm EFT} = \mathcal{K}_2 \left[\frac{4}{3} \ln \frac{M_\Lambda^2}{m_e^2} + \frac{2}{3}\right] \simeq 1.39 \times 10^{-15} \,,$$
$$a_e^{(4)\,\rm EW}([u,d,s]; p > M_\Lambda)_{\rm QPM} = \mathcal{K}_2 \left[2 \ln \frac{M_Z^2}{M_\Lambda^2}\right] \simeq 1.04 \times 10^{-15} \,,$$

and together with

$$\begin{aligned} a_e^{(4)\,\rm EW}([e,\mu,c])_{QPM} &= -\mathcal{K}_2 \left[3 \ln \frac{M_Z^2}{m_e^2} + 3 \ln \frac{M_Z^2}{m_\mu^2} - 4 \ln \frac{M_Z^2}{M_c^2} + \frac{23}{6} - \frac{8}{9}\pi^2\right] \\ &\simeq -\mathcal{K}_2 \times 75.32 \simeq -4.77 \times 10^{-15} \,, \end{aligned}$$

yield the complete estimate for the 1st plus 2nd family

[38] The result is essentially the same as

$$a_\mu^{\rm EW} = (154 \pm 1[\rm had] \pm 2[m_H, m_t, 3-loop]) \times 10^{-11}$$

of Czarnecki, Marciano and Vainshtein [284], which also agrees numerically with the one

$$a_\mu^{\rm EW} = (152 \pm 1[\rm had]) \times 10^{-11}$$

obtained by Knecht, Peris, Perrottet and de Rafael [312].

Table 15
Summary of weak 2–loop effects contributing to a_e in units 10^{-15}. Fermion triangle loops: 1st, 2nd and 3rd family LO, fermion loops NLL and bosonic loops (with equation numbers, last 3 entries rescaled as described in the text).

$[eud]$ LO Eq. (250)	$[\mu sc]$ LO Eq. (251)	$[\tau bt]$ LO Eq. (211)	NLL Eq. (237)	bosonic Eqs. (239,241)
-1.86±0.16	-1.15±0.07	-1.91±0.02	-1.09±0.19	$-1.02^{+0.35}_{-0.25}$

$$a_e^{(4)\,\mathrm{EW}}\left(\begin{bmatrix} e,u,d \\ \mu,c,s \end{bmatrix}\right) = -\mathcal{K}_2\ \left[\frac{5}{3}\ln\frac{M_\Lambda^2}{m_e^2} + 3\ln\frac{M_\Lambda^2}{m_\mu^2} - 4\ln\frac{M_\Lambda^2}{M_c^2} + \frac{19}{6} - \frac{8}{9}\pi^2\right]$$
$$\simeq -\mathcal{K}_2\ \times 36.85(46) \simeq -2.33(3)\times 10^{-15}\,. \tag{249}$$

The large N_c QCD inspired LMD result Eq. (234) for the 1st family translates into

$$a_e^{(4)\,\mathrm{EW}}([e,u,d]) \simeq -\mathcal{K}_2\left\{\frac{1}{3}\left(-r_\pi\,(r_\pi+2)\sqrt{1-\frac{4}{r_\pi}}\left[\ln\frac{-2}{r_\pi\sqrt{1-\frac{4}{r_\pi}}-r_\pi+2}\right]\right.\right.$$
$$\left.\left. + r_\pi^2\ln r_\pi - 2r_\pi - 3\right) + \ln\frac{M_\rho^2}{m_e^2} - \frac{M_\rho^2}{M_{a_1}^2-M_\rho^2}\ln\frac{M_{a_1}^2}{M_\rho^2} - \frac{8\pi^2}{9} + \frac{11}{6}\right\}$$
$$\simeq -\mathcal{K}_2\ \times 29.41(2.56) = -1.86(16)\times 10^{-15}\,, \tag{250}$$

with $r_\pi = m_\pi^2/m_e^2$. For the 2nd family Eq. (235) reads

$$a_e^{(4)\,\mathrm{EW}}([\mu,c,s]) \simeq -\mathcal{K}_2\ \left[\frac{2}{3}\ \ln\frac{M_\phi^2}{M_{\eta'}^2} - \frac{2}{3}\ \ln\frac{M_{\eta'}^2}{m_\eta^2}\right.$$
$$\left. + \frac{1}{3}\frac{M_\phi^2-m_\eta^2}{M_{f_1}^2-M_\phi^2}\ln\frac{M_{f_1}^2}{M_\phi^2} + 4\ln\frac{M_c^2}{M_\phi^2} + 3\ln\frac{M_\phi^2}{m_\mu^2} + 2\right]$$
$$\simeq -\mathcal{K}_2\ \times 18.19(1.16) \simeq -1.15(7)\times 10^{-11}\,. \tag{251}$$

The LL approximation Eq. (242) for a_e is given by

$$a_{e\,\mathrm{LL}}^{(4)\,\mathrm{EW}} = -\mathcal{K}_2\left\{\left[\frac{161}{9} + \frac{27}{9}(1-4s_W^2)^2\right]\ln\frac{M_Z}{m_e}\right.$$
$$\left. - \sum_{f\in F} N_f Q_f\left[12\,T_f^3\,Q_f - \frac{8}{9}\left(T_f^3 - 2Q_f s_W^2\right)\left(1-4s_W^2\right)\right]\ln\frac{M_Z}{m_f}\right\}$$
$$\simeq -14.62\times 10^{-15}\,, \tag{252}$$

where the sum extends over $F = \mu,\tau,u,d,s,c,b$.

Note that the contributions Eqs. (211) and (237) scale with $x_{(e\mu)}$. The bosonic contributions only depend on the external fermion mass and we may use the full 2–loop result Eq. (241) together with Eq. (239) to calculate $c_0^{\mathrm{bos},2L}$ which is equal for μ and e and we obtain $a_e^{(4)\,\mathrm{EW}}(\mathrm{bosonic}) = -1.02^{+0.35}_{-0.25}\times 10^{-15}$. Results are collected in Table 15.

As a result we obtain the total weak 2–loop contribution

$$a_e^{(4)\,\mathrm{EW}} \simeq (-7.03 \pm 0.35[m_H,m_t] \pm 0.23[\mathrm{had}])\times 10^{-15}\,. \tag{253}$$

The total weak contribution thus is given by

$$a_e^{\mathrm{EW}} \simeq (38.54 \pm 0.35[m_H,m_t] \pm 0.23[\mathrm{had}])\times 10^{-15}\,. \tag{254}$$

Note that the leading log approximation in Eq. (252) utilizing constituent quarks in this case is quite far off from the result in Eq. (253). Using this approximation we would get the smaller value $a_e^{\mathrm{EW}} \simeq 30.95\times 10^{-15}$, which was used frequently in the past.

Table 16
Standard model theory and experiment comparison [in units 10^{-11}].

Contribution	Value	Error	Equation	References
QED incl. 4-loops+LO 5-loops	116 584 718.1	0.2	(99)	[317]
Leading hadronic vacuum polarization	6 903.0	52.6	(113)	[174]
Subleading hadronic vacuum polarization	-100.3	1.1	(139)	[160]
Hadronic light–by–light	116.0	39.0	(200)	[318]
Weak incl. 2-loops	153.2	1.8	(245)	[319]
Theory	116 591 790.0	64.6	–	
Experiment	116 592 080.0	63.0	(41)	[92]
Exp. - The. 3.2 standard deviations	290.0	90.3	–	

7. Muon g-2: Theory versus Experiment

A new stage in testing theory and new physics scenarios has been reached with the BNL muon $g-2$ experiment, which was able to reduce the experimental uncertainty by a factor 14 to $\sim 63\times10^{-11}$. We already have summarized the experimental status in Sect. 2.2. The world average experimental muon magnetic anomaly, dominated by the very precise BNL result, now is [92]

$$a_\mu^{\rm exp} = 1.16592080(63)\times 10^{-3} \tag{255}$$

(relative uncertainty 0.54ppm), which confronts the SM prediction (see Table 16)

$$a_\mu^{\rm the} = 1.16591790(65)\times 10^{-3}\ . \tag{256}$$

As ever before, but on a order of magnitude higher level, the anomalous magnetic moment of the muon provides one of the most precise tests of quantum field theory as a basic framework of elementary particle theory and of QED and the electroweak SM in particular. But not only that, it also constrains physics beyond the SM severely. In fact the $3.2\,\sigma$ deviation between theory and experiment

$$\delta a_\mu^{\rm NP?} = a_\mu^{\rm exp} - a_\mu^{\rm the} = (290 \pm 90)\ \times 10^{-11}\ , \tag{257}$$

could be a hint for new physics. Before we discuss possibilities to explain this deviation assuming it to be *a clear indication of something missing*, we first will summarize the SM prediction and recall what are the most relevant effects.

7.1. *Standard Model Prediction*

In the previous sections, we have discussed in detail the various contributions which enter the theoretical prediction of a_μ. We summarize them in Table 16. Input parameters were specified in Sect. 3 and Appendix A. What we notice is that a new quality of "diving into the depth of quantum corrections" has been achieved: the 8th order QED [$\sim 381\times10^{-11}$], the weak correction up to 2nd order [$\sim 153\times10^{-11}$] and the hadronic light–by–light scattering [$\sim 116\times10^{-11}$] are now in the focus. The hadronic vacuum polarization effects which played a significant role already for the last CERN experiment now is a huge effect of more than 11 SD's. As a non–perturbative effect it still has to be evaluated largely in terms of experimental data with unavoidable experimental uncertainties which yield the biggest contribution to the uncertainty of theoretical predictions. However, due to substantial progress in the measurement of total hadronic e^+e^-–annihilation cross–sections, the uncertainty from this source has reduced to a remarkable $\sim 53\times10^{-11}$ only. This source

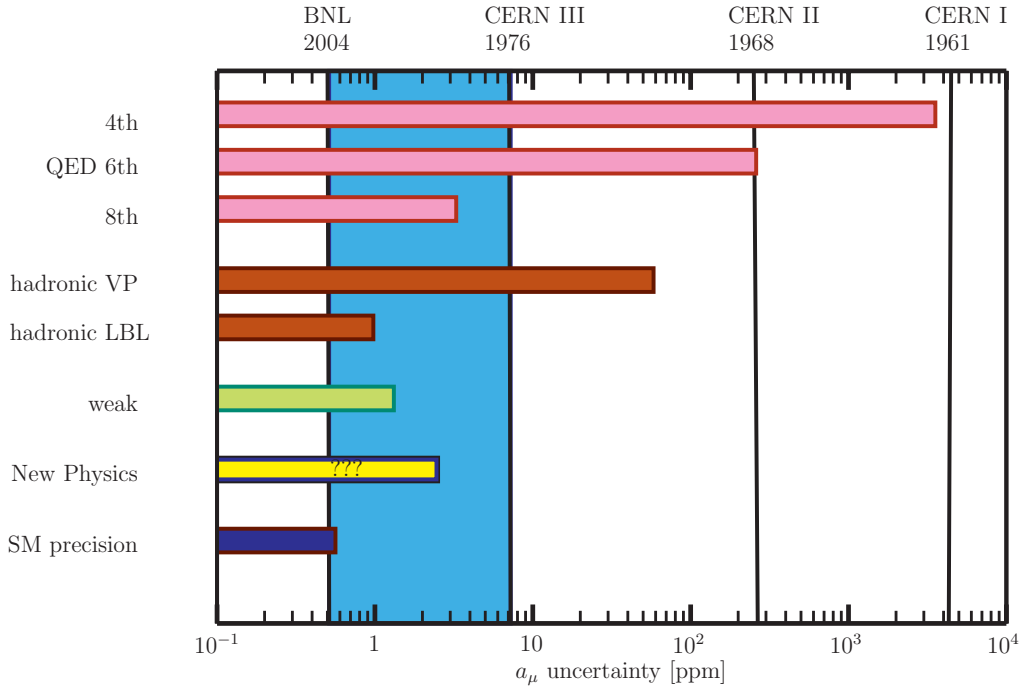

Fig. 41. Sensitivity of $g-2$ experiments to various contributions. The increase in precision with the BNL $g-2$ experiment is shown as a gray (blue) vertical band. New Physics is illustrated by the deviation $(a_\mu^{\rm exp} - a_\mu^{\rm the})/a_\mu^{\rm exp}$.

of error now is only slightly larger than the uncertainty in the theoretical estimates of the hadronic light–by–light scattering contribution [$\sim 39 \times 10^{-11}$]. Nevertheless, we have a solid prediction with a total uncertainty of $\sim 65 \times 10^{-11}$, which is essentially equal to the experimental error of the muon $g-2$ measurement.

Fig. 41 illustrates the sensitivity to various contributions and how it developed in history. The high sensitivity of a_μ to physics from not too high scales M above m_μ, which is scaling like $(m_\mu/M)^2$, and the more than one order of magnitude improvement of the experimental accuracy has raised many previously negligible SM contributions to relevance. We also have reached an exciting level of sensitivity to New Physics. "New Physics" is displayed in the figure as the ppm deviation of Eq. (257) which is $3.2\,\sigma$. We note that the theory error is somewhat larger than the experimental one. It is fully dominated by the uncertainty of the hadronic low energy cross–section data, which determine the hadronic vacuum polarization and, partially, from the uncertainty of the hadronic light–by–light scattering contribution.

In any case we now have a much more detailed test of the present established theory of the fundamental forces and the particle spectrum than we had before the BNL experiment. At the same time the muon $g-2$ provides insight to possible new physics entering at scales below about 1 TeV. For what concerns the interpretation of the actual deviation between theory and experiment, we have to remember that such high precision physics is extremely challenging for both experiment and for theory and it is not excluded that some small effect has been overlooked or underestimated at some place. To our present knowledge, it is hard to imagine that a $3\,\sigma$ shift could be explained by known physics or underestimated systematic uncertainties, theoretical and/or experimental. Thus New Physics seems a likely interpretation, if it is not an experimental fluctuation (0.27% chance).

It should be noted that the result Eq. (256) is obtained when relying on the published e^+e^-–data for the evaluation of the hadronic vacuum polarization. If isospin rotated hadronic τ–decay spectral functions, corrected for known isospin violations, are included, a substantially larger value for $a_\mu^{\rm had}$ results: $\delta a_\mu(+\tau) \sim 150 \times 10^{-11}$ and the "discrepancy" Eq. (257) reduces to about $1.4\,\sigma$ only, which would mean that there is agreement between theory and experiment. However, as pointed out in Ref. [217] recently, an increase of the hadronic vacuum polarization would also increase the value of $\alpha(M_Z)$ and as a consequence lower the

indirect Higgs mass bound from LEP precision experiments. In fact the indirect upper Higgs mass bound, $m_H < 153$ GeV would move to $m_H < 133$ GeV, closer to be in conflict with the direct exclusion bound of $m_H > 114$ GeV. This possibility in any case would lead to an interesting tension for the Standard Model to be in conflict with experimental facts.

Note that the theoretical predictions obtained by different authors in general differ by the leading order hadronic vacuum polarization contribution listed in Tab. 4 and/or by a different choice of the hadronic light–by–light scattering contribution which we have collected in Tab. 13. The deviation between theory and experiment then ranges from 0.7 to 4.2 σ's. The smallest difference is obtained when including the isospin rotated τ–data in calculating $a_\mu^{\rm had}$, as in [177], together with the LbL estimate [257], the largest using the $a_\mu^{\rm had}$ estimate [184] together with the LbL estimate [17] (also see Fig. 7.1 in Ref. [46]).

7.2. *New Physics Contributions*

Although the SM is very well established as a renormalizable QFT and describes essentially all experimental data of laboratory and collider experiments, it is well established that the SM is *not* able to explain a number of fundamental facts. The SM fails to account for the existence of non–baryonic cold dark matter (at most 10% is normal baryonic matter), the matter–antimatter asymmetry in the universe, which requires baryon–number B and lepton–number L violation at a level much higher than in the SM, the problem of the cosmological constant and so on. Also, a "complete" theory should include the 4th force of gravity in a natural way and explain the huge difference between the weak and the Planck scale (hierarchy problem). So, new physics is there but how is it realized? What can the muon $g-2$ tell us about new physics?

New physics contributions, which we know must exist, are part of any measured number. If we confront an accurately predictable observable with a sufficiently precise measurement of it, we should be able to see that our theory is incomplete. New physics is due to states or interactions which have not been seen by other experiments, either by a lack of sensitivity or, because the new state was too heavy to be produced at existing experimental facilities or, because the signal was still buried in the background. At the high energy frontier LEP and the Tevatron have set limits on many species of possible new particles predicted in a plenitude of models which extend the SM. The Particle Data Group [104] includes a long list of possible states which have not been seen, which translates into an experimental lower bound for the mass. In contrast to the direct searches at the high energy frontier, new physics is expected to change a_μ indirectly, by virtual loop–contributions. In general, assuming Eq. (257) to be a true effect, the result allows to constrain the parameter space of extensions of the SM.

The simplest possibility is to add a 4th fermion family of sequential fermions, where the neutrino has to have a large mass ($m_{\nu'} > 45$ GeV) as additional light (nearly massless) neutrinos have been excluded by LEP. The present bounds read $m_L > 100$ GeV for a heavy lepton and $m_{b'} \gtrsim 200$ GeV for a heavy quark.

Similarly, there could exist additional gauge bosons, like from an extra $U(1)'$. This would imply an additional Z boson, a sequential Z' which would mix with the SM Z and the photon. More attractive are extensions which solve some real or thought shortcomings of the SM. This includes Grand Unified Theories (GUT) [320] which attempt to unify the strong, electromagnetic and weak forces, which correspond to three different factors of the local gauge group of the SM, in one big simple local gauge group

$$G_{\rm GUT} \supset SU(3)_c \otimes SU(2)_L \otimes U(1)_Y \equiv G_{\rm SM}$$

which is assumed to be spontaneously broken in at least two steps

$$G_{\rm GUT} \to SU(3)_c \otimes SU(2)_L \otimes U(1)_Y \to SU(3)_c \otimes U(1)_{\rm em} \; .$$

Coupling unification is governed by the renormalization group evolution of $\alpha_1(\mu)$, $\alpha_2(\mu)$ and $\alpha_3(\mu)$, corresponding to the SM group factors $U(1)_Y$, $SU(2)_L$ and $SU(3)_c$, with the experimentally given low energy values, typically at the Z mass scale, as starting values evolved to very high energies, the *GUT scale* $M_{\rm GUT}$ where couplings should meet. Within the SM the three couplings do not unify, thus unification requires new physics as predicted by a GUT extension [321]. Also extensions like the left–right (LR) symmetric model

are of interest. The simplest possible unifying group is $SU(5)$ which, however, is ruled out by the fact that it predicts protons to decay faster than allowed by observation. GUT models like $SO(10)$ or the exceptional group E_6 not only unify the gauge group, thereby predicting many additional gauge bosons, they also unify quarks and leptons in GUT matter multiplets. Now quarks and leptons directly interact via the *leptoquark* gauge bosons X and Y which carry color, fractional charge ($Q_X = -4/3$, $Q_Y = -1/3$) as well as baryon and lepton number. Thus GUTs are violating B as well as L, yet with $B - L$ still conserved. The proton may now decay via $p \to e^+\pi^0$ or many other possible channels. The experimental proton lifetime $\tau_{\rm proton} > 2 \times 10^{29}$ years at 90% C.L. requires the extra gauge bosons to exhibit masses of about $M_{\rm GUT} > 10^{16}$ GeV and excludes $SU(5)$ as it predicts unification at too low scales. Note that the stability of the proton requires $M_{\rm GUT}$ to lie not more than a factor 1000 below the Planck scale. In general GUTs also have additional normal gauge bosons, extra W's and Z's which mix with the SM gauge bosons. Present bounds here are $M_{Z',W'} > 600 - 800$ GeV depending on the GUT scenario. Contributions from such extra gauge bosons may be estimated from the weak one–loop contributions by rescaling with $(M_W/M_{W'_{\rm SM}})^2 \sim 0.01$ and hence 1% of 19.5×10^{-10} only, an effect much too small to be of relevance.

In deriving bounds on New Physics it is important to respect constraints not only from a_μ and the direct bounds from the particle data tables, but also from other precision observables which are sensitive to new physics via radiative corrections. Important examples are the electroweak precision observables [322,323]: $M_W = 80.392(29)$ GeV , $\sin^2\Theta^\ell_{\rm eff} = 0.23153(16)$, and $\rho_0 = 1.0002^{+0.0007}_{-0.0004}$, which are all precisely measured and precisely predicted by the SM or in extensions of it. The SM predictions use the very precisely known independent input parameters α, G_μ and M_Z, but also the less precisely known top mass $m_t = 172.6 \pm 1.4$ GeV , [324] (the dependence on other fermion masses is usually weak, the one on the unknown Higgs is only logarithmic and already fairly well constrained by experimental data). The effective weak mixing parameter essentially determines $m_H = 114^{+45}_{-33}$ GeV at 68% C.L. (not taking into account M_W). The parameter ρ_0 is the tree level (SM radiative corrections subtracted) ratio of the low energy effective weak neutral to charged current couplings: $\rho = G_{\rm NC}/G_{\rm CC}$ where $G_{\rm CC} \equiv G_\mu$. This parameter is rather sensitive to new physics. Equally important are constraints by the B–physics branching fractions [325] ${\rm BR}(b \to s\gamma) = (3.55 \pm 0.24^{+0.09}_{-0.10} \pm 0.03) \times 10^{-4}$, ${\rm BR}(B_s \to \mu^+\mu^-) < 1.0 \times 10^{-7}$ (95% C.L.) .

Concerning flavor physics, in particular the B factories Belle at KEK and BaBar at SLAC have set new milestones in confirming the flavor structure as inferred by the SM. In the latter FCNC are absent at tree level due to the GIM mechanism and CP-violation and flavor mixing patterns seem to be realized in nature precisely as implemented by the three fermion–family CKM mixing scheme. Many new physics models have serious problems to accommodate this phenomenologically largely confirmed structure in a natural way. Therefore, the criterion of *Minimal Flavor Violation* (MFV) [326] has been conjectured as a framework for constructing low energy effective theories which include the SM Lagrangian without spoiling its flavor structure. The SM fermions are grouped into three families with two $SU(2)_L$ doublets (Q_L and L_L) and three $SU(2)_L$ singlets (U_R, D_R and E_R) and the largest group of unitary transformations which commutes with the gauge group is $G_F = U(3)^5$ [327]. The latter may be written more specifically as

$$G_F = SU(3)^3_q \otimes SU(3)^2_\ell \otimes U(1)_B \otimes U(1)_L \otimes U(1)_Y \otimes U(1)_{PQ} \otimes U(1)_{E_R}$$

with $SU(3)^3_q = SU(3)_{Q_L} \otimes SU(3)_{U_R} \otimes SU(3)_{D_R}$ and $SU(3)^2_\ell = SU(3)_{L_L} \otimes SU(3)_{E_R}$. The SM Yukawa interactions break the subgroup $SU(3)^3_q \otimes SU(3)^2_\ell \otimes U(1)_{PQ} \otimes U(1)_{E_R}$. However, one may introduce three dimensionless auxiliary fields

$$Y_U \sim (3, \bar{3}, 1)_{SU(3)^3_q} \ , \ Y_D \sim (3, 1, \bar{3})_{SU(3)^3_q} \ , \ Y_E \sim (3, \bar{3})_{SU(3)^2_\ell}$$

which provide a convenient bookkeeping for constructing MFV effective theories. Formally the auxiliary fields allow to write down MFV compatible interactions as G_F invariant effective interactions. The MVF criterion requires that a viable dynamics of flavor violation is completely determined by the structure of the ordinary SM Yukawa couplings. Most of the promising and seriously considered new physics models, which we will consider below, belong to the class of MFV extensions of the SM. Examples are the R-parity conserving two doublet Higgs models, the R-parity conserving minimal supersymmetric extension of the SM [328] and the Littlest Higgs model without T-parity.

Table 17
Typical New Physics scales required to satisfy $\Delta a_\mu^{\rm NP} = \delta a_\mu$ in Eq. (257).

$\mathcal{C}$	1	α/π	$(\alpha/\pi)^2$
$M_{\rm NP}$	$2.0^{+0.4}_{-0.3}$ TeV	100^{+21}_{-13} GeV	5^{+1}_{-1} GeV

One important monitor for new physics is the electric dipole moment which we briefly discussed towards the end of Sect. 1. The EDM is a direct measure of T–violation, which in a QFT is equivalent to a CP–violation. Since extensions of the SM in general exhibit additional sources of CP violation, EDMs are very promising probes of new physics. An anomalously large EDM of the muon d_μ would influence the a_μ extraction from the muon precession data as discussed earlier. We may ask whether d_μ could be responsible for the observed deviation in a_μ. In fact Eq. (37) tells us that a non–negligible d_μ would increase the observed a_μ, and we may estimate

$$|d_\mu| = \frac{1}{2}\frac{e}{m_\mu}\sqrt{(a_\mu^{\rm exp})^2 - (a_\mu^{\rm SM})^2} = (2.42 \pm 0.41) \times 10^{-19}\, e\cdot{\rm cm}\,. \tag{258}$$

This also may be interpreted as an upper limit $d_\mu < 2.7 \times 10^{-19}\, e\cdot$cm. Recent advances in experimental techniques will allow to perform much more sensitive experiments for electrons, neutrons and neutral atoms [329]. For new efforts to determine d_μ at much higher precision see [9,330]. In the following we will assume that d_μ is in fact negligible, and that the observed deviation has other reasons. As mentioned after Eq. (37), in the SM and viable extensions of it d_μ is expected to be much smaller that what could be of relevance here (see [6,7]).

As mentioned many times, the general form of contributions from states of mass $M_{\rm NP} \gg m_\mu$ takes the form

$$a_\mu^{\rm NP} = \mathcal{C}\,\frac{m_\mu^2}{M_{\rm NP}^2} \tag{259}$$

where naturally $\mathcal{C} = O(\alpha/\pi)$ ($\sim$ lowest order a_μ), like for the weak contributions Eq. (203), but now from interactions and states not included in the SM. New fermion loops may contribute similarly to a τ–lepton by

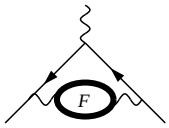

$$a_\mu^{(4)}({\rm vap}, F) = \sum_F Q_F^2 N_{cF}\left[\frac{1}{45}\left(\frac{m_\mu}{m_F}\right)^2 + \cdots\right]\left(\frac{\alpha}{\pi}\right)^2, \tag{260}$$

which means $\mathcal{C} = O((\alpha/\pi)^2)$. Note that the τ contribution to a_μ is 42×10^{-11} only, while the 3 σ effect we are looking for is 290×10^{-11}. As the direct lower limit for a sequential fermion is about 100 GeV such effects cannot account for the observed deviation [39].

A rough estimate of the scale $M_{\rm NP}$ required to account for the observed deviation is given in Table 17. An effective tree level contribution would extend the sensibility to the very interesting 2 TeV range, however, we know of no compelling scenario where this is the case.

[39] It should be noted that heavy sequential fermions are constrained severely by the ρ–parameter (NC/CC effective coupling ratio), if doublet members are not nearly mass degenerate. However, a doublet (ν_L, L) with $m_{\nu_L} = 45$ GeV and $m_L = 100$ GeV only contributes $\Delta\rho \simeq 0.0008$ which is within the limit from LEP electroweak fits [322]. Not yet included is a similar type of contribution from the 4th family (t', b') doublet mass–splitting, which also would add a positive term

$$\Delta\rho = \frac{\sqrt{2}G_\mu}{16\pi^2}\,3\,|m_{t'}^2 - m_{b'}^2| + \cdots\,.$$

In this context it should be mentioned that the so called *custodial symmetry* of the SM which predicts $\rho_0 = 1$ at the tree level (independent of any parameter of the theory, which implies that it is not subject to subtractions due to parameter renormalization) is one of the severe constraints to extensions of the SM (see [331])

7.2.1. *Generic Contributions from Physics beyond the SM*

Common to many of the extensions of the SM are predictions of new states: scalars S, pseudoscalars P, vectors V or axialvectors A, neutral or charged. They contribute via one–loop lowest order type diagrams shown in Fig. 42. Here, we explicitly assume all fermions to be Dirac fermions. Besides the SM fermions, μ in particular, new heavy fermions F of mass M may be involved, but fermion number is assumed to be conserved, like in $\Delta\mathcal{L}_S = f\bar{\psi}_\mu\psi_F S + \text{h.c.}$, which will be different in supersymmetric (SUSY) extensions discussed below, where fermion number violating Majorana fermions necessarily must be there. Note that

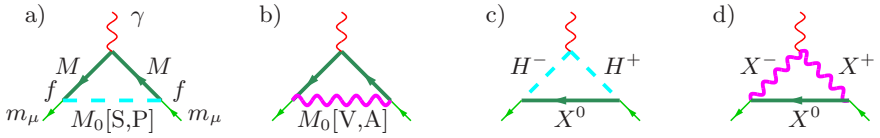

Fig. 42. Possible New Physics contributions. Neutral boson exchange: a) scalar or pseudoscalar and b) vector or axialvector, flavor changing or not. New charged bosons: c) scalars or pseudoscalars, d) vector or axialvector.

massive spin 1 boson exchange contributions in general have to be considered within the context of a gauge theory, in order to control gauge invariance and unitarity. We will present corresponding contributions in the unitary gauge calculated with dimensional regularization. We first discuss neutral boson exchange contributions from diagrams a) and b). Exotic neutral bosons of mass M_0 coupling to muons with coupling strength f would contribute [19,332]

$$\Delta a_\mu^{\rm NP} = \frac{f^2}{4\pi^2}\,\frac{m_\mu^2}{M_0^2}\,L,\;\; L = \frac{1}{2}\int\limits_0^1 {\rm d}x\,\frac{Q(x)}{(1-x)\,(1-\lambda^2\,x)+(\epsilon\lambda)^2\,x}\;, \tag{261}$$

where $Q(x)$ is a polynomial in x which depends on the type of coupling:

$$\begin{aligned}
&\text{Scalar} && : Q_{\rm S} = \; x^2\,(1+\epsilon-x)\\
&\text{Pseudoscalar} && : Q_{\rm P} = \; x^2\,(1-\epsilon-x)\\
&\text{Vector} && : Q_{\rm V} = 2x\,(1-x)\,(x-2\,(1-\epsilon)) \;+\lambda^2\,(1-\epsilon)^2\,Q_{\rm S}\\
&\text{Axialvector} && : Q_{\rm A} = 2x\,(1-x)\,(x-2\,(1+\epsilon)) \;+\lambda^2\,(1+\epsilon)^2\,Q_{\rm P}
\end{aligned}$$

with $\epsilon = M/m_\mu$ and $\lambda = m_\mu/M_0$. As an illustration we first consider the regime of a heavy boson of mass M_0 and $m_\mu, M \ll M_0$ for which one gets

$$\begin{aligned}
L_{\rm S} &= \;\;\frac{M}{m_\mu}\left(\ln\frac{M_0}{M}-\frac{3}{4}\right)+\frac{1}{6} \;\stackrel{M=m_\mu}{=}\; \ln\frac{M_0}{m_\mu}-\frac{7}{12},\\
L_{\rm P} &= -\frac{M}{m_\mu}\left(\ln\frac{M_0}{M}-\frac{3}{4}\right)+\frac{1}{6} \;\stackrel{M=m_\mu}{=}\; -\ln\frac{M_0}{m_\mu}+\frac{11}{12},\\
L_{\rm V} &= \;\;\frac{M}{m_\mu}-\frac{2}{3} \;\stackrel{M=m_\mu}{=}\; \frac{1}{3},\\
L_{\rm A} &= -\frac{M}{m_\mu}-\frac{2}{3} \;\stackrel{M=m_\mu}{=}\; -\frac{5}{3}\;.
\end{aligned} \tag{262}$$

In accordance with the MFV requirement it is more realistic to assume a flavor conserving neutral current $M = m_\mu$ as given by the second form. Typical contributions are shown in Fig. 43. Taking the coupling small enough such that a perturbative expansion in f makes sense, we take $f/(2\pi) = 0.1$, only the scalar exchange could account for the observed deviation with a scalar mass 480 GeV $< M_0 <$ 690 GeV. Pseudoscalar and axialvector yield the wrong sign. The vector exchange is too small.

As we will see later, in SUSY and littlest Higgs extensions the leading contributions actually come from the regime $m_\mu \ll M, M_0$ with $M \sim M_0$, which is of enhanced FCNC type, and thus differs from the case just presented in Eq. (262). For the combinations of fixed chirality up to terms of order $O(m_\mu/M)$ one gets

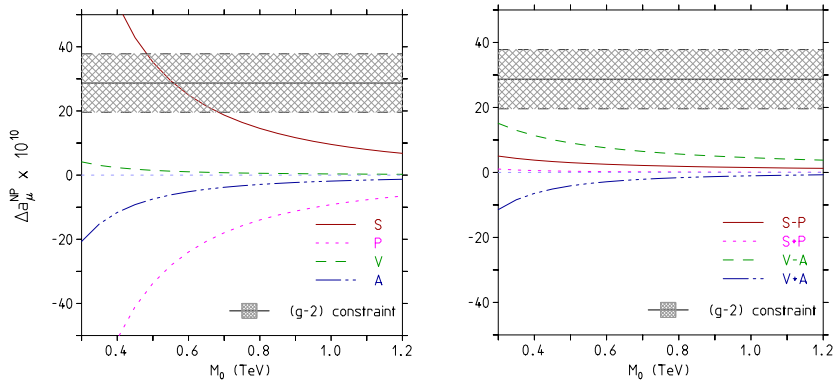

(a) Case: $m_\mu = M \ll M_0$ (b) Case: $m_\mu \ll M_0 = M$

Fig. 43. Single particle one–loop induced NP effects from Eq. (261) for $f^2/(4\pi^2) = 0.01$ (Note, a typical EW SM coupling would be $e^2/(4\pi^2 \cos^2\Theta_W) = 0.003$). S,P,V,A denote scalar, pseudoscalar, vector and axialvector exchange. Panel (a) uses Eq. (262) for $M = m_\mu$, panel (b) the chiral combinations in Eq. (263) for $M = M_0$, with the large combinations $L_S - L_P$ and $L_V - L_A$ rescaled by the muon Yukawa coupling m_μ/v in order to compensate for the huge pre-factor M/m_μ (see text).

$$
\begin{aligned}
L_S + L_P &= \frac{1}{6\,(1-z)^4}\,\left[2 + 3z - 6z^2 + z^3 + 6z\ln z\right] = \frac{1}{12}\,F_1^C(z),\\
L_S - L_P &= \frac{-M}{2m_\mu\,(1-z)^3}\,\left[3 - 4z + z^2 + 2\ln z\right] = \frac{M}{3m_\mu}\,F_2^C(z),\\
L_V + L_A &= \frac{-1}{6\,(1-z)^4}\,\left[8 - 38z + 39z^2 - 14z^3 + 5z^4 - 18z^2\ln z\right] = -\frac{13}{12}\,F_3^C(z),\\
L_V - L_A &= \frac{M}{2m_\mu\,(1-z)^3}\,\left[4 - 3z - z^3 + 6z\ln z\right] = \frac{M}{m_\mu}\,F_4^C(z),
\end{aligned}
\tag{263}
$$

where $z = (M/M_0)^2 = O(1)$ and the functions F_i^C are normalized to $F_i^C(1) = 1$. The possible huge enhancement factors M/m_μ, in some combination of the amplitudes, typical for flavor changing transitions, may be compensated due to radiative contributions to the muon mass (as discussed below) or by a corresponding Yukawa coupling $f \propto y_\mu = \sqrt{2}\,m_\mu/v$, as it happens in SUSY or little Higgs extensions of the SM.

The second class of possible new physics transitions due to charged S,P,V and A modes are represented by the diagrams c) and d) in Fig. 42. It amounts to replace L in Eq. (261) according to

$$
\Delta a_\mu^{\rm NP} = \frac{f^2}{4\pi^2}\,\frac{m_\mu^2}{M_0^2}\,L,\;\; L = \frac{1}{2}\int\limits_0^1 {\rm d}x\,\frac{Q(x)}{(\epsilon\lambda)^2\,(1-x)\,(1-\epsilon^{-2}\,x) + x}\;,
\tag{264}
$$

where again $Q(x)$ is a polynomial in x which depends on the type of coupling:

$$
\begin{aligned}
&\text{Scalar} && : Q_{\rm S} = -\,x\,(1-x)\,(x+\epsilon)\\
&\text{Pseudoscalar} && : Q_{\rm P} = -\,x\,(1-x)\,(x-\epsilon)\\
&\text{Vector} && : Q_{\rm V} = -2\,x^2\,(1+x-2\epsilon) + \lambda^2\,(1-\epsilon)^2\,Q_{\rm S}\\
&\text{Axialvector} && : Q_{\rm A} = -2\,x^2\,(1+x+2\epsilon) + \lambda^2\,(1+\epsilon)^2\,Q_{\rm P}
\end{aligned}
$$

Again, results for V and A are in the unitary gauge calculated with dimensional regularization. For a heavy boson of mass M_0 and $m_\mu, M \ll M_0$ one finds

$$
\begin{aligned}
L_{\rm S} &= -\frac{1}{4}\frac{M}{m_\mu} - \frac{1}{12} \overset{M=m_\mu}{=} -\frac{1}{3}\;, \quad L_{\rm P} = \frac{1}{4}\frac{M}{m_\mu} - \frac{1}{12} \overset{M=m_\mu}{=} \frac{1}{6}\;,\\
L_{\rm V} &= \frac{M}{m_\mu} - \frac{5}{6} \overset{M=m_\mu}{=} \frac{1}{6}\;, \quad L_{\rm A} = -\frac{M}{m_\mu} - \frac{5}{6} \overset{M=m_\mu}{=} -\frac{11}{6}\;.
\end{aligned}
\tag{265}
$$

The second form given is for a flavor conserving charged current transition with $M = m_\mu$.

Also for the charged boson exchanges the regime $m_\mu \ll M, M_0$ with $M \sim M_0$ is of interest in SUSY and littlest Higgs extensions of the SM and we find

$$
\begin{aligned}
L_S + L_P &= \frac{-1}{6\,(1-z)^4}\,\left[1 - 6z + 3z^2 + 2z^3 - 6z^2\ln z\right] = -\frac{1}{12}\,F_1^N(z),\\
L_S - L_P &= \frac{-M}{2m_\mu\,(1-z)^3}\,\left[1 - z^2 + 2z\ln z\right] = -\frac{M}{6m_\mu}\,F_2^N(z),\\
L_V + L_A &= \frac{-1}{6\,(1-z)^4}\,\left[10 - 43\,z + 78\,z^2 - 49\,z^3 + 4\,z^4 + 18\,z^3\ln z\right] = -\frac{5}{3}\,F_3^N(z),\\
L_V - L_A &= \frac{M}{m_\mu\,(1-z)^3}\,\left[4 - 15\,z + 12\,z^2 - z^3 - 6\,z^2\ln z\right] = \frac{2M}{m_\mu}\,F_4^N(z),
\end{aligned}
\tag{266}
$$

where $z = (M/M_0)^2 = O(1)$ and the functions F_i^N are normalized to $F_i^N(1) = 1$.

At $O((\alpha/\pi)^2)$ new physics may enter via vacuum polarization and we may write corresponding contributions as a dispersion integral Eq. (68):

$$
\Delta a_\mu^{\rm NP} = \frac{\alpha}{\pi}\int\limits_0^\infty \frac{{\rm d}s}{s}\frac{1}{\pi}\,{\rm Im}\,\Delta\Pi_\gamma^{\rm NP}(s)\,K(s)\,.
$$

Since, we are looking for contributions from heavy yet unknown states of mass $M \gg m_\mu$, and ${\rm Im}\Delta\Pi_\gamma^{\rm NP}(s) \neq 0$ for $s \geq 4M^2$ only, we may safely approximate $K(s) \simeq \frac{1}{3}\frac{m_\mu^2}{s}$ for $s \gg m_\mu^2$ such that, with $\frac{1}{\pi}\,{\rm Im}\,\Delta\Pi_\gamma^{\rm NP}(s) = \frac{\alpha(s)}{\pi}\,R^{\rm NP}(s)$

$$
\Delta a_\mu^{\rm NP} = \frac{1}{3}\frac{\alpha}{\pi}\left(\frac{m_\mu}{M}\right)^2 L\ ,\quad \frac{L}{M^2} = \frac{\alpha}{3\pi}\int\limits_0^\infty \frac{{\rm d}s}{s^2}R^{\rm NP}(s)\,.
$$

An example is a heavy lepton given by Eq. (260). A heavy narrow vector meson resonance of mass M_V and electronic width $\Gamma(V \to e^+e^-)$ (which is $O(\alpha^2)$) contributes $R_V(s) = \frac{9\pi}{\alpha^2}\,M_V\,\Gamma(V \to e^+e^-)\,\delta(s - M_V^2)$ such that $L = \frac{3\Gamma(V\to e^+e^-)}{\alpha M_V}$ and hence

$$
\Delta a_\mu^{\rm NP} = \frac{m_\mu^2\,\Gamma(V \to e^+e^-)}{\pi M_V^3} = \frac{4\alpha^2\,\gamma_V^2\,m_\mu^2}{3M_V^2}\,.
\tag{267}
$$

For $\gamma_V = 0.1$ and $M_V = 200$ GeV we get $\Delta a_\mu \sim 2\times 10^{-13}$. The hadronic contribution of a 4th family quark doublet assuming $m_{b'} = m_{t'} = 200$ GeV would yield $\Delta a_\mu \sim 5.6\times 10^{-14}$ only. Unless there exists a new type of strong interactions like Technicolor[40] [333,334,335], new strong interaction resonances are not expected, because new heavy sequential quarks would be too shortlived to be able to form resonances. As we know, due to the large mass and the large mass difference $m_t \gg m_b$, the top quark is the first quark which decays, via $t \to Wb$, as a bare quark before it has time to form hadronic resonances. This is not so surprising as the top Yukawa coupling responsible for the weak decay is stronger than the strong interaction constant.

New physics effects here may be easily buried in the uncertainties of the hadronic vacuum polarization. In any case, we expect $O((\alpha/\pi)^2)$ terms from heavy states not yet seen to be too small to play a role here.

In general the effects related to single diagrams, discussed in this paragraph, are larger than what one expects in a viable extension of the SM, usually required to be a renormalizable QFT and to exhibit gauge interactions which typically cause large cancellations between different contributions. But even if one ignores possible cancellations, all the examples considered so far show how difficult it actually is to reconcile the observed deviation with NP effects not ruled out already by LEP or Tevatron new physics searches, and

[40] Searches for Technicolor states like color–octet techni–ρ were negative up to 260 to 480 GeV depending on the decay mode.

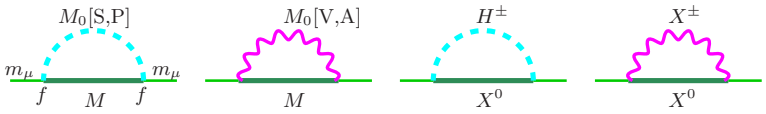

Fig. 44. Lepton self–energy contributions induced by the new interactions appearing in Fig. 42 may generate m_μ as a radiative correction effect.

if we adopt the phenomenologically preferred MFV restriction. The latter means to try to avoid conflicts with other experimental facts. Apparently a more sophisticated extension of the SM is needed which is able to produce substantial radiative corrections in the low energy observable a_μ while the new particles have escaped detection at accelerator facilities so far and only produce small higher order effects in other electroweak precision observables. In fact supersymmetric extensions of the SM precisely allow for such a scenario, as we will discuss below.

7.2.2. *Flavor Changing Processes*

We already have seen that flavor changing processes could give large contributions to a_μ. As pointed out in [27] taking into account just the vertex diagrams could be very misleading. The argument is that the same interactions and heavy states which could contribute to $a_\mu^{\rm NP}$ according to Fig. 42 would contribute to the muon self energy, via the diagrams Fig. 44. By imposing chiral symmetry to the SM, i.e. setting the SM Yukawa couplings to zero, lepton masses could be radiatively induced by flavor changing $f\bar\psi_\mu\psi_F S+$h.c. and $f\bar\psi_\mu\,{\rm i}\,\gamma_5\psi_F P+$h.c. interactions ($F$ a heavy fermion, S a scalar and P a pseudoscalar) in a hierarchy $m_\mu \ll M_F \ll M_S, M_P$. Then with $m_\mu \propto f^2 M_F$ and $a_\mu \propto f^2 m_\mu M_F/M^2_{S,P}$ one obtains $a_\mu = \mathcal{C}\, m_\mu^2/M^2_{S,P}$ with $\mathcal{C} = O(1)$, and the interaction strength f has dropped from the ratio. The problem is that a convincing approach of generating the lepton/fermion spectrum by radiative effects is not easy to accommodate. Of course it is a very attractive idea to replace the Yukawa term, put in by hand in the SM, by a mechanism which allows us to understand or even calculate the known fermion mass-spectrum, exhibiting a tremendous hierarchy of about 13 orders of magnitude of vastly different couplings/masses [from m_{ν_e} to m_t]. The radiatively induced values must reproduce this pattern and one has to explain why the same effects which make up the muon mass do not contribute to the electron mass. Again the needed hierarchy of fermion masses is only obtained by putting it in by hand in some way. In the scenario of radiatively induced lepton masses one has to require the family hierarchy like $f_e^2 M_{F_e}/f_\mu^2 M_{F_\mu} \simeq m_e/m_\mu$, $f_P \equiv f_S$ in order to get a finite cut–off independent answer, and $M_0 \to M_S \neq M_P$, such that $m_\mu = \frac{f_\mu^2\, M_{F_\mu}}{16\pi^2}\,\ln\frac{M_S^2}{M_P^2}$ which is positive provided $M_S > M_P$.

Another aspect of flavor changing transition in the lepton sector is the following: after neutrino oscillations and herewith right–handed singlet neutrinos and neutrino masses have been established, also lepton number violating transitions like $\mu^\pm \to e^\pm\gamma$, see Fig. 45, are in the focus of further searches. The corresponding contributions here read

$$
\begin{aligned}
L_{\rm S}^\mu &\simeq \frac{1}{6} \quad , \quad L_{\rm S}^e \simeq \frac{m_\mu}{m_e}\left(\ln\frac{M_0}{m_\mu}-\frac{3}{4}\right),\\
L_{\rm P}^\mu &\simeq \frac{1}{6} \quad , \quad L_{\rm P}^e \simeq -\frac{m_\mu}{m_e}\left(\ln\frac{M_0}{m_\mu}-\frac{3}{4}\right),\\
L_{\rm V}^\mu &\simeq \frac{2}{3} \quad , \quad L_{\rm V}^e \simeq \frac{m_\mu}{m_e},\\
L_{\rm A}^\mu &\simeq -\frac{2}{3} \quad , \quad L_{\rm A}^e \simeq -\frac{m_\mu}{m_e}\,.
\end{aligned}
$$

The latter flavor changing transitions are strongly constrained, first by direct rare decay search experiments which were performed at the Paul Scherrer Institute (PSI) and second, with the advent of the much more precise measurement of a_e. For example, for a scalar exchange mediating $e \to \mu \to e$ with $f^2/(4\pi^2) \simeq 0.01$ and $M_0 \simeq 100$ GeV we obtain $\Delta a_e^{NP} \simeq 33\times 10^{-11}$ which is ruled out by $a_e^{\rm exp} - a_e^{\rm the} \sim 1\times 10^{-11}$. Either M_0 must be heavier or the coupling smaller: $f^2/(4\pi^2) < 0.0003$. The present limit for the branching fraction

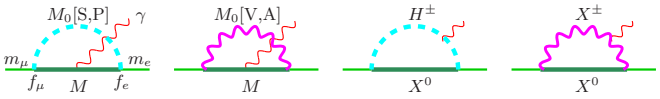

Fig. 45. $\mu \to e\gamma$ transitions by new interactions (overall flavor changing version of Fig. 42).

$Br(\mu \to e\gamma)$ is 1.2×10^{-11}, which will be improved to 10^{-13} at PSI by a new experiment [336] (see also [337]) .

At present the most important constraints from flavor changing transitions are the ones obtained with quarks [325]. In particular the $b \to s\gamma$ branching fraction given before provides an interesting constraint for the SUSY parameter space as we will discuss below. Note that models exhibiting tree level FCNCs are not in the class of MFV theories, nevertheless a_e and a_μ can provide useful constraints on such processes.

7.2.3. *Two-Higgs Doublet Models*

One possibility of extending the SM is to modify the Higgs sector where one could add scalar singlets, an additional doublet, a Higgs triplet and so on. From a theoretical point of view the case with two Higgs doublets is very attractive. General two Higgs doublet models (2HDM) are interesting as they predict 4 additional physical spin 0 bosons. In terms of the components of the two doublet fields Φ_i $(i = 1, 2)$ of fixed hypercharge $Y_i = (-1, +1)$, the new physical scalars are the two scalars h and H, the pseudoscalar A and the charged Higgses $H^\pm$:

$$h = -\sin\alpha\,\eta_1 + \cos\alpha\,\eta_2\,, \qquad A = -\sin\beta\,\chi_1 + \cos\beta\,\chi_2\,,$$
$$H = \cos\alpha\,\eta_1 + \sin\alpha\,\eta_2\,, \qquad H^\pm = -\sin\beta\,\phi_1^\pm + \cos\beta\,\phi_2^\pm\,.$$

Two Higgs doublets are needed in Minimal Supersymmetric extensions of the SM (MSSM). One reason is supersymmetry itself, the other is anomaly cancellation of the SUSY partners of the Higgses. In the minimal SUSY models the masses of the extra Higgses at tree level are severely constrained by the following mass- and coupling-relationships:

$$m_\pm^2 = M_W^2 + m_A^2\,, \quad m_{H,h}^2 = \frac{1}{2}\left(M_Z^2 + m_A^2 \pm \sqrt{(M_Z^2 - m_A^2)^2 + 4M_Z^2 m_A^2 \sin^2 2\beta}\right),$$
$$\tan(2\alpha) = \tan(2\beta)\,\frac{m_A^2 + M_Z^2}{m_A^2 - M_Z^2}\,, \quad \sin^2(\alpha - \beta) = \frac{m_H^2}{m_A^2}\,\frac{M_Z^2 - m_H^2}{M_Z^2 + m_A^2 - 2m_H^2}\,.$$

Only two independent parameters are left, which we may choose to be $\tan\beta$ and m_A. In the phenomenologically interesting region of enhanced $\tan\beta$ together with a light Higgs for the CP-even part of the Higgs sector we have $\alpha \simeq \beta$, which we assume in the following.

In 2HDMs many new real and virtual processes, like $W^\pm H^\mp \gamma$ transitions, are the consequence. Present bounds on scalars are $m_{H^\pm} > 80$ GeV and $m_A + m_h > 90$ GeV. In general, in type I models, fermions get contributions to their masses from the vev's of both Higgs scalars. Phenomenologically preferred and most interesting are the type II models where a discrete symmetry guarantees that the upper and the lower entries of the fermion doublets get their masses from different vev's ($m_t \propto v_2$, $m_b \propto v_1$) in order to prevent FCNC's [338]. Only the type II models satisfy the MFV criterion. Such models are also interesting because one easily may get $m_t \gg m_b$ without having vastly different Yukawa couplings. Notice, however, that the experimental bounds on $\Delta r = 1 - \pi\alpha/(\sqrt{2}G_\mu M_Z^2 \cos^2\Theta_W \sin^2\Theta_W)$, with $\cos^2\Theta_W = M_W^2/M_Z^2$ and $\Delta\rho$, seem to require a top with a large Yukawa coupling, not just a large top mass. In addition if $\tan\beta = v_2/v_1 \sim m_t/m_b$ the bottom Yukawa coupling is about equal to the top Yukawa coupling and would practically cancel the top quark contribution [41] . Anyway, the possibility of two Higgs doublets is an interesting option and

[41] The virtual top effect contributing to the radiative corrections of $\rho = 1 + \Delta\rho$ allowed a determination of the top mass prior to the discovery of the top by direct production at Fermilab in 1995. The LEP precision determination of $\Delta\rho = \frac{\sqrt{2}G_\mu}{16\pi^2}\,3\,|m_t^2 - m_b^2|$ (up to subleading terms) from precision measurements of Z resonance parameters yields $m_t = 172.3^{+10.2}_{-7.6}$ GeV in excellent agreement with the direct determination $m_t = 172.6(1.4)$ GeV [324] at the Tevatron.

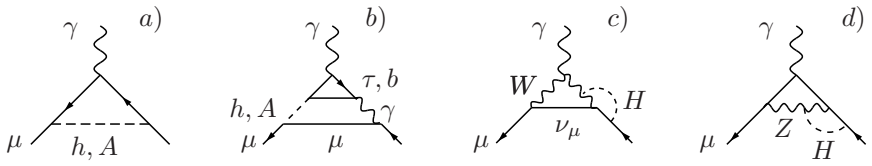

Fig. 46. Leading 2HDM graphs a) and b) contributing to a_μ. Diagrams c) and d), with $H \to h, H, A$, are examples of subleading bosonic contributions which are modified with respect to the SM weak bosonic contributions due to the extended Higgs structure.

therefore has been studied extensively [338]–[344] in the past.

The SM Higgs contribution Eq. (204) is tiny, due to the fact that the $H\bar{\mu}\mu$ Yukawa coupling $y_\mu = \sqrt{2}\, m_\mu/v$ is very small because the SM Higgs VEV is large: $v = 246.221(1)$ GeV. In 2HDMs of type II the Yukawa couplings may be enhanced by large factors $\tan\beta = v_2/v_1$. This is particularly important for the heavier fermions. The relevant couplings read

$$\begin{aligned}
&Hf\bar{f},\ f = b,t && -\frac{g}{2}\left(\ \frac{m_b}{M_W}\frac{\cos\alpha}{\cos\beta},\ \frac{m_t}{M_W}\frac{\sin\alpha}{\sin\beta}\right)\\
&hf\bar{f},\ \ f = b,t && -\frac{g}{2}\left(-\frac{m_b}{M_W}\frac{\sin\alpha}{\cos\beta},\ \frac{m_t}{M_W}\frac{\cos\alpha}{\sin\beta}\right)\\
&Af\bar{f},\ f = b,t && -\gamma_5\frac{g}{2}\left(\ \frac{m_b}{M_W}\tan\beta,\ \ \frac{m_t}{M_W}\cot\beta\right)\\
&H^+ b\bar{t} && \frac{g}{\sqrt{2}}\left(\ \frac{m_b}{M_W}\tan\beta\,\frac{1+\gamma_5}{2} + \frac{m_t}{M_W}\cot\beta\,\frac{1-\gamma_5}{2}\right) V_{tb}\ .
\end{aligned} \tag{268}$$

The couplings for the other fermions are given by analogous expressions. For example, the coupling for the τ may be obtained by substituting $m_t \to 0,\ \ m_b \to m_\tau$.

For the contributions from the diagrams Fig. 46a, using Eqs. (261,262) for $M = m_\mu$ and $M_0 = m_h, m_A$ and coupling $f^2 = \sqrt{2} G_\mu m_\mu^2 \tan^2\beta$ we obtain, assuming $m_h, m_A \gg m_\mu$

$$\begin{aligned}
a_\mu^{(2)\,\mathrm{2HDM}}(h) &\simeq \frac{\sqrt{2} G_\mu m_\mu^2}{4\pi^2}\,\tan^2\beta\,\frac{m_\mu^2}{m_h^2}\,\left(\ln\frac{m_h^2}{m_\mu^2} - \frac{7}{6}\right) > 0\ ,\\
a_\mu^{(2)\,\mathrm{2HDM}}(A) &\simeq \frac{\sqrt{2} G_\mu m_\mu^2}{4\pi^2}\,\tan^2\beta\,\frac{m_\mu^2}{m_A^2}\,\left(-\ln\frac{m_A^2}{m_\mu^2} + \frac{11}{6}\right) < 0\ .
\end{aligned} \tag{269}$$

At 2–loops the Barr–Zee diagram Fig. 46b yields an enhanced contribution, which can exceed the 1–loop result. The enhancement factor m_b^2/m_μ^2 actually compensates the suppression by α/π as $(\alpha/\pi)\times(m_b^2/m_\mu^2) \sim 4 > 1$

$$a_\mu^{(4)\,\mathrm{2HDM}}(h,A) = \frac{\sqrt{2} G_\mu\, m_\mu^2}{16\pi^2}\,\frac{\alpha}{\pi}\,4\,\tan^2\beta\,\sum_{i=h,A;f} N_{cf} Q_f^2\, F_i(z_{if}), \tag{270}$$

with $z_{if} = m_f^2/m_i^2$ $(i = h, A)$ and

$$\begin{aligned}
F_h(z) &= z\int_0^1 \mathrm{d}x\,\frac{2x(1-x)-1}{x(1-x)-z}\,\ln\frac{x(1-x)}{z} \;=\; -2z(\ln z + 2) + (2z-1)\,F_A(z),\\
F_A(z) &= \int_0^1 \mathrm{d}x\,\frac{z}{x(1-x)-z}\,\ln\frac{x(1-x)}{z} \;=\; \frac{2z}{y}\left\{\mathrm{Li}_2\left(1-\frac{1-y}{2z}\right) - \mathrm{Li}_2\left(1-\frac{1+y}{2z}\right)\right\},
\end{aligned} \tag{271}$$

with $y = \sqrt{1-4z}$. The non–observation of processes like $\Upsilon \to H + \gamma$ sets stringent lower bounds on the scalar masses. Together with the LEP bounds this prevents large 2HDM contribution to a_μ. As an illustration we present values for $\tan\beta = 10[40]$, $m_h = 100$ GeV and $m_A = 100[300]$ GeV in units of 10^{-11}:

$(m_h, m_A, \tan\beta)$	$a_\mu^{(2)}(h)$	$a_\mu^{(2)}(A)$	$a_\mu^{(4)}(h)$	$a_\mu^{(4)}(A)$	sum
$(100, 100, 10)$	0.65	-0.62	-2.31	2.88	0.61
$(100, 100, 40)$	10.45	-9.89	-36.90	46.09	9.74
$(100, 300, 10)$	0.65	-0.08	-2.31	0.55	-1.18
$(100, 300, 40)$	10.45	-1.30	-36.90	8.85	-18.90

If $m_A \sim m_h$ the contributions largely cancel. Assuming m_h to be in the 100 GeV region, to get a large $m_A - m_h$ mass splitting requires a large m_A, which however yields a large contribution of the disfavored negative sign. This means that the muon $g-2$ constraint gives a bound on m_A which, however, strongly depends on $\tan\beta$ (see e.g. [342]–[346] for a more detailed discussion). Besides the dominant 2-loop contributions form Fig. 46b a 2–loop calculation of the 2HDM contributions, including diagrams like Figs. 46c,d, within the context of the MSSM has been presented in [315]. If one identifies m_h with m_H of the SM the correction is found to be small: $a_\mu^{\rm bos,2L}(\text{MSSM} - \text{SM}) < 3 \times 10^{-11}$ in the parameter range $m_A \gtrsim 50$ GeV and $\tan\beta \lesssim 50$. In fact, in the LL approximation, the 2HDM sector in the MSSM at 2–loops does not change the SM result. The reason is that at the 1–loop level the electroweak SM result numerically remains practically unchanged, because the additional 2HDM diagrams all are suppressed by the small Yukawa coupling of the μ (like the SM Higgs contribution).

7.2.4. *Supersymmetry*

The most promising theoretical scenarios for new physics are supersymmetric extensions of the SM, in particular the minimal supersymmetric Standard Model. This "minimal" extension of the SM, which doubles the particle spectrum of the SM equipped with an additional Higgs doublet, is the natural possibility to solve the Higgs hierarchy problem of the SM. It predicts a low lying Higgs close to the current experimental bound and allows for a GUT extension where $G_{\rm GUT}$ is broken to $G_{\rm SM}$ at a low scale, in the phenomenologically interesting region around 1 TeV.

Supersymmetry implements a symmetry mapping

$$\text{boson} \overset{\rm Q}{\leftrightarrow} \text{fermion}$$

between bosons and fermions, by changing the spin by $\pm 1/2$ units [347]. The SUSY algebra [graded Lie algebra] $\left\{Q_\alpha, \overline{Q}_\beta\right\} = -2\,(\gamma^\mu)_{\alpha\beta}\,P_\mu\,;\; P_\mu = (H, \vec{P})$, P_μ the generators of space–time translations, Q_α four component Majorana (neutral) spinors and $\overline{Q}_\alpha = \left(Q^+\gamma^0\right)_\alpha$ the Pauli adjoint, is the only possible non–trivial unification of internal and space–time symmetry in a quantum field theory. The Dirac matrices in the Majorana representation play the role of the structure constants. The SUSY extension of the SM associates with each SM state X a supersymmetric "sstate" $\tilde{X}$ where sfermions are bosons and sbosons are fermions. The superpartners for leptons, quarks, gauge and Higgs bosons are called sleptons, squarks, gauginos and higgsinos, respectively. In addition there must be at least one extra Higgs doublet which also has its SUSY partners. Thus it is the 2HDM (II) extension of the SM which is subject to global supersymmetrization. The minimal SUSY extension of the SM assumes that the SM is "completed" by adding Majorana fermions and scalars, with no new spin 1 bosons and no new Dirac fermions.

We restrict ourselves to a discussion of the MSSM which usually is thought as a renormalizable low energy effective theory emerging from a supergravity (SUGRA) model which is obtained upon gauging global SUSY. SUGRA must include the spin 2 graviton and its superpartner, the spin 3/2 gravitino. Such a QFT is necessarily non–renormalizable [348]. Nevertheless, it is attractive to consider the MSSM as a low energy effective theory of a non–renormalizable SUGRA scenario with $M_{\rm Planck} \to \infty$ [349]. SUSY is spontaneously broken in the hidden sector by fields with no $SU(3)_c \otimes SU(2)_L \otimes U(1)_Y$ quantum numbers and which couple to the observable sector only gravitationally. $M_{\rm SUSY}$ denotes the SUSY breaking scale and the gravitino acquires a mass

$$m_{3/2} \sim M_{\rm SUSY}^2 / M_{\rm Planck}$$

with $M_{\rm Planck}$ the inherent scale of gravity.

SUSY is not realized as a perfect symmetry in nature. SUSY partners of the known SM particles have not yet been observed because sparticles in general are heavier than the known particles. Like in the SM, where the local gauge symmetry is broken by the Higgs mechanism, SUGRA is broken at some higher scale $M_{\rm SUSY}$ by a super–Higgs mechanism. The Lagrangian exhibits global supersymmetry softly broken at a scale $M_{\rm SUSY}$ commonly taken to coincide with the "new physics scale" $\Lambda_{\rm NP} \simeq 1$ TeV, where the SM is expected to loose its validity. If one assumes the sparticles all to have masses below $M_{\rm SUSY}$, then relatively light sparticles around 100 GeV are expected in the spectrum. The MSSM scenario is characterized by the following features:

– the gauge group is the SM gauge group with couplings $g_1 = e/\cos\Theta_W$, $g_2 = e/\sin\Theta_W$ and $g_3 = \sqrt{4\pi\alpha_s}$ and no new heavy gauge bosons besides the W and Z exist;
– there are no new matter fields besides the quarks and leptons and two Higgs doublets which are needed to provide supersymmetric masses to quarks and leptons;
– it follows that gauge- and Yukawa-couplings of the sparticles are all fixed by supersymmetry in terms of the SM couplings;
– in spite of some constraints, masses and mixings of the sparticles remain quite arbitrary.

In general, SUSY extensions of the SM lead to Flavor Changing Neutral Currents (FCNC) and un-suppressed CP–violation, which are absent or small, respectively, in the SM and known to be suppressed in nature. Therefore one assumes that

– flavor- and CP-violation is as in the SM, namely coming from the (now supersymmetrized) Yukawa couplings only.

This implies that at some grand unification scale M_X there is a universal mass term for all scalars as well as a universal gaugino mass term, i. e. the SUSY-breaking Majorana masses of the gauginos are equal at M_X. Note that an elegant way to get rid of the mentioned problems is to impose that

– R-parity, even for particles, odd for sparticles, is conserved.

This is a strong assumption implying that sparticles must be produced in pairs and that there exists an absolutely stable *lightest supersymmetric particle* (LSP), the lightest neutralino. Thus all sparticles at the end decay into the LSP plus normal matter. The LSP is a Cold Dark Matter (CDM) candidate [350] if it is neutral and colorless. From the precision mapping of the anisotropies in the cosmic microwave background, the Wilkinson Microwave Anisotropy Probe (WMAP) collaboration has determined the relic density of cold dark matter to [351]

$$\Omega_{\rm CDM}{\rm h}^2 = 0.1126 \pm 0.0081 \; . \tag{272}$$

This sets severe constraints on the SUSY parameter space [352,353,354] and defines the constrained MSSM (CMSSM) scenario (see also [355]). Note that SUSY in general is providing a new source for CP–violation which could help in understanding the matter–antimatter asymmetry $n_B = (n_b - n_{\bar b})/n_\gamma \simeq 6 \times 10^{-10}$ present in our cosmos. Low energy precision tests of supersymmetry and present experimental constraints are reviewed and discussed in [356]. For a topical review on supersymmetry, the different symmetry breaking scenarios and the muon magnetic moment see [357].

A question is: what should cause R–parity to be conserved? It just means that certain couplings one usually would assume to be there are excluded. If R is not conserved, sparticles may be produced singly and the LSP is not stable and would not provide a possible explanation of CDM. Mechanisms which mimic approximate R–parity conservation are known and usually based on a supersymmetric Froggatt-Nielsen model which assumes a spontaneously broken horizontal local $U(1)_X$ symmetry [358,359,360,361,362,363,364,365].

The SUGRA scenario leads to universal masses for all SUSY partners:

– s–matter: $m_{\tilde q} = m_{\tilde \ell} = m_{\tilde H} = m_{1/2} \sim m_{3/2}$
– gauginos: $M_3 = M_2 = M_1 = m_0 \sim m_{3/2}$

where M_3, M_2 and M_1 are the mass scales of the spartners of the gauge bosons in $SU(3)_c$, $SU(2)_L$ and $U(1)_Y$, respectively. The non–observation of any sparticles so far requires a mass bound of about $m_{3/2} \sim 100 \div 1000$ GeV , which is of the order of the weak scale 246 GeV.

In general one expects different masses for the different types of gauginos:

– M' the $U(1)_Y$ gaugino mass ,

– M the $SU(2)_L$ gaugino mass ,
– $m_{\tilde{g}}$ the $SU(3)_c$ gluino mass .
However, the grand unification assumption

$$M' = \frac{5}{3}\tan^2\Theta_W\, M \;= \frac{5}{3}\frac{\alpha}{\cos^2\Theta_W\,\alpha_s}\, m_{\tilde{g}}$$

leads back to the minimal SUGRA (mSUGRA) scenario [42] . A very attractive feature of this scenario is the fact that the known SM Yukawa couplings now may be understood by evolving couplings from the GUT scale down to low energy by the corresponding RG equations. This also implies the form of the muon Yukawa coupling $y_\mu \propto \tan\beta$, as

$$y_\mu = \frac{m_\mu}{v_1} = \frac{m_\mu\, g_2}{\sqrt{2} M_W\, \cos\beta} \tag{273}$$

where $1/\cos\beta \approx \tan\beta$. This enhanced coupling is central for the discussion of the SUSY contributions to a_μ. In spite of the fact that SUSY and GUT extensions of the SM have completely different motivations and in a way are complementary, supersymmetrizing a GUT is very popular as it allows coupling constant unification together with a low SUSY breaking scale which promises nearby new physics. Actually, supersymmetric $SU(5)$ circumvents the problems of the normal $SU(5)$ GUT and provides a viable phenomenological framework. The extra GUT symmetry requirement is attractive also because it reduces the number of independent parameters.

While supersymmetrizing the SM fixes all gauge and Yukawa couplings of the sparticles, there are a lot of free parameters to fix the SUSY breaking and masses, such that mixings of the sparticles remain quite arbitrary: the mass eigenstates of the gaugino–Higgsino sector are obtained by unitary transformations which mix states with the same conserved quantum numbers (in particular the charge):

$$\chi_i^+ = V_{ij}\psi_j^+ \;,\; \chi_i^- = U_{ij}\psi_j^- \;,\; \chi_i^0 = N_{ij}\psi_j^0 \tag{274}$$

where ψ_j^a denote the spin 1/2 sparticles of the SM gauge bosons and the two Higgs doublets. In fact, a SUSY extension of the SM in general exhibits more than 100 parameters, while the SM has 28 (including neutrino masses and mixings).

The main theoretical motivation for a supersymmetric extension of the SM is the **hierarchy** or **naturalness** problem. In the SM the Higgs mass is the only mass which is not protected by a symmetry, which implies the existence of quadratic divergences in the Higgs self–energy [43] . If we assume that, like in the SM, the Higgs boson is not a (quasi-) Goldstone boson, then the only known symmetry which requires this scalar particle to be massless in the symmetry limit is supersymmetry [44] . Simply because a scalar is now always a supersymmetric partner of a fermion which is required to be massless by chiral symmetry. Thus only in a supersymmetric theory it is natural to have a "light" Higgs, in fact in a SUSY extension of the SM, the lightest scalar h^0, which corresponds to the SM Higgs, is bounded to have mass $m_{h^0} \leq M_Z$ at tree level. This bound receives large radiative corrections from the $t/\tilde{t}$ sector, which changes the upper bound to [367]

$$m_{h^0} \leq \left(1 + \frac{\sqrt{2}G_\mu}{2\pi^2\,\sin^2\beta}\, 3m_t^4\, \ln\left(\frac{m_{\tilde{t}_1}\, m_{\tilde{t}_2}}{m_t^2}\right) + \cdots\right) M_Z \tag{275}$$

which in any case is well below 200 GeV. For an improved bound obtained by including the 2–loop corrections we refer to [368].

[42] The difference between CMSSM and mSUGRA is that in the latter one fixes the Higgsino mixing mass parameter μ by demanding a radiative breaking of the EW symmetry.
[43] In the SM the quadratic divergence in the Higgs mass counterterm at 1–loop is $\delta m_H^2 \sim 6(\Lambda/v)^2(m_H^2 + M_Z^2 + 2M_W^2 - 4m_f^2)$ and is absent if the Higgs mass is tuned to $m_H \simeq (4(m_t^2 + m_b^2) - M_Z^2 - 2M_W^2)^{1/2} \sim 318$ GeV [366], which can be considered to be ruled out by experiment.
[44] Other "solutions" of the hierarchy problem are the little Higgs models, in which the Higgs is a quasi-Goldstone boson which attains its mass through radiative corrections, and the extra dimension scenarios where the effective cut–off can be low (see below).

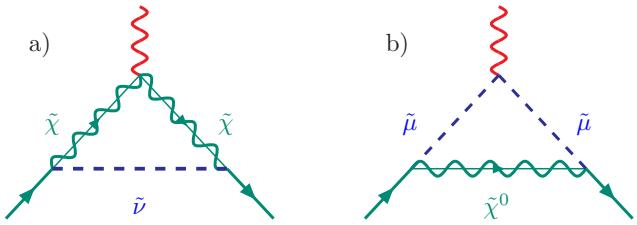

Fig. 47. Leading SUSY contributions to $g-2$ in supersymmetric extension of the SM. Diagrams a) and b) correspond to diagrams a) and b) of Fig. 42, respectively.

It is worthwhile to mention that in an exactly supersymmetric theory the anomalous magnetic moment must vanish, as observed by Ferrara and Remiddi in 1974 [369]:

$$a_\mu^{\rm tot} = a_\mu^{\rm SM} + a_\mu^{\rm SUSY} = 0 \; .$$

Thus, since $a_\mu^{\rm SM} > 0$, in the SUSY limit, in the unbroken theory, we must have

$$a_\mu^{\rm SUSY} < 0 \; .$$

However, we know that SUSY must be drastically broken. All super–partners of existing particles seem to be too heavy to be produced up to now. If SUSY is broken a_μ may have either sign. In fact, the 3 standard deviation $(g_\mu - 2)$–discrepancy requires $a_\mu^{\rm SUSY} > 0$, of the same sign as the SM contribution and of at least the size of the weak contribution [$\sim 200 \times 10^{-11}$] (see Fig. 41).

The leading SUSY contributions, like the weak SM contributions, are due to one–loop diagrams. Most interesting are the ones which get enhanced for large $\tan\beta$. Such supersymmetric contributions to a_μ stem from sneutrino–chargino and smuon–neutralino loops, see Fig. 47, and yield [45]

$$a_\mu^{{\rm SUSY}\,(1)} = a_\mu^{\chi^\pm} + a_\mu^{\chi^0} \; , \tag{276}$$

$$a_\mu^{\chi^\pm} = \frac{g_2^2}{32\pi^2} \, \frac{m_\mu^2}{M_{\rm SUSY}^2} \, {\rm sign}(\mu M_2) \, \tan\beta \left[1 + O(\frac{1}{\tan\beta}, \frac{M_W}{M_{\rm SUSY}}) \right] \; , \tag{277}$$

$$a_\mu^{\chi^0} = \frac{g_1^2 - g_2^2}{192\pi^2} \, \frac{m_\mu^2}{M_{\rm SUSY}^2} \, {\rm sign}(\mu M_2) \, \tan\beta \left[1 + O(\frac{1}{\tan\beta}, \frac{M_W}{M_{\rm SUSY}}) \right] \; , \tag{278}$$

where as usual we expanded in $1/\tan\beta$ and in $M_W/M_{\rm SUSY}$ because we expect that SUSY partners of SM particles are heavier. Parameters have been taken to be real and M_1 and M_2 of the same sign [46] . The couplings g_1 and g_2 denote the $U(1)_Y$ and $SU(2)_L$ gauge couplings, respectively, and y_μ is the muon's Yukawa coupling Eq. (273). The interesting aspect of the SUSY contribution to a_μ is that they are enhanced for large $\tan\beta$ in contrast to SUSY contributions to electroweak precision observables, which mainly affect $\Delta\rho$

[45] The precise result may be easily obtained from the generic 1-loop results of Sect. 7.2.1 with the appropriate choice of couplings (see Eq. (274)). One obtains [370,371]

$$a_\mu^{\chi^\pm} = \frac{m_\mu}{16\pi^2} \sum_k \left\{ \frac{m_\mu}{12 m^2_{\tilde{\nu}_\mu}} (|c_k^L|^2 + |c_k^R|^2) \, F_1^C(x_k) + \frac{m_{\chi_k^\pm}}{3 m^2_{\tilde{\nu}_\mu}} {\rm Re}\,[c_k^L c_k^R] \, F_2^C(x_k) \right\} \; ,$$

$$a_\mu^{\chi^0} = \frac{m_\mu}{16\pi^2} \sum_{i,m} \left\{ -\frac{m_\mu}{12 m^2_{\tilde{\mu}_m}} (|n_{im}^L|^2 + |n_{im}^R|^2) \, F_1^N(x_{im}) + \frac{m_{\chi_i^0}}{3 m^2_{\tilde{\mu}_m}} {\rm Re}\,[n_{im}^L n_{im}^R] \, F_2^N(x_{im}) \right\} \; ,$$

where $k = 1, 3$ and $i = 1, ..., 4$ denote the chargino and neutralino indices, $m = 1, 2$ is the smuon index, and the couplings are given by $c_k^L = -g_2 \, V_{k1}$, $c_k^R = y_\mu \, U_{k2}$, $n_{im}^L = \frac{1}{\sqrt{2}} \, (g_1 N_{i1} + g_2 N_{i2}) \, U_{m1}^{\tilde{\mu}\,*} - y_\mu N_{i3} \, U_{m2}^{\tilde{\mu}\,*}$ and $n_{im}^R = \sqrt{2}\, g_1 N_{i1} \, U_{m2}^{\tilde{\mu}} + y_\mu N_{i3} \, U_{m1}^{\tilde{\mu}}$. The kinematical variables are the mass ratios $x_k = m^2_{\chi_k^\pm}/m^2_{\tilde{\nu}_\mu}$, $x_{im} = m^2_{\chi_i^0}/m^2_{\tilde{\mu}_m}$, and the one–loop vertex functions are given in Eqs. (263) and (266).

[46] In the MSSM the parameters $\mu \, A_f$ and $\mu M_{1,2,3}$ in general are complex. However, not all phases are observable. In particular, one may assume M_2 to be real and positive without loss of generality.

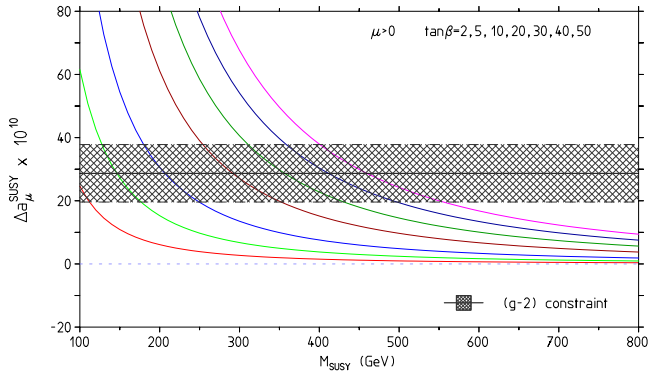

Fig. 48. Constraint on large tanβ SUSY contributions as a function of $M_{\rm SUSY}$.

which determines the ρ–parameter and contributes to $M_W = M_W(\alpha, G_\mu, M_Z, \cdots)$. The anomalous magnetic moment thus may be used to constrain the SUSY parameter space in a specific way. Altogether one obtains

$$a_\mu^{\rm SUSY} \simeq \frac{\mathrm{sign}(\mu M_2)\,\alpha(M_Z)}{8\pi \sin^2\Theta_W}\,\frac{\left(5+\tan^2\Theta_W\right)}{6}\,\frac{m_\mu^2}{M_{\rm SUSY}^2}\,\tan\beta\left(1-\frac{4\alpha}{\pi}\ln\frac{M_{\rm SUSY}}{m_\mu}\right) \tag{279}$$

with $M_{\rm SUSY}$ a typical SUSY loop mass and the sign is determined by the Higgsino mass term μ. Here we also included the leading 2–loop QED logarithm as an RG improvement factor [310], which amounts to parametrize the one-loop result in terms of the running $\alpha(M_{\rm SUSY})$. Note that $M_{\rm SUSY}$ in the logarithm is the mass of the lightest charged SUSY particle. In Fig. 48 contributions are shown for various values of $\tan\beta$. Above $\tan\beta \sim 5$ and $\mu > 0$ the SUSY contributions from the diagrams Fig. 47 easily could explain the observed deviation Eq. (257) with SUSY states of masses in the interesting range 100 to 500 GeV.

In the large $\tan\beta$ regime we have

$$\left|a_\mu^{\rm SUSY}\right| \simeq 123\times 10^{-11}\left(\frac{100\ \mathrm{GeV}}{M_{\rm SUSY}}\right)^2\tan\beta\ . \tag{280}$$

$a_\mu^{\rm SUSY}$ generally has the same sign as the μ–parameter. The deviation Eq. (257) requires positive sign(μ) and if identified as a SUSY contribution

$$M_{\rm SUSY} \simeq (65.5\ \mathrm{GeV})\sqrt{\tan\beta}\ . \tag{281}$$

Negative μ models give the opposite sign contribution to a_μ and are strongly disfavored. For $\tan\beta$ in the range $2 \sim 40$ one obtains

$$M_{\rm SUSY} \simeq 93 - 414\ \mathrm{GeV}\ , \tag{282}$$

precisely the range where SUSY particles are often expected. For a more elaborate discussion and further references we refer to [27,357].

A remarkable 2–loop calculation within the MSSM has been performed by Heinemeyer, Stöckinger and Weiglein [372,315]. They evaluated the exact 2–loop correction of the SM 1–loop contributions Figs. 8 and 37. These are all diagrams where the μ–lepton number is carried only by μ and/or ν_μ. In other words SM diagrams with an additional insertion of a closed sfermion– or charginos/neutralino–loop. These are diagrams like the electroweak ones Fig. 38 with the SM fermion–loops replaced by closed $\tilde\chi$–loops plus diagrams obtained be replacing $W^\pm$ with $H^\pm$. Thus the full 2–loop result from the class of diagrams with closed sparticle loops is known. This class of SUSY contributions is interesting because it has a parameter dependence completely different from the one of the leading SUSY contribution and can be large in regions of parameter space where the 1–loop contribution is small. The second class of corrections are the 2–loop corrections to the SUSY 1–loop diagrams Fig. 47, where the μ–lepton number is carried also by $\tilde\mu$ and/or $\tilde\nu_\mu$. This class of corrections is expected to have the same parameter dependence as the leading SUSY 1–loop

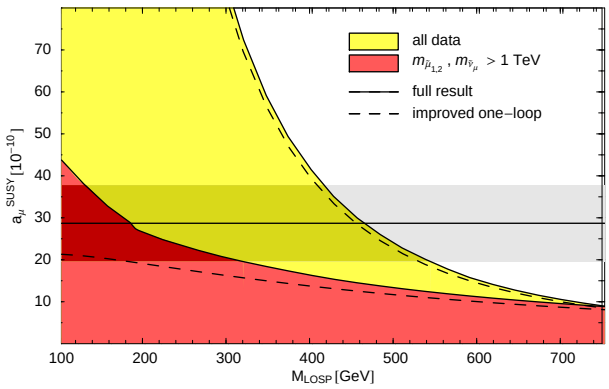

Fig. 49. Allowed values of MSSM contributions to a_μ as a function of the mass of the Lightest Observable SUSY Particle $M_{\rm LOSP}$, from an MSSM parameter scan with $\tan\beta = 50$. The 3σ region corresponding to the deviation (257) is indicated as a horizontal band. The light gray region corresponds to all input parameter points that satisfy the experimental constraints from b–decays, m_h and $\Delta\rho$. In the middle gray region, smuons and sneutrinos are heavier than 1 TeV. The dashed lines correspond to the contours that arise from ignoring the 2–loop corrections from chargino/neutralino– and sfermion–loop diagrams. Courtesy of D. Stöckinger [357].

ones and only the leading 2–loop QED corrections are known [310] as already included in Eq. (279). Results which illustrate our brief discussion are shown in Fig. 49. The contributions of the 2HDM sector of the MSSM have been discussed earlier in Sect. 7.2.3.

The results for the SUSY contributions to a_μ up to the two-loops is given by [357] [47]

$$a_\mu^{\rm SUSY} = a_\mu^{\rm SUSY,1L}\left(1 - \frac{4\alpha}{\pi}\log\frac{M_{\rm SUSY}}{m_\mu}\right) + a_\mu^{(\chi\gamma H)} + a_\mu^{(\tilde f\gamma H)} + a_\mu^{(\chi\{W,Z\}H)} + a_\mu^{(\tilde f\{W,Z\}H)} + a_\mu^{\rm SUSY,ferm,2L} + a_\mu^{\rm SUSY,bos,2L} + \dots\,. \tag{283}$$

The labels $(\chi\gamma H)$ etc identify contributions from Fig. 46b type diagrams which would be labeled by $(\tau h\gamma)$, with possible replacements $\gamma \to V = \gamma, Z, W^\pm$, $h \to H = h, H, A, H^\pm$ and $\tau^\mp \to X = \chi^\mp, \chi^0, \tilde f$. Contributions (XVV) correspond to Fig. 38a,d with corresponding substitutions. The remaining terms $a_\mu^{\rm SUSY,ferm,2L}$ and $a_\mu^{\rm SUSY,bos,2L}$ denote small terms like the fermionic contribution Fig. 46b and the bosonic contributions Figs. 46c,d, which differ from the SM result due to the modified Higgs structure. The ellipsis denote the known but negligible 2–loop contributions as well as the missing 2–loop and higher order contributions.

[47] All leading terms come from Barr-Zee type diagrams. In terms of the functions Eq. (271) the results read [340,341,373,374,375]

$$a_\mu^{(\chi\gamma H)} = \frac{\sqrt{2}G_\mu m_\mu^2}{8\pi^2}\,\frac{\alpha}{\pi}\sum_{k=1,2}\left[\,{\rm Re}\,[\lambda_\mu^A\lambda^A_{\chi_k^+}]\,F_A(m^2_{\chi_k^+}/m_A^2) + \sum_{S=h,H}{\rm Re}\,[\lambda_\mu^S\lambda^S_{\chi_k^+}]\,F_h(m^2_{\chi_k^+}/m_S^2)\right],$$

$$a_\mu^{(\tilde f\gamma H)} = \frac{\sqrt{2}G_\mu m_\mu^2}{8\pi^2}\,\frac{\alpha}{\pi}\sum_{\tilde f=\tilde t,\tilde b,\tilde\tau}\sum_{i=1,2}\left[\sum_{S=h,H}(N_cQ^2)_{\tilde f}\,{\rm Re}\,[\lambda_\mu^S\lambda^S_{\tilde f_i}]\,F_{\tilde f}(m^2_{\tilde f_i}/m_S^2)\right],$$

with $F_{\tilde f}(z) = z\,(2 + \ln z - F_A(z))/2$ and couplings (see Eqs. (268, 274))

$$\lambda_\mu^{h,H,A} = (-\sin\alpha/\cos\beta, \cos\alpha/\cos\beta, \tan\beta)\,,$$
$$\lambda^{h,H,A}_{\chi_k^+} = \sqrt{2}M_W/m_{\chi_k^+}\,(U_{k1}V_{k2}\,(\cos\alpha, \sin\alpha, -\cos\beta) + U_{k2}V_{k1}(-\sin\alpha, \cos\alpha, -\sin\beta))\,,$$
$$\lambda^{h,H}_{\tilde\tau_i} = 2m_\tau/(m^2_{\tilde\tau_i}\cos\beta)\,(-\mu^*\,(\cos\alpha, \sin\alpha) + A_\tau\,(-\sin\alpha, \cos\alpha))\,(U^{\tilde\tau_{i1}})^*U^{\tilde\tau_{i2}}\,.$$

The last expression given for the $\tilde\tau$ applies to the $\tilde b$ with $\tau \to b$ everywhere, and for the $\tilde t$ with $\tau \to t$ together with $(\mu, \cos\beta, \cos\alpha, \sin\alpha) \to (-\mu, \sin\beta, \sin\alpha, -\cos\alpha)$.

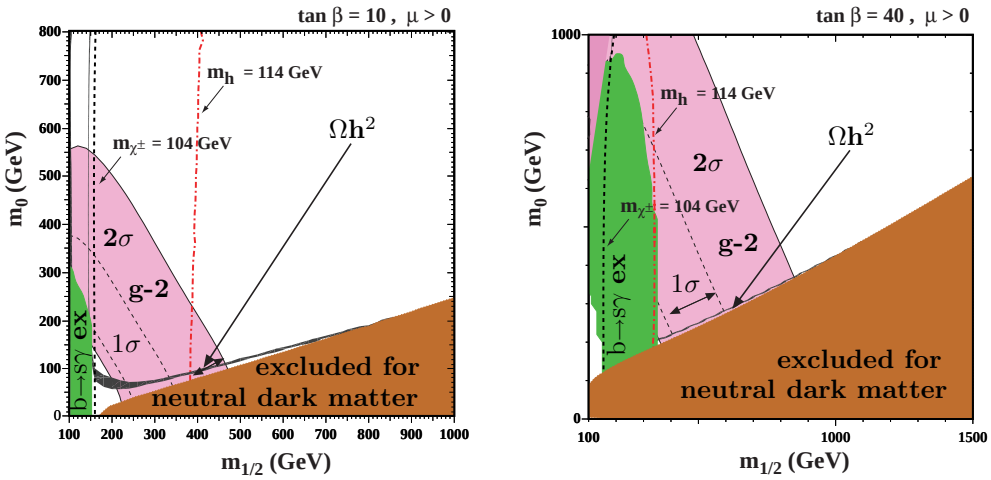

Fig. 50. The $(m_0, m_{1/2})$ plane for $\mu > 0$ for (a) $\tan\beta = 10$ and (b) $\tan\beta = 40$ in the constrained MSSM scenario (which includes mSUGRA). The allowed region by the cosmological neutral dark matter constraint Eq. (272) is shown by the black parabolic shaped region. The disallowed region where $m_{\tilde{\tau}_1} < m_\chi$ has dark shading. The regions excluded by $b \to s\gamma$ have medium shading (left). The $g_\mu - 2$ favored region at the 2 σ $[(290 \pm 180) \times 10^{-11}]$ (between dashed lines the 1 σ $[(290 \pm 90) \times 10^{-11}]$ band) level has medium shading. The LEP constraint on $m_{\chi^\pm} = 104$ GeV and $m_h = 114$ GeV are shown as near vertical lines. Plot courtesy of K. Olive updated from [352].

For the potentially enhanced Barr-Zee type contributions the following simple approximations have been given [372,315,357]:

$$a_\mu^{(\chi VH)} \approx \quad 11 \times 10^{-10} \left(\frac{\tan\beta}{50}\right) \left(\frac{100\ \text{GeV}}{M_{\text{SUSY}}}\right)^2 \ \text{sign}(\mu M_2), \tag{284}$$

$$a_\mu^{(\tilde{t}\gamma H)} \approx -13 \times 10^{-10} \left(\frac{\tan\beta}{50}\right) \left(\frac{m_t}{m_{\tilde{t}}}\right) \left(\frac{\mu}{20 M_H}\right) \ \text{sign}(X_t), \tag{285}$$

$$a_\mu^{(\tilde{b}\gamma H)} \approx -3.2 \times 10^{-10} \left(\frac{\tan\beta}{50}\right) \left(\frac{m_b \tan\beta}{m_{\tilde{b}}}\right) \left(\frac{A_b}{20 M_H}\right) \ \text{sign}(\mu)\ . \tag{286}$$

The parameter X_t is determined by the SUSY breaking parameter A_f, μ and $\tan\beta$ by $X_t = A_t - \mu^* \cot\beta$. Like for the leading 1–loop case, the first approximation applies if all SUSY masses are approximately equal (e.g. $\mu \sim M_2 \sim m_A$) (but the relevant masses are different in the two cases), and the second and third are valid if the stop/sbottom mixing is large and the relevant stop/sbottom and Higgs masses are of similar size. We refer to the review by Stöckinger [357] for a more detailed presentation of the higher order SUSY effects.

In comparison to $g_\mu - 2$, the SM prediction of M_W [376], as well as of other electroweak observables, as a function of m_t for given α, G_μ and M_Z, is in much better agreement with the experimental result (1 σ), although the MSSM prediction for suitably chosen MSSM parameters is slightly favored by the data [377]. Thus large extra corrections to the ones of the SM are not tolerated. The leading radiative shift of M_W by SUSY contributions enters via $\Delta\rho$. As we know, $\Delta\rho$ is most sensitive to weak isospin splitting and in the SM is dominated by the contribution from the (t, b)–doublet. In the SUSY extension of the SM these effects are enhanced by the contributions from the four SUSY partners $\tilde{t}_{\text{L,R}}, \tilde{b}_{\text{L,R}}$ of t, b, which can be as large as the SM contribution itself for $m_{1/2} \ll m_t$ [light SUSY], and tends to zero for $m_{1/2} \gg m_t$ [heavy SUSY]. It is important to note that these contributions are not enhanced by $\tan\beta$. Thus, provided $\tan\beta$ enhancement is at work, it is quite natural to get a larger SUSY contribution to $g_\mu - 2$ than to M_W, otherwise some tension between the two constraints would be there as M_W prefers the heavy SUSY domain.

Assuming the very restricted CMSSM scenario, besides the direct limits from LEP and Tevatron, presently, the most important constraints come from $(g-2)_\mu$, $b \to s\gamma$ and from the dark matter relic density (cosmo-

logical bound on CDM) given in Eq. (272) [352,353]. Due to the precise value of $\Omega_{\rm CDM}$, the lightest SUSY fermion (sboson) of mass m_0 is given as a function of the lightest SUSY boson (sfermion) with mass $m_{1/2}$ within a narrow band. In fact only a part of the relic cold dark matter need be neutralinos, such that $\Omega_{\rm CDM}$ is an upper bound only. This is illustrated in Fig. 50 together with the constraints from $g_\mu - 2$ Eq. (257) and $b \to s\gamma$. Since m_h for given $\tan\beta$ is fixed by $m_{1/2}$ via Eq. (275) with $\min(m_{\tilde{t}_i}; i = 1, 2) \sim m_{1/2}$, the allowed region is to the right of the (almost vertical) line $m_h = 114$ GeV which is the direct LEP bound. Again there is an interesting tension between the SM like lightest SUSY Higgs mass m_h which in case the Higgs mass goes up from the present limit to higher values requires heavier sfermion masses and/or lower $\tan\beta$, while a_μ prefers light sfermions and large $\tan\beta$. Another lower bound from LEP is the line characterizing $m_{\chi^\pm} > 104$ GeV. The CDM bound gives a narrow hyperbola like shaped band. The cosmology bound is harder to see in the $\tan\beta = 40$ plot, but it is the strip up the $\chi - \tilde{\tau}$ degeneracy line, the border of the excluded region (dark) which would correspond to a charged LSP which is not allowed. The small shaded region in the upper left is excluded due to no electroweak symmetry breaking (EWSB) there. The latter must be tuned to reproduce the correct value for M_Z. The $\tan\beta = 40$ case is much more favorable, since $g_\mu - 2$ selects the part of the WMAP strip which has a Higgs above the LEP bound. Within the CMSSM the discovery of the Higgs and the determination of its mass would essentially fix m_0 and $m_{1/2}$.

Since the SM prediction [378] for the $b \to s\gamma$ rate $\mathrm{BR}(b \to s\gamma) = (3.15 \pm 0.23) \times 10^{-4}$ is in good agreement with the experimental value, only small extra radiative corrections are allowed (1.5 σ). In SUSY extensions of the SM [379], this excludes light $m_{1/2}$ and m_0 from light to larger values depending on $\tan\beta$. Ref. [378] also illustrates the updated $b \to s\gamma$ bounds on M_{H^+} (> 295 GeV for $2 \leq \tan\beta$) in the 2DHM (Type II) [380].

It is truly remarkable that in spite of the different highly non–trivial dependencies on the MSSM parameters, with $g - 2$ favoring definitely $\mu > 0$, $\tan\beta$ large and/or light SUSY states, there is a common allowed range, although a quite narrow one, depending strongly on $\tan\beta$.

In general less constrained versions of the MSSM or other SUSY extensions of the SM (see e.g. [381]) are much harder to pin down or even to disprove. Certainly, the muon $g - 2$ plays an important role for the upcoming LHC searches. Note that the 3 σ deviation (if real) requiring $\mathrm{sign}(\mu)$ positive and $\tan\beta$ preferably large, poses constraints which hardly can be obtained from a hadron collider. In any case, the muon $g - 2$ would yield important hints for constraining the SUSY parameter space, if SUSY would show up at the LHC.

7.2.5. *Little Higgs models*

The Higgs mass in the SM is not protected by any symmetry and turns out to be quadratically sensitive to the cutoff Λ. This leads to the well-known hierarchy or fine-tuning problem, in particular, if the SM is embedded in some grand unified theory or if gravity (and thus the Planck scale) enters.

Less known is the the so-called "little hierarchy problem" [382]. We can view the SM as an effective field theory (EFT) with a cutoff and parametrize new physics in terms of higher-dimensional operators which are suppressed by inverse powers of the cutoff Λ. Precision tests of the SM at low energies and at LEP/SLC point to a small Higgs mass of order 100 GeV and have not shown any significant deviations from the SM. This in turn translates into a cutoff of about $\Lambda \sim 5 - 10$ TeV which is slightly more than an order of magnitude above the electroweak scale and thus requires fine-tuning at the percent level only.

An attractive set of solutions to this little hierarchy problem are the little Higgs models [383,384]. In these models, the Higgs boson is a pseudo-Goldstone boson of a global symmetry which is spontaneously broken at a scale f. This symmetry protects the Higgs mass from getting quadratic divergences at one loop, even in the presence of gauge and Yukawa interactions. The electroweak symmetry is broken via the Coleman-Weinberg mechanism [385] and the Higgs mass is generated radiatively, which leads naturally to a light Higgs boson $m_H \sim (g^2/4\pi)f \approx 100$ GeV, if the scale $f \sim 1$ TeV.[48] In contrast to supersymmetric theories, here the new states at the TeV-scale which cancel the quadratic divergences arising from the top quark, gauge boson and Higgs boson loops, respectively, have the same spin as the corresponding SM particles. The little Higgs model can then be interpreted as an EFT up to a new cutoff scale of $\Lambda \sim 4\pi f \sim 10$ TeV.

[48] If one implements the Coleman-Weinberg mechanism directly in the SM, the Higgs mass would be fixed at about 10 GeV [386] which as we know is ruled out by experiment.

Among the different versions of this approach, the littlest Higgs model [387] achieves the cancellation of quadratic divergences with a minimal number of new degrees of freedom. The global symmetry breaking pattern is $SU(5) \to SO(5)$ and an $[SU(2) \times U(1)]^2$ gauge symmetry is imposed, that is broken down at the scale f to the diagonal subgroup $SU(2)_L \times U(1)_Y$, which is identified with the SM gauge group. This leads to four heavy gauge bosons $A_H, W_H^{\pm}, Z_H$ with masses $\sim f$ in addition to the SM gauge fields. The SM Higgs doublet is part of an assortment of pseudo-Goldstone bosons which result from the spontaneous breaking of the global symmetry. The multiplet of Goldstone bosons contains a heavy $SU(2)$ complex triplet scalar Φ as well. Furthermore, a vector-like heavy quark that can mix with the top quark is postulated. It turns out, however, that electroweak precision data put very strong constraints on the littlest Higgs model. Typically one obtains the bound $f \gtrsim 3-5$ TeV in most of the natural parameter space, unless specific choices are made for fermion representations or hypercharges [388]. Since f effectively acts as a cutoff for loops with SM particles, this reintroduces a little hierarchy between the Higgs boson mass and the scale f.

These constraints from electroweak precision data can be bypassed by imposing a discrete symmetry in the model, called T-parity [389]. In the littlest Higgs model with T-parity (LHT) [390], this discrete symmetry maps the two pairs of gauge groups $SU(2)_i \times U(1)_i, i = 1, 2$ into each other, forcing the corresponding gauge couplings to be equal, with $g_1 = g_2$ and $g_1' = g_2'$. All SM particles, including the Higgs doublet, are even under T-parity, whereas the four additional heavy gauge bosons and the Higgs triplet are T-odd. The top quark has now two heavy fermionic partners, T_+ (T-even) and T_- (T-odd). For consistency of the model, one has to introduce additional heavy, T-odd vector-like fermions u_H^i, d_H^i, e_H^i and ν_H^i $(i = 1, 2, 3)$ for each SM quark and lepton field. For further details on the LHT, we refer the reader to Refs. [390,391,392,393].

In the LHT there are no tree-level corrections to electroweak precision observables and there is no dangerous Higgs triplet vev v' that violates the custodial symmetry of the SM grossly. This relaxes the constraints on the model from electroweak precision data and allows a relatively small value of f in certain regions of the parameter space. As shown in Refs. [392,394,395], a scale f as low as 500 GeV is compatible in the LHT with electroweak precision data. Furthermore, if T-parity is exact, the lightest T-odd particle, typically the heavy, neutral partner of the photon, A_H, is stable and can be a good dark matter candidate [391,394,396]. The LHT can thus serve as an attractive alternative to supersymmetric or extra-dimensional models.

a_μ in the Littlest Higgs model: The contribution to the muon $g-2$ in the Littlest Higgs model has been calculated in Refs. [397,398,399]. The relevant diagrams are of the generic type shown in Figs. 42c, 42d. Ref. [397] only considered the effect of loops containing the new heavy gauge bosons A_H, W_H and Z_H and found that even the contribution from the lightest of them, A_H, which could have a mass as low as 200 GeV, is very small. Typically, they obtain $a_\mu^{\rm LH} < 1 \times 10^{-11}$ in all of the allowed parameter space, assuming that the symmetry breaking scale fulfills $f > 1$ TeV. Soon afterwards it was, however, pointed out in Ref. [398] that this calculation was incomplete. In fact, the couplings of the ordinary SM gauge fields W and Z to SM fermions are modified in the Littlest Higgs model by factors $\left(1 + \mathcal{O}(v^2/f^2)\right)$ and thus lead to a modification of the usual one-loop SM electroweak contribution to the muon $g-2$. This leads in general to a bigger effect than loops involving new heavy particles. For instance, for $f = 1$ TeV, they obtain in some region of the allowed parameter space a contribution of about

$$a_\mu^{\rm LH} \sim 10 \times 10^{-11}, \tag{287}$$

i.e. a factor 10 larger than the value quoted above. Nevertheless, even this larger value cannot explain the observed discrepancy between the measured value and the SM prediction of $a_\mu^{\rm exp} - a_\mu^{\rm SM} = (290 \pm 90) \times 10^{-11}$ from Eq. (257). Furthermore, as mentioned above, electroweak precision data actually constrain the value of the symmetry breaking scale f to lie above $3-5$ TeV [388]. For such high values of f, the corrections to the W and Z couplings are much smaller and the contribution to a_μ becomes again tiny. In addition, for higher values of f, the new heavy particles also become heavier and thus their contribution in loops is even more suppressed.

In Ref. [399] a slightly modified version of the Littlest Higgs models was studied, which included lepton number violating terms. These terms which involve the complex Higgs triplet field Φ were first introduced in Ref. [400] to generate neutrino masses. The corresponding new Yukawa couplings Y_{ab}, where a, b denote different generations, and the vev v' of the Higgs triplet have to satisfy the relation $Y_{ab} v' \sim 10^{-10}$ GeV in order to lead to neutrino masses in the expected range. Assuming that v' is of the order of 10^{-10} GeV, which

requires, however, a substantial amount of (unnatural) fine-tuning, one could in principle have $Y_{ab} \sim \mathcal{O}(1)$. The contribution to the anomalous magnetic moment then reads, in the limit $m_\phi \gg m_i, i = e, \mu, \tau$,

$$a_\mu^{\rm LNV-LH} = \sum_{i=e,\mu,\tau} \frac{3}{16\pi^2} \frac{m_\mu^2}{m_\Phi^2} |Y_{\mu i}|^2. \tag{288}$$

Thus for $m_\phi \sim 1$ TeV and $Y_{\mu i} \sim 1-3$ one can obtain $a_\mu^{\rm LNV-LH} \sim (60-600) \times 10^{-11}$ and thus "explain" the observed discrepancy. On the other hand, in the same paper [399], the authors study the lepton number violating decay $\mu^- \to e^+ e^- e^-$ which is also induced by the new terms in the Lagrangian. From the bound $\mathrm{BR}(\mu^- \to e^+ e^- e^-) < 1 \times 10^{-12}$ on the corresponding branching ratio they then obtain bounds on the Yukawa couplings Y_{ab}. For instance, for $m_\phi \sim 1$ TeV, the relation $Y_{ee}^* Y_{\mu e} < 0.2 \times 10^{-5}$ has to hold in order not to violate the bound on the branching ratio. It therefore seems questionable whether one can really obtain the above quoted large value for a_μ where $Y_{ab} \sim 1$ is needed. In any case a perturbative treatment would be obsolete.

a_μ in the Littlest Higgs model with T-parity: The value of the muon $g-2$ in the Littlest Higgs model with T-parity (LHT) was studied in Refs. [401,402,403]. Leading contributions are given by 1–loop diagrams of the type shown in Figs. 42c, 42d. While the conclusions of the papers concerning the anomalous magnetic moment agree qualitatively, Ref. [403] disagrees with the analytic expressions for the contributions given in the earlier two papers.

The main difference to the Little Higgs model without T-parity is, that in the LHT the couplings of the SM gauge bosons W, Z to SM fermions are unchanged. Therefore only loops involving new heavy particles contribute to a_μ. In addition to diagrams involving the (T-odd) heavy gauge bosons, the new T-odd heavy "mirror leptons" ℓ_H^i and neutrinos ν_H^i $(i = 1, 2, 3)$ can now appear in the loops. Assuming that bounds on slepton searches at LEP apply roughly also to these leptons in the LHT, they could be as light as 200-300 GeV. Furthermore, since the electroweak precision tests allow scales as low as $f \sim 500$ GeV, the "heavy" photon can be rather light, $M_{A_H} \sim 65$ GeV (also W_H and Z_H will be around 300 GeV). Nevertheless, in both Ref. [402] and Ref. [403] it was found that [49]

$$a_\mu^{\rm LHT} < 12 \times 10^{-11}, \tag{289}$$

even for such choices of the parameters at the boundary of the region allowed by EW precision test and direct searches. Therefore, the discrepancy between the experimental value and the SM prediction for a_μ cannot be explained within the LHT. In fact, it was pointed out in Ref. [403] that the muon $g-2$ is actually one way to discriminate the LHT from the MSSM. The main reason for the relatively small value of $a_\mu^{\rm LHT}$ compared to the MSSM is the absence of any enhancement factor, like a large $\tan\beta$.

On the other hand, the small value of $a_\mu^{\rm LHT}$ also implies that one can, at present, not obtain any strong new bounds on the parameters of the LHT. This is in contrast to many lepton number violating processes which were also discussed in Refs. [402,403]. Some of these processes could be detectable with new experiments in the coming years. These potentially large effects are due to the fact that the LHT, in contrast to the Littlest Higgs model without T-parity (or the MSSM), does not belong to the class of Minimal Flavor Violation (MFV) [326] models.

7.2.6. *Extra Dimensions*

String theory requires at least 6 extra spatial dimensions (beyond the 3 we know). The extra dimensions are assumed to be curled up (compactified). The compactification radius R is not (yet) predictable from

[49] In terms of the generic functions given in Eqs. (263,266) the results reads

$$a_\mu^{\rm LHT} = \frac{\sqrt{2} G_\mu m_\mu^2}{32\pi^2} \frac{v^2}{f^2} \sum_{i=1}^{3} \left|V_{H\ell}^{i\mu}\right|^2 \left[L_1(y_i) - L_2(y_i) + \frac{1}{5} L_1(y_i')\right]$$

where $L_1(z) = -\frac{13}{24} F_3^C(z)$ and $L_2(z) = -\frac{5}{3} F_3^N(z)$ with $y_i = m_{\ell_H^i}^2 / M_{W_H}^2$ and $y_i' = a y_i$ where $a = 5/\tan^2\Theta_W$ and $V_{H\ell}^{i\mu}$ are the couplings (denoted by f in Fig. 42).

string dynamics and thus must be considered as a free parameter which phenomenologically could be as low as $R^{-1} \sim 300$ GeV [404]–[409]. Phenomenological bounds on extra dimensions have been reviewed in [410]. Originally proposed by Kaluza and Klein [411], the rejuvenation of theories with extra dimensions came with the observation [406] that such scenarios could provide an alternative solution (besides supersymmetry or little Higgs models) of the hierarchy problem, as for phenomenological reasons $1/R$ can be low and pretty close to the electroweak scale. A true solution of the hierarchy problem would require a dynamical explanation for the low value of $1/R$, of course. Extra dimension models projected down to the 4–dimensional Minkowski space are non-renormalizable effective theories and in general require a cut-off, usually identified with the effective Planck constant, which will be defined below [50]. Naive momentum cut-off truncation of the excitation spectrum usually spoils gauge invariance [412,413] and more sophisticated constructions are necessary. However, as we will see, some quantities in theories with one extra dimension, in particular the anomalous magnetic moment, are actually finite.

If particles are created they can disappear into the extra dimension and become invisible except, in some scenarios, from missing energy and momentum, which would be observable in laboratory experiments. On a phenomenological level there are many possibilities concerning the number of dimensions, the size of the compactified directions and the type of particles which may move into them. The prototype mechanism has been proposed by Kaluza-Klein (KK), noticing that a 5-dimensional theory is able to describe simultaneously gravitational and electromagnetic interactions. In extra dimension scenarios one considers a D dimensional spacetime with $\Delta = D - 4$ extra space dimensions. The space is factorized into Minkowski space times a Δ–dimensional torus of radius R: $M^4 \times T^\Delta$. The torus has finite volume $V_\Delta = (2\pi R)^\Delta$. The SM fields are fields on M^4, which is called the brane or "the wall". Spacetime vectors are of the form $z^A = (x^\mu, y^i)$ and a scalar field, for example, takes the form

$$\phi(x,y) = \sum_{\vec{n}} \frac{\varphi^{(\vec{n})}(x)}{\sqrt{V_\Delta}} \exp\left(\mathrm{i}\frac{\vec{n}\cdot\vec{y}}{R}\right) \tag{290}$$

and the sum is discrete because the extra dimensions are of finite size R. When compactified on a circle of radius R, the M^4 fields $\varphi^{(\vec{n})}$ are the KK excitations and represent particles propagating in M^4 with masses $m^2_{(\vec{n})} = |\vec{n}|^2/R^2 + m_0^2$. m_0 is the mass of the zero mode. The masses of the KK states depend on the geometry of the extra dimensions. Gravity extends over D dimensions and the Einstein action reads

$$S_G = \frac{\overline{M}_D^{2+\Delta}}{2} \int \mathrm{d}^4x\, \mathrm{d}^\Delta y \sqrt{-\mathrm{Det}\, g}\, \mathcal{R}(g) \tag{291}$$

where g is the metric, $\mathcal{R}$ the scalar curvature and $\overline{M}_D$ the reduced Planck mass of the D–dimensional theory. Integrating out the extra coordinates under the hypothesis of factorization one obtains $\overline{M}_{Pl} = M_{Pl}/\sqrt{8\pi} = (\sqrt{8\pi\, G_N})^{-1} = 2.4 \times 10^{18}$ GeV (G_N Newton's gravitational constant) from the relation

$$\overline{M}^2_{\mathrm{Pl}} = \overline{M}_D^{2+\Delta}\, V_\Delta = \overline{M}_D^{2+\Delta}\, (2\pi R)^\Delta = M_D^{2+\Delta}\, R^\Delta\ . \tag{292}$$

Here, by a redefinition, factors 2π have been absorbed into M_D which is to be considered as a fundamental D–dimensional Planck mass.

The most direct consequence of extra dimensions is due to the graviton (G) excitations, if we assume that SM fields are confined to the brane and do not propagate in the additional dimensions [414]. The KK gravitons then couple to ordinary matter like the muon via the energy–momentum tensor $T^{\mu\nu}$ with coupling proportional to $\sqrt{G_N}$ such that

$$\Delta a_\mu^{\mathrm{KK}}(\mathrm{G}) = \frac{G_N m_\mu^2}{2\pi} \sum_{(\vec{n})} w(m_\mu^2, m^2_{(\vec{n})}) \approx \frac{G_N m_\mu^2\, S_\Delta\, R^\Delta}{2\pi} \int \mathrm{d}s\, s^{\Delta/2-1}\, w(m_\mu^2, s)\ ,$$

[50] In $D > 4$ coupling constants like gauge couplings carry a dimension m^{4-D} and therefore the D–dimensional field theories with extra dimensions are non-renormalizable

where we have replaced the sum by an integral, because the mass splittings are tiny especially for the heavier states which dominate the integral. $S_\Delta = 2\pi^{\Delta/2}/\Gamma(\Delta/2)$ is the surface of the Δ–dimensional sphere. While the contribution from a KK state is finite the integral is divergent due to the fact that the heavier states appear with increasing multiplicity. One can show that $w(m_\mu^2, s) \to c$ as $s \to \infty$ with $c = 5$ [414]. With a cut-off $\Lambda = \lambda\, M_\Delta$ one obtains

$$\Delta a_\mu^{\rm KK}({\rm G}) = \frac{c\lambda^\Delta}{4\pi^2}\frac{\pi^{\Delta/2}}{\Delta\Gamma(\Delta/2)}\frac{m_\mu^2}{M_D^2}\,. \tag{293}$$

In addition there exists a *radion field* due to the fluctuation of the radius, a spin 0 field which couples to the trace T^μ_μ. This radion yields a tiny contribution only [414] and will not be considered further. Using Eq. (293), we in principle can get a constraint on M_D which strongly depends on Δ, however. For $\Delta = 2$ severe constraints from cosmology and astrophysics exist, requiring $M_6 >$ a few TeV [410]. If $\Delta = 6$ (as required by string theory) the bound is much weaker and actually comes from the colliders LEP and Tevatron $M_{10} > 600$ -700 GeV. The bound Eq. (257) interpreted as $\delta a_\mu < 380 \times 10^{-11}$ requires $M_{10} > 980$ GeV [for M_5 one gets 610 GeV as a limit].

Another simple extra dimensions scenario is the one where only the gauge bosons propagate into the extra dimensions, while fermions and the Higgs remains in ordinary space. The Lagrangian in M^4 reads

$$\mathcal{L}_{\rm int} = \sum_{i=A,Z,W} g_i j_i^\mu \left(A_{\mu i} + \sqrt{2}\sum_{n=1}^{\infty} A_{\mu i}^{(n)} \right) \tag{294}$$

where $g_i = \sqrt{\pi R}\, g_i^{(D)}$ are the 4–dimensional effective couplings, rescaled from the D–dimensional theory. The fields $A_{\mu i}^{(n)}$ denote the KK excitations, the zero mode Lagrangian is the SM one. The masses M_n of the gauge–boson KK excitations are related to the masses M_0 of the zero-mode gauge bosons (i.e. the normal SM gauge bosons) by

$$M_n^2 = M_0^2 + n^2/R^2 \text{ with } \; n^2 = \sum_{i=1}^{\Delta} n_i^2 \tag{295}$$

and their couplings g_n are given by $g_n = \sqrt{2}\, g$, where g is the standard coupling of the zero mode. Relative to the SM, the extra effects $a_\mu^{\rm KK}$ to $g-2$ from a KK-tower of states are proportional to a factor $\sum_n D_n \frac{m_\mu^2}{M_n^2}$, where D_n is the degeneracy of the nth KK mode [414]–[421]. For $\Delta = 1$ we have $D_n = 1$ and thus

$$\sum_n D_n \frac{m_\mu^2}{M_n^2}/(m_\mu\, R)^2 = \sum_n \frac{D_n}{(M_0\, R)^2 + n^2} = \sum_n \frac{1}{(M_0\, R)^2 + n^2} \approx \sum_n \frac{1}{n^2} = \frac{\pi^2}{6} \tag{296}$$

In general all SM particles propagate into the extra dimensions and affect physics in the $D = 4$ subspace. In the Appelquist, Chang and Dobrescu model [408] with one universal extra dimension (UED) compactified as S^1/Z_2 (even number of additional dimensions are compactified as T^2/Z_2) there is only one new parameter $1/R$ the compactification scale. Universal refers to the property that all SM fields propagate into the extra dimensions. The interaction of all KK modes among themselves and with the SM fields are all expressed in $1/R$ and the SM parameters. One thus obtains the prediction [419,420]

$$\Delta a_\mu^{(2)\,\rm KK} = -\frac{g^2}{8\pi^2}\,\frac{3 - 4s^2 + \Delta/2\,(3 + 8s^2)}{12c^2}\,\sum_n D_n \frac{m_\mu^2}{M_n^2} \tag{297}$$

using $s^2 = \sin^2\Theta_W = 0.231$ one obtains

$$\Delta a_\mu^{(2)\,\rm KK} = -24.8 \times 10^{-11}\,(1 + 1.2\,\Delta)\, S_{\rm KK} \tag{298}$$

with $S_{\rm KK} = \sum_n \frac{6 D_n}{\pi^2}\left[\frac{300\ {\rm GeV}}{M_n}\right]^2$. This sum is convergent only for a single extra dimension where $D_n = 1$ and where the smallest value allowed for $1/R$ is about ~ 300 GeV , giving $S_{\rm KK} \approx 1$ and one finds

$$\Delta a_\mu^{(2)\,\mathrm{KK}} = -0.276 \cdot a_\mu^{(2)\,\mathrm{EW}} = -53.7[-24.8] \times 10^{-11} \; . \tag{299}$$

which differs numerically from the value -12.8×10^{-11} given in [420] and is closer to the -40×10^{-11} estimated in [419]. Given in brackets the value when scalar modes are not included, which corresponds and essentially agrees with the result in Eq. (301) [at $1/R = 300$ GeV the result is -20.4×10^{-11}] below. Note that the Δ scalar components of the D dimensional gauge fields for $D = 5$ enhance the effect by a factor 2. Another interesting scenario proposed by Barbieri, Hall and Nomura [407] assumes an extension of the SM to $D = 5$ dimensions, with N=1 supersymmetry, compactified on $M^4 \times S^1/(Z_2 \times Z_2')$ with a compactification scale $1/R \sim 370 \pm 70$ GeV. Again, the model allows for unambiguous predictions depending on R and the SM parameters only. The modification of $g-2$ has been worked out in [421] and reads

$$\Delta a_\mu^{(2)\,\mathrm{KK}} = -\frac{g^2}{192}\,\frac{11-18s^2}{12c^2}\,(m_\mu\,R)^2 \tag{300}$$

Numerically, for $1/R = 370 \pm 70$ GeV, it is given by

$$\Delta a_\mu^{(2)\,\mathrm{KK}} = -0.07^{+0.04}_{-0.02} \cdot a_\mu^{(2)\,\mathrm{EW}} = -(13.6^{+7.1}_{-4.0}) \times 10^{-11} \tag{301}$$

which again for any sensible value of R yields a result well inside the uncertainties of the SM prediction.

A number of authors have obtained results of similar size but of opposite sign [414,415,416,417]. The corrections of large extra dimension scenarios are rather small, below 1σ, for sensible values of the compactification radius R, typically 10% - 25% of the weak SM contribution and inside the uncertainties of the hadronic contribution. In more than one extra dimension a second cut-off $M_S \gg 1/R$ must come into play in a calculation of a_μ and the predictive power is reduced in general. The positive graviton KK contribution also for $D = 5$ requires a cut–off. Using $M_D \sim 1.2 \times 10^{13}$ for $D = 5$ and $1/R \sim 300$ GeV a contribution is practically absent; a phenomenological cut–off $M_5 \sim 3$ TeV, however, would yield $\Delta a_\mu^{\mathrm{KK}}(\mathrm{G}) \sim 15 \times 10^{-11}$ which would compete with other type of extra dimensions contributions.

7.2.7. *Anomalous Gauge Couplings*

It is a common belief that the SM is a low energy effective theory which results from an expansion in E/Λ, where E is a laboratory energy scale and Λ is the intrinsic cut–off of nature at the "microscopic" level. In this case it is natural to ask for corrections to the SM as a renormalizable low energy effective theory by operators of higher dimension. But also compositeness scenarios would lead to the same structure of effective interactions. Here we only consider P–conserving anomalous interactions of the $WW\gamma$–type as an illustration. It is a correction to the weak 1–loop contribution from diagram Fig. 37a. The most natural non-standard couplings correspond to an anomalous magnetic dipole moment (see [422] and references therein)

$$\mu_W = \frac{e}{2m_W}(1+\kappa+\lambda) \tag{302}$$

and an anomalous electric quadrupole moment

$$Q_W = -\frac{e}{2m_W}(\kappa-\lambda) \; . \tag{303}$$

In the SM, local gauge symmetry, which is mandatory for renormalizability of the SM, requires $\kappa = 1$ and $\lambda = 0$. These anomalous couplings yield the following contribution to a_μ [423]:

$$a_\mu(\kappa,\lambda) \simeq \frac{G_\mu m_\mu^2}{4\sqrt{2}\pi^2}\left[(\kappa-1)\ln\frac{\Lambda^2}{m_W^2} - \frac{1}{3}\lambda\right] \; . \tag{304}$$

Actually, the modification spoils renormalizability and one has to work with a cut–off Λ in order to get a finite answer as usual in an effective theory. For $\Lambda \simeq 1$ TeV LEP data from $e^+e^- \to W^+W^-$ production find bounds $\kappa - 1 = -0.027 \pm 0.045$, $\lambda = -0.028 \pm 0.021$ [104,424]. Applying the LEP bounds we can get not more than $a_\mu(\kappa,0) \simeq (-3.3 \pm 5.3) \times 10^{-10}$, $a_\mu(1,\lambda) \simeq (0.2 \pm 1.6) \times 10^{-10}$, and thus the observed deviation cannot be due to anomalous $WW\gamma$ couplings. The constraint on those couplings from $g-2$ is at least an order

of magnitude weaker than the one from LEP. This also illustrates that a_μ is not per se the most suitable observable for testing physics at the high end of scales.

8. Outlook and Conclusions

The measurement of a_μ is one of the most stringent tests for "new physics" scenarios, thanks to the current impressive precision. The Brookhaven muon $g-2$ experiment marks a new milestone in precision physics, with a 14–fold improvement over the previous CERN experiment. The precision achieved by the experiment E821 at BNL at the end was still statistics dominated and just running the experiment a little longer could have reduced the error down to the original goal of $\pm 40 \times 10^{-11}$. The recent result of the Brookhaven experiment has highlighted a 3σ discrepancy with the present SM prediction and hence makes comparisons with reliable predictions from extensions of the SM very interesting. Most interestingly, there is now a high tension between the $g-2$ constraints and other precisely measured observables, which provides very useful hints for where to look for the "new physics" at the upcoming high energy frontier experiments at the Large Hadron Collider (LHC) at CERN. This is a strong motivation for a next-generation $g-2$ experiment [425].

8.1. *Future Experimental Possibilities*

As a possible follow–up experiment of E821 a proposal for an upgraded experiment E969 has been submitted some time ago [111,426]. Considerations aim at $\sim 15 \times 10^{-11}$ experimental precision. The BNL storage ring would remain the key element. Different options are discussed for Brookhaven and for Fermilab in the USA and for JPARC in Japan. A higher rate and less background would be important and this requires several changes in the experiment. At JPARC with a high-intensity 30 GeV proton beam one could realize a backward decay beam which allows a better separation of muons and pions. A similar effect could be achieved using backward muons together with a muon accumulator ring at Fermilab or with a longer beam line. At FNAL statistics could be increased by a factor 25 due to the higher repetition rate of muon fills in the ring.

In order to further reduce the systematic errors one would also require a more uniform magnetic field and an improved centering of the muon beam and an improvement of the calibration. For the detection and analysis of the precession signal one could use a complementary method of determining ω_a by measuring the energy versus time in place of events versus time. The monitoring detectors would be improved by a better segmentation. A reduction of the pileup and muon losses (better kicker) would allow for further improvements.

This all looks very promising and will likely happen in a not too far future. For the theory side this represents a tremendous challenge. Some possible improvements and open problems will be discussed in the following outlook.

8.2. *Theory: Critical Assessment of Theoretical Errors and Open Problems*

8.2.1. *QED*

A first type of problems concerns the extremely complex four– and five–loop calculations, so far almost exclusively done by Kinoshita and his collaborators, which require cross checks by independent groups. Indeed new more effective numerical methods are being developed at present [427]. The 5–loop calculations are just at the beginning [148,150,151]. Here the problem is to master the exponentially growing complexity with increasing order of perturbation theory. Only a very high level of automatization of such calculations will allow us to get reliable results within a reasonable time. Of course the increasing computational power available will also be a key factor. As such kind of calculations are needed in many other branches of particle physics, like for understanding and analyzing LHC data or for future precision experiments with an e^+e^- linear collider like the ILC or at CLIC, there is little doubt that big progress will be made in all kinds of challenging perturbative calculations.

8.2.2. *Hadronic vacuum polarization*

The main conceptual problems remain with the hadronic contributions which are limiting the theoretical precision. The hadronic vacuum polarization requires substantial improvement and will depend very much on new improved e^+e^-–annihilation experiments in particular in the range up to 2.5 GeV. A serious effort in improving calculations of radiative corrections to these hadron production processes will be urgently needed. In the region including many–hadron final states inclusive versus exclusive approaches can provide important cross checks for estimating the true uncertainties. A major step in the reduction of the uncertainties are expected from VEPP-2000 [428] and from a possible "high-energy" option DAFNE-2 at Frascati [429]. Also important are forthcoming hadronic cross section measurements at BES III (Beijing) [430], CLEOc (Cornell/USA), and last but not least, additional very useful results from radiative return measurements are expected from the B–factories BaBar and Belle.

Since hadronic τ–decay spectra and $e^+e^- \to$ hadrons data should be related by isospin symmetry one expects to be able to further reduce the errors by including the τ data. However, one observes substantial yet unexplained deviations between these data, and therefore usually one does not include the τ data. A solution of this e^+e^- vs. τ puzzle also would help to improve the determination of $a_\mu^{\rm had}$.

A better theory supported method in determining in particular the dominating low energy $\pi\pi$ channel is possible. The theory of the pion form–factor, based on exploiting analyticity, unitarity and the low energy chiral expansion, looks very promising for future improvements [176]. This interesting framework systematically takes into account the constraints from the experimentally well determined $\pi\pi$–scattering phase shifts. However, in order to be able to fully exploit this approach one has to reduce the presently existing inconsistencies between the different measurements of the modulus of the pion form factor. Furthermore, in such a theory-driven approach to the lowest order hadronic vacuum polarization contribution, higher order corrections shown in Fig. 29d) would then have to be added "by hand" using some hadronic models for the corresponding 4-point function $\langle VVVV\rangle$. In this context it is important to remind that future experiments must attempt to actually measure these final state radiation effects [431,432].

With more precise values for the QCD parameters, in particular the quark masses m_c and m_b [433]–[438], one will be able to make more precise pQCD calculations of the photon self-energy in the Euclidean region, at $Q^2 = -q^2 \gtrsim (2.5\ {\rm GeV})^2$, say. There, the light quarks are essentially massless and also can be treated perturbatively. This will allow us to calculate $a_\mu^{\rm had}$ via the Adler function [234,235,174], by exploiting more extensively and in a well controlled way pQCD. This would provide determinations of $a_\mu^{\rm had}$ in a manner which is less dependent on experimental data and their uncertainties.

An important long term project are non-perturbative calculations of the vacuum polarization function in lattice QCD [439]. Since we know that the hadronic vacuum polarization is dominated by the contribution from the ρ–resonance, it is crucial to have the physical ρ "in the box", i.e. it requires to simulate at physical parameters (quark masses) and in full QCD including the u, d, s and c quarks. The advantage is that for calculating $a_\mu^{\rm had}$ the photon vacuum polarization is needed at Euclidean momenta only, which is directly accessible to lattice simulations. The aim of a precision at the 0.5% level needed in future, is certainly very hard to reach. But also less precise results would be very important in view of the existing problems, which we have discussed in Sect. 4. Note, however, that again higher order radiative effects are not included in a lattice study of the two-point function $\langle VV\rangle$.

8.2.3. *Hadronic light-by-light scattering*

In contrast to the hadronic vacuum polarization contribution to a_μ, no direct connection with experimental data can be made for hadronic light-by-light scattering and, very likely, we have to rely on models in the foreseeable future. Because of the increased accuracy of a potential future $g-2$ experiment and the expected substantial reduction of the error of the other hadronic contributions to a_μ, in particular the hadronic vacuum polarization, also a reconsideration of the hadronic light–by–light contribution is certainly needed. Whereas some control over the pseudoscalar and axial vector contributions has been achieved by implementing many experimental and theoretical constraints, this is not the case for the other contributions, like the dressed pion loop, the scalar exchanges and the dressed quark loop. Unless one succeeds in getting a much better control on the corresponding model uncertainties, it will be very difficult to reduce the final overall error

of the hadronic light-by-light scattering contribution below the "guesstimate" of $\pm 40 \times 10^{-11}$ quoted in Section 5.2.

In view of recent and foreseeable progress in computer performance, and using recently developed much more efficient computer simulation algorithms, we expect that lattice QCD will be able to provide a useful estimate in coming years. Exploratory studies [440,441] actually look rather promising. Recall that one has to integrate the relevant QCD four-point function $\langle VVVV \rangle$ over the full phase space of the three off-shell photons, which is much more complicated than what has been done in the lattice studies for the hadronic vacuum polarization contribution to $g-2$ [439]. However, even a number for the light-by-light scattering contribution with an error of 50% (but "reliable" !) would be very helpful to complement the other approaches.

In the following, we suggest some potential ways of improvement. Probably only a collaborative effort of all interested people (maybe in the form of a hadronic light-by-light scattering working group) can lead to real progress and to a final estimate for the central value and its error, which is trustworthy.

The first, most important point is that one has to have one consistent framework (model) for all contributions, since the splitting into different contributions is model dependent as stressed in Sect. 5. A priori this was already the case for the two existing full evaluations by Bijnens et al. [243] using the ENJL model and Kinoshita et al. [242,245] employing the HLS model, but only to a certain extent. In both cases the general framework had to be adjusted for some contributions, in particular for the pseudoscalar exchange and the charged pion loop. However, as soon as one tries to "improve" ("repair") the model for one contribution, one has to make sure that this is consistent for the other contributions.

One purely phenomenological approach would be to use some resonance Lagrangian which contains the lowest lying and possibly heavier states, where all the couplings have been determined by some physical processes (e.g. from resonance decays or from the contribution of these resonances to the production of a certain number of pions in e^+e^- scattering [442,443,444], etc.). It should be kept in mind with such an approach that for instance different formalisms can be used to describe vector mesons (vector field, antisymmetric tensor field, massive Yang-Mills, etc.). Even imposing chiral and gauge invariance does not uniquely fix the corresponding Lagrangian and certain couplings might be absent in one particlar model, unless one adds terms with more derivatives or more resonance fields. Furthermore, there is no consistent chiral counting to discard certain terms as higher order in p^2 in such a resonance Lagrangian.

Note that even if all parameters in such a resonance Lagrangian can be fixed by some decay or scattering processes, this does not guarantee that integrating over the photon momenta in hadronic light-by-light scattering, or by performing loops with resonances, will lead to ultraviolet finite results. In general, these resonance Lagrangians are non-renormalizable and we will need some momentum cutoff or some new counter-terms with a priori unknown finite coefficients. The question is whether varying the cutoff in some "reasonable" range, like 1-2 GeV, will lead to a stable result, if the high momentum region is modeled by a (dressed) quark loop. Note, however, that Ref. [294] does not include the dressed light quark loops as a separate contribution. It is assumed to be already covered by using the short-distance constraint from Ref. [257] on the pseudoscalar-pole contribution. This issue certainly needs to be clarified.

Another approach is based on the large-N_c framework advocated in Ref. [254]. One tries to write ansätze in terms of exchanged resonances for all the relevant QCD Green's functions and matches them with QCD short distance constraints and the chiral Lagrangian at low energies. In principle, also in this case one can use some chiral and gauge-invariant resonance Lagrangian and then fix (some of) the coefficients by matching with QCD at high energies. The advantage of the Lagrangian approach, in contrast to the LMD or LMD+V ansätze used in Refs. [17,257], is that for instance crossing symmetry is automatically fulfilled and that the connection between the parameters which enter in different Green's functions is explicit. Also in this case one has to fix the other parameters in the Lagrangian using some experimental input. The problem is that in such an approach one has to start with the most general effective Lagrangian and this will lead to many unknown parameters. This is in contrast with the above phenomenological approach, where only those couplings are introduced, which are "needed" to describe a particular process.

For both approaches it is crucial to have as much experimental information as possible, e.g. data for various form factors (on-shell and off-shell), to constrain these model Lagrangians or to check their consistency, if some parameters are fixed by QCD short-distance constraints. A new important constraint for the internal

$\pi^0\gamma\gamma$–vertex would be a measurement of $\mathcal{F}_{\pi^{0*}\gamma^*\gamma}(m_\pi^2, -Q^2, -Q^2)$, which should be possible at future high luminosity machines.

One problem with the resonance Lagrangian approach is how to go beyond the leading order in N_c. In most cases, such resonance Lagrangians are only used at tree-level, which corresponds to the leading order in N_c. How can one consistently include loops with resonances (some progress has been made, see Refs. [445,444]) and how can we account for finite width effects ? Maybe the latter point is not so relevant for hadronic light-by-light scattering, since one can always evaluate the contribution to $g-2$ in Euclidean space in order to avoid physical poles and thresholds. A somehow related problem concerns the scalars. Can we really use a simple resonance Lagrangian, which usually assumes narrow states ? Often the scalar states are very broad or it is not clear, whether they are really some $q\bar{q}$ bound states or rather some four quark states or meson molecules. Furthermore, how can we constrain the scalar sector theoretically, i.e. by matching with QCD short-distance constraints, since the scalars directly couple to the non-perturbative vacuum of QCD.

One important step within such a resonance Lagrangian framework would then be to check that the so far neglected contributions from heavier states, like π' or some tensor mesons, are really small. Furthermore, one should check how stable the final result is, if we include such heavier resonance states and, at the same time, integrate in the (dressed) quark loop only the high-momentum region above all those resonances, e.g. from 1.5 GeV upwards (quark-hadron duality). One problem might be that the quark loop also serves as some sort of counterterm to absorb the cutoff dependence of the integrals including the resonances. If there is no matching between low and high momenta, the final result will likely be very dependent on the exact choice of the cutoff.

The same four-point function $\langle VVVV \rangle$ which is relevant for hadronic light-by-light scattering also enters at higher order in the hadronic vacuum polarization (hadronic blob with an additional photon attached to itself, see Fig. 29d)), although of course in a different kinematical region. It would be a good cross-check on all models for hadronic light-by-light scattering, if they could successfully predict this contribution. In the more recent $\pi\pi$ cross-section measurements, this contribution is usually included in the data for $e^+e^- \to$ hadrons. In fact experiments always have to apply cuts to the photon spectrum and the missing hard final state radiation is added "by hand", assuming sQED to provide a reasonable approximation.

Finally, it might be useful to complement these approaches using resonance models with a more theoretical framework, where one tries to identify different contributions in the full light-by-light scattering amplitude in a dispersive framework, looking for the one-pion cut, the two-pion cut, etc., in the spirit of the theory of the pion form factor developed in Refs. [176,446]. It might also be interesting whether one could make some model-independent statements (exact low-energy theorems) in some particular limits, e.g. to identify the dominant contribution, if $m_\mu \to 0, m_\pi \to 0$ with the ratio m_μ/m_π fixed to its physical value. For instance, can one prove without resorting to some particular Feynman diagram with model-dependent form factors, that the leading term is completely given by the (undressed) "charged pion loop". Even if one might not be able, with such an approach, to obtain precise numerical predictions for the light-by-light scattering contribution in the real world, the knowledge of the result in some limits could help to check the consistency of calculations within some models or on the lattice, e.g. the size and sign of different contributions, like from scalar exchanges. Some progress in this direction has been achieved in the effective field theory approach described in Sect. 5.3, where the leading logarithmically enhanced terms for large N_c have been identified.

It remains to be seen, whether such a concerted effort can reliably predict the light-by-light scattering contribution to a_μ with an error comparable with the final goal of a future experiment, i.e. about $\pm 15 \times 10^{-11}$. Of course, the corresponding contribution to the electron $a_e^{\mathrm{LbL;had}}$ should also be evaluated at the same time. We hope that some progress can be achieved by taking into account the issues which have been brought up in this Section and in the recent literature [17,257,41]. If not, hadronic light-by-light scattering might be the future roadblock to strongly constrain new physics models, in case a new muon $g-2$ experiment will be carried out in the future.

Another possibility, proposed by Remiddi some time ago, would be to increase the precision of independent measurements of α by a factor 20 and then use a_e together with improved QED and SM calculations and determine a_μ(unpredicted) assuming that it is proportional to m_ℓ^2: thus from

$$a_\mu = a_\mu(\text{predicted}) + a_\mu(\text{unpredicted}) \ ,$$

$$a_e = a_e(\text{predicted}) + (m_e/m_\mu)^2 \times a_\mu(\text{unpredicted}) \,,$$

we could determine a_μ(unpredicted). This quantity would, however, not only include the hard to pin down hadronic contributions, but also unaccounted new physics effects which scale with m_ℓ^2. Unfortunately, the leading hadronic contributions are due to the ρ^0 resonance in the hadronic vacuum polarization or to light states like π^0–exchange in light-by-light scattering, which do not scale in this simple manner in general. Nevertheless, such attempts to constrain whatever kinds of physics would be certainly very interesting.

8.3. *Conclusions*

The BNL muon $g-2$ experiment has stimulated significant progress in theory as well as in hadronic cross–section measurements. QED and electroweak contributions are well established at the required level of precision. Fortunately, substantial experimental improvements of the e^+e^-–annihilation data allowed to reduce the uncertainties of the theoretical prediction to match the experimental precision, although there remain some as yet not understood deviations in particular between different $\pi\pi$ cross–section measurements. Here also a clarification of the e^+e^- vs. τ puzzle seems to be crucial for a better understanding of possible experimental and/or theoretical problems. The main problem at present is the limited precision of the e^+e^- data in the range between 1 and 2 GeV. We expect further improvements by about a factor 2 in accuracy of $a_\mu^{\rm had}$ after VEPP-2000, DAΦNE-II, CESRc and $c-\tau$–factories [Beijing], as well as further results from radiative return measurements at DAΦNE and the B–factories, will be available. The hadronic light–by–light scattering contribution will then be limiting further progress in the prediction of $g_\mu - 2$. The actual 3.2 σ deviation between $a_\mu^{\rm exp}$ and $a_\mu^{\rm the}$ opens plenty of room for speculations about its origin and we hope it is a true effect, due to physics beyond the Standard Model.

Even if there are some serious limitations in controlling the hadronic effects (see also [217]), the current very precise SM prediction of the muon anomalous magnetic moment is pretty safe and a real triumph for the SM, which incorporates, except from gravity, all particle interactions within the unifying framework of a spontaneously broken $SU(3)_c \otimes SU(2)_L \otimes U(1)_Y$ gauge theory with 3 families of leptons and quarks. The muon anomalous magnetic moment is a pure quantum observable, unambiguously predicted by the SM, and known at a precision which unfolds the whole spectrum of physics incorporated in the SM. Only the Higgs boson, due to its tiny coupling to light fermions, is far from playing a relevant role. The muon anomaly's sensitivity to new physics is largest to nearby new states or new effective interactions, while too heavy states yield too small effects to be seen. At the same time light states are severely constrained in particular by the LEP and Tevatron new physics searches. In any case the muon $g-2$ with its 3σ disagreement / agreement between theory and experiment provides important constraints to parameters of new physics models as outlined in some detail above. It certainly also helps to disentangle the plentitude of possibilities we have to go beyond the SM and can complement upcoming new physics searches at the LHC.

An improved muon $g-2$ experiment would challenge new efforts to improve the accuracy of the theoretical prediction and corroborate the existence of physics beyond the SM which we belief must be there in any case.

Acknowledgments

We would like to thank Oliver Bär, Gilberto Colangelo, Jürg Gasser, Andrei Kataev, Wolfgang Kluge, Heiri Leutwyler, Peter Minkowski, Stefan Müller, Federico Nguyen, Giulia Pancheri, Ximo Prades, Rainer Sommer, Arkady Vainshtein and Graziano Venanzoni for numerous stimulating discussions and for correspondence. A.N. is grateful to Marc Knecht, Michel Perrottet and Eduardo de Rafael for many discussions and the pleasant collaboration on the hadronic light-by-light scattering contribution. F.J. gratefully acknowledges the kind hospitality at Frascati National Laboratory and thanks Staszek Jadach and his team from the Niewodniczanski Nuclear Physics Institute at Krakow and Karol Kołodziej and his Colleagues from the Institute of Physics of the University of Silesia at Katowice for the kind hospitality extended to him. A.N. thanks the Institute for Theoretical Physics at the University of Bern, the Centre de Physique Théorique in Marseille, the Theory Group at DESY Zeuthen and the Institute for Theoretical Physics at ETH Zürich for the hospitality during some stages of writing this review. F.J. gratefully acknowledges support by the

Alexander von Humboldt Foundation through the Foundation of Polish Science. This work was supported in part by the EU grants MTKD-CT2004-510126, in partnership with the CERN Physics Department and with the TARI Program under contract RII3-CT-2004-506078, and by the Department of Atomic Energy, Government of India, under a 5-Years Plan Project.

Appendix A. Some Standard Model parameters, ζ values and polylogarithms

For calculating the weak contributions we need the Fermi constant

$$G_\mu = 1.16637(1) \times 10^{-5}\ \mathrm{GeV}^{-2}\ , \tag{A.1}$$

the weak mixing parameter (here defined by $\sin^2\Theta_W = 1 - M_W^2/M_Z^2$)

$$\sin^2\Theta_W = s_W^2 = 0.22276(56) \tag{A.2}$$

and the masses of the intermediate gauge bosons Z and W (see [104,322])

$$M_Z = 91.1876 \pm 0.0021\ \mathrm{GeV}\ ,\ M_W = 80.398 \pm 0.025\ \mathrm{GeV}\ . \tag{A.3}$$

In the SM the Higgs particle the mass is constrained by LEP data to the range [322]

$$114\ \mathrm{GeV} < m_H < 144\ \mathrm{GeV}(\text{at } 95\%\ \text{C.L.})\ . \tag{A.4}$$

In calculations of hadronic contributions we will use the charged pion mass

$$m_{\pi^\pm} = 139.570\,18\,(35)\mathrm{MeV}\ , \tag{A.5}$$

and the neutral pion mass m_{π^0} which has the value

$$m_{\pi^0} = 134.976\,6\,(6)\mathrm{MeV}\ . \tag{A.6}$$

In some cases quark masses are needed. For the light quarks $q = u, d, s$ we give $m_q = \bar{m}_q(\mu = 2\ \mathrm{GeV})$, for the heavier $q = c, b$ the values at the mass as a scale $m_q = \bar{m}_q(\mu = \bar{m}_q)$ and for $q = t$ the pole mass:

$$\begin{aligned} m_u &= \ \ 3 \pm 1\,\mathrm{MeV} \qquad m_d = \ \ 6 \pm 2\,\mathrm{MeV} \qquad m_s = \ \ 105 \pm 25\,\mathrm{MeV} \\ m_c &= 1.25 \pm 0.10\,\mathrm{GeV} \qquad m_b = 4.25 \pm 0.15\,\mathrm{GeV} \qquad m_t = 172.6 \pm 1.4\,\mathrm{GeV}\ . \end{aligned} \tag{A.7}$$

When using constituent quark masses we will adopt the values

$$M_u = M_d = 300\,\mathrm{MeV}\ ,\ \ M_s = 500\,\mathrm{MeV}\ ,\ \ M_c = 1.5\,\mathrm{GeV}\ ,\ \ M_b = 4.5\,\mathrm{GeV}\ . \tag{A.8}$$

It should be noted that for u, d and s quarks such large effective light quark masses violate basic chiral Ward-Takahashi identities of low energy QCD. The latter requires values like those in Eq. (A.7) for the so called *current quark masses* to properly account for the pattern of chiral symmetry breaking.
Typically, analytic results for higher order terms may be expressed in terms of the Riemann zeta function

$$\zeta(n) = \sum_{k=1}^{\infty} \frac{1}{k^n} \tag{A.9}$$

and of the polylogarithmic integrals

$$\mathrm{Li}_n(x) = \frac{(-1)^{n-1}}{(n-2)!} \int_0^1 \frac{\ln^{n-2}(t)\ln(1-tx)}{t} dt = \sum_{k=1}^{\infty} \frac{x^k}{k^n}\ , \tag{A.10}$$

where the dilogarithm $\mathrm{Li}_2(x)$ is often referred to as the Spence function. The series representation holds for $|x| \leq 1$. The dilogarithm is an analytic function with the same cut as the logarithm. Useful relations are

$$\mathrm{Li}_2(x) = -\mathrm{Li}_2(1-x) + \frac{\pi^2}{6} - \ln x \ln(1-x),$$
$$\mathrm{Li}_2(x) = -\mathrm{Li}_2(\frac{1}{x}) - \frac{\pi^2}{6} - \frac{1}{2}\ln^2(-x),$$
$$\mathrm{Li}_2(x) = -\mathrm{Li}_2(-x) + \frac{1}{2}\mathrm{Li}_2(x^2)\ . \tag{A.11}$$

Special values are:

$$\mathrm{Li}_2(0) = 0\ ,\ \ \mathrm{Li}_2(1) = \frac{\pi^2}{6}\ ,\ \ \mathrm{Li}_2(-1) = -\frac{\pi^2}{12}\ ,\ \ \mathrm{Li}_2(\frac{1}{2}) = \frac{\pi^2}{12} - \frac{1}{2}(\ln 2)^2\ . \tag{A.12}$$

Special $\zeta(n)$ values we will need are

$$\zeta(2) = \frac{\pi^2}{6}\ ,\ \zeta(3) = 1.202\ 056\ 903\cdots\ ,\ \zeta(4) = \frac{\pi^4}{90}\ ,\ \zeta(5) = 1.036\ 927\ 755\cdots\ . \tag{A.13}$$

Also the constants

$$\mathrm{Li}_n(1) = \zeta(n)\ ,\ \ \mathrm{Li}_n(-1) = -[1-2^{1-n}]\,\zeta(n),$$
$$a_4 \equiv \mathrm{Li}_4(\frac{1}{2}) = \sum_{n=1}^{\infty} 1/(2^n n^4) = 0.517\ 479\ 061\ 674\cdots\ , \tag{A.14}$$

related to polylogarithms, will be needed for the evaluation of analytical results.

References

[1] W. Gerlach, O. Stern, Zeits. Physik **8** (1924) 110
[2] G. E. Uhlenbeck, S. Goudsmit, Naturwissenschaften **13** (1925) 953; Nature **117** (1926) 264
[3] C. D. Anderson, S. H. Neddermeyer, Phys. Rev. **50** (1936) 263; S. H. Neddermeyer, C. D. Anderson, Phys. Rev. **51** (1937) 884
[4] C. D. Anderson, Phys. Rev. **43** (1933) 491
[5] P. A. M. Dirac, Proc. Roy. Soc. A **126** (1930) 360
[6] F. Hoogeveen, Nucl. Phys. B **341** (1990) 322
[7] W. Bernreuther, M. Suzuki, Rev. Mod. Phys. **63** (1991) 313 [Erratum-ibid. **64** (1992) 633]
[8] B. C. Regan, E. D. Commins, C. J. Schmidt, D. DeMille, Phys. Rev. Lett. **88** (2002) 071805
[9] F. J. M. Farley et al., Phys. Rev. Lett. **93** (2004) 052001; M. Aoki et al. [J-PARC Letter of Intent]: *Search for a Permanent Muon Electric Dipole Moment at the* $10^{-24}\, e\cdot cm$ *Level*, `http://www-ps.kek.jp/jhf-np/LOIlist/pdf/L22.pdf`
[10] V. B. Berestetskii, O. N. Krokhin, A. X. Klebnikov, Zh. Eksp. Teor. Fiz. **30** (1956) 788 [Sov. Phys. JETP **3** (1956) 761]; W. S. Cowland, Nucl. Phys. B **8** (1958) 397
[11] K. Ackerstaff et al. [OPAL Collab.], Phys. Lett. B **431** (1998) 188; M. Acciarri et al. [L3 Collab.], Phys. Lett. B **434** (1998) 169; W. Lohmann, Nucl. Phys. B (Proc. Suppl.) **144** (2005) 122
[12] R. M. Carey et al., Phys. Rev. Lett. **82** (1999) 1632
[13] H. N. Brown et al. [Muon (g-2) Collaboration], Phys. Rev. D **62** (2000) 091101
[14] H. N. Brown et al. [Muon (g-2) Collaboration], Phys. Rev. Lett. **86** (2001) 2227
[15] G. W. Bennett et al. [Muon g-2 Collaboration], Phys. Rev. Lett. **89** (2002) 101804 [Erratum-ibid. **89** (2002) 129903]
[16] G. W. Bennett et al. [Muon g-2 Collaboration], Phys. Rev. Lett. **92** (2004) 161802
[17] M. Knecht, A. Nyffeler, Phys. Rev. D **65** (2002) 073034
[18] J. Bailey, E. Picasso, Progr. Nucl. Phys. **12** (1970) 43
[19] B. E. Lautrup, A. Peterman, E. de Rafael, Phys. Reports 3C (1972) 193
[20] F. Combley, E. Picasso, Phys. Reports **14C** (1974) 1
[21] F. J. M. Farley, Contemp. Phys. **16** (1975) 413
[22] T. Kinoshita, *Quantum Electrodynamics*, 1st edn (World Scientific, Singapore 1990) pp 997, and contributions therein
[23] F. J. M. Farley, E. Picasso, In: *Quantum Electrodynamics*, ed by T. Kinoshita (World Scientific, Singapore 1990) p 479; Adv. Ser. Direct. High Energy Phys. **7** (1990) 479
[24] T. Kinoshita, W. J. Marciano, In: *Quantum Electrodynamics*, ed. T. Kinoshita (World Scientific, Singapore 1990) pp 419–478

[25] V. W. Hughes, T. Kinoshita, Rev. Mod. Phys. **71** (1999) S133
[26] A. Czarnecki, W. J. Marciano, Nucl. Phys. B (Proc. Suppl.) **76** (1999) 245
[27] A. Czarnecki, W. J. Marciano, Phys. Rev. D **64** (2001) 013014
[28] V. W. Hughes, *The anomalous magnetic moment of the muon*. In: Intern. School of Subnuclear Physics: 39th Course: New Fields and Strings in Subnuclear Physics, Erice, Italy, 29 Aug - 7 Sep 2001; Int. J. Mod. Phys. A **18S1** (2003) 215
[29] E. de Rafael, *The muon g-2 revisited*. In: XVI Les Rencontres de Physique de la Vallee d'Aoste: Results and Perspectives in Particle Physics, La Thuile, Aosta Valley, Italy, 3-9 Mar 2002; hep-ph/0208251
[30] K. P. Jungmann, Nucl. Phys. News **12** (2002) 23
[31] A. Nyffeler, Acta Phys. Polon. B **34** (2003) 5197; Nucl. Phys. B (Proc. Suppl.) **131** (2004) 162; hep-ph/0305135
[32] M. Knecht, *The anomalous magnetic moment of the muon: A theoretical introduction*, In: 41st International University School of Theoretical Physics: Flavor Physics (IUTP 41), Schladming, Styria, Austria, 22-28 Feb 2003; hep-ph/0307239
[33] F. J. M. Farley, Y. K. Semertzidis, Prog. Part. Nucl. Phys. **52** (2004) 1
[34] D. W. Hertzog, W. M. Morse, Annu. Rev. Nucl. Part. Sci. **54** (2004) 141
[35] M. Passera, J. Phys. G **31** (2005) R75; Phys. Rev. D **75** (2007) 013002
[36] K. P. Jungmann, *Precision Measurements at the Frontiers of Standard Theory: The Magnetic Anomaly of Leptons*, DPG Frühjahrstagung, Berlin, 4-9 March 2005
[37] P. J. Mohr, B. N. Taylor, Rev. Mod. Phys. **72** (2000) 351
[38] P. J. Mohr, B. N. Taylor, Rev. Mod. Phys. **77** (2005) 1
[39] T. Kinoshita, Nucl. Phys. B (Proc. Suppl.) **144** (2005) 206
[40] K. Melnikov, A. Vainshtein, *Theory of the muon anomalous magnetic moment*, (Springer, Berlin, 2006) 176 p
[41] J. Bijnens, J. Prades, Mod. Phys. Lett. A **22** (2007) 767
[42] M. Passera, Nucl. Phys. Proc. Suppl. **169** (2007) 213
[43] J. P. Miller, E. de Rafael, B. L. Roberts, Rept. Prog. Phys. **70** (2007) 795
[44] F. Jegerlehner, Acta Phys. Polon. B **38** (2007) 3021
[45] S. Eidelman, *Standard Model Predictions for $g-2$*, presented at the Intern. Workshop on Tau Lepton Physics, TAU08 Novosibirsk, Russia, September 22-25, 2008
[46] F. Jegerlehner, *The Anomalous Magnetic Moment of the Muon*, STMP 226, (Springer, Berlin Heidelberg 2008) 426 p
[47] W. Pauli, Zeits. Phys. **43** (1927) 601
[48] P. A. M. Dirac, Proc. Roy. Soc. A **117** (1928) 610; A **118** (1928) 351
[49] L. E. Kinster, W. V. Houston, Phys. Rev. **45** (1934) 104
[50] P. Kusch, Science **123** (1956) 207; Physics Today **19** (1966) 23
[51] S. Tomonaga, Riken Iho, Progr. Theor. Phys. **1** (1946) 27; J. Schwinger, Phys. Rev. **74** (1948) 1439; R. P. Feynman, Phys. Rev. **76** (1949) 749; F. Dyson, Phys. Rev. **75** (1949) 486, ibid. 1736
[52] J. S. Schwinger, Phys. Rev. **73** (1948) 416
[53] J. E. Nafe, E. B. Nelson, I. I. Rabi, Phys. Rev. **71** (1947) 914
[54] D. E. Nagle, R. S. Julian, J. R. Zacharias, Phys. Rev. **72** (1947) 971
[55] G. Breit, Phys. Rev. **72** (1947) 984
[56] P. Kusch, H. M. Foley, Phys. Rev. **73** (1948) 421; Phys. Rev. **74** (1948) 250
[57] W. E. Lamb Jr, R. C. Retherford, Phys. Rev. **72** (1947) 241
[58] H. A. Bethe, Phys. Rev. **72** (1947) 339; N. M. Kroll, W. E. Lamb Jr, Phys. Rev. **75** (1949) 388; V. Weisskopf, J. B. French, Phys. Rev. **75** (1949) 1240
[59] W. H. Luisell, R. W. Pidd, H. R. Crane, Phys. Rev. **91** (1953) 475; ibid. **94** (1954) 7; A. A. Schupp, R. W. Pidd, H. R. Crane, Phys. Rev. **121** (1961) 1; H. R. Crane, Sci. American **218** (1968) 72
[60] T. D. Lee, C. N. Yang, Phys. Rev. **104** (1956) 254
[61] R. L. Garwin, L. Lederman, M. Weinrich, Phys. Rev. **105** (1957) 1415
[62] J. I. Friedman, V .L. Telegdi, Phys. Rev. **105** (1957) 1681
[63] R. L. Garwin, D. P. Hutchinson, S. Penman, G. Shapiro, Phys. Rev. **118** (1960) 271
[64] G. Charpak, F. J. M. Farley, R. L. Garwin, T. Muller, J. C. Sens, V. L. Telegdi, A. Zichichi, Phys. Rev. Lett. **6** (1961) 128; G. Charpak, F. J. M. Farley, R. L. Garwin, T. Muller, J. C. Sens, A. Zichichi, Nuovo Cimento **22** (1961) 1043; Phys. Lett. **1**B (1962) 16
[65] G. Charpak, F. J. M. Farley, R. L. Garwin, T. Muller, J. C. Sens, A. Zichichi, Nuovo Cimento **37** (1965) 1241
[66] F. J. M. Farley, J. Bailey, R. C. A. Brown, M. Giesch, H. Jöstlein, S. van der Meer, E. Picasso, M. Tannenbaum, Nuovo Cimento **45** (1966) 281
[67] J. Bailey et al., Phys. Lett. B **28** (1968) 287
[68] J. Bailey, W. Bartl, G. von Bochmann, R. C. A. Brown, F. J. M. Farley, M. Giesch, H. Jöstlein, S. van der Meer, E. Picasso, R. W. Williams, Nuovo Cimento A **9** (1972) 369
[69] J. Aldins, T. Kinoshita, S. J. Brodsky, A. J. Dufner, Phys. Rev. Lett. **23** (1969) 441; Phys. Rev. D **1** (1970) 2378
[70] V. Bargmann, L. Michel, V. A. Telegdi, Phys. Rev. Lett. **2** (1959) 435
[71] J. Bailey et al. [CERN Muon Storage Ring Collaboration], Phys. Lett. B **67** (1977) 225 [Phys. Lett. B **68** (1977) 191]
[72] N. Cabibbo, R. Gatto, Phys. Rev. Lett. **4** (1960) 313, Phys. Rev. **124** (1961) 1577
[73] C. Bouchiat, L. Michel, J. Phys. Radium **22** (1961) 121
[74] L. Durand, III., Phys. Rev. **128** (1962) 441; Erratum-ibid. **129** (1963) 2835

[75] T. Kinoshita, R. J. Oakes, Phys. Lett. **25**B (1967) 143
[76] M. Gourdin, E. de Rafael, Nucl. Phys. B **10** (1969) 667
[77] V. L. Auslander, G. I. Budker, Ju. N. Pestov, A. V. Sidorov, A. N. Skrinsky. A. G. Kbabakhpashev, Phys. Lett. B **25** (1967) 433
[78] J. E. Augustin et al., Phys. Lett. B **28** (1969), 503, 508, 513, 517
[79] T. Kinoshita, B. Nizic, Y. Okamoto, Phys. Rev. Lett. **52** (1984) 717; Phys. Rev. D **31** (1985) 2108
[80] L. M. Barkov et al., Nucl. Phys. B **256** (1985) 365
[81] J. A. Casas, C. Lopez, F. J. Ynduráin, Phys. Rev. D **32** (1985) 736
[82] F. Jegerlehner, Z. Phys. C **32** (1986) 195
[83] S. Eidelman, F. Jegerlehner, Z. Phys. C **67** (1995) 585; F. Jegerlehner, Nucl. Phys. (Proc. Suppl.) C **51** (1996) 131
[84] J. Z. Bai et al. [BES Collaboration], Phys. Rev. Lett. **84** (2000) 594; Phys. Rev. Lett. **88** (2002) 101802
[85] R. R. Akhmetshin et al. [CMD-2 Collaboration], Phys. Lett. B **578** (2004) 285
[86] A. Aloisio et al. [KLOE Collaboration], Phys. Lett. B **606** (2005) 12
[87] S. Weinberg, Physica A **96** (1979) 327; J. Gasser, H. Leutwyler, Annals Phys. **158** (1984) 142; J. Gasser, H. Leutwyler, Nucl. Phys. B **250** (1985) 465
[88] G. Ecker, J. Gasser, A. Pich, E. de Rafael, Nucl. Phys. B **321** (1989) 311; G. Ecker, J. Gasser, H. Leutwyler, A. Pich, E. de Rafael, Phys. Lett. B **223** (1989) 425
[89] F. Scheck, Leptons, Hadrons and Nuclei, North Holland, Amsterdam (1983)
[90] R. Barbieri, E. Remiddi, Phys. Lett. B **49** (1974) 468; Nucl. Phys. B **90** (1975) 233
[91] J. Bailey et al. [CERN-Mainz-Daresbury Collaboration], Nucl. Phys. B **150** (1979) 1
[92] G. W. Bennett et al. [Muon g-2 Collaboration], Phys. Rev. D **73** (2006) 072003
[93] G. T. Danby et al., Nucl. Instr. and Methods Phys. Res. **A 457** (2001) 151
[94] Y. K. Semertzidis, Nucl. Instr. and Methods Phys. Res. **A503** (2003) 458
[95] E. Efstathiadis et al., Nucl. Instr. and Methods Phys. Res. **A496** (2002) 8
[96] L. H. Thomas, Phil. Mag. **3** (1927) 1; B. W. Montague, Phys. Rept. **113** (1984) 1; J. S. Bell, CERN-75-11, 38p (1975)
[97] R. Prigl et al., Nucl. Instr. and Methods Phys. Res. **A374** (1996) 118; X. Fei, V. Hughes, R. Prigl, Nucl. Instr. and Methods Phys. Res. **A394** (1997) 349
[98] W. Liu et al., Phys. Rev. Lett. **82** (1999) 711
[99] T. Kinoshita, M. Nio, Phys. Rev. D **53** (1996) 4909; M. Nio, T. Kinoshita, Phys. Rev. D **55** (1997) 7267; T. Kinoshita, hep-ph/9808351
[100] A. Czarnecki, S. I. Eidelman, S. G. Karshenboim, Phys. Rev. D **65** (2002) 053004; S. G. Karshenboim, V. A. Shelyuto, Phys. Lett. B **517** (2001) 32
[101] G. Charpak et al., Phys. Rev. Lett. **6** (1961) 128; G. Charpak et al., Nuovo Cimento **22** (1961) 1043
[102] J. Bailey et al., Phys. Lett. B **28** (1968) 287; Nuovo Cimento A **9** (1972) 369
[103] S. Eidelman et al. [Particle Data Group], Phys. Lett. B **592** (2004) 1
[104] W.-M. Yao et al. [Particle Data Group], J. Phys. G **33** (2006) 1, URL `http://pdg.lbl.gov`
[105] B. C. Odom, D. Hanneke, B. D'Urso, G. Gabrielse, Phys. Rev. Lett. **97** (2006) 030801
[106] D. Hanneke, S. Fogwell, G. Gabrielse, Phys. Rev. Lett. **100** (2008) 120801
[107] G. Gabrielse, D. Hanneke, T. Kinoshita, M. Nio, B. Odom, Phys. Rev. Lett. **97** (2006) 030802 [Erratum-ibid. **99** (2007) 039902]
[108] T. Aoyama, M. Hayakawa, T. Kinoshita, M. Nio, Phys. Rev. Lett. **99** (2007) 110406; Phys. Rev. D **77** (2008) 053012
[109] T. Kinoshita, B. Nizic, Y. Okamoto, Phys. Rev. D **41** (1990) 593
[110] T. Appelquist, J. Carrazone, Phys. Rev. D **11** (1975) 2856
[111] B. L. Roberts, Nucl. Phys. B (Proc. Suppl.) **131** (2004) 157; R. M. Carey et al, Proposal of the BNL Experiment E969, 2004; J-PARC Letter of Intent L17
[112] A. Petermann, Helv. Phys. Acta **30** (1957) 407; Nucl. Phys. **5** (1958) 677
[113] C. M. Sommerfield, Phys. Rev. **107** (1957) 328; Ann. Phys. (N.Y.) **5** (1958) 26
[114] M. V. Terentev, Sov. Phys. JETP **16** (1963) 444 [Zh. Eksp. Teor. Fiz. **43** (1962) 619]
[115] J. A. Mignaco, E. Remiddi, Nuovo Cim. A **60** (1969) 519; R. Barbieri, E. Remiddi, Phys. Lett. B **49** (1974) 468; Nucl. Phys. B **90** (1975) 233; R. Barbieri, M. Caffo, E. Remiddi, Phys. Lett. B **57** (1975) 460; M. J. Levine, E. Remiddi, R. Roskies, Phys. Rev. D **20** (1979) 2068; S. Laporta, E. Remiddi, Phys. Lett. B **265** (1991) 182; S. Laporta, Phys. Rev. D **47** (1993) 4793; Phys. Lett. B **343** (1995) 421; S. Laporta, E. Remiddi, Phys. Lett. B **356** (1995) 390
[116] S. Laporta, E. Remiddi, Phys. Lett. B **379** (1996) 283
[117] T. Kinoshita, Phys. Rev. Lett. **75** (1995) 4728
[118] M. Caffo, E. Remiddi, S. Turrini, Nucl. Phys. B **141** (1978) 302; M. Caffo, S. Turrini, E. Remiddi, Phys. Rev. D **30** (1984) 483; E. Remiddi, S. P. Sorella, Lett. Nuovo Cim. **44** (1985) 231; S. Laporta, Phys. Lett. B **312** (1993) 495
[119] A. L. Kataev, Phys. Lett. B **284** (1992) 401; R. N. Faustov, A. L. Kataev, S. A. Larin, V. V. Starshenko, Phys. Lett. B **254** (1991) 241; D. J. Broadhurst, A. L. Kataev, O. V. Tarasov, Phys. Lett. B **298** (1993) 445; P. A. Baikov, D. J. Broadhurst, hep-ph/9504398
[120] J. P. Aguilar, D. Greynat, E. de Rafael, Phys. Rev. D **77** (2008) 093010
[121] T. Kinoshita, W. B. Lindquist, Phys. Rev. Lett. **47** (1981) 1573
[122] T. Kinoshita, W. B. Lindquist, Phys. Rev. D **27** (1983) 867; Phys. Rev. D **27** (1983) 877; Phys. Rev. D **27** (1983) 886; Phys. Rev. D **39** (1989) 2407; Phys. Rev. D **42** (1990) 636

[123] T. Kinoshita, In: *Quantum Electrodynamics*, ed by T. Kinoshita (World Scientific, Singapore 1990) pp 218–321
[124] T. Kinoshita, Phys. Rev. D **47** (1993) 5013
[125] V. W. Hughes, T. Kinoshita, Rev. Mod. Phys. **71** (1999) S133
[126] T. Kinoshita, M. Nio, Phys. Rev. Lett. **90** (2003) 021803; Phys. Rev. D **70** (2004) 113001
[127] T. Kinoshita, M. Nio, Phys. Rev. D **73** (2006) 013003
[128] R.S. Van Dyck, P.B. Schwinberg, H.G. Dehmelt, Phys. Rev. Lett. **59** (1987) 26
[129] P. Cladé et al., Phys. Rev. Lett. **96** (2006) 033001
[130] V. Gerginov et al., Phys. Rev. A **73** (2006) 032504
[131] H. Suura, E. Wichmann, Phys. Rev. **105** (1957) 1930; A. Petermann, Phys. Rev. **105** (1957) 1931
[132] H. H. Elend, Phys. Lett. **20** (1966) 682; Erratum-ibid. **21** (1966) 720
[133] B. E. Lautrup, E. de Rafael, Nuovo Cim. A **64** (1969) 322
[134] B. Lautrup, Phys. Lett. B **69** (1977) 109
[135] B. E. Lautrup, E. de Rafael, Nucl. Phys. B **70** (1974) 317
[136] S. G. Gorishnii, A. L. Kataev, S. A. Larin, L. R. Surguladze, Phys. Lett. B **256** (1991) 81; S. G. Gorishnii, A. L. Kataev, S. A. Larin, Phys. Lett. B **273** (1991) 141 [Erratum-ibid. B **275** (1992) 512; Erratum-ibid. B **341** (1995) 448]
[137] G. Li, R. Mendel, M. A. Samuel, Phys. Rev. D **47** (1993) 1723
[138] T. Kinoshita, Nuovo Cim. B **51** (1967) 140;
T. Kinoshita, W. B. Lindquist, Phys. Rev. D **27** (1983) 867
[139] B. E. Lautrup, E. de Rafael, Phys. Rev. **174** (1968) 1835;
B. E. Lautrup, M. A. Samuel, Phys. Lett. B **72** (1977) 114
[140] M. A. Samuel, G. Li, Phys. Rev. D **44** (1991) 3935 [Errata-ibid. D **46** (1992) 4782; D **48** (1993) 1879]
[141] S. Laporta, Nuovo Cim. A **106** (1993) 675
[142] S. Laporta, E. Remiddi, Phys. Lett. B **301** (1993) 440
[143] J. H. Kühn, A. I. Onishchenko, A. A. Pivovarov, O. L. Veretin, Phys. Rev. D **68** (2003) 033018
[144] A. Czarnecki, M. Skrzypek, Phys. Lett. B **449** (1999) 354
[145] S. Friot, D. Greynat, E. de Rafael, Phys. Lett. B **628** (2005) 73
[146] S. G. Karshenboim, Phys. Atom. Nucl. **56** (1993) 857 [Yad. Fiz. **56N6** (1993) 252]
[147] S. Laporta, Phys. Lett. B **338** (1994) 522
[148] T. Kinoshita, M. Nio, Phys. Rev. D **73** (2006) 053007
[149] A. L. Kataev, Nucl. Phys. Proc. Suppl. **155** (2006) 369; hep-ph/0602098; Phys. Rev. D **74** (2006) 073011
[150] T. Aoyama, M. Hayakawa, T. Kinoshita, M. Nio and N. Watanabe, Phys. Rev. D **78** (2008) 053005
[151] P. A. Baikov, K. G. Chetyrkin and C. Sturm, Nucl. Phys. Proc. Suppl. **183** (2008) 8
[152] V. B. Berestetskii, O. N. Krokhin, A. K. Khelbnikov, Sov. Phys. JETP **3** (1956) 761 [Zh. Eksp. Teor. Fiz. **30** (1956) 788]
[153] S. J. Brodsky, E. de Rafael, Phys. Rev. **168** (1968) 1620
[154] B. E. Lautrup, M. A. Samuel, Phys. Lett. B **72** (1977) 114
[155] T. Kinoshita, Phys. Rev. Lett. **61** (1988) 2898
[156] M. A. Samuel, Phys. Rev. D **45** (1992) 2168
[157] R. Barbieri, E. Remiddi, Nucl. Phys. B **90** (1975) 233
[158] R. Barbieri, E. Remiddi, Phys. Lett. B **57** (1975) 273
[159] S. Laporta, P. Mastrolia, E. Remiddi, Nucl. Phys. B **688** (2004) 165; P. Mastrolia, E. Remiddi, Nucl. Phys. B (Proc. Suppl.) **89** (2000) 76
[160] F. Jegerlehner, Nucl. Phys. Proc. Suppl. **162** (2006) 22
[161] K. Adel, F. J. Yndurain, hep-ph/9509378
[162] D. H. Brown, W. A. Worstell, Phys. Rev. D **54** (1996) 3237
[163] R. Alemany, M. Davier, A. Höcker, Eur. Phys. J. C **2** (1998) 123
[164] M. Davier, A. Höcker, Phys. Lett. B **419** (1998) 419; Phys. Lett. B **435** (1998) 427
[165] F. Jegerlehner, In: *Radiative Corrections*, ed by J. Solà (World Scientific, Singapore 1999) pp 75–89
[166] A. D. Martin, J. Outhwaite, M. G. Ryskin, Phys. Lett. B **492** (2000) 69; Eur. Phys. J. C **19** (2001) 681
[167] M. R. Whalley, J. Phys. G **29** (2003) A1
[168] A. E. Blinov et al., Z. Phys. C **70** (1996) 31
[169] V. M. Aulchenko et al. [CMD-2 Collaboration], JETP Lett. **82** (2005) 743 [Pisma Zh. Eksp. Teor. Fiz. **82** (2005) 841]; R. R. Akhmetshin et al., JETP Lett. **84** (2006) 413 [Pisma Zh. Eksp. Teor. Fiz. **84** (2006) 491]; Phys. Lett. B **648** (2007) 28
[170] F. Nguyen [for the KLOE Collaboration], Nucl. Phys. Proc. Suppl. **181-182** (2008) 106; F. Ambrosino et al. [KLOE Collaboration], Phys. Lett. B **670** (2009) 285; G. Venanzoni [for the KLOE Collaboration], *Pion form factor at KLOE*, presented at the Intern. Workshop on Tau Lepton Physics, TAU08 Novosibirsk, Russia, September 22-25, 2008
[171] M. N. Achasov et al. [SND Collaboration], J. Exp. Theor. Phys. **103** (2006) 380 [Zh. Eksp. Teor. Fiz. **130** (2006) 437]
[172] B. Aubert et al. [BABAR Collaboration], Phys. Rev. D **70** (2004) 072004; **71** (2005) 052001; **73** (2006) 012005; **73** (2006) 052003
[173] B. Aubert et al. [BABAR Collaboration], Phys. Rev. D **76** (2007) 012008; ibid. 092005; ibid. 092006; D **77** (2008) 092002
[174] F. Jegerlehner, Nucl. Phys. Proc. Suppl. **181-182** (2008) 26
[175] M. Davier [for the BABAR Collaboration], *Precision Measurement of the* $e^+e^- \to \pi^+\pi^-(\gamma)$ *Cross Section with the ISR Method*, presented at the Intern. Workshop on Tau Lepton Physics, TAU08 Novosibirsk, Russia, September 22-25, 2008

[176] H. Leutwyler, *Electromagnetic form factor of the pion*, hep-ph/0212324; G. Colangelo, Nucl. Phys. Proc. Suppl. **131** (2004) 185; ibid. **162** (2006) 256
[177] M. Davier, S. Eidelman, A. Höcker, Z. Zhang, Eur. Phys. J. C **27** (2003) 497; ibid. **31** (2003) 503
[178] S. Ghozzi, F. Jegerlehner, Phys. Lett. B **583** (2004) 222
[179] S. Narison, Phys. Lett. B **568** (2003) 231
[180] V. V. Ezhela, S. B. Lugovsky, O. V. Zenin, hep-ph/0312114
[181] K. Hagiwara, A. D. Martin, D. Nomura, T. Teubner, Phys. Lett. B **557** (2003) 69; Phys. Rev. D **69** (2004) 093003
[182] J. F. de Troconiz, F. J. Yndurain, Phys. Rev. D **71** (2005) 073008
[183] S. Eidelman, *Status of* $(g_\mu - 2)/2$ *in Standard Model*, in "HIGH ENERGY PHYSICS, ICHEP '06", proceedings of the 33rd Intern. Conference on High Energy Physics 2006, Moscow (Russia), eds. A. Sissakian, G. Kozlov and E. Kolganova, World Scientific, Singapore, 2007) p. 547; M. Davier, Nucl. Phys. Proc. Suppl. **169** (2007) 288
[184] K. Hagiwara, A. D. Martin, D. Nomura, T. Teubner, Phys. Lett. B **649** (2007) 173; T. Teubner, Nucl. Phys. Proc. Suppl. **181-182** (2008) 20
[185] A. Bramòn, E. Etim, M. Greco, Phys. Lett. **39**B (1972) 514
[186] V. Barger, W. F. Long, M. G. Olsson, Phys. Lett. **60**B (1975) 89
[187] J. Calmet, S. Narison, M. Perrottet, E. de Rafael, Phys. Lett. B **61** (1976) 283; Rev. Mod. Phys. **49** (1977) 21
[188] S. Narison, J. Phys. G: Nucl. Phys. **4** (1978) 1849
[189] Ľ. Martinovič, S. Dubnička, Phys. Rev. D **42** (1990) 884
[190] A. Z. Dubničková, S. Dubnička, P. Strizenec, Dubna-Report, JINR-E2-92-28, 1992
[191] V. N. Baier, V. S. Fadin, Phys. Lett. B **27** (1968) 223
[192] S. Spagnolo, Eur. Phys. J. C **6** (1999) 637; A. B. Arbuzov, E. A. Kuraev, N. P. Merenkov, L. Trentadue, JHEP **12** (1998) 009; S. Binner, J. H. Kühn, K. Melnikov, Phys. Lett. B **459** (1999) 279; M. I. Konchatnij, N. P. Merenkov, JETP Lett. **69** (1999) 811; V. A. Khoze et al., Eur. Phys. J. C **18** (2001) 481
[193] M. Benayoun, S. I. Eidelman, V. N. Ivanchenko, Z. K. Silagadze, Mod. Phys. Lett. A **14** (1999) 2605
[194] H. Czyż, J. H. Kühn, Eur. Phys. J. C **18** (2001) 497; G. Rodrigo, A. Gehrmann-De Ridder, M. Guilleaume, J. H. Kühn, Eur. Phys. J. C **22** (2001) 81; G. Rodrigo, H. Czyż, J. H. Kühn, M. Szopa, Eur. Phys. J. C **24** (2002) 71; H. Czyż, A. Grzelińska, J. H. Kühn, G. Rodrigo, Eur. Phys. J. C **27** (2003) 563; Eur. Phys. J. C **33** (2004) 333; Eur. Phys. J. C **39** (2005) 411
[195] H. Czyż, A. Grzelinska, Acta Phys. Polon. B **38** (2007) 2989
[196] W. Kluge, Nucl. Phys. Proc. Suppl. **181-182**, 280 (2008)
[197] A. B. Arbuzov, V. A. Astakhov, A. V. Fedorov, G. V. Fedotovich, E. A. Kuraev, N. P. Merenkov, JHEP **9710** (1997) 006
[198] V. A. Khoze, M. I. Konchatnij, N. P. Merenkov, G. Pancheri, L. Trentadue, O. N. Shekhovzova, Eur. Phys. J. C **18** (2001) 481
[199] A. Hoefer, J. Gluza, F. Jegerlehner, Eur. Phys. J. C **24** (2002) 51
[200] A. B. Arbuzov, G. V. Fedotovich, F. V. Ignatov, E. A. Kuraev, A. L. Sibidanov, Eur. Phys. J. C **46** (2006) 689
[201] J. Gluza, A. Hoefer, S. Jadach, F. Jegerlehner, Eur. Phys. J. C **28** (2003) 261
[202] Y. S. Tsai, Phys. Rev. D **4** (1971) 2821 [Erratum-ibid. D **13** (1976) 771];
S. I. Eidelman, V. N. Ivanchenko, Phys. Lett. B **257** (1991) 437; Nucl. Phys. Proc. Suppl. **40** (1995) 131; ibid. **55C** (1997) 181
[203] R. Barate et al. [ALEPH Collaboration], Z. Phys. C **76** (1997) 15; Eur. Phys. J. C **4** (1998) 409; S. Schael et al. [ALEPH Collaboration], Phys. Rept. **421** (2005) 191
[204] K. Ackerstaff et al. [OPAL Collaboration], Eur. Phys. J. C **7** (1999) 571
[205] S. Anderson et al. [CLEO Collaboration], Phys. Rev. D **61** (2000) 112002
[206] M. Fujikawa, H. Hayashii, S. Eidelman [for the Belle Collaboration], Phys. Rev. D **78**, 072006 (2008); H. Hayashii [for the Belle Collaboration], $\tau \to 2\pi\nu_\tau$ *at Belle*, presented at the Intern. Workshop on Tau Lepton Physics, TAU08 Novosibirsk, Russia, September 22-25, 2008
[207] M. Davier, A. Höcker, Z. Zhang, Rev. Mod. Phys. **78** (2006) 1043
[208] W. J. Marciano, A. Sirlin, Phys. Rev. Lett. **61** (1988) 1815
[209] E. Braaten, C. S. Li, Phys. Rev. D **42** (1990) 3888
[210] R. Decker, M. Finkemeier, Nucl. Phys. B **438** (1995) 17
[211] J. Erler, Rev. Mex. Fis. **50** (2004) 200
[212] V. Cirigliano, G. Ecker, H. Neufeld, Phys. Lett. B **513** (2001) 361; JHEP **0208** (2002) 002
[213] F. Flores-Baez, A. Flores-Tlalpa, G. Lopez Castro, G. Toledo Sanchez, Phys. Rev. D **74** (2006) 071301; F. V. Flores-Baez, G. L. Castro, G. Toledo Sanchez, Phys. Rev. D **76** (2007) 096010
[214] K. Maltman, C. E. Wolfe, Phys. Rev. D **73** (2006) 013004
[215] M. Davier, eConf **C0209101** (2002) WE03 [hep-ex/0301035]
[216] M. Benayoun, P. David, L. DelBuono, O. Leitner, H. B. O'Connell, Eur. Phys. J. C **55** (2008) 199; Nucl. Phys. Proc. Suppl. 181-182 (2008) 161; M. Benayoun, arXiv:0805.1835 [hep-ph]
[217] M. Passera, W. J. Marciano and A. Sirlin, Phys. Rev. D **78**, 013009 (2008); arXiv:0809.4062 [hep-ph]
[218] P. A. M. Dirac, Théorie du positron. In: *Septième Conseile de Physique Solvay: Structure et propriétés des noyaux atomique, October 22-29, 1933*, (Gauthier-Villars, Paris 1934), pp.203-230; P. A. M. Dirac, Proc. Cambridge. Phil. Soc. **30** (1934) 150

[219] J. Schwinger, Phys. Rev. **75** (1949) 651
[220] R. P. Feynman, Phys. Rev. **76** (1949) 749
[221] R. Jost, J. M. Luttinger, Helv. Phys. Acta **23** (1950) 201
[222] H. Fritzsch, Phys. Rev. D **10** (1974) 1624; H. Fritzsch, H. Leutwyler, Report CALT-68-416, 1974
[223] T. Appelquist, H. Georgi, Phys. Rev. D **8** (1973) 4000; A. Zee, Phys. Rev. D **8** (1973) 4038
[224] K. G. Chetyrkin, A. L. Kataev, F. V. Tkachov, Phys. Lett. B **85** (1979) 277; M. Dine, J. Sapirstein, Phys. Rev. Lett. **43** (1979) 668; W. Celmaster, R. J. Gonsalves, Phys. Rev. Lett. **44** (1980) 560; K. G. Chetyrkin, Phys. Lett. B **391** (1997) 402
[225] S. G. Gorishnii, A. L. Kataev, S. A. Larin, Phys. Lett. B **259** (1991) 144; L. R. Surguladze, M. A. Samuel, Phys. Rev. Lett. **66** (1991) 560 [Erratum-ibid. **66** (1991) 2416]
[226] P. A. Baikov, K. G. Chetyrkin, J. H. Kühn, Phys. Rev. Lett. **88** (2002) 012001; Phys. Rev. D **67** (2003) 074026; Phys. Lett. B **559** (2003) 245; Phys. Rev. Lett. **101** (2008) 012002
[227] V. A. Novikov, L. B. Okun, M. A. Shifman, A. I. Vainshtein, M. B. Voloshin, V. I. Zakharov, Phys. Rept. **41** (1978) 1
[228] K. G. Chetyrkin, J. H. Kühn, Phys. Lett. B **342** (1995) 356; K. G. Chetyrkin, R. V. Harlander, J. H. Kühn, Nucl. Phys. B **586** (2000) 56 [Erratum-ibid. B **634** (2002) 413]
[229] R. V. Harlander, M. Steinhauser, Comput. Phys. Commun. **153** (2003) 244
[230] E. D. Bloom, F. J. Gilman, Phys. Rev. Lett. **25** (1970) 1140; Phys. Rev. D **4** (1971) 2901
[231] E. C. Poggio, H. R. Quinn, S. Weinberg, Phys. Rev. D **13** (1976) 1958
[232] M. A. Shifman, *Quark–hadron duality*, hep-ph/0009131
[233] S. L. Adler, Phys. Rev. D **10** (1974) 3714; A. De Rujula, H. Georgi, Phys. Rev. D **13** (1976) 1296
[234] S. Eidelman, F. Jegerlehner, A. L. Kataev, O. Veretin, Phys. Lett. B **454** (1999) 369
[235] F. Jegerlehner, J. Phys. G **29** (2003) 101 [hep-ph/0104304]; Nucl. Phys. Proc. Suppl. **126** (2004) 325
[236] M.A. Shifman, A.I. Vainshtein, V.I. Zakharov, Nucl. Phys. B **147** (1979) 385
[237] B. Krause, Phys. Lett. B **390** (1997) 392
[238] J. S. Schwinger, *Particles, sources, and fields*, Vol. 3 (Addison–Wesley, Redwood City (USA) 1989), p. 99; see also: M. Drees, K. i. Hikasa, Phys. Lett. B **252** (1990) 127, where a misprint in Schwinger's formula is corrected
[239] K. Melnikov, Int. J. Mod. Phys. A **16** (2001) 4591
[240] J. J. Sakurai, Annals of Phys. (NY) **11** (1960) 1; H. Joos, Acta Phys. Austriaca Suppl. **4** (1967); N. M. Kroll, T. D. Lee, B. Zumino, Phys. Rev. **157** (1967) 1376
[241] H. Kolanoski, P. Zerwas, Two-Photon Physics, In: *High Energy Electron-Positron Physics*, ed. A. Ali, P. Söding, (World Scientific, Singapore 1988) pp 695–784; D. Williams et al. [Crystal Ball Collaboration], SLAC-PUB-4580, 1988, unpublished
[242] M. Hayakawa, T. Kinoshita, A. I. Sanda, Phys. Rev. Lett. **75** (1995) 790; Phys. Rev. D **54** (1996) 3137
[243] J. Bijnens, E. Pallante, J. Prades, Phys. Rev. Lett. **75** (1995) 1447 [Erratum-ibid. **75** (1995) 3781]; Nucl. Phys. B **474** (1996) 379; [Erratum-ibid. **626** (2002) 410]
[244] E. de Rafael, Phys. Lett. B **322** (1994) 239
[245] M. Hayakawa, T. Kinoshita, Phys. Rev. D **57** (1998) 465 [Erratum-ibid. D **66** (2002) 019902]
[246] J. Wess, B. Zumino, Phys. Lett. B **37** (1971) 95
[247] E. Witten, Nucl. Phys. B **223** (1983) 422
[248] S. L. Adler, Phys. Rev. **177** (1969) 2426; J. S. Bell, R. Jackiw, Nuovo Cim. **60A** (1969) 47; W. A. Bardeen, Phys. Rev. **184** (1969) 1848
[249] M. Knecht, A. Nyffeler, M. Perrottet, E. de Rafael, Phys. Rev. Lett. **88** (2002) 071802
[250] S. J. Brodsky, G. R. Farrar, Phys. Rev. Lett. **31** (1973) 1153; Phys. Rev. D **11** (1975) 1309
[251] G. 't Hooft, Nucl. Phys. B **72** (1974) 461; ibid. **75** (1974) 461
[252] A. V. Manohar, Hadrons in the $1/N$ Expansion, In: *At the frontier of Particle Physics*, ed M. Shifman, (World Scientific, Singapore 2001) Vol. 1, pp 507–568
[253] H. Leutwyler, Nucl. Phys. Proc. Suppl. **64** (1998) 223; R. Kaiser, H. Leutwyler, Eur. Phys. J. C **17** (2000) 623
[254] S. Peris, M. Perrottet, E. de Rafael, JHEP **9805** (1998) 011; M. Knecht, S. Peris, M. Perrottet, E. de Rafael, Phys. Rev. Lett. **83** (1999) 5230
[255] I. Blokland, A. Czarnecki, K. Melnikov, Phys. Rev. Lett. **88** (2002) 071803
[256] M. J. Ramsey-Musolf, M. B. Wise, Phys. Rev. Lett. **89** (2002) 041601
[257] K. Melnikov, A. Vainshtein, Phys. Rev. D **70** (2004) 113006
[258] J. L. Rosner, Ann. Phys. (N.Y.) **44**, 11 (1967). Implicitly, the method of Gegenbauer polynomials was already used in the following papers: M. Baker, K. Johnson,, R. Willey, Phys. Rev. **136**, B1111 (1964); **163**, 1699 (1967); M. J. Levine, R. Roskies, Phys. Rev. D **9**, 421 (1974); M. J. Levine, E. Remiddi,, R. Roskies, *ibid.* **20**, 2068 (1979); R. Z. Roskies, E. Remiddi,, M. J. Levine, in *Quantum Electrodynamics* [22], p. 162
[259] H. J. Behrend et al. [CELLO Collaboration], Z. Phys. C **49** (1991) 401
[260] J. Gronberg et al. [CLEO Collaboration], Phys. Rev. D **57** (1998) 33
[261] G. P. Lepage, S. J. Brodsky, Phys. Rev. D **22** (1980) 2157; S. J. Brodsky, G. P. Lepage, Phys. Rev. D **24** (1981) 1808
[262] A. V. Efremov, A. V. Radyushkin, Phys. Lett. B **94** (1980) 245; A. V. Radyushkin, R. Ruskov, Phys. Lett. B **374** (1996) 173; A. V. Radyushkin, Acta Phys. Polon. B **26** (1995) 2067
[263] S. Ong, Phys. Rev. D **52** (1995) 3111; P. Kroll, M. Raulfs, Phys. Lett. B **387** (1996) 848

[264] F. del Aguila, M. K. Chase, Nucl. Phys. B **193** (1981) 517; E. Braaten, Phys. Rev. D **28** (1983) 524; E. P. Kadantseva, S. V. Mikhailov, A. V. Radyushkin, Yad. Fiz. **44** (1986) 507 [Sov. J. Nucl. Phys. **44** (1986) 326]
[265] A. Khodjamirian, Eur. Phys. J. C **6** (1999) 477
[266] M. Knecht, A. Nyffeler, Eur. Phys. J. C **21** (2001) 659
[267] B. Moussallam, Phys. Rev. D **51** (1995) 4939; M. Knecht, S. Peris, M. Perrottet, E. de Rafael in Ref. [254]
[268] A. Nyffeler, Nucl. Phys. Proc. Suppl. **116** (2003) 225
[269] N. S. Craigie, J. Stern, Phys. Rev. D **26** (1982) 2430
[270] A. Nyffeler, arXiv:0901.1172 [hep-ph]
[271] V. M. Belyaev and Y. I. Kogan, Sov. J. Nucl. Phys. **40** (1984) 659 [Yad. Fiz. **40** (1984) 1035]
[272] B. L. Ioffe, A. V. Smilga, Nucl. Phys. B **232** (1984) 109
[273] V. Mateu, J. Portoles, Eur. Phys. J. C **52** (2007) 325
[274] S. Narison, Phys. Lett. B **666** (2008) 455
[275] A. Vainshtein, Phys. Lett. B **569** (2003) 187
[276] A. E. Dorokhov, Eur. Phys. J. C **42** (2005) 309
[277] V. Y. Petrov, M. V. Polyakov, R. Ruskov, C. Weiss and K. Goeke, Phys. Rev. D **59** (1999) 114018; K. Goeke, H. C. Kim, M. M. Musakhanov and M. Siddikov, Phys. Rev. D **76** (2007) 116007
[278] I. I. Balitsky and A. V. Yung, Phys. Lett. B **129** (1983) 328
[279] I. I. Balitsky, A. V. Kolesnichenko and A. V. Yung, Sov. J. Nucl. Phys. **41** (1985) 178 [Yad. Fiz. **41** (1985) 282]
[280] P. Ball, V. M. Braun, N. Kivel, Nucl. Phys. B **649** (2003) 263
[281] S. Bethke, J. Phys. G **26** (2000) R27 [arXiv:hep-ex/0004021]
[282] E. V. Shuryak, A. I. Vainsthein, Nucl. Phys. B **199** (1982) 451
[283] V. A. Novikov, M. A. Shifman, A. I. Vainshtein, M. B. Voloshin, V. I. Zakharov, Nucl. Phys. B **237** (1984) 525
[284] A. Czarnecki, W. J. Marciano, A. Vainshtein, Phys. Rev. D **67** (2003) 073006 [Erratum-ibid. D **73** (2006) 119901]
[285] A. Czarnecki, W. J. Marciano, A. Vainshtein, Acta Phys. Polon. B **34** (2003) 5669
[286] M. Knecht, S. Peris, M. Perrottet, E. de Rafael, JHEP **0403** (2004) 035
[287] S. L. Adler, W. A. Bardeen, Phys. Rev. **182** (1969) 1517
[288] G. 't Hooft, In: *Recent Developments in Gauge Theories*, Proceedings of the Summer-Institute, Cargese, France, 1979, ed by G. 't Hooft et al., NATO Advanced Study Institute Series B: Physics Vol. 59 (Plenum Press, New York 1980)
[289] J. Bijnens, F. Persson, arXiv:hep-ph/0106130
[290] E. Bartos, A. Z. Dubnickova, S. Dubnicka, E. A. Kuraev, E. Zemlyanaya, Nucl. Phys. B **632** (2002) 330
[291] A. E. Dorokhov and W. Broniowski, Phys. Rev. D **78**, 073011 (2008)
[292] J. Bijnens, E. Gamiz, E. Lipartia, J. Prades, JHEP **0304** (2003) 055
[293] C. Amsler *et al.* [Particle Data Group], Phys. Lett. B **667** (2008) 1
[294] J. Prades, E. de Rafael, A. Vainshtein, arXiv:0901.0306 [hep-ph]
[295] J. Bijnens, C. Bruno, E. de Rafael, Nucl. Phys. B **390** (1993) 501
[296] J. Bijnens, E. de Rafael, H. q. Zheng, Z. Phys. C **62** (1994) 437
[297] J. Bijnens, J. Prades, Z. Phys. C **64** (1994) 475
[298] J. Bijnens, J. Prades, Acta Phys. Polon. B **38** (2007) 2819; J. Prades, Nucl. Phys. Proc. Suppl. **181-182** (2008) 15
[299] A. Nyffeler, Nucl. Phys. Proc. Suppl. **121** (2003) 187
[300] L. Ametller, Phys. Scripta **T99** (2002) 45 [arXiv:hep-ph/0111278]
[301] A. A. Pivovarov, Phys. Atom. Nucl. **66** (2003) 902 [Yad. Fiz. **66** (2003) 934]
[302] J. Erler, G. T. Sanchez, Phys. Rev. Lett. **97** (2006) 161801
[303] R. Barbieri, E. Remiddi, Hadronic contributions to the muon g-2. In: *The second DAΦNE physics handbook, Vol. II*, eds L. Maiani et al. (INFN-LNF,Frascati 1995) pp 467–470
[304] G. 't Hooft, Nucl. Phys. B **33** (1971) 173; **35** (1971) 167; G. 't Hooft, M. Veltman, Nucl. Phys. B **50** (1972) 318
[305] R. Jackiw, S. Weinberg, Phys. Rev. D **5** (1972) 2396; I. Bars, M. Yoshimura, Phys. Rev. D **6** (1972) 374; G. Altarelli, N. Cabibbo, L. Maiani, Phys. Lett. B **40** (1972) 415; W. A. Bardeen, R. Gastmans, B. Lautrup, Nucl. Phys. B **46** (1972) 319; K. Fujikawa, B. W. Lee, A. I. Sanda, Phys. Rev. D **6** (1972) 2923
[306] E. A. Kuraev, T. V. Kukhto, A. Schiller, Sov. J. Nucl. Phys. **51** (1990) 1031 [Yad. Fiz. **51** (1990) 1631]; T. V. Kukhto, E. A. Kuraev, A. Schiller, Z. K. Silagadze, Nucl. Phys. **B 371** (1992) 567
[307] C. Bouchiat, J. Iliopoulos, P. Meyer, Phys. Lett. **38**B (1972) 519; D. Gross, R. Jackiw, Phys. Rev. D **6** (1972) 477; C. P. Korthals Altes, M. Perrottet, Phys. Lett. **39**B (1972) 546
[308] S. Peris, M. Perrottet, E. de Rafael, Phys. Lett. B **355** (1995) 523
[309] A. Czarnecki, B. Krause, W. Marciano, Phys. Rev. D **52** (1995) R2619
[310] G. Degrassi, G. F. Giudice, Phys. Rev. **58D** (1998) 053007
[311] E. D'Hoker, Phys. Rev. Lett. **69** (1992) 1316
[312] M. Knecht, S. Peris, M. Perrottet, E. de Rafael, JHEP **0211** (2002) 003
[313] F. Jegerlehner, O. V. Tarasov, Phys. Lett. B **639** (2006) 299
[314] A. Czarnecki, B. Krause, W. J. Marciano, Phys. Rev. Lett. **76** (1996) 3267
[315] S. Heinemeyer, D. Stöckinger, G. Weiglein, Nucl. Phys. B **699** (2004) 103
[316] T. Gribouk, A. Czarnecki, Phys. Rev. D **72** (2005) 053016
[317] Ref. [148] with updated value for α from Ref. [106]; see also Refs. [52],[112]–[159]

[318] see Refs. [243,242,245,31,257] and this work
[319] see Refs. [308,309,314,310,312,284,315,316]
[320] J. C. Pati, A. Salam, Phys. Rev. Lett. **31** (1973) 661; Phys. Rev. D **8** (1973) 1240; H. Georgi, S. L. Glashow, Phys. Rev. Lett. **32** (1974) 438
[321] J. R. Ellis, S. Kelley, D. V. Nanopoulos, Phys. Lett. B **249** (1990) 441; ibid **260** (1991) 131; U. Amaldi, W. de Boer, H. Fürstenau, Phys. Lett. B **260** (1991) 447; P. Langacker, M. x. Luo, Phys. Rev. D **44** (1991) 817
[322] LEP Electroweak Working Group (LEP EWWG),
`http://lepewwg.web.cern.ch/LEPEWWG/plots/summer2006`
[ALEPH, DELPHI, L3, OPAL, SLD Collaborations], *Precision electroweak measurements on the Z resonance*, Phys. Rept. **427** (2006) 257;
`http://lepewwg.web.cern.ch/LEPEWWG/Welcome.html` (March 2008 update); (see also: Tevatron Electroweak Working Group, arXiv:0808.0147 [hep-ex]).
[323] J. Erler, P. Langacker, *Electroweak model and constraints on new physics* in W. M. Yao et al. [Particle Data Group], J. Phys. G **33** (2006) 1
[324] [Tevatron Electroweak Working Group and CDF Collaboration and D0 Collab.], arXiv:0803.1683 [hep-ex].
[325] Heavy Flavor Averaging Group (HFAG),
`http://www.slac.stanford.edu/xorg/hfag/`
`http://www-cdf.fnal.gov/physics/new/bottom/bottom.html`
[326] G. D'Ambrosio, G. F. Giudice, G. Isidori, A. Strumia, Nucl. Phys. B **645** (2002) 155
[327] R. S. Chivukula, H. Georgi, Phys. Lett. B **188** (1987) 99
[328] W. Altmannshofer, A. J. Buras, D. Guadagnoli, JHEP **0711** (2007) 065
[329] I. B. Khriplovich, S. K. Lamoreaux, CP Violation without Strangeness: Electric Dipole Moments of Particles, Atoms, and Molecules, (Springer, Berlin, 1997)
[330] A. Adelmann, K. Kirch, hep-ex/0606034
[331] M. Czakon, J. Gluza, F. Jegerlehner, M. Zrałek, Eur. Phys. J. C **13** (2000) 275
[332] J. P. Leveille, Nucl. Phys. B **137** (1978) 63
[333] C. T. Hill, E. H. Simmons, Phys. Rept. **381** (2003) 235 [Erratum-ibid. **390** (2004) 553]
[334] E. Eichten and K. Lane, Phys. Lett. B **669**, 235 (2008)
[335] R. Foadi, M. T. Frandsen, T. A. Ryttov, F. Sannino, Phys. Rev. D **76** (2007) 055005; T. A. Ryttov, F. Sannino, Phys. Rev. D **76** (2007) 105004
[336] S. Ritt [MEG Collaboration], Nucl. Phys. Proc. Suppl. **162** (2006) 279
[337] R. Barbieri, L. J. Hall, Phys. Lett. B **338** (1994) 212; R. Barbieri, L. J. Hall, A. Strumia, Nucl. Phys. B **445** (1995) 219; J. Hisano, D. Nomura, Phys. Rev. D **59** (1999) 116005
[338] S. L. Glashow, S. Weinberg, Phys. Rev. D **15** (1977) 1958
[339] S. M. Barr, A. Zee, Phys. Rev. Lett. **65** (1990) 21 [Erratum-ibid. **65** (1990) 2920]
[340] D. Chang, W. F. Chang, C. H. Chou, W. Y. Keung, Phys. Rev. D **63** (2001) 091301
[341] K. M. Cheung, C. H. Chou, O. C. W. Kong, Phys. Rev. D **64** (2001) 111301
[342] M. Krawczyk, Acta Phys. Polon. B **33** (2002) 2621; PoS **HEP2005** (2006) 335 [hep-ph/0512371]
[343] K. Cheung, O. C. W. Kong, Phys. Rev. D **68** (2003) 053003
[344] A. Wahab El Kaffas, P. Osland, O. Magne Ogreid, Phys. Rev. D **76** (2007) 095001
[345] J. Ellis, T. Hahn, S. Heinemeyer, K. A. Olive, G. Weiglein, JHEP **0710** (2007) 092
[346] S. Marchetti, S. Mertens, U. Nierste, D. Stöckinger, arXiv:0808.1530 [hep-ph]
[347] J. Wess, B. Zumino, Nucl. Phys. B **70** (1974) 39; R. Haag, J. T. Lopuszanski, M. Sohnius, Nucl. Phys. B **88** (1975) 257
[348] D. Z. Freedman, P. van Nieuwenhuizen, S. Ferrara, Phys. Rev. D **13** (1976) 3214; S. Deser, B. Zumino, Phys. Lett. B **62** (1976) 335; R. Barbieri, S. Ferrara, C. A. Savoy, Phys. Lett. B **119** (1982) 343
[349] H. P. Nilles, Phys. Rep. **110** (1984) 1; H. E. Haber, G. L. Kane, Phys. Rep. **117** (1985) 75; L. Ibáñez, Beyond the Standard Model. In: CERN Yellow Report, CERN 92-06 (1992) 131-237
[350] J. R. Ellis, J. S. Hagelin, D. V. Nanopoulos, K. A. Olive, M. Srednicki, Nucl. Phys. B **238** (1984) 453
[351] C. L. Bennett et al. [WMAP Collaboration], Astrophys. J. Suppl. **148** (2003) 1; D. N. Spergel et al. [WMAP Collaboration], Astrophys. J. Suppl. **148** (2003) 175
[352] J. R. Ellis, K. A. Olive, Y. Santoso, V. C. Spanos, Phys. Lett. B **565** (2003) 176; Phys. Rev. D **71** (2005) 095007; K. A. Olive, arXiv:0806.1208 [hep-ph]
[353] H. Baer, A. Belyaev, T. Krupovnickas, A. Mustafayev, JHEP **0406** (2004) 044; J. Ellis, S. Heinemeyer, K. A. Olive, G. Weiglein, *Indications of the CMSSM mass scale from precision electroweak data*, hep-ph/0604180
[354] J. R. Ellis, S. Heinemeyer, K. A. Olive, A. M. Weber, G. Weiglein, JHEP **0708** (2007) 083
[355] M. Cirelli, M. Kadastik, M. Raidal, A. Strumia, arXiv:0809.2409 [hep-ph]
[356] M. J. Ramsey-Musolf and S. Su, Phys. Rept. **456**, 1 (2008)
[357] D. Stöckinger, J. Phys. G: Nucl. Part. Phys. 34 (2007) 45; Nucl. Phys. Proc. Suppl. **181-182** (2008) 32
[358] C. D. Froggatt, H. B. Nielsen, Nucl. Phys. B **147** (1979) 277
[359] G. F. Giudice, A. Masiero, Phys. Lett. B **206**, 480 (1988)
[360] E. Dudas, S. Pokorski, C. A. Savoy, Phys. Lett. B **356** (1995) 45
[361] P. Binetruy, S. Lavignac, P. Ramond, Nucl. Phys. B **477**, 353 (1996)

[362] K. Choi, E. J. Chun, H. D. Kim, Phys. Lett. B **394**, 89 (1997)
[363] J. M. Mira, E. Nardi, D. A. Restrepo, Phys. Rev. D **62**, 016002 (2000)
[364] A. S. Joshipura, R. D. Vaidya, S. K. Vempati, Phys. Rev. D **62**, 093020 (2000)
[365] H. K. Dreiner, M. Thormeier, Phys. Rev. D **69** (2004) 053002
[366] M. Veltman, Acta Phys. Polon. **B12** (1981) 437
[367] H. E. Haber, R. Hempfling, Phys. Rev. Lett. **66** (1991) 1815
[368] R. Hempfling, A. H. Hoang, Phys. Lett. B **331** (1994) 99; S. Heinemeyer, W. Hollik, G. Weiglein, Phys. Lett. B **455** (1999) 179; Phys. Rept. **425** (2006) 265
[369] S. Ferrara, E. Remiddi, Phys. Lett. B **53** (1974) 347
[370] J. L. Lopez, D. V. Nanopoulos, X. Wang, Phys. Rev. D **49** (1994) 366; U. Chattopadhyay, P. Nath, Phys. Rev. D **53** (1996) 1648; T. Moroi, Phys. Rev. D **53** (1996) 6565 [Erratum-ibid. D **56** (1997) 4424]
[371] S. P. Martin, J. D. Wells, Phys. Rev. D **64** (2001) 035003
[372] S. Heinemeyer, D. Stöckinger, G. Weiglein, Nucl. Phys. B **690** (2004) 62
[373] A. Arhrib, S. Baek, Phys. Rev. D **65**, 075002 (2002)
[374] C. H. Chen, C. Q. Geng, Phys. Lett. B **511**, 77 (2001)
[375] T. F. Feng, X. Q. Li, L. Lin, J. Maalampi, H. S. Song, Phys. Rev. D **73** (2006) 116001
[376] M. Awramik, M. Czakon, A. Freitas, G. Weiglein, Phys. Rev. **D 69** (2004) 053006
[377] S. Heinemeyer, W. Hollik, D. Stöckinger, A. M. Weber, G. Weiglein, JHEP **0608** (2006) 052.
[378] M. Misiak et al., Phys. Rev. Lett. **98** (2007) 022002
[379] R. Barbieri, G. F. Giudice, Phys. Lett. B **309** (1993) 86; M. Carena, D. Garcia, U. Nierste, C. E. M. Wagner, Phys. Lett. B **499** (2001) 141
[380] L. F. Abbott, P. Sikivie, M. B. Wise, Phys. Rev. D **21** (1980) 1393; M. Ciuchini, G. Degrassi, P. Gambino, G. F. Giudice, Nucl. Phys. B **527** (1998) 21
[381] V. Barger, C. Kao, P. Langacker, H. S. Lee, Phys. Lett. B **614** (2005) 67
[382] R. Barbieri, A. Strumia, hep-ph/0007265; Phys. Lett. B **462**, 144 (1999)
[383] N. Arkani-Hamed, A. G. Cohen, H. Georgi, Phys. Lett. B **513**, 232 (2001); N. Arkani-Hamed, A. G. Cohen, T. Gregoire, J. G. Wacker, JHEP **0208**, 020 (2002)
[384] M. Schmaltz, D. Tucker-Smith, Ann. Rev. Nucl. Part. Sci. **55**, 229 (2005); M. Perelstein, Prog. Part. Nucl. Phys. **58**, 247 (2007); M. C. Chen, Mod. Phys. Lett. A **21**, 621 (2006); E. Accomando *et al.*, hep-ph/0608079, Chapter 7
[385] S. R. Coleman, E. Weinberg, Phys. Rev. D **7**, 1888 (1973)
[386] J. R. Ellis, M. K. Gaillard, D. V. Nanopoulos, C. T. Sachrajda, Phys. Lett. B **83** (1979) 339
[387] N. Arkani-Hamed, A. G. Cohen, E. Katz, A. E. Nelson, JHEP **0207**, 034 (2002)
[388] C. Csaki *et al.*, Phys. Rev. D **67**, 115002 (2003); J. L. Hewett, F. J. Petriello, T. G. Rizzo, JHEP **0310**, 062 (2003); C. Csaki *et al.*, Phys. Rev. D **68**, 035009 (2003); M. Perelstein, M. E. Peskin, A. Pierce, Phys. Rev. D **69**, 075002 (2004); M. C. Chen, S. Dawson, Phys. Rev. D **70**, 015003 (2004); W. Kilian, J. Reuter, Phys. Rev. D **70**, 015004 (2004); G. Marandella, C. Schappacher, A. Strumia, Phys. Rev. D **72**, 035014 (2005)
[389] H. C. Cheng, I. Low, JHEP **0309**, 051 (2003); JHEP **0408**, 061 (2004)
[390] I. Low, JHEP **0410**, 067 (2004)
[391] J. Hubisz, P. Meade, Phys. Rev. D **71**, 035016 (2005)
[392] J. Hubisz, P. Meade, A. Noble, M. Perelstein, JHEP **0601**, 135 (2006)
[393] C. R. Chen, K. Tobe, C. P. Yuan, Phys. Lett. B **640**, 263 (2006)
[394] M. Asano, S. Matsumoto, N. Okada, Y. Okada, Phys. Rev. D **75**, 063506 (2007)
[395] R. S. Hundi, B. Mukhopadhyaya, A. Nyffeler, Phys. Lett. B **649**, 280 (2007)
[396] A. Birkedal, A. Noble, M. Perelstein, A. Spray, Phys. Rev. D **74**, 035002 (2006); C. S. Chen, K. Cheung and T. C. Yuan, Phys. Lett. B **644**, 158 (2007)
[397] S. C. Park, J. Song, Phys. Rev. D **69** (2004) 115010
[398] R. Casalbuoni, A. Deandrea, M. Oertel, JHEP **0402** (2004) 032 (Erratum added online)
[399] S. R. Choudhury, N. Gaur, A. Goyal, Phys. Rev. D **72** (2005) 097702
[400] W. Kilian, J. Reuter, Phys. Rev. D **70** (2004) 015004; J. Y. Lee, JHEP **0506** (2005) 060; T. Han, H. E. Logan, B. Mukhopadhyaya, R. Srikanth, Phys. Rev. D **72** (2005) 053007; A. Goyal, AIP Conf. Proc. **805** (2006) 302 [arXiv:hep-ph/0506131]
[401] A. Goyal, hep-ph/0609095
[402] S. R. Choudhury *et al.*, Phys. Rev. D **75** (2007) 055011
[403] M. Blanke *et al.*, JHEP **0705** (2007) 013
[404] I. Antoniadis, Phys. Lett. B **246** (1990) 377
[405] I. Antoniadis, M. Quiros, Phys. Lett. B **392** (1997) 61
[406] N. Arkani-Hamed, S. Dimopoulos, G. R. Dvali, Phys. Lett. B **429** (1998) 263
[407] R. Barbieri, L. J. Hall, Y. Nomura, Phys. Rev. D **63** (2001) 105007
[408] T. Appelquist, H. C. Cheng, B. A. Dobrescu, Phys. Rev. D **64** (2001) 035002
[409] G. F. Giudice, J. D. Wells, *Extra Dimensions*, in [104]
[410] J. L. Hewett, M. Spiropulu, Ann. Rev. Nucl. Part. Sci. **52** (2002) 397
[411] Th. Kaluza, Sitz. Preuss. Akad. 966 (1921); O. Klein, Z. Phys. **37** (1926) 895

[412] C. T. Hill, S. Pokorski, J. Wang, Phys. Rev. D **64** (2001) 105005
[413] N. Arkani-Hamed, A. G. Cohen, H. Georgi, Phys. Rev. Lett. **86** (2001) 4757
[414] M. L. Graesser, Phys. Rev. D **61** (2000) 074019
[415] P. Nath, M. Yamaguchi, Phys. Rev. D **60** (1999) 116006
[416] R. Casadio, A. Gruppuso, G. Venturi, Phys. Lett. B **495** (2000) 378
[417] S. C. Park, H. S. Song, Phys. Lett. B **523** (2001) 161
[418] K. Agashe, N. G. Deshpande, G. H. Wu, Phys. Lett. B **511** (2001) 85
[419] T. G. Rizzo, Phys. Rev. D **64** (2001) 095010
[420] T. Appelquist, B. A. Dobrescu, Phys. Lett. B **516** (2001) 85
[421] G. Cacciapaglia, M. Cirelli, G. Cristadoro, Nucl. Phys. B **634** (2002) 230
[422] F. Jegerlehner, Nucl. Phys. B (Proc. Suppl.) **37** (1994) 129 and references therein
[423] P. Mery, S. E. Moubarik, M. Perrottet, F. M. Renard, Z. Phys. C **46** (1990) 229
[424] LEP Electroweak Working Group (LEP EWWG), `http://lepewwg.web.cern.ch/LEPEWWG/lepww/tgc/`
[425] D. W. Hertzog, J. P. Miller, E. de Rafael, B. Lee Roberts, D. Stöckinger, arXiv:0705.4617 [hep-ph]
[426] D. W. Hertzog, Nucl. Phys. Proc. Suppl. **181-182** (2008) 5
[427] S. Laporta, E. Remiddi, Nucl. Phys. Proc. Suppl. **181-182** (2008) 10
[428] B. Khazin, Nucl. Phys. Proc. Suppl. **181-182** (2008) 376; S. Eidelman, Nucl. Phys. Proc. Suppl. **162** (2006) 323
[429] G. Venanzoni, Acta Phys. Polon. B **38** (2007) 3421; F. Ambrosino et al., Eur. Phys. J. C **50** (2007) 729
[430] J. Zhang, *Status of BEPCII/BESIII and physics preparation*, presented at "Int. Workshop "e^+e^- Collisions from Φ to Ψ", April 7 – 10, 2008, LNF-INFN, Frascati
[431] J. Gluza, A. Hoefer, S. Jadach, F. Jegerlehner, Eur. Phys. J. C **28** (2003) 261
[432] G. Pancheri, O. Shekhovtsova, G. Venanzoni, Phys. Lett. B **642** (2006) 342
[433] J. H. Kühn, M. Steinhauser, C. Sturm, Nucl. Phys. B **778** (2007) 192
[434] R. Boughezal, M. Czakon, T. Schutzmeier, Phys. Rev. D **74** (2006) 074006
[435] M. Della Morte, N. Garron, M. Papinutto, R. Sommer, JHEP **0701** (2007) 007
[436] G. M. de Divitiis, M. Guagnelli, R. Petronzio, N. Tantalo, F. Palombi, Nucl. Phys. B **675** (2003) 309
[437] J. Rolf, S. Sint [ALPHA Collab.], JHEP **0212** (2002) 007
[438] J. Heitger, R. Sommer [ALPHA Collaboration], JHEP **0402** (2004) 022
[439] T. Blum, Phys. Rev. Lett. **91** (2003) 052001; M. Göckeler *et al.* [QCDSF Collaboration], Nucl. Phys. B **688** (2004) 135; C. Aubin, T. Blum, Phys. Rev. D **75** (2007) 114502
[440] M. Hayakawa, T. Blum, T. Izubuchi, N. Yamada, PoS **LAT2005** (2006) 353 [arXiv:hep-lat/0509016]
[441] P. Rakow [for the QCDSF Collaboration], *The hadronic light-by-light contribution to the anomalous magnetic moment of the muon: a lattice approach*, Talk at Lattice 2008, Williamsburg, Virginia, USA, 2008 July 14-19
[442] S. I. Eidelman, Z. K. Silagadze, E. A. Kuraev, Phys. Lett. B **346** (1995) 186
[443] J. Juran, P. Lichard, Phys. Rev. D **78** (2008) 017501
[444] S. Ivashyn, A. Y. Korchin, Eur. Phys. J. C **54** (2008) 89
[445] I. Rosell, J. J. Sanz-Cillero, A. Pich, JHEP **0408** (2004) 042; I. Rosell, P. Ruiz-Femenia, J. Portoles, JHEP **0512** (2005) 020; I. Rosell, arXiv:hep-ph/0701248
[446] H. Leutwyler, G. Colangelo, private communication